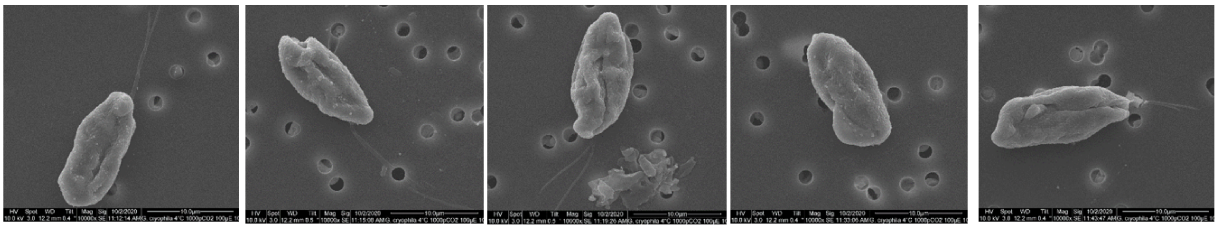

Ecophysiological response of Southern Ocean cryptophytes to temperature, CO_2, light and iron availability

Marianne Camoying

Dissertation

16 January 2025

Ecophysiological response of Southern Ocean cryptophytes to temperature, CO_2, light and iron availability

Marianne Camoying

Dissertation zur Erlangung des akademischen Grades eines

Doktors der Naturwissenschaften

Dr. rer. nat.

Universität Bremen

Fachbereich 2

16 January 2025

EXAMINATION COMMITTEE

Examiner / Chairperson: Prof. Dr. Christian Wild
University of Bremen
Fachbereich 2 Biologie/Chemie
Bremen, Germany

Examiner: Prof. Dr. Tilmann Harder
University of Bremen
Bremen, Germany
Fachbereich 2 Biologie/Chemie
Bremen, Germany

Examiner: Dr. Scarlett Trimborn (PhD Supervisor)
Alfred Wegener Institute for Polar and Marine Research
Bremerhaven, Germany

Examiner / Reviewer 1: Prof. Dr. Sven Kranz
Department of BioSciences, Rice University
Houston, Texas, USA

Reviewer 2: Prof. Dr. Natalie Cohen
Department of Marine Sciences and Skidaway Institute of Oceanography
University of Georgia
Savannah, Georgia, USA

Date of colloquium: 16 January 2025

To Nanay and Tatay, my siblings, my nephew -Lawin, and my husband…

Summary

The Southern Ocean (SO) is one of the most susceptible regions in the world to climate change. The on-going increase in anthropogenic carbon dioxide (CO_2) concentration in the atmosphere and warming have already brought changes in the composition and abundance of phytoplankton communities in the SO. These changes, however, would not only affect the Antarctic food web, but would also influence the ability of the SO to export carbon as well as absorb heat, which on a bigger scale, potentially impact the global climate and global biogeochemical cycles.

The Western Antarctic Peninsula (WAP) is one of the most productive regions in the SO. Over the past decades, the WAP region has been experiencing rapid warming and these warming events have been reported to cause shifts in phytoplankton community structure such as the increasing occurrence and dominance of cryptophytes in coastal WAP waters. Despite already being well-recognized as an important component of the WAP phytoplankton community, cryptophytes still remain less-studied compared to diatoms and haptophytes.

The most dominant cryptophyte species in the SO belongs to the genus *Geminigera*. So far, the limited studies available on the key Antarctic cryptophyte species *Geminigera cryophila* have focused mainly on determining the single effects of various environmental drivers (CO_2, warming, light, Fe) on its physiology, but studies looking at the interactive effects of these stressors are still lacking. Hence, it is the main objective of this thesis to fill these knowledge gaps by conducting laboratory and field incubation experiments to determine how the combination of multiple climate drivers would affect the ecophysiology of SO cryptophytes.

Specifically, ***Publication 1*** explored the combined effects of Fe limitation and ocean acidification (OA) which refers to the decrease in oceans' pH due mainly to the uptake of CO_2 from the atmosphere, on the growth, carbon production, trace metal quotas and photophysiology of *G. cryophila* in comparison to the response of a key SO diatom species *Pseudo-nitzschia subcurvata*. ***Publication 1*** reveals that indeed, *G. cryophila* has a high Fe requirement as it was strongly impacted by low Fe supply, but it also exhibited a modest increase in growth and carbon production in response to OA in conjunction with high Fe condition. In contrast, the Antarctic diatom *P. subcurvata* coped well with Fe limitation, but it was not able to take advantage of the high CO_2 concentration. The trace metal quotas of the two species were also differently affected by OA and Fe limitation. While Cu:C ratios were enhanced in *P. subcurvata* in response to low Fe supply and OA, *G. cryophila* maintained similar Cu:C ratios in all treatments. This observation may be associated with the potentially limited suite of Fe uptake strategies that cryptophytes employ (i.e. absence of Cu-dependent high affinity Fe uptake mechanism) compared to diatoms or the

inability to reduce its cellular Fe demand (i.e. by replacing the Fe-requiring electron carrier cytochrome c6 with the Cu-containing plastocyanin). Hence, *G. cryophila* was strongly impacted by low Fe availability.

Publication 2 aimed at characterizing the combined effects of temperature, OA and light availability on *G. cryophila*. It is shown here that the cryptophyte has a narrow thermal window compared to diatoms and haptophytes, reaching maximum growth at 4 °C while it stopped growing already at 8 °C. ***Publication 2*** demonstrates that increasing temperature (up to 4 °C) alleviated the negative effects of high light (500 µmol photons m^{-2} s^{-1}) under ambient pCO_2. It is also revealed here that *G. cryophila* is better adapted to medium irradiances (100 µmol photons m^{-2} s^{-1}) and also corroborates the findings of ***Publication 1*** that this species has a high tolerance to OA.

In ***Publication 3***, shipboard incubation experiments were conducted to examine the responses of two distinct phytoplankton communities in the WAP coastal region and in the Drake Passage, to increasing light and Fe availability as projected by SO climate models. Both communities exhibited enhanced growth and carbon production in response to increasing Fe and light availability, but differed in the magnitude of the increase. The coastal flagellate-dominated assemblage, wherein a significant number of cryptophytes was encountered, displayed a lower degree of carbon production increase compared to the open ocean diatom-dominated community. This could be attributed to the higher Fe requirement of flagellates which was not fulfilled due to their potentially less efficient Fe uptake strategy, in line with the observations in ***Publication 1***. Likewise, in agreement with ***Publication 2***, the flagellate-dominated assemblage also benefited from medium irradiances (80 µmol photons m^{-2} s^{-1}), but it did not exhibit further enhancement in carbon production at the higher light treatment (150 µmol photons m^{-2} s^{-1}). This indicates, as also noted in ***Publication 1***, that Fe has a stronger influence on the physiology of cryptophytes compared to that of light.

Overall, the results of this thesis provide an explanation on why cryptophytes are commonly distributed in Fe-rich coastal regions of the SO. In line with the results of previous studies, this thesis also highlights the potential of cryptophytes to take advantage of the on-going OA and warming events in the WAP region. However, given that OA and warming may potentially modify the bioavailability of Fe in the SO, this thesis also emphasizes the need for conducting studies on the Fe requirement and Fe uptake strategies being employed by cryptophytes. Considering the proposed hypothesis that cryptophytes have a limited suite of Fe uptake strategies, it would also be helpful to study the factors that induces mixotrophy in cryptophytes as this is one strategy that they could utilize to access the needed nutrients for growth. A deeper understanding of the ecophysiology of cryptophytes is important to better ascertain its influence on the overall carbon production and export in the SO and its role in shaping the Antarctic trophic food web.

Zusammenfassung

Das Südpolarmeer ist eine der anfälligsten Regionen der Welt für den Klimawandel. Der anhaltende Anstieg der anthropogenen Kohlenstoffdioxidkonzentration (CO_2) in der Atmosphäre und die Erwärmung haben bereits zu Veränderungen in der Zusammensetzung der Phytoplanktongemeinschaften im Südpolarmeer geführt. Diese Veränderungen würden sich jedoch nicht nur auf das Nahrungsnetz der Antarktis auswirken, sondern auch auf die Fähigkeit des Südpolarmeeres, Kohlenstoff zu exportieren und Wärme zu absorbieren, was sich in größerem Maßstab potenziell auf das globale Klima und die globalen biogeochemischen Kreisläufe auswirken könnte.

Die Westantarktische Halbinsel ist eine der produktivsten Regionen der Antarktis. In den letzten Jahrzehnten kam es in dieser Region zu einer raschen Erwärmung, und es wurde berichtet, dass diese Wärmeperioden zu Veränderungen in der Struktur der Phytoplanktongemeinschaft führten, wie beispielsweise dem zunehmenden Vorkommen und der Dominanz von Cryptophyten in den Küstengewässern der Westantarktischen Halbinsel. Obwohl Cryptophyten bereits als wichtiger Bestandteil der Phytoplanktongemeinschaft der Westantarktischen Halbinsel anerkannt sind, sind sie im Vergleich zu Kieselalgen und Haptophyten immer noch weniger erforscht.

Die dominanteste Cryptophytenart im Südpolarmeer gehört zum Gattung *Geminigera*. Bislang haben sich die wenigen Studien, die über die antarktischen Cryptophytenart *Geminigera cryophila* verfügbar sind, hauptsächlich auf die Untersuchung der jeweiligen Auswirkungen verschiedener Umwelteinflüsse (CO_2, Erwärmung, Licht, Fe) auf ihre Physiologie konzentriert, aber es fehlen Studien, die sich mit den interaktiven Effekten dieser Stressoren befassen. Daher besteht das Hauptziel dieser Arbeit darin, diese Wissenslücke durch die Durchführung von Labor- und Feldinkubationsexperimenten zu schließen, um zu bestimmen, wie sich die Kombination mehrerer Klimatreiber auf die Ökophysiologie von Cryptophyten im Südlichen Ozean auswirkt.

Publikation 1 untersuchte die kombinierten Auswirkungen von Fe-Limitation und Ozeanversauerung, bei der es sich um die Abnahme des pH-Wertes des Ozeans handelt, die hauptsächlich auf die Aufnahme von CO_2 aus der Atmosphäre zurückzuführen ist, auf Wachstum, Kohlenstoffproduktion, Spurenmetallquotas und Photophysiologie von *G. cryophila* im Vergleich zur Reaktion einer antarktischen Schlüsselart, der Diatomee *Pseudonitzschia subcurvata*. ***Publikation 1*** zeigt, dass *G. cryophila* tatsächlich einen hohen Fe-Bedarf hat, da sie bei geringem Fe-Gehalt des Meerwassers stark beeinträchtigt war, aber die Studie zeigte auch einen leichten Anstieg des Wachstums und der Kohlenstoffproduktion als Reaktion auf Ozeanversauerung in Verbindung mit einer hohen Fe-Verfügbarkeit. Im Gegensatz dazu kam die antarktische Kieselalge *P. subcurvata* gut mit der Fe-Limitierung zurecht, war aber nicht in der Lage, die hohe CO_2-Konzentration ausnutzen. Auch die

Spurenmetallquotas der beiden Arten wurden durch die Ozeanversauerung und die Fe-Limitation unterschiedlich beeinflusst. Während die Cu:C-Verhältnisse in *P. subcurvata* als Reaktion auf niedrige Fe-Versorgung und Ozeanversauerungerhöht war, behielt *G. cryophila* unter allen Bedingungen ähnliche Cu:Cu-Quotas bei. Diese Beobachtung könnte mit der begrenzten Auswahl an Fe-Aufnahmestrategien zusammenhängen, die Cryptophyten im Vergleich zu Diatomeen haben (d. h. das Fehlen eines Cu-abhängigen Fe-Aufnahmemechanismus mit hoher Affinität) oder mit der Unfähigkeit, ihren zellulären Fe-Bedarf zu reduzieren (d. h. durch Ersetzen des Fe-abhänigigen Elektonenträgers Cytochrom c6 durch das Cu-haltige Plastocyanin). Daher wurde *G. cryophila* stark von der geringen Fe-Verfügbarkeit beeinträchtigt.

Publikation 2 zielte darauf ab, die kombinierten Auswirkungen von Temperatur, Ozeanversauerung und Lichtverfügbarkeit auf *G. cryophila* zu charakterisieren. Es zeigt sich, dass der Cyptophyt im Vergleich zu Kieselalgen und Haptophyten nur ein schmales thermisches Fenster hat und sein maximales Wachstum bei 4 °C erreicht, während er bereits bei 8 °C aufhört zu wachsen. ***Publikation 2*** zeigt ebenso, dass steigende Temperaturen (bis zu 4 °C) die negativen Auswirkungen von starkem Licht (500 µmol Photonen m^{-2} s^{-1}) unter Umgebungs-pCO_2 mildern. Es wurde außerdem nachgewiesen, dass *G. cryophila* besser an mittlere Bestrahlungsstärken (100 µmol Photonen m^{-2} s^{-1}) angepasst ist und zusätzlich das Ergebnis von ***Publikation 1*** bestätigt, dass diese Art eine hohe Toleranz gegenüber Ozeanversauerung aufweist.

In ***Publikation 3*** wurden Inkubationsexperimente an Bord des Forschungseisbrechers FS Polarstern durchgeführt, um die Reaktionen von zwei unterschiedlichen Phytoplanktongemeinschaften an der Antarktischen Halbinsel und in der Drake-Passage auf zunehmende Licht- und Fe-Verfügbarkeit zu untersuchen, die von Klimamodellen vorhergesagt werden. Beide Gemeinschaften zeigten ein gesteigertes Wachstum und eine erhöhte Kohlenstoffproduktion als Reaktion auf die zunehmende Verfügbarkeit von Eisen und Licht, die Höhe des Anstiegs unterschied sich jedoch. Die von Flagellaten dominierte Phytoplanktongemeinschaft an der Küste, in der eine beträchtliche Anzahl von Cryptophyten angetroffen wurde, zeigte einen geringeren Anstieg der Kohlenstoffproduktion im Vergleich zu der von Kieselalgen dominierten Gemeinschaft im offenen Ozean. In Übereinstimmung mit den Beobachtungen von ***Publikation 1*** könnte dies auf den höheren Fe-Bedarf der Flagellaten zurückgeführt werden, der aufgrund ihrer potenziell weniger effizienten Fe-Aufnahmestrategie nicht erfüllt wurde. Ebenfalls im Einklang mit den Ergebnissen von ***Publikation 2*** profitierte die von Flagellaten dominierte Gemeinschaft auch von den mittleren Bestrahlungsstärken (80 µmol Photonen m^{-2} s^{-1}), jedoch ohne weitere Verbesserung der Kohlenstoffproduktion bei höheren Lichtintensitäten (150 µmol Photonen m^{-2} s^{-1}). Dies deutet, wie auch in ***Publikation 1*** festgestellt, stark darauf hin, dass Fe einen stärkeren Einfluss als Licht auf die Physiologie von Cryptophyten hat.

Insgesamt liefern die Ergebnisse dieser Arbeit eine Erklärung dafür, warum Cryptophyten häufig in den eisenreichen Küstenregionen des Südpolarmeeres vorkommen. Im Einklang mit den Ergebnissen früherer Studien unterstreicht diese Arbeit das Potenzial

von Cryptophyten, von der fortwährenden Ozeanversauerung und den erhöhten Temperaturen an der Antarktischen Halbinsel zu profitieren. Da Ozeanversauerung und Erwärmung jedoch möglicherweise die Bioverfügbarkeit von Fe im Südpolarmeer verändern können, zeigt diese Arbeit allerdings auch die Notwendigkeit auf, in Zukunft Studien zum Fe-Bedarf und den Fe-Aufnahmestrategien der Cryptophyten durchzuführen. In Anbetracht der vorgeschlagenen Hypothese, dass Cryptophyten nur über eine begrenzte Auswahl an Fe-Aufnahmestrategien verfügen, wäre es sehr hilfreich, die Faktoren zu untersuchen, die bei Cryptophyten Mixotrophie induzieren, da dies eine Strategie ist, die sie potenziell nutzen könnten, um an die für das Wachstum benötigten Nährstoffe zu gelangen. Es ist weiterhin wichtig, ein tieferes Verständnis der Ökophysiologie von Cryptophyten zu erlangen, um ihren Einfluss auf die Produktion und den Export von Kohlenstoff im Südpolarmeer sowie ihre Rolle bei der Gestaltung des trophischen Nahrungsnetzes der Antarktis besser zu ermitteln.

Contents

List of Figures

List of Tables

Chapter 1

General Introduction

1.1 The importance of the Southern Ocean

The Southern Ocean (SO) is an important region to study because it does not only serve as home to a diversity of marine organisms (i.e. whales, penguins, krill, seals), but it also plays a significant role in controlling the Earth's climate as well as the global biogeochemical cycles. It is responsible for approximately 50 % of the oceanic uptake of anthropogenic carbon dioxide (CO_2) and also accounts for more than 75 % of the global ocean heat uptake (Frölicher et al., 2015). Since the dissolution of CO_2 in seawater is salinity- and temperature-dependent, the cold waters of polar regions are able to absorb more CO_2 than the warm waters of the tropical oceans. The transport of the dissolved CO_2 into the deep ocean depends on two processes: the physical and the biological carbon pump (BCP). The physical carbon pump is driven by ocean dynamics and air-sea gas exchange, with the Antarctic Circumpolar Current (ACC) and the formation of bottom water through the sinking of very dense, salty and CO_2-enriched water, controlling the strength of the solubility pump in the SO. On the other hand, the BCP which is mainly dependent on primary producers, consists of two components namely, the soft-tissue pump and the carbonate (counter) pump. The soft-tissue pump involves the transport of organic carbon from the water surface to depths while the carbonate (counter) pump involves the precipitation of calcium carbonate by calcifiers which lowers alkalinity and can result in net CO_2 outflow to the atmosphere. The physical pump is said to be responsible for 70 % of the total CO_2 uptake of the SO and the remaining 30 % is attributed to the BCP (Henley et al., 2020).

The ability of the SO to act as a sink for CO_2 and heat therefore depends on the efficiency of both the physical and BCP. To set the context and frame the scope and objectives of this thesis, the impacts of various climate drivers on the BCP, more specifically on the soft-tissue pump driven by SO phytoplankton, will be addressed in this section.

1.1.1 Iron and light - the main controlling factors of primary production in the Southern Ocean

Almost half of the total global primary production is attributed to phytoplankton (Field et al., 1998). Phytoplankton are microscopic organisms that are able to perform photosynthesis by using water and the light energy from the sun to convert inorganic CO_2 into particulate organic carbon (Fischer et al., 2016). Hence, they have a major influence on the amount of CO_2 that is removed from the atmosphere, and the amount of carbon that is exported into the ocean floor (Martin, 1990; Tortell et al., 2008).

In the SO, being the largest high-nutrient, low-chlorophyll region (HNLC) in the world, the concentrations of macronutrients (i.e. nitrate, phosphate and silicate) are normally in excess, but this does not result in high primary production due to the low concentration of the trace metal iron (Fe) (Martin et al., 1990a,b; Boyd et al., 2007). Fe plays an important role in controlling the phytoplankton primary production in the SO because it is needed in various cellular processes such as nitrogen and carbon fixation, pigment synthesis as well as in the photosynthetic electron transport chain (Raven et al., 1999; Strzepek and Harrison, 2004; Behrenfeld and Milligan, 2013; Twining and Baines, 2013). In particular, the thylakoid membrane inside the chloroplast of cells receives the highest allocation of Fe because it is where the Fe-rich photochemical reaction centers (Photosystem II (PSII), 1 Fe atom; Photosystem I (PSI), 12 Fe atoms) are assembled together with the light harvesting complexes and several Fe-requiring electron carriers (Figure 1.1; Behrenfeld and Milligan, 2013). These complexes are involved in the light-dependent reaction during photosynthesis wherein water is oxidized to produce excess protons and electrons, which are needed in the production of adenosine triphosphate (ATP) and nicotinamide adenine dinucleotide phosphate (NADPH). These two photosynthates are further required for carbon fixation during the light-independent reaction process or the Calvin-Benson Cycle (Falkowski and Raven, 2013). Hence, Fe limitation typically results in reduced photosynthetic efficiency (F_v/F_m) as well as a decrease in growth and carbon production of SO phytoplankton (e.g. Strzepek et al., 2012; Petrou et al., 2014; Koch and Trimborn, 2019; Andrew et al., 2019). Indeed, previous Fe-fertilization experiments in the SO have resulted in enhanced growth and biomass of phytoplankton communities (e.g. Smetacek et al., 2012; Coale et al., 2004).

Aside from the overall low concentrations of Fe in most parts of the SO (especially in open ocean regions), more than 99 % of dissolved Fe in the field are bound to organic ligands which phytoplankton cannot freely access (Hassler et al., 2012). Hence, SO phytoplankton need to invoke various strategies to decrease their Fe requirement. Under Fe limitation, phytoplankton in general typically reduce their cell size and increase their surface area to volume ratio to enhance the diffusive uptake of Fe (Sunda and Huntsman, 1995; Maldonado and Price, 1996). Some phytoplankton species occurring in HNLC regions have also been observed to substitute Fe-rich enzymes or compounds with the ones that require less Fe or totally do not need Fe (La Roche et al., 1993; La Roche et al., 1995, 1996). For example, in the electron transport chain, the Fe-requiring cytochrome c_6 can be replaced by the copper-containing plastocyanin (Peers and Price, 2006) or flavodoxin (no Fe atom) can be partially used instead of ferrodoxin (2 Fe atoms) (La Roche et al., 1993, Ferreira and Straus, 1994). Fe-limited phytoplankton were also observed to induce the operation of high affinity Fe uptake systems (Maldonado and Price, 2001; Shaked et al.,

2005; Morrissey et al., 2015; Behnke and LaRoche, 2020). Some phytoplankton species were even found to be capable of acquiring and storing large quantities of Fe through the use of ferritins (termed as luxury Fe uptake) (Marchetti et al., 2009; Cohen et al., 2018) under high Fe supply.

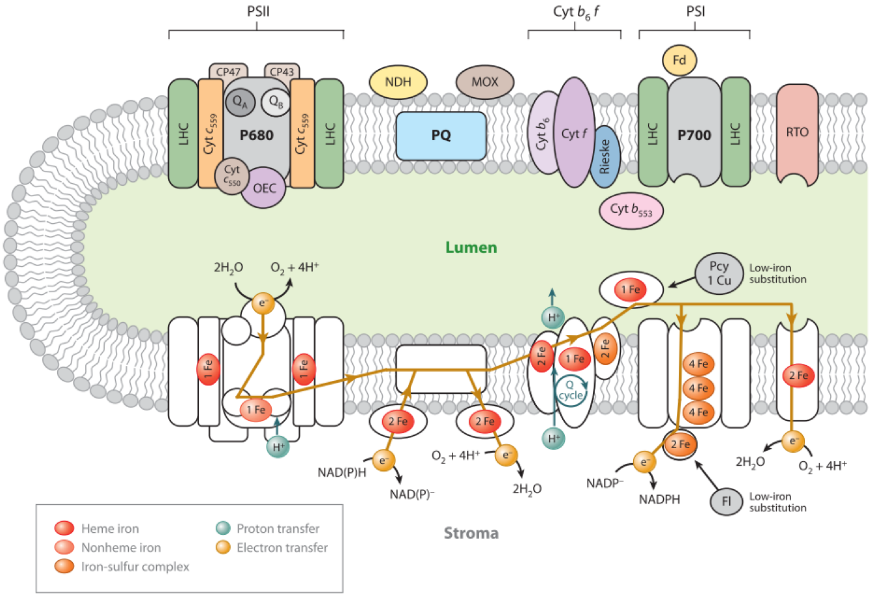

Figure 1.1. Thylakoid membrane architecture of oxygenic photoautotrophs reflecting the Fe allocation in the photosynthetic electron transport chain. The Photosystem II reaction center (P680) requires 1 Fe atom while that of Photosytem I (P700) requires 12 Fe atoms. The Fe requirements of various electron carriers which include ferredoxin (Fd) as well as the different types of cytochrome (Cyt), are also shown. Figure is taken from Behrenfeld and Milligan (2013), with permission from the primary author.

Besides Fe, light availability also influences significantly the growth and carbon production of SO phytoplankton (Sunda and Huntsman, 1997; Smith and Lancelot, 2004; Boyd, 2002). This is due to the fact that for most of the year, SO phytoplankton communities are exposed to very low light intensities, and higher irradiances only become available to them at the start of austral spring. While temperate phytoplankton have been observed to increase their Fe requirement under low light conditions (Fe-light antagonism, Sunda and Huntsman, 1997; Maldonado et al., 1999), SO phytoplankton were found to employ a different photophysiological strategy to enhance light absorption without increasing their cellular Fe demand. Specifically, SO phytoplankton were observed to increase the size of their light harvesting antennae rather than increasing the number of their Fe-rich photochemical reaction center units (Strzepek et al., 2012, 2019).

The influence of both Fe and light availability on SO phytoplankton, however, has been shown to be modulated further by other climate drivers such as ocean acidification (OA) (e.g. Feng et al., 2010; Koch and Trimborn, 2019; Hoppe et al., 2013; Pausch et al., 2022) and warming (e.g. Rose et al., 2009; Andrew et al., 2019). The influence of these drivers on SO phytoplankton would strongly depend on their species-specific Fe requirement,

the efficiency of their Fe uptake systems and their adaptive mechanisms in dealing with low Fe and varying light availability. All these aspects will be discussed in detail in the succeeding subsections.

1.2 Susceptibility of the Southern Ocean to climate change

Over the past decades, the SO has been reported to experience the impacts of climate change such as ocean acidification. Due to anthropogenic activities, the atmospheric CO_2 concentration is projected to reach levels between 750 and 1000 µatm by the end of this century (Constable et al., 2022). As CO_2 dissolves in seawater, it reacts with H_2O to form carbonic acid (H_2CO_3) which dissociates into bicarbonate (HCO_3^-) and releases a proton (H^+). Another proton forms when bicarbonate further dissociates into carbonate ion (CO_3^-). The increase in H^+ concentration lowers the pH of the seawater, a process that leads to ocean acidification. Another climate driver that affects SO is the increase of the global mean sea surface temperature also caused by the increasing CO_2 concentration in the atmosphere. OA and warming would not only directly affect SO phytoplankton, but these two factors together can also potentially alter the availability of Fe and light to primary producers.

1.2.1 Climate-driven changes in the Western Antarctic Peninsula (WAP): the emerging dominance of cryptophytes

One of the most susceptible regions in the SO to climate change is the Western Antarctica Peninsula (WAP). It is a unique region to study because of its particular northeast to southwest geographic orientation and also being exposed to strong westerly winds and oceanic circulation (Ducklow et al., 2013). Because of this geographic orientation, the northern region is usually characterized by shorter ice season and more maritime conditions while the southern areas are characterized by a longer ice season and more continental conditions (Ducklow et al., 2013). The WAP coastal region is one of the most productive areas in the SO characterized by vast, seasonal phytoplankton blooms (Vernet et al., 2008; Ducklow et al., 2013). Since coastal WAP waters generally have high availability of nutrients (Kim et al., 2018; Carvalho et al., 2020), phytoplankton productivity in the region is primarily being attributed to the stratification of the upper water column which influences the amount of light reaching the phytoplankton assemblages (Vernet et al., 2008; Carvalho et al., 2020).

Two of the major phytoplankton groups that contribute to the overall carbon production in the WAP are diatoms and haptophytes. Diatoms belong to the class Bacillariophyceae and are characterized by having siliceous cell walls or frustules (Battarbee et al., 2001). Phytoplankton blooms in coastal Antarctic waters are mainly dominated by this group. The haptophyte group (Class Prymnesiophyceae), mainly represented by the genus *Phaeocystis*, can occur as small, solitary cells having two flagella or forms prominent blooms composed of large colonies wherein cells are enclosed in a gelatinous, mucopolysaccharide

matrix (Hamm et al., 1999; Smith and Trimborn, 2024). The typical seasonal phytoplankton succession in the WAP is characterized by the dominance of autotrophic flagellates (such as *Phaeocystis*) during spring, which are then replaced by the diatom group toward summer when water column stratification strengthens (van Leeuwe et al., 2020; Smith and Trimborn, 2024). When nutrients become depleted later in the season, diatoms die down and are replaced by a mixed group of small-sized nanoflagellates.

Global warming, however, has been shown to cause a number of environmental changes in the WAP (Henley et al., 2020; Kerr et al., 2018; Moffat and Meredith, 2018). Since 1950, the WAP has warmed by 7 °C and exhibited a 100-day decline in sea ice duration (Ducklow et al., 2013). This led to the decrease in sea ice extent (Stammerjohn et al., 2008, 2012), warming and freshening of the upper ocean (Meredith and King, 2005) and thus, deepening of the mixed layer (Brown et al., 2019) due to stronger water column stratification. Along with these environmental changes, alterations in the structure and distribution of phytoplankton communities in coastal WAP regions have also been reported (Garibotti et al., 2005; Montes-Hugo et al., 2009). Specifically, over the past decades, the increasing occurrence and dominance during summer of another nanoflagellate group, the cryptophytes, have been observed in several studies (Moline and Prézelin, 1996; Moline et al., 2004; Mendes et al., 2013, 2018; Schofield et al., 2017; Brown et al., 2021).

For instance, using a 20-year (1992 -2012) time series data on the phytoplankton composition from the US Palmer Research Station off the Antarctic Peninsula, it has been shown that diatoms and cryptophytes were the top two most dominant phytoplankton groups during the summer season (Saba et al., 2014; Schofield et al., 2017). Distinct temporal patterns in the distribution of cryptophytes were also evident wherein higher relative cryptophyte abundances were generally observed during the years of low biomass than in high chlorophyll years (Figure 1.2, Schofield et al., 2017). Previous studies have also reported that diatoms and cryptophytes tend to have separate ecological niches wherein cryptophytes are specifically associated with low salinity and highly-illuminated surface waters (Garibotti et al., 2003; Schofield et al., 2017).

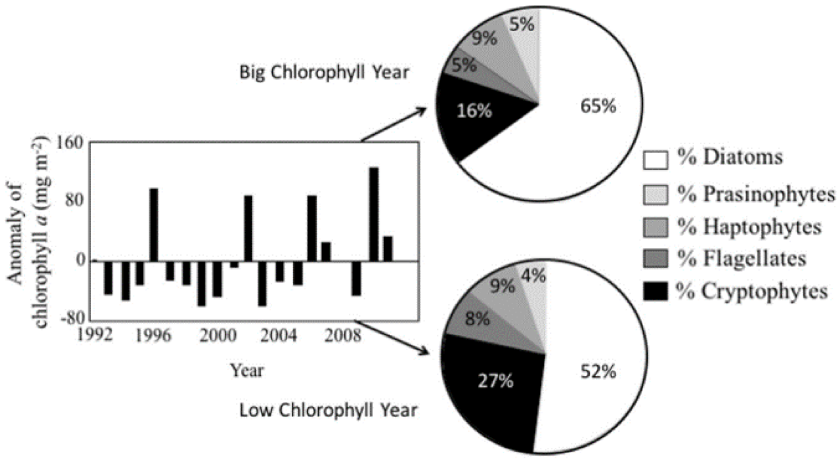

Figure 1.2. Pie charts show the average relative abundance of different phytoplankton groups in the WAP over the full summer season during the period 1992 - 2012. It is shown here that diatoms and cryptophytes were the top main contibutors to the total phytoplankoton biomass in the region. The 20-year time series data represent samples collected at the United States Palmer Research Station through the Palmer Long Term Ecological Research program. Figure is taken from Schofield et al. (2017), with permission from the primary author.

Despite the reported increasing dominance of cryptophytes in the WAP, knowledge on their ecophysiology is still scarce relative to that of the diatom and haptophyte groups. This dissertation aimed at addressing this research gap by determining the influence of major climate drivers such as warming and OA in conjunction with different light and Fe availabilities on the yet less-studied ecologically important Antarctic cryptophyte group.

1.2.2 The biology of cryptophytes

Cryptophytes (or cryptomonads) are single-celled algae ($\sim 5-50$ µm), belonging to the phylum Cryptophyta, which were formerly grouped together with diatoms and haptophytes under the supergroup Chromalveolata. Due to the advancements in the field of phylogenomics and the increase in availability of molecular datasets of eukaryotes, a new classification has been proposed wherein cryptophytes and haptophytes were separated from diatoms and were placed under their own supergroups- Cryptista and Haptista, respectively (Figure 1.3; Burki et al., 2020).

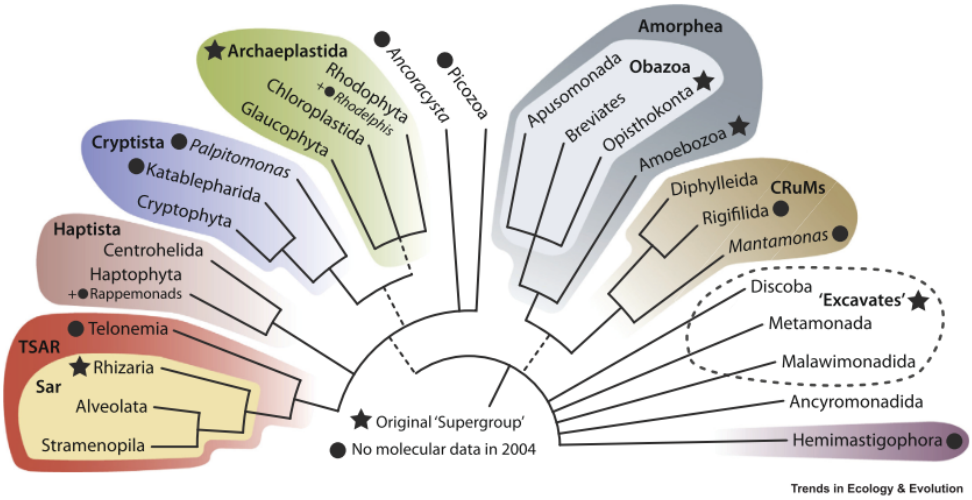

Figure 1.3. Schematic tree of eukaryotes showing the proposed new supergroups - Cryptista and Haptista. Figure is taken from Burki et al. (2020), with permission from the primary author.

Cryptophytes evolved from secondary endosymbiosis between a eukaryotic host and a red alga symbiont (Douglas and Penny, 1999; Douglas et al., 2001; Gould et al., 2008). The engulfed red alga then evolved into a plastid, allowing the cryptophyte to capture light through photosynthesis. Aside from having the major photosynthetic pigments chlorophyll *a* and c_2 and alloxanthin, cryptophytes also contain an additional light-harvesting complex composed of nitrogen-rich phycobiliprotein pigments (Hoef-Emden and Archibald, 2017), similar to cyanobacteria (Grossman et al., 1993; MacColl, 1998). However, unlike in cyanobacteria wherein phycobiliproteins form an aggregate (referred to as phycobilisome) and are attached to the outer stroma side of the thylakoid membrane, phycobiliproteins in cryptophytes are not arranged into a phycobilisome and are found instead in the thylakoid lumen (Hoef-Emden and Archibald, 2017). The phycoerythrin of cryptophyte evolved into another biliprotein, a so-called phycocyanin mimicking the blue phycocyanin in cyanobacteria (Glazer and Wedemayer, 1995). As reported by Hill and Rowan (1989) and Hoef-Emden (2008), there are three types of phycoerythrin and five types of phycocyanin present in cryptophytes, and each species is reported to contain only a single type of phycobiliprotein.

While most cryptophytes are capable of photosynthesis, there are also other species that can either be heterotrophic (plastid-lacking) or mixotrophic (Izaguirre et al., 2012; Gast et al., 2014). Mixotrophy (the ability to employ both autotrophic and heterotrophic nutrition) has been reported in several cryptophyte species (e.g. Epstein and Shiaris, 1992; Laybourn-Parry et al., 2005; Sinistro et al., 2006; Izaguirre et al., 2012; Yoo et al., 2017). Hence, mixotrophy may indeed provide cryptophytes a competitive advantage over other phytoplankton groups under conditions of extreme carbon and nutrient limitation.

Cryptophytes are ubiquitous in nature. They can be found in polar, temperate and tropical regions as well as in freshwater, marine and brackish environments (Klaveness,

1988; Hill, 1991; Garibotti et al., 2003; Hoef-Emden, 2007). In fact, some species have been reported to thrive in both low and high salinity waters (Meyer and Pienaar, 1984; Hoef-Emden, 2014). Due to their fragile cells, they are easily overlooked during sampling and thus their overall global distribution tends to be underestimated. They are not known to be toxin-producing species. They are rich in bioactive compounds such as polyunsaturated fatty acids and phytosterols which could be used for medical, pharmaceutical and food science research (Abidizadegan et al., 2021).

Cryptophytes are characterized by having a flattened asymmetrical cell and possess two flagella which allow to them to be motile. They are capable of vertical migration and also form palmellae (cell accumulation embedded in mucus) which they may utilize to avoid predators (Klaveness, 1988). Some species have also been reported to form globular and thick-walled cysts as resting stages especially during unfavorable environmental conditions (Lichtlé, 1979,Lichtlé, 1980).

The most abundant cryptophyte species identified from the SO belongs to the genus *Geminigera* (Brown et al., 2021). Almost all laboratory studies on Antarctic cryptophytes were conducted with the species *Geminigera cryophila* (Basionym: *Cryptomonas cryophila* D.L. Taylor and C.C. Lee), which is currently the only SO cryptophyte species being cultured in the laboratory. The very first isolate of *G. cryophila* was from the water sample collected beneath the pack ice in the Weddell Sea in February 1968 (Taylor and Lee, 1971). Cells measure between 15-17 µm in length, 8-10 µm in height and have a width of 3-5 µm. *G. cryophila* contains the phycobiliprotein phycoerythrin (PC-PE 545; Hoef-Emden, 2008). So far, it is the only described cryptophyte species with distinct lipid droplets/accumulations, which are said to be associated to its polar habitat (Taylor and Lee, 1971). Further, it has been observed to be capable of mixotrophy (McKie-Krisberg et al., 2015; Gast et al., 2014). The laboratory experiments conducted in this thesis focused only on *G. cryophila* (Figure 1.4).

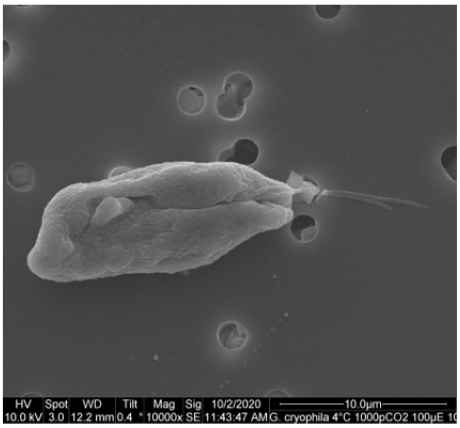

Figure 1.4. Scanning electron micropcopy image of *Geminigera cryophila*. Source: M.Camoying

1.3 Physiological responses of different Southern Ocean phytoplankton groups to climate drivers

1.3.1 Single effects of ocean acidification (OA)

The production of particulate organic carbon (POC) by phytoplankton during the light-independent reaction in photosynthesis is primarily hindered by the low affinity of the enzyme Ribulose-1,5- bisphosphate carboxylase-oxygenase (RubisCO) for its CO_2 substrate. Moreover, due to the very low concentration of aqueous CO_2 in seawater (Zeebe and Wolf-Gladrow, 2001), phytoplankton cannot solely rely on the diffusive uptake of CO_2 to saturate RubisCO with its substrate (Badger et al., 1998). To counteract this, several phytoplankton operate the so-called carbon concentrating mechanisms (CCMs; Giordano et al., 2005; Reinfelder, 2011). Several phytoplankton groups, especially the earliest evolved groups such as cyanobacteria and dinoflagellates, have been observed already to operate highly efficient CCMs compared to diatoms and haptophytes (Van de Waal et al., 2019). CCM operation is highly energy intensive, which involves the active transport of CO_2 and bicarbonate (HCO_3^-) through the cell membranes and the interconversion between CO_2 and HCO_3^- (both inside and outside the cell) which is facilitated by the enzyme carbonic anhydrase (CA), preventing further the diffusive outflow of CO_2 (Hopkinson et al., 2011). Thus, the increase in the concentration of CO_2 in surface waters resulting from OA may lead to CCM downregulation (Hopkinson et al., 2011), allowing the cells to save energy (Reinfelder, 2011) and potentially enhance phytoplankton growth.

Field and laboratory CO_2-incubation experiments on SO phytoplankton have reported diverging results. For instance, growth and community composition of natural SO assemblages have been shown to be influenced by OA (Feng et al., 2010; Hoppe et al., 2013; Trimborn et al., 2017a) while laboratory experiments have reported that the growth of Antarctic diatom cultures was not enhanced by increasing pCO_2 (Boelen et al., 2011; Hoppe et al., 2015; Trimborn et al., 2017b). OA even led to reduced growth and/or POC production of the Antarctic diatoms *Fragilariopsis curta* and *Odontella weisflogii* (Heiden et al., 2016). Nevertheless, based on a meta-analysis on the responses of SO phytoplankton to OA, negative effects on the cell's physiology becomes evident only when Antarctic phytoplankton are exposed to pCO_2 levels higher than 1000 µatm (Hancock et al., 2020). Indeed, the growth of several SO diatoms *Pseudo-nitzschia subcurvata* (Trimborn et al., 2013; Zhu et al., 2017), *Chaetoceros debilis* (Trimborn et al., 2013, 2017b), *C. brevis* (Boelen et al., 2011), *Fragilariopsis kurguelensis* (Trimborn et al., 2017b) and *Proboscia alata* (Hoogstraten et al., 2012) remained unaffected by increasing CO_2 (< 1000 µatm). The haptophyte *Phaeocystis antarctica* was also not affected by OA (Trimborn et al., 2017b; Koch et al., 2019). The absence of positive OA effects on SO phytoplankton could be related to the small "energy savings" from CCM downregulation due to the low half-saturation constant of RubisCO for its CO_2 substrate at low temperatures (Kranz et al., 2015; Young et al., 2015).

In comparison to diatoms and haptophytes, the key Antarctic cryptophyte species *Geminigera cryophila* has been shown to grow well under OA (Trimborn et al., 2019), in line with the observations in the field for the general cryptophyte group (Sommer et al.,

2015; Schulz et al., 2017; Donahue et al., 2019). Cryptophytes have also been reported to grow within a broad pH range (i.e. at both lower and upper extreme of the pH spectrum). The freshwater species *Cryptomonas* sp., for example, was reported to tolerate low pH values such as 4.4 up to high values such as 9.65 (Weisse and Stadler, 2006) while the temperate marine cryptophyte *Teleaulax amphioxeia* was able to grow from pH 6.0 (Gaillard et al., 2020) up to 9.4 (Smith and Hansen, 2007). Another cryptophyte species *Rhodomonas marina* was reported to maintain maximum growth rates within the pH range of 7.1 and 9.5 (Berge et al., 2010) and to survive even up to a pH of 9.9 (Schmidt and Hansen, 2001). In the coastal areas of the SO, where cryptophytes are commonly observed (Mendes et al., 2013), CO_2 concentrations can become very low towards the end of the summer bloom. Under these conditions of high pH and very low CO_2 concentrations, cryptophytes may potentially acquire carbon and other nutrients from ingesting bacteria (phagotrophy).

With respect to low pH, it still remains unclear how cryptophytes remain unaffected as they are able to grow even under very low pH values (i.e. pH 4.4; Weisse and Stadler, 2006). In acidic environments, phytoplankton cells require a great amount of ATP in order to maintain neutral cytosolic pH (Messerli et al., 2005). In connection to this, the acidophilic green alga *Chlamydomonas eustigma* has been reported to have highly expressed genes encoding for the enzymes phosphagen kinases (PK) and amidinotransferase (AMGT) in contrast to the neutrophilic species *Chlamydomonas reinhardtii* (Hirooka et al., 2017). The two enzymes are assumed to play a significant role in maintaining cellular pH under acidic conditions by increasing the ATP supply in the cell. Interestingly, the cryptophyte *Guillardia* was also found to have the same PK and AMGT genes (Hirooka et al., 2017; Yano and Suzuki, 2022), which may therefore potentially explain why cryptophytes are able to thrive in acidic environments.

It still needs to be investigated whether the yet less-studied Antarctic cryptophyte *G. cryophila* also has this ability to tolerate a wide pH spectrum. Moreover, experiments which aim to determine how other climate stressors such as warming and increasing light availability would influence the response of SO cryptophytes to OA, are important and this is addressed in this thesis.

1.3.2 Single effects of warming

The increase of the concentration of greenhouse gas CO_2 in the atmosphere will not only cause acidification of the oceans, but will also lead to warming, as has been observed already in some regions of the Antarctic Peninsula. Indeed, changes in phytoplankton community composition due to warming have already been documented such as the increased occurrence of the cryptophytes in these coastal waters (Moline et al., 2004; Montes-Hugo et al., 2009).

Compared to tropical phytoplankton, which are already close to experiencing their thermal limit, polar phytoplankton, on the other hand, are reported to be less susceptible to global warming since their optimum growth temperatures (T_{opt}) are higher than the temperature of their ambient environment (Thomas et al., 2012). Increasing temperatures generally leads to higher growth rates in phytoplankton and growth starts to decline once temperatures go beyond their T_{opt} (Eppley, 1972). A T_{opt} of 5.2 °C has been calculated

for Antarctic phytoplankton in general (Coello-Camba and Agustí, 2017), a value that is two times higher than their current growth temperature in the field ($\sim$ 0 – 2 °C). SO phytoplankton may benefit from the increased enzymatic reactions at higher temperatures (i.e. increase carboxylation rates of the enzyme RuBisCO, Young et al., 2015). Indeed, several studies have already reported the strong positive effect of increasing temperature on phytoplankton primary productivity in the SO (Boyd et al., 2015; Spackeen et al., 2018). For instance, the growth rates of the haptophyte *P. antarctica* (Zhu et al., 2017; Andrew et al., 2019) as well as of the diatoms *Chaetoceros flexuous* and *Thalassiosira antarctica* (Andrew et al., 2019) were enhanced when exposed to temperatures up to 5 °C. On the other hand, the diatom *Pseudo-nitzschia subcurvata* exhibited a much higher temperature requirement as maximum growth was reached only at 8 °C. Interestingly, *P. subcurvata* exhibited a narrower upper thermal limit (T_{max}) at 10 °C compared to *P. antarctica*, which has been observed to maintain positive growth until 14 °C (Buma et al., 1991; Zhu et al., 2017). Such information on the thermal performance curve of the key Antarctic cryptophyte species *G. cryophila* is, however, still lacking. Besides the study of Wang and Smith (2021) which reported the ability of the cryptophyte to tolerate and achieve the highest growth at 4 °C and that of van de Poll and Nassif (2023) where *G. cryophila* was grown at 7 °C under verly low light, no study has been conducted yet to determine its overall thermal capacity.

Clearly, it is imperative to conduct experiments which aim at determining the thermal performance curves of various Antarctic phytoplankton species to better predict the effects of future warming on SO primary productivity.

1.3.3 Single effects of increasing light availability

One of the projected consequences of warming in the SO is increased water column stratification (Thomas et al., 2012; Meredith et al., 2019), which would in turn lead to shoaling of the mixed layer depth and thus expose phytoplankton to higher light intensities (Marinov et al., 2010). Similar to temperature, phytoplankton also have different light requirements for optimal growth. Thus, Antarctic phytoplankton are expected to exhibit differential responses to the projected increase of light availability in the SO, as have been observed already in previous studies (Heiden et al., 2016; Trimborn et al., 2017b). For example, the diatom *Fragilariopsis curta* exhibited earlier saturation of photosynthesis at 20 µmol photons m^{-2} s^{-1} while *Odontella weisflogii* only reached maximum POC production at 200 µmol photons m^{-2} s^{-1} (Heiden et al., 2016). The growth of the diatom *Chaetoceros debilis* was also stimulated in response to increasing irradiance while that of the haptophyte *P. antarctica* remained unaffected (Trimborn et al., 2017b). In a field incubation experiment with natural phytoplankton communities in the WAP, *Phaeocystis* spp. reached similar high cell abundances across all light treatments (4-7, 30-50 and 150-200 µmol photons m^{-2} s^{-1}) while diatoms of different size-classes showed strong group-specific responses to the different light availability (Biggs et al., 2022).

These group- and species-specific responses to light are mainly controlled by the ability of phytoplankton to undergo photo-acclimation. In response to super-saturating light, phytoplankton downregulate light absorption by decreasing the concentration of their light harvesting pigments and increasing the amount of pigments for light protection

(Kropuenske et al., 2010; Van De Poll et al., 2011). Excess excitation energy can also be dissipated through non-photochemical quenching (NPQ, Lavaud et al., 2007) such as the rapid response (in seconds) to high light stress by releasing heat via the xanthophyll cycle pigments (diadinoxanthin and diatoxanthin) triggered by changes in the thylakoid proton gradient (Holt et al., 2004; Milligan et al., 2012). The second form of NPQ is the so-called state transition, which involves the balancing of light energy between photosystems through the movement of light harvesting antennae complexes from PSII to PSI. The third type is the quenching of the PSII reactions center, which is associated to protein damage or the reversible down-regulation of PSII (Milligan et al., 2012).

With regard to the photo-acclimation response of cryptophytes to increasing light, some species have been shown to employ the photoprotective non-xanthophyll dependent NPQ (Funk et al., 2011; Kaňa et al., 2012, 2019) as well as to regulate light energy distribution through state transition (Cheregi et al., 2015). Moreover, unlike diatoms, cryptophytes are capable of actively moving away from extreme light through phototaxis (Häder et al., 1987; Kaňa et al., 2019), thus providing them longer protection against photoinhibition. In line with this, field observation in the SO reported the dominance of cryptophytes in stratified, well-illuminated coastal waters (Mendes et al., 2018). It has also been shown in a laboratory experiment that the cryptophyte *G. cryophila* was able to tolerate a wide range of light intensities (up to 535 µmol photons m^{-2} s^{-1}; Mendes et al., 2023). In fact, a different strain of *G. cryophila* (Trimborn et al., 2019) was observed to maintain similar high growth and carbon production rates between 20 and 200 µmol photons m^{-2} s^{-1} irradiance. However, unlike in Mendes et al. (2023), the cryptophyte was drastically impacted when grown at 500 µmol photons m^{-2} s^{-1} (Trimborn et al., 2019). The discrepancy between the observations of Mendes et al. (2023) and Trimborn et al. (2019) may indicate that other environmental factors potentially play a role in modulating the ability of the cryptophyte to tolerate high irradiances.

Warming is also projected to strengthen the westerly winds, which would consequently lead to increased water column mixing, thereby transporting phytoplankton to deeper water layers and exposing them to low light availability. Although it was not an objective of this thesis to examine the response of *G. cryophila* to very low irradiances, previous studies have reported the ability of other cryptophyte species to enhance light capture through the use of their additional phycobiliprotein light harvesting complexes. Multiple-stressor experiments are indeed necessary to shed more light on how the ecophysiology Antarctic cryptophytes will be influenced by OA in conjunction with other climate drivers.

1.3.4 Interactive effects of OA, warming and increasing light

While it is important to first understand the individual effects of OA, warming and increasing light on SO phytoplankton, in the future, however, these climate drivers will not occur in isolation. Hence, it is imperative to examine the combined effects of these three factors on SO phytoplankton.

Previous studies have shown how the ecophysiological responses of Antarctic phytoplankton to a single stressor were modified when they are further exposed simultaneously to other environmental factors. SO phytoplankton in general are reported be less suscepti-

ble to OA (Hancock et al., 2020), however, the combination of OA and high irradiance was found to promote either positive or negative effects on their growth and carbon production (Heiden et al., 2016; Trimborn et al., 2017b). Shifts in community composition such as the dominance of dinoflagellates under OA and high light conditions, were also observed in field incubation experiments on natural SO phytoplankton assemblages (Donahue et al., 2019). In the case of the diatoms *Fragilariopsis kerguelensis* and *Chaetoceros debilis*, their growth and POC production, were reduced under OA in combination with 200 µmol photons m^{-2} s^{-1} irradiance (Trimborn et al., 2017b). This observation is in line with the response of natural phytoplankton assemblages of the South China Sea, which exhibited decreased primary production rates due to the combined effects of OA and high light (Gao et al., 2012). The authors hypothesized that CCM downregulation under OA potentially reduces the energetic costs of phytoplankton, thus they become more prone to high light stress or photoinhibition. Opposed to diatoms, the haptophye *P. antarctica* was observed to be more tolerant to OA and high irradiance (Trimborn et al., 2017b, Heiden et al., 2019).

With regard to the cryptophyte group, the combination of OA and high light was found to be beneficial for the cryptophyte *G. cryophila*, wherein OA enabled it to grow at the high light level of 500 µmol photons m^{-2} s^{-1} while at the same light intensity, its growth was drastically impacted at ambient pCO_2 (Trimborn et al., 2019). It still remains unclear how *G. cryophila* benefits exactly from OA especially under high irradiances and thus pinpointing the need for further investigation.

As discussed in the previous subsection, phytoplankton species have different thermal functional response curves and temperature has a strong influence on their physiological response to other environmental drivers. It has been shown that the exposure of the SO diatom *Pseudo-nitzschia subcurvata* to 8 °C warming and increasing pCO_2 led to enhanced growth rates while this combination had no beneficial effects for *Phaeocystis antarctica* (Zhu et al., 2017). This was due to the fact that the diatom has a wider maximal thermal limit (14 °C) compared to the haptophyte, which was no longer able to maintain positive growth at 10 °C (Zhu et al., 2017). As for the cryptophyte *G. cryophila*, its response to increasing temperatures and CO_2 has not yet been tested.

Another important stressor combination to SO phytoplankton in the future is the interactive effects of warming and high light availability. It has been shown in a laboratory incubation experiment by Andrew et al. (2019) that the growth rates of the SO phytoplankton *Chaetoceros flexuosus*, *P. antarctica*, *Proboscia enermis* and *Thalassiosira antarctica* were strongly enhanced in response to 5 °C temperature and 200 µmol photons m^{-2} s^{-1} irradiance. The cryptophyte *Rhodomonas salina* also exhibited an increasing trend in growth rates when exposed to increasing temperatures (5 – 20 °C) and light intensities (10 – 150 µmol photons m^{-2} s^{-1}) (Hammer et al., 2002). Whether *G. cryophila* would benefit as well from future warming and high light still needs to be investigated. This thesis addresses this knowledge gap by conducting laboratory experiments on the combined effects of there 3 factors - warming, OA and increasing light, on the ecophysiology of the yet less-studied cryptophyte *G. cryophila*.

1.4 The responses of Antarctic phytoplankton to different light and Fe availability are modulated by other climate stressors

Climate stressors such as OA and warming may potentially affect the bioavailability of Fe as well as modify the Fe requirement of SO phytoplankton. In fact, OA and warming have been shown to directly affect the solubility of Fe as well as its complexation with organic ligands (Millero et al., 2009; Breitbarth et al., 2010; Hassler et al., 2013; Gledhill et al., 2015). For instance, OA was shown to enhance Fe bioavailability due to weakening of Fe binding with ligands (Millero et al., 2009; Gledhill et al., 2015). This supposed positive OA effect on the bioavailability of Fe, however, was not reflected in the response of model diatom and coccolithophore cultures as their Fe uptake rates decreased under OA (Shi et al., 2010). In line with the observations of Shi et al. (2010), the natural SO phytoplankton community from the Weddell Sea which was exposed to Fe-limiting conditions (with the addition of the Fe chelator hydroxamate siderophore B) also did not exhibit CO_2-dependent increases in carbon fixation (Hoppe et al., 2013).

Although the solubility of Fe in artificial seawater has been observed to decrease at higher temperatures (Liu and Millero, 1999), the combination of warming and high Fe supply was found to promote synergistic positive effects on the growth of SO phytoplankton (Rose et al., 2009; Andrew et al., 2019). On the other hand, increasing light can alleviate Fe limitation of phytoplankton in cold regions such as in the SO by increasing the concentration of dissolved inorganic Fe via photolysis of Fe chelates (Sunda and Huntsman, 2003, 2011). This positive light effect on Fe availability, however, may be countered by warming (Sunda and Huntsman, 2011).

While SO climate change models project an overall increasing Fe supply in the future (Henley et al., 2020), the concomitant OA and warming events may potentially decrease the bioavailability of Fe as well as reduce the Fe uptake rates of SO phytoplankton (Shi et al., 2010; Liu and Millero, 1999), as previously discussed. The Antarctic cryptophyte *G. cryophila* has already been shown to be strongly affected by Fe limitation alone (Koch and Trimborn, 2019). It remains unknown, however, how other stressors, such as OA, will influence its ecophysiological response to Fe limitation. Moreover, while a number of studies have already characterized the Fe uptake mechanism of diatoms (Behnke and LaRoche, 2020 and references therein), nothing is known yet on the Fe uptake strategy of cryptophytes. It is endeavored that the findings of this thesis can provide insights into the Fe requirement and uptake strategies of cryptophytes.

1.5 Thesis aims and scope

As discussed in the preceding subsections, despite the increasing occurrence and dominance of cryptophytes in coastal Antarctic waters (e.g. Moline et al., 2004; Montes-Hugo et al., 2009; Mendes et al., 2018), they still remain less-studied compared to SO diatoms and haptophytes. SO studies which aim at providing a mechanistic explanation on the

emerging dominance of cryptophytes in the field as well as how they will be influenced by the combination of different climate drivers (i.e. warming, OA, light), are still lacking. Hence, this thesis addresses these knowledge gaps and presents results from laboratory experiments on the key SO cryptophyte species *Geminigera cryophila* as well as from field incubation experiments on SO natural phytoplankton assemblages. Overall, this thesis aims to gain new insights into the ecophysiology of cryptophytes and its response to future climate change scenarios projected for the SO.

***Publication 1*: Response of *G. cryophila* and *Pseudo-nitzschia* to OA and Fe limitation**

Building upon the findings of a previous study that showed the strong influence of Fe on the cryptophyte *G. cryophila* (Koch and Trimborn, 2019), *Publication 1* aimed at investigating how growth, carbon production and cellular trace metal quotas of *G. cryophila* would be influenced by Fe limitation in combination with OA. The physiological responses of the cryptophyte were then compared to the open ocean SO diatom *Pseudo-nitzschia subcurvata*. Results of *Publication 1* highlight the higher Fe requirement of the cryptophyte relative to the diatom as well as the modest positive influence of OA on the growth of *G. cryophila*, specifically under higher Fe availability.

Publication 2*: The combined effects of temperature, pCO_2 and light on *G. cryophila

Besides the warming experiment conducted in this thesis, there are only two other studies available so far which investigated the effects of temperature on *G. cryophila*. In the study of Wang and Smith (2021), another strain of *G. cryophila* was grown only up to a maximum temperature of 4 °C at which the highest growth rate was observed. On the other hand, the study of van de Poll and Nassif (2023) had a different objective which was to investigate the ability of the cryptophyte to recover from prolonged darkness under two different temperatures (4 and 7 °C). Nevertheless, the authors were able to show that *G. cryophila* could grow at a higher temperature of 7 °C, but this was in conjunction with very low irradiance (15 µmol photons m^{-2} s^{-1}). While the thermal growth response curve of several SO diatoms (Zhu et al., 2017; Andrew et al., 2019) and the haptophyte *Phaeocystis antarctica* (Zhu et al., 2017) have already been characterized, little is known about the thermal tolerance of *G. cryophila*. Hence, to increase our knowledge on the thermal tolerance of *G. cryophila*, the first objective of *Publication 2* was to determine the functional thermal response of the cryptophyte, being exposed up to 8 °C. The second objective was to investigate the combined effects of temperature, OA and increasing light intensities on the growth, carbon production and photophysiology of the cryptophyte. *Publication 2* highlights that *G. cryophila* has a lower upper thermal limit for growth compared to diatoms and haptophytes. It is also shown here that *G. cryophila* was impacted by high light (500 µmol photons m^{-2} s^{-1}) under ambient pCO_2 in line with the findings of Trimborn et al. (2019). Increasing temperature (4 °C), however, alleviated the negative effects of high light on the growth and carbon production of *G. cryophila*.

***Publication 3*: Response of two natural SO phytoplankton communities to increasing**

light and Fe availability

In *Publication 3*, two field incubation experiments were conducted to investigate the response of contrasting phytoplankton communities in the WAP coastal region and in the Drake Passage, to increasing light and Fe availability as projected by SO climate models. Growth, carbon production and the photoacclimation strategy of the flagellate-dominated coastal assemblage, wherein cryptophytes were one of the most abundant groups, were characterized and compared to a diatom-dominated open ocean community. *Publication 3* showed that carbon production was enhanced in both communities in response to increasing light and Fe availability, but the magnitude of increase was lower in the flagellate-dominated community compared to the diatom-dominated assemblage. The differential response of the two communities to Fe and light could be attributed to the specific Fe requirement of the dominant phytoplankton groups in the assemblage, whereby the higher Fe requirement of the flagellate-dominated community was potentially not fulfilled due to their less efficient Fe uptake strategy.

Synthesis

In the Synthesis section, the main findings of this thesis are summarized and discussed in a broader context. Specifically, the ecophysiology of cryptophytes under present-day conditions and how they respond to future climate change scenarios are discussed. The ecological implications of these observations and future research perspectives which emerged in the framework of this thesis, are also presented.

1.6 List of first-author publications and declaration of own contribution

Publication 1

Camoying, M. G., K. Bischof, J. K. Geuer, B. P. Koch, and S. Trimborn. 2022. In contrast to diatoms, cryptophytes are susceptible to iron limitation, but not to ocean acidification.

Published in Physiologia Plantarum

Content: Laboratory experiments were conducted to investigate the response of the Antarctic cryptophyte *Geminigera cryophila* and the Antarctic diatom *Pseudo-nitzschia subcurvata* to increasing pCO_2 levels and Fe availability. The findings of this study show that in contrast to the open ocean diatom, the cryptophyte was strongly impacted by Fe limitation, but was not susceptible to ocean acidification.

Contribution: S. Trimborn and I designed the experiment. I performed the experiments and also conducted the data analysis. I wrote the manuscript and revised it with the help of the co-authors.

Publication 2

Camoying, M. G., and S. Trimborn. 2023. Physiological response of an Antarctic cryptophyte to increasing temperature, CO_2, and irradiance.

Published in Limnology and Oceanography

Content: Laboratory experiments were conducted to determine the thermal response curve of the Antarctic cryptophyte *Geminigera cryophila*. Its response to the combined effects of warming, ocean acidification and increasing light intensities was also investigated. The findings of this study reveal that *G. cryophila* has a narrow thermal limit for growth compared to other Antarctic phytoplankton. Also, OA had no effect no effect on *G. cryophila* and increasing temperature (4 °C) alleviated the negative effects of high light (500 µmol photons m^{-2} s^{-1}) on its growth and carbon production.

Contribution: I designed and performed the experiments. I also did the data analysis. I wrote the manuscript and revised it with the help of my co-author.

Publication 3

Camoying, M.G., Koch, F., Stimpfle, J., Pausch, F., Hassler, C., and S. Trimborn. 2024. Distinct responses of diatom- and flagellate-dominated Antarctic phytoplankton communities to altered iron and light supply.

Published in Frontiers in Marine Science – Global Change and the Future Ocean

Content: Field incubation experiments were conducted to determine the ecophysiological responses of two distinct SO phytoplankton assemblages to varying light and Fe availabilities. The findings of this study demonstrate that both the diatom- and flagellate-

dominated communities enhanced their carbon production in response to increasing light intensity and Fe addition. The magnitude of the increase, however, differed between the two communities, being higher in the former than the latter, which could be attributed to the different Fe demand and Fe uptake capabilities of diatoms and flagellates.

Contribution: F. Koch and S. Trimborn conducted the field experiments. J. Stimpfle did the microscopic counting of the diatom phytoplankton community. F. Pausch supported the pigment analysis. I did the data analyses with the help of the co-authors. I wrote the manuscript and revised it with the help of the co-authors.

1.7 References

Abidizadegan, M., Peltomaa, E., and Blomster, J. (2021). The potential of cryptophyte algae in biomedical and pharmaceutical applications. *Frontiers in Pharmacology*, 11(February):1–17.

Andrew, S. M., Morell, H. T., Strzepek, R. F., Boyd, P. W., and Ellwood, M. J. (2019). Iron availability influences the tolerance of Southern Ocean phytoplankton to warming and elevated irradiance. *Frontiers in Marine Science*, 6(November):1–12.

Badger, M. R., Andrews, T. J., Whitney, S. M., Ludwig, M., Yellowlees, D. C., Leggat, W., and Price, G. D. (1998). The diversity and coevolution of Rubisco, plastids, pyrenoids, and chloroplast-based CO_2-concentrating mechanisms in algae. *Canadian Journal of Botany*, 76(6):1052–1071.

Battarbee, R. W., Jones, V. J., Flower, R. J., Cameron, N. G., Bennion, H., Carvalho, L., and Juggins, S. (2001). *Diatoms*, pages 155–202. Springer Netherlands, Dordrecht.

Behnke, J. and LaRoche, J. (2020). Iron uptake proteins in algae and the role of Iron Starvation-Induced Proteins (ISIPs). *European Journal of Phycology*, 55(3):339–360.

Behrenfeld, M. J. and Milligan, A. J. (2013). Photophysiological expressions of iron stress in phytoplankton. *Annual Review of Marine Science*, 5(1):217–246.

Berge, T., Daugbjerg, N., Andersen, B. B., and Hansen, P. J. (2010). Effect of lowered pH on marine phytoplankton growth rates. *Marine Ecology Progress Series*, 416:79–91.

Biggs, T. E., Rozema, P. D., Evans, C., Timmermans, K. R., Meredith, M. P., Pond, D. W., and Brussaard, C. P. (2022). Control of Antarctic phytoplankton community composition and standing stock by light availability. *Polar Biology*, 45(11):1635–1653.

Boelen, P., van de Poll, W. H., van der Strate, H. J., Neven, I. A., Beardall, J., and Buma, A. G. (2011). Neither elevated nor reduced CO_2 affects the photophysiological performance of the marine Antarctic diatom *Chaetoceros brevis*. *Journal of Experimental Marine Biology and Ecology*, 406(1-2):38–45.

Boyd, P. W. (2002). Environmental factors controlling phytoplankton processes in the Southern Ocean. *Journal of Phycology*, 38(5):844–861.

Boyd, P. W., Jickells, T., Law, C. S., Blain, S., Boyle, E. A., Buesseler, K. O., Coale, K. H., Cullen, J. J., De Baar, H. J., Follows, M., Harvey, M., Lancelot, C., Levasseur, M., Owens, N. P., Pollard, R., Rivkin, R. B., Sarmiento, J., Schoemann, V., Smetacek, V., Takeda, S., Tsuda, A., Turner, S., and Watson, A. J. (2007). Mesoscale iron enrichment experiments 1993-2005: Synthesis and future directions. *Science*, 315(5812):612–617.

Boyd, P. W., Lennartz, S. T., Glover, D. M., and Doney, S. C. (2015). Biological ramifications of climate-change-mediated oceanic multi-stressors. *Nature Climate Change*, 5(1):71–79.

Breitbarth, E., Bellerby, R. J., Neill, C. C., Ardelan, M. V., Meyerhöfer, M., Zöllner, E., Croot, P. L., and Riebesell, U. (2010). Ocean acidification affects iron speciation during a coastal seawater mesocosm experiment. *Biogeosciences*, 7(3):1065–1073.

Brown, M. S., Bowman, J. S., Lin, Y., Feehan, C. J., Moreno, C. M., Cassar, N., Marchetti, A., and Schofield, O. M. (2021). Low diversity of a key phytoplankton group along the West Antarctic Peninsula. *Limnology and Oceanography*, 66(6):2470–2480.

Brown, M. S., Munro, D. R., Feehan, C. J., Sweeney, C., Ducklow, H. W., and Schofield, O. M. (2019). Enhanced oceanic CO_2 uptake along the rapidly changing West Antarctic Peninsula. *Nature Climate Change*, 9(9):678–683.

Buma, A. G. J., Bano, N., Veldhuis, M. J. W., and Kraay, G. W. (1991). Comparison of the pigmentation of two strains of the prymnesiophyte *Phaeocystis* sp. *Netherlands Journal of Sea Research*, 27(2):173–182.

Burki, F., Roger, A. J., Brown, M. W., and Simpson, A. G. (2020). The New Tree of Eukaryotes. *Trends in Ecology and Evolution*, 35(1):43–55.

Carvalho, F., Fitzsimmons, J. N., Couto, N., Waite, N., Gorbunov, M., Kohut, J., Oliver, M. J., Sherrell, R. M., and Schofield, O. (2020). Testing the canyon hypothesis: Evaluating light and nutrient controls of phytoplankton growth in penguin foraging hotspots along the West Antarctic Peninsula. *Limnology and Oceanography*, 65(3):455–470.

Cheregi, O., Kotabová, E., Prášil, O., Schröder, W. P., Kaňa, R., and Funk, C. (2015). Presence of state transitions in the cryptophyte alga *Guillardia theta*. *Journal of Experimental Botany*, 66(20):6461–6470.

Coale, K. H., Johnson, K. S., Chavez, F. P., Buesseler, K. O., Barber, R. T., Brzezinski, M. A., Cochlan, W. P., Millero, F. J., Falkowski, P. G., Bauer, J. E., Wanninkhof, R. H., Kudela, R. M., Altabet, M. A., Hales, B. E., Takahashi, T., Landry, M. R., Bidigare, R. R., Wang, X., Chase, Z., Strutton, P. G., Friederich, G. E., Gorbunov, M. Y., Lance, V. P., Hilting, A. K., Hiscock, M. R., Demarest, M., Hiscock, W. T., Sullivan, K. F., Tanner, S. J., Gordon, R. M., Hunter, C. N., Elrod, V. A., Fitzwater, S. E., Jones, J. L., Tozzi, S., Koblizek, M., Roberts, A. E., Herndon, J., Brewster, J., Ladizinsky, N., Smith, G., Cooper, D., Timothy, D., Brown, S. L., Selph, K. E., Sheridan, C. C., Twining, B. S., and Johnson, Z. I. (2004). Southern Ocean Iron Enrichment Experiment: Carbon Cycling in High- and Low-Si Waters. *Science*, 304(5669):408–414.

Coello-Camba, A. and Agustí, S. (2017). Thermal thresholds of phytoplankton growth in polar waters and their consequences for a warming polar ocean. *Frontiers in Marine Science*, 4.

Cohen, N. R., Mann, E., Stemple, B., Moreno, C. M., Rauschenberg, S., Jacquot, J. E., Sunda, W. G., Twining, B. S., and Marchetti, A. (2018). Iron storage capacities and associated ferritin gene expression among marine diatoms. *Limnology and Oceanography*, 63(4):1677–1691.

Constable, A., Harper, S., Dawson, J., Holsman, K., Mustonen, T., Piepenburg, D., and Rost, B. (2022). *Cross-Chapter Paper 6: Polar Regions*, pages 2319–2368. Cambridge University Press, Cambridge, UK and New York, USA.

Donahue, K., Klaas, C., Dillingham, P. W., and Hoffmann, L. J. (2019). Combined effects of ocean acidification and increased light intensity on natural phytoplankton communities from two Southern Ocean water masses. *Journal of Plankton Research*, 41:30–45.

Douglas, S., Zauner, S., Fraunholz, M., Beaton, M., Penny, S., Deng, L. T., Wu, X., Reith, M., Cavalier-Smith, T., and Maier, U. G. (2001). The highly reduced genome of an enslaved algal nucleus. *Nature*, 410(6832):1091–1096.

Douglas, S. E. and Penny, S. L. (1999). The plastid genome of the cryptophyte alga, *Guillardia theta*: Complete sequence and conserved synteny groups confirm its common ancestry with red algae. *Journal of Molecular Evolution*, 48(2):236–244.

Ducklow, H. W., Fraser, W. R., Meredith, M. P., Stammerjohn, S. E., Doney, S. C., Martinson, D. G., Sailley, S. F., Schofield, O. M., Steinberg, D. K., Venables, H. J., and Amsler, C. D. (2013). West Antarctic peninsula: An ice-dependent coastal marine ecosystem in transition. *Oceanography*, 26(3):190–203.

Eppley, R. W. (1972). Temperature and phytoplankton growth in the sea. *Fishery Bulletin*, 70(4):1063–1085.

Epstein, S. S. and Shiaris, M. P. (1992). Size-selective grazing of coastal bacterioplankton by natural assemblages of pigmented flagellates, colorless flagellates, and ciliates. *Microbial Ecology*, 23(3):211–225.

Falkowski, P. G. and Raven, J. A. T. A. T. T. (2013). Aquatic Photosynthesis (Second Edition).

Feng, Y., Hare, C. E., Rose, J. M., Handy, S. M., DiTullio, G. R., Lee, P. A., Smith, W. O., Peloquin, J., Tozzi, S., Sun, J., Zhang, Y., Dunbar, R. B., Long, M. C., Sohst, B., Lohan, M., and Hutchins, D. A. (2010). Interactive effects of iron, irradiance and CO_2 on Ross Sea phytoplankton. *Deep-Sea Research Part I: Oceanographic Research Papers*, 57(3):368–383.

Ferreira, F. and Straus, N. A. (1994). Iron deprivation in cyanobacteria. *Journal of Applied Phycology*, 6(2):199–210.

Field, C. B., Behrenfeld, M. J., Randerson, J. T., and Falkowski, P. (1998). Primary production of the biosphere: Integrating terrestrial and oceanic components. *Science (New York, N.Y.)*, 281(5374):237–240.

Fischer, W. W., Hemp, J., and Johnson, J. E. (2016). Evolution of oxygenic photosynthesis. *Annual Review of Earth and Planetary Sciences*, 44:647–683.

Frölicher, T. L., Sarmiento, J. L., Paynter, D. J., Dunne, J. P., Krasting, J. P., and Winton, M. (2015). Dominance of the Southern Ocean in anthropogenic carbon and heat uptake in CMIP5 models. *Journal of Climate*, 28(2):862–886.

Funk, C., Alami, M., Tibiletti, T., and Green, B. R. (2011). High light stress and the one-helix LHC-like proteins of the cryptophyte *Guillardia theta*. *Biochimica et Biophysica Acta - Bioenergetics*, 1807(7):841–846.

Gaillard, S., Charrier, A., Malo, F., Carpentier, L., Bougaran, G., Hégaret, H., Réveillon, D., Hess, P., and Séchet, V. (2020). Combined effects of temperature, irradiance, and pH on *Teleaulax amphioxeia* (Cryptophyceae) physiology and feeding ratio for its predator *Mesodinium rubrum* (Ciliophora). *Journal of Phycology*, 56(3):775–783.

Gao, K., Xu, J., Gao, G., Li, Y., Hutchins, D. A., Huang, B., Wang, L., Zheng, Y., Jin, P., Cai, X., Häder, D. P., Li, W., Xu, K., Liu, N., and Riebesell, U. (2012). Rising CO_2 and increased light exposure synergistically reduce marine primary productivity. *Nature Climate Change*, 2:519–523.

Garibotti, I. A., Vernet, M., and Ferrario, M. E. (2005). Annually recurrent phytoplanktonic assemblages during summer in the seasonal ice zone west of the Antarctic Peninsula (Southern Ocean). *Deep-Sea Research Part I: Oceanographic Research Papers*, 52(10):1823–1841.

Garibotti, I. A., Vernet, M., Ferrario, M. E., Smith, R. C., Ross, R. M., and Quetin, L. B. (2003). Phytoplankton spatial distribution patterns along the Western Antarctic Peninsula (Southern Ocean). *Marine Ecology Progress Series*, 261:21–39.

Gast, R. J., McKie-Krisberg, Z. M., Fay, S. A., Rose, J. M., and Sanders, R. W. (2014). Antarctic mixotrophic protist abundances by microscopy and molecular methods. *FEMS Microbiology Ecology*, 89(2):388–401.

Giordano, M., Beardall, J., and Raven, J. A. (2005). CO_2 concentrating mechanisms in algae: Mechanisms, environmental modulation, and evolution. *Annual Review of Plant Biology*, 56:99–131.

Glazer, A. N. and Wedemayer, G. J. (1995). Cryptomonad biliproteins — an evolutionary perspective. *Photosynthesis Research*, 46(1):93–105.

Gledhill, M., Achterberg, E. P., Li, K., Mohamed, K. N., and Rijkenberg, M. J. (2015). Influence of ocean acidification on the complexation of iron and copper by organic ligands in estuarine waters. *Marine Chemistry*, 177:421–433.

Gould, S. B., Waller, R. F., and McFadden, G. I. (2008). Plastid evolution. *Annual review of plant biology*, 59:491–517.

Grossman, A. R., Schaefer, M. R., Chiang, G. G., and Collier, J. L. (1993). The phycobilisome, a light-harvesting complex responsive to environmental conditions. *Microbiological reviews*, 57(3):725–749.

Häder, D.-P., Rhiel, E., and Wehrmeyer, W. (1987). Phototaxis in the marine flagellate *Cryptomonas maculata*. *Journal of Photochemistry and Photobiology B: Biology*, 1(1):115–122.

Hamm, C., Simson, D. A., Merkel, R., and Smetacek, V. (1999). Colonies of *Phaeocystis globosa* are protected by a thin but tough skin. *Marine Ecology Progress Series 187:*, pages 101–111.

Hammer, A., Rhena, S., and Hedrink, S. (2002). Light and temperature acclimation of *Rhodomonas salina* (Cryptophyceae): Photosynthetic performance. *Aquatic Microbial Ecology*, 29:287–2965.

Hancock, A. M., King, C. K., Stark, J. S., McMinn, A., and Davidson, A. T. (2020). Effects of ocean acidification on Antarctic marine organisms: A meta-analysis. *Ecology and Evolution*, 10(10):4495–4514.

Hassler, C. S., Legiret, F.-E., and Butler, E. C. (2013). Measurement of iron chemical speciation in seawater at 4 °C: The use of competitive ligand exchange–adsorptive cathodic stripping voltammetry. *Marine Chemistry*, 149:63–73.

Hassler, C. S., Schoemann, V., Boye, M., Tagliabue, A., Rozmarynowycz, M., and Mckay, R. M. (2012). Iron bioavailability in the Southern Ocean. *Oceanography and Marine Biology: An Annual Review*, 50:1–64.

Heiden, J. P., Bischof, K., and Trimborn, S. (2016). Light intensity modulates the response of two Antarctic diatom species to ocean acidification. *Frontiers in Marine Science*, 3.

Heiden, J. P., Völkner, C., Jones, E. M., van de Poll, W. H., Buma, A. G. J., Meredith, M. P., de Baar, H. J. W., Bischof, K., Wolf-Gladrow, D., and Trimborn, S. (2019). Impact of ocean acidification and high solar radiation on productivity and species composition of a late summer phytoplankton community of the coastal Western Antarctic Peninsula. *Limnology and Oceanography*, 64(4):1716–1736.

Henley, S. F., Cavan, E. L., Fawcett, S. E., Kerr, R., Monteiro, T., Sherrell, R. M., Bowie, A. R., Boyd, P. W., Barnes, D. K., Schloss, I. R., Marshall, T., Flynn, R., and Smith, S. (2020). Changing biogeochemistry of the Southern Ocean and its ecosystem implications. *Frontiers in Marine Science*, 7:1–31.

Hill, D. R. A. (1991). A revised circumscription of *Cryptomonas* (Cryptophyceae) based on examination of Australian strains. *Phycologia*, 30(2):170–188.

Hill, D. R. A. and Rowan, K. S. (1989). The biliproteins of the Cryptophyceae. *Phycologia*, 28(4):455–463.

Hirooka, S., Hirose, Y., Kanesaki, Y., Higuchi, S., Fujiwara, T., Onuma, R., Era, A., Ohbayashi, R., Uzuka, A., Nozaki, H., Yoshikawa, H., and ya Miyagishima, S. (2017). Acidophilic green algal genome provides insights into adaptation to an acidic environment. *Proceedings of the National Academy of Sciences*, 114(39):E8304–E8313.

Hoef-Emden, K. (2007). Revision of the genus *Cryptomonas* (Cryptophyceae) II: Incongruences between the classical morphospecies concept and molecular phylogeny in smaller pyrenoid-less cells. *Phycologia*, 46(4):402–428.

Hoef-Emden, K. (2008). Molecular phylogeny of phycocyanin-containing cryptophyte evolution of biliproteins and geographical distribution. *Journal of Phycology*, 44(4):985–993.

Hoef-Emden, K. (2014). Osmotolerance in the Cryptophyceae: Jacks-of-all-trades in the *Chroomonas* Clade. *Protist*, 165(2):123–143.

Hoef-Emden, K. and Archibald, J. M. (2017). *Cryptophyta (Cryptomonads): In: Archibald, J., Simpson, A., Slamovits, C. (eds) Handbook of the Protists*, pages 851–891. Springer International Publishing, Cham.

Holt, N. E., Fleming, G. R., and Niyogi, K. K. (2004). Toward an understanding of the mechanism of Nonphotochemical Quenching in green plants. *Biochemistry*, 43(26):8281–8289.

Hoogstraten, A., Timmermans, K. R., and de Baar, H. J. W. (2012). Morphological and physiological effects in *Proboscia alata* (Bacillariophyceae) grown under different light and CO_2 conditions of the modern Southern Ocean. *Journal of Phycology*, 48(3):559–568.

Hopkinson, B. M., Dupont, C. L., Allen, A. E., and Morela, F. M. (2011). Efficiency of the CO_2-concentrating mechanism of diatoms. *Proceedings of the National Academy of Sciences of the United States of America*, 108(10):3830–3837.

Hoppe, C. J., Holtz, L. M., Trimborn, S., and Rost, B. (2015). Ocean acidification decreases the light-use efficiency in an Antarctic diatom under dynamic but not constant light. *New Phytologist*, 207(1):159–171.

Hoppe, C. J. M., Hassler, C. S., Payne, C. D., Tortell, P. D., Rost, B., and Trimborn, S. (2013). Iron limitation modulates ocean acidification effects on Southern Ocean phytoplankton communities. *PLOS ONE*, 8(11):e79890.

Izaguirre, I., Sinistro, R., Schiaffino, M. R., Sánchez, M. L., Unrein, F., and Massana, R. (2012). Grazing rates of protists in wetlands under contrasting light conditions due to floating plants. *Aquatic Microbial Ecology*, 65(3):221–232.

Kaňa, R., Kotabová, E., Šedivá, B., and Kuthanová Trsková, E. (2019). Photoprotective strategies in the motile cryptophyte alga *Rhodomonas salina* —role of non-photochemical quenching, ions, photoinhibition, and cell motility. *Folia Microbiologica*, 64(5):691–703.

Kaňa, R., Kotabová, E., Sobotka, R., and Prášil, O. (2012). Non-photochemical quenching in cryptophyte alga *Rhodomonas salina* is located in chlorophyll *a*/*c* antennae. *PLoS ONE*, 7(1).

Kerr, R., Mata, M. M., Mendes, C. R. B., and Secchi, E. R. (2018). Northern Antarctic Peninsula: A marine climate hotspot of rapid changes on ecosystems and ocean dynamics. *Deep-Sea Research Part II: Topical Studies in Oceanography*, 149:4–9.

Kim, H., Ducklow, H. W., Abele, D., Ruiz Barlett, E. M., Buma, A. G. J., Meredith, M. P., Rozema, P. D., Schofield, O. M., Venables, H. J., and Schloss, I. R. (2018). Inter-decadal

variability of phytoplankton biomass along the coastal West Antarctic Peninsula. *Philosophical Transactions of the Royal Society A: Mathematical, Physical and Engineering Sciences*, 376(2122):20170174.

Klaveness, D. (1988). Ecology of the Cryptomonadida: A first review. in C. D. Sandgren (ed.), Growth and reproductive strategies of freshwater phytoplankton. *Cambridge: Cambridge University Press.*, pages 105–133.

Koch, F., Beszteri, S., Harms, L., and Trimborn, S. (2019). The impacts of iron limitation and ocean acidification on the cellular stoichiometry, photophysiology, and transcriptome of *Phaeocystis antarctica*. *Limnology and Oceanography*, 64(1):357–375.

Koch, F. and Trimborn, S. (2019). Limitation by Fe, Zn, Co, and B_{12} results in similar physiological responses in two Antarctic phytoplankton species. 6:514.

Kranz, S. A., Young, J. N., Hopkinson, B. M., Goldman, J. A. L., Tortell, P. D., and Morel, F. M. M. (2015). Low temperature reduces the energetic requirement for the CO_2 concentrating mechanism in diatoms. *New Phytologist*, 205(1):192–201.

Kropuenske, L. R., Mills, M. M., Van Dijken, G. L., Alderkamp, A. C., Mine Berg, G., Robinson, D. H., Welschmeyer, N. A., and Arrigo, K. R. (2010). Strategies and rates of photoacclimation in two major Southern Ocean phytoplankton taxa: *Phaeocystis antarctica* (haptophyta) and *Fragilariopsis cylindrus* (Bacillariophyceae). *Journal of Phycology*, 46(6):1138–1151.

La Roche, J., Geider, R. J., Graziano, L. M., Murray, H., and Lewis, K. (1993). Induction of specific proteins in eukaryotic algae grown under iron-, phosphorus-, or nitrogen-deficient conditions. *Journal of Phycology*, 29(6):767–777.

La Roche, J., Murray, H., Orellana, M., and Newton, J. (1995). Flavodoxin expression as an indicator of iron limitation in marine diatoms. *Journal of Phycology*, 31(4):520–530.

La Roche, J. L., Boyd, P. W., McKay, R. M. L., and Geider, R. J. (1996). Flavodoxin as an in situ marker for iron stress in phytoplankton. *Nature*, 382(6594):802–805.

Lavaud, J., Strzepek, R. F., and Kroth, P. G. (2007). Photoprotection capacity differs among diatoms: Possible consequences on the spatial distribution of diatoms related to fluctuations in the underwater light climate. *Limnology and Oceanography*, 52(3):1188–1194.

Laybourn-Parry, J., Marshall, W. A., and Marchant, H. J. (2005). Flagellate nutritional versatility as a key to survival in two contrasting Antarctic saline lakes. *Freshwater Biology*, 50(5):830–838.

Lichtlé, C. (1979). Effects of nitrogen deficiency and light of high intensity on *Cryptomonas rufescens* (Cryptophyceae). *Protoplasma*, 101(4):283–299.

Lichtlé, C. (1980). Effects of nitrogen deficiency and light of high intensity on Cryptomonas rufescens (Cryptophyceae). *Protoplasma*, 102:11–19.

Liu, X. and Millero, F. J. (1999). The solubility of iron hydroxide in sodium chloride solutions. *Geochimica et Cosmochimica Acta*, 63(19):3487–3497.

MacColl, R. (1998). Cyanobacterial phycobilisomes. *Journal of structural biology*, 124(2-3):311–334.

Maldonado, M. T., Boyd, P. W., Harrison, P. J., and Price, N. M. (1999). Co-limitation of phytoplankton growth by light and Fe during winter in the NE subarctic Pacific Ocean. *Deep-Sea Research Part II: Topical Studies in Oceanography*, 46(11-12):2475–2485.

Maldonado, M. T. and Price, N. M. (1996). Influence of N substrate on Fe requirements of marine centric diatoms. *Marine Ecology Progress Series*, 141(1-3):161–172.

Maldonado, M. T. and Price, N. M. (2001). Reduction and transport of organically bound iron by *Thalassiosira oceanica* (Bacillariophyceae). *Journal of Phycology*, 37(2):298–310.

Marchetti, A., Parker, M. S., Moccia, L. P., Lin, E. O., Arrieta, A. L., Ribalet, F., Murphy, M. E. P., Maldonado, M. T., and Armbrust, E. V. (2009). Ferritin is used for iron storage in bloom-forming marine pennate diatoms. *Nature*, 457(7228):467–470.

Marinov, I., Doney, S. C., and Lima, I. D. (2010). Response of ocean phytoplankton community structure to climate change over the 21st century: Partitioning the effects of nutrients, temperature and light. *Biogeosciences*, 7(12):3941–3959.

Martin, J. H. (1990). Glacial-interglacial CO_2 change: The Iron Hypothesis. *Paleoceanography*, 5(1):1–13.

Martin, J. H., Fitzwater, S. E., and Gordon, R. M. (1990a). Iron deficiency limits phytoplankton growth in Antarctic waters. *Global Biogeochemical Cycles*, 4(1):5–12.

Martin, J. H., Gordon, R. M., and Fitzwater, S. E. (1990b). Iron in Antarctic waters. *Nature*, 345(6271):156–158.

McKie-Krisberg, Z. M., Gast, R. J., and Sanders, R. W. (2015). Physiological responses of three species of Antarctic mixotrophic phytoflagellates to changes in light and dissolved nutrients. *Microbial Ecology*, 70(1):21–29.

Mendes, C. R. B., Costa, R. R., Ferreira, A., Jesus, B., Tavano, V. M., Dotto, T. S., Leal, M. C., Kerr, R., Islabão, C. A., Franco, A. d. O. d. R., Mata, M. M., Garcia, C. A. E., and Secchi, E. R. (2023). Cryptophytes: an emerging algal group in the rapidly changing Antarctic Peninsula marine environments. *Global Change Biology*, (January):1–18.

Mendes, C. R. B., Tavano, V. M., Dotto, T. S., Kerr, R., de Souza, M. S., Garcia, C. A. E., and Secchi, E. R. (2018). New insights on the dominance of cryptophytes in Antarctic coastal waters: A case study in Gerlache Strait. *Deep-Sea Research Part II: Topical Studies in Oceanography*, 149:161–170.

Mendes, C. R. B., Tavano, V. M., Leal, M. C., de Souza, M. S., Brotas, V., and Garcia, C. A. E. (2013). Shifts in the dominance between diatoms and cryptophytes during three late summers in the Bransfield Strait (Antarctic Peninsula). *Polar Biology*, 36(4):537–547.

Meredith, M., Sommerkorn, M., Cassota, S., Derksen, C., Ekaykin, A., Hollowed, A., Kofinas, G., Mackintosh, A., Melbourne-Thomas, J., Muelbert, M. M. C., Ottersen, G., Pritchard, H., Schuur, E. A. G., Boyd, P., Hobbs, W., and Hodgson-Johnston, I. (2019). Polar Regions.

Meredith, M. P. and King, J. C. (2005). Rapid climate change in the ocean west of the Antarctic Peninsula during the second half of the 20th century. *Geophysical Research Letters*, 32(19):1–5.

Messerli, M. A., Amaral-Zettler, L. A., Zettler, E., Jung, S. K., Smith, P. J., and Sogin, M. L. (2005). Life at acidic pH imposes an increased energetic cost for a eukaryotic acidophile. *Journal of Experimental Biology*, 208:569–2579.

Meyer, S. R. and Pienaar, R. N. (1984). Mitosis and cytokinesis in *Chroomonas africana* Meyer and Pienaar (Cryptophyceae). *South African Journal of Botany*, 3(5):320–330.

Millero, F. J., Woosley, R., Ditrolio, B., and Waters, J. (2009). Effect of ocean acidification on the speciation of metals in seawater. *Oceanography*, 22:72–85.

Milligan, A. J., Aparicio, U. A., and Behrenfeld, M. J. (2012). Fluorescence and nonphotochemical quenching responses to simulated vertical mixing in the marine diatom *Thalassiosira weissflogii*. *Marine Ecology Progress Series*, 448:67–78.

Moffat, C. and Meredith, M. (2018). Shelf-ocean exchange and hydrography west of the Antarctic Peninsula: A review.

Moline, M. A., Claustre, H., Frazer, T. K., Schofield, O., and Vernet, M. (2004). Alteration of the food web along the Antarctic Peninsula in response to a regional warming trend. *Global Change Biology*, 10(12):1973–1980.

Moline, M. A. and Prézelin, B. B. (1996). Long-term monitoring and analyses of physical factors regulating variability in coastal Antarctic phytoplankton biomass, in situ productivity and taxonomic composition over subseasonal, seasonal and interannual time scales. *Marine Ecology Progress Series*, 145(1-3):143–160.

Montes-Hugo, M., Doney, S. C., Ducklow, H. W., Fraser, W., Martinson, D., Stammerjohn, S. E., and Schofield, O. (2009). Recent changes in phytoplankton communities associated with rapid regional climate change along the Western Antarctic Peninsula. *Science*, 323(5920):1470 LP – 1473.

Morrissey, J., Sutak, R., Paz-Yepes, J., Tanaka, A., Moustafa, A., Veluchamy, A., Thomas, Y., Botebol, H., Bouget, F. Y., McQuaid, J. B., Tirichine, L., Allen, A. E., Lesuisse, E., and Bowler, C. (2015). A novel protein, ubiquitous in marine phytoplankton, concentrates iron at the cell surface and facilitates uptake. *Current Biology*, 25(3):364–371.

Pausch, F., Koch, F., Hassler, C., Bracher, A., Bischof, K., and Trimborn, S. (2022). Responses of a natural phytoplankton community from the Drake Passage to two predicted climate change scenarios. *Frontiers in Marine Science*, 9(February):1–18.

Peers, G. and Price, N. M. (2006). Copper-containing plastocyanin used for electron transport by an oceanic diatom. *Nature*, 441(7091):341–344.

Petrou, K., Trimborn, S., Rost, B., Ralph, P. J., and Hassler, C. S. (2014). The impact of iron limitation on the physiology of the Antarctic diatom *Chaetoceros simplex*. *Marine Biology*, 161(4):925–937.

Raven, J. A., Evans, M. C., and Korb, R. E. (1999). The role of trace metals in photosynthetic electron transport in O_2-evolving organisms. *Photosynthesis Research*, 60(2-3):111–149.

Reinfelder, J. R. (2011). Carbon concentrating mechanisms in eukaryotic marine phytoplankton. pages 291–317.

Rose, J. M., Feng, Y., Ditullio, G. R., Dunbar, R. B., Hare, C. E., Lee, P. A., Lohan, M., Long, M., Smith, W. O., Sohst, B., Tozzi, S., Zhang, Y., and Hutchins, D. A. (2009). Synergistic effects of iron and temperature on Antarctic phytoplankton and microzooplankton assemblages. *Biogeosciences*, 6(12):3131–3147.

Saba, G. K., Fraser, W. R., Saba, V. S., Iannuzzi, R. A., Coleman, K. E., Doney, S. C., Ducklow, H. W., Martinson, D. G., Miles, T. N., Patterson-Fraser, D. L., Stammerjohn, S. E., Steinberg, D. K., and Schofield, O. M. (2014). Winter and spring controls on the summer food web of the coastal West Antarctic Peninsula. *Nature Communications*, 5.

Schmidt, L. E. and Hansen, P. J. (2001). Allelopathy in the prymnesiophyte *Chrysochromulina polylepis*: Effect of cell concentration, growth phase and pH. *Marine Ecology Progress Series*, 216:67–81.

Schofield, O., Saba, G., Coleman, K., Carvalho, F., Couto, N., Ducklow, H., Finkel, Z., Irwin, A., Kahl, A., Miles, T., Montes-Hugo, M., Stammerjohn, S., and Waite, N. (2017). Decadal variability in coastal phytoplankton community composition in a changing West Antarctic Peninsula. *Deep-Sea Research Part I: Oceanographic Research Papers*, 124:42–54.

Schulz, K. G., Bach, L. T., Bellerby, R. G. J., Bermúdez, R., Büdenbender, J., Boxhammer, T., Czerny, J., Engel, A., Ludwig, A., Meyerhöfer, M., Larsen, A., Paul, A. J., Sswat, M., and Riebesell, U. (2017). Phytoplankton blooms at increasing levels of atmospheric carbon dioxide: Experimental evidence for negative effects on prymnesiophytes and positive on small picoeukaryotes. *Frontiers in Marine Science*, 4.

Shaked, Y., Kustka, A. B., and Morel, F. M. (2005). A general kinetic model for iron acquisition by eukaryotic phytoplankton. *Limnology and Oceanography*, 50(3):872–882.

Shi, D., Xu, Y., Hopkinson, B. M., and Morel, F. M. M. (2010). Effect of ocean acidification on iron availability to marine phytoplankton. *Science*, 327(5966):676–679.

Sinistro, R., Izaguirre, I., and Asikian, V. (2006). Experimental study on the microbial plankton community in a South American wetland (Lower Paraná River Basin) and the effect of the light deficiency due to the floating macrophytes. *Journal of Plankton Research*, 28(8):753–768.

Smetacek, V., Klaas, C., Strass, V. H., Assmy, P., Montresor, M., Cisewski, B., Savoye, N., Webb, A., D'Ovidio, F., Arrieta, J. M., Bathmann, U., Bellerby, R., Berg, G. M., Croot, P., Gonzalez, S., Henjes, J., Herndl, G. J., Hoffmann, L. J., Leach, H., Losch, M., Mills, M. M., Neill, C., Peeken, I., Röttgers, R., Sachs, O., Sauter, E., Schmidt, M. M., Schwarz, J., Terbrüggen, A., and Wolf-Gladrow, D. (2012). Deep carbon export from a Southern Ocean iron-fertilized diatom bloom. *Nature*, 487(7407):313–319.

Smith, M. and Hansen, P. J. (2007). Interaction between *Mesodinium rubrum* and its prey: Importance of prey concentration, irradiance and pH. *Marine Ecology Progress Series*, 338:61–70.

Smith, W. O. and Lancelot, C. (2004). Bottom-up versus top-down control in phytoplankton of the Southern Ocean. *Antarctic Science*, 16(4):531–539.

Smith, W. O. and Trimborn, S. (2024). *Phaeocystis*: A Global Enigma. *Annual Review ofMarine Science*, pages 417–441.

Sommer, U., Paul, C., and Moustaka-Gouni, M. (2015). Warming and ocean acidification effects on phytoplankton - From species shifts to size shifts within species in a mesocosm experiment. *PLoS ONE*, 10(5):1–17.

Spackeen, J. L., Sipler, R. E., Bertrand, E. M., Xu, K., McQuaid, J. B., Walworth, N. G., Hutchins, D. A., Allen, A. E., and Bronk, D. A. (2018). Impact of temperature, CO_2, and iron on nutrient uptake by a late-season microbial community from the Ross Sea, Antarctica. *Aquatic Microbial Ecology*, 82(2):145–159.

Stammerjohn, S., Massom, R., Rind, D., and Martinson, D. (2012). Regions of rapid sea ice change: An inter-hemispheric seasonal comparison. *Geophysical Research Letters*, 39(6):1–8.

Stammerjohn, S. E., Martinson, D. G., Smith, R. C., and Iannuzzi, R. A. (2008). Sea ice in the Western Antarctic Peninsula region: Spatio-temporal variability from ecological and climate change perspectives. *Deep Sea Research Part II: Topical Studies in Oceanography*, 55(18):2041–2058.

Strzepek, R. F., Boyd, P. W., and Sunda, W. G. (2019). Photosynthetic adaptation to low iron, light, and temperature in Southern Ocean phytoplankton. *Proceedings of the National Academy of Sciences of the United States of America*, 116(10):4388–4393.

Strzepek, R. F. and Harrison, P. J. (2004). Photosynthetic architecture differs in coastal and oceanic diatoms. *Nature*, 431(7009):689–692.

Strzepek, R. F., Hunter, K. A., Frew, R. D., Harrison, P. J., and Boyd, P. W. (2012). Iron-light interactions differ in Southern Ocean phytoplankton. *Limnology and Oceanography*, 57(4):1182–1200.

Sunda, W. and Huntsman, S. (2003). Effect of pH, light, and temperature on Fe–EDTA chelation and Fe hydrolysis in seawater. *Marine Chemistry*, 84(1):35–47.

Sunda, W. G. and Huntsman, S. A. (1995). Iron uptake and growth limitation in oceanic and coastal phytoplankton. *Marine Chemistry*, 50(1-4):189–206.

Sunda, W. G. and Huntsman, S. A. (1997). Interrelated influence of iron, light and cell size on marine phytoplankton growth. *Nature*, 390(6658):389–392.

Sunda, W. G. and Huntsman, S. A. (2011). Interactive effects of light and temperature on iron limitation in a marine diatom: Implications for marine productivity and carbon cycling. *Limnology and Oceanography*, 56(4):1475–1488.

Taylor, D. L. and Lee, C. C. (1971). A new cryptomonad from Antarctica: *Cryptomonas cryophila* sp. nov. *Archiv für Mikrobiologie*, 75(4):269–280.

Thomas, M. K., Kremer, C. T., Klausmeier, C. A., and Litchman, E. (2012). A global pattern of thermal adaptation in marine phytoplankton. *Science*, 338(6110):1085–1088.

Tortell, P. D., Payne, C. D., Li, Y., Trimborn, S., Smith, W. O., Riesselman, C., Dunbar, R. B., Sedwick, P., and Ditullio, G. R. (2008). CO_2 sensitivity of Southern Ocean phytoplankton. 35:1–5.

Trimborn, S., Brenneis, T., Hoppe, C. J., Laglera, L. M., Norman, L., Santos-Echeandía, J., Völkner, C., Wolf-Gladrow, D., and Hassler, C. S. (2017a). Iron sources alter the response of Southern Ocean phytoplankton to ocean acidification. *Marine Ecology Progress Series*, 578:35–50.

Trimborn, S., Brenneis, T., Sweet, E., and Rost, B. (2013). Sensitivity of Antarctic phytoplankton species to ocean acidification: Growth, carbon acquisition, and species interaction. *Limnology and Oceanography*, 58(3):997–1007.

Trimborn, S., Thoms, S., Brenneis, T., Heiden, J. P., Beszteri, S., and Bischof, K. (2017b). Two Southern Ocean diatoms are more sensitive to ocean acidification and changes in irradiance than the prymnesiophyte *Phaeocystis antarctica*. *Physiologia Plantarum*, 160(2):155–170.

Trimborn, S., Thoms, S., Karitter, P., and Bischof, K. (2019). Ocean acidification and high irradiance stimulate the photo-physiological fitness, growth and carbon production of the Antarctic cryptophyte *Geminigera cryophila*. *Biogeosciences*, 16(15):2997–3008.

Twining, B. S. and Baines, S. B. (2013). The trace metal composition of marine phytoplankton. *Annual Review of Marine Science*, 5:191–215.

van de Poll, W. and Nassif, A. (2023). The interacting effect of prolonged darkness and temperature on photophysiological characteristics of three antarctic phytoplankton species. *Journal of Phycology*, 59(5):1053–1063.

Van De Poll, W. H., Lagunas, M., De Vries, T., Visser, R. J., and Buma, A. G. (2011). Non-photochemical quenching of chlorophyll fluorescence and xanthophyll cycle responses after excess PAR and UVR in *Chaetoceros brevis*,*Phaeocystis antarctica* and coastal Antarctic phytoplankton. *Marine Ecology Progress Series*, 426:119–131.

Van de Waal, D. B., Brandenburg, K. M., Keuskamp, J., Trimborn, S., Rokitta, S., Kranz, S. A., and Rost, B. (2019). Highest plasticity of carbon-concentrating mechanisms in earliest evolved phytoplankton. *Limnology and Oceanography Letters*.

van Leeuwe, M. A., Webb, A. L., Venables, H. J., Visser, R. J., Meredith, M. P., Elzenga, J. T. M., and Stefels, J. (2020). Annual patterns in phytoplankton phenology in Antarctic coastal waters explained by environmental drivers. *Limnology and Oceanography*, 65(7):1651–1668.

Vernet, M., Martinson, D., Iannuzzi, R., Stammerjohn, S., Kozlowski, W., Sines, K., Smith, R., and Garibotti, I. (2008). Primary production within the sea-ice zone west of the Antarctic Peninsula: I—sea ice, summer mixed layer, and irradiance. *Deep Sea Research Part II: Topical Studies in Oceanography*, 55(18):2068–2085. Palmer, Antarctica Long Term Ecological Research.

Wang, X. and Smith, W. O. (2021). Phytoplankton growth at low temperatures: results from low temperature incubations. *Journal of Plankton Research*, 43(5):633–641.

Weisse, T. and Stadler, P. (2006). Effect of pH on growth, cell volume, and production of freshwater ciliates, and implications for their distribution. *Limnology and Oceanography*, 51(4):1708–1715.

Yano, D. and Suzuki, T. (2022). Phosphagen kinases from five groups of eukaryotic protists (Choanomonada, Alveolate, Stramenopiles, Haptophyta, and Cryptophyta): Diverse enzyme activities and phylogenetic relationship with metazoan enzymes. *Comparative Biochemistry and Physiology Part B: Biochemistry and Molecular Biology*, 257:110663.

Yoo, Y. D., Seong, K. A., Jeong, H. J., Yih, W., Rho, J. R., Nam, S. W., and Kim, H. S. (2017). Mixotrophy in the marine red-tide cryptophyte *Teleaulax amphioxeia* and ingestion and grazing impact of cryptophytes on natural populations of bacteria in Korean coastal waters. *Harmful Algae*, 68(May 2005):105–117.

Young, J. N., Goldman, J. A., Kranz, S. A., Tortell, P. D., and Morel, F. M. (2015). Slow carboxylation of Rubisco constrains the rate of carbon fixation during Antarctic phytoplankton blooms. *New Phytologist*, 205(1):172–181.

Zeebe, R. E. and Wolf-Gladrow, D. (2001). CO_2 in seawater: Equilibrium, Kinetics, Isotopes. *Elsevier Science*.

Zhu, Z., Qu, P., Gale, J., Fu, F., and Hutchins, D. A. (2017). Individual and interactive effects of warming and CO_2 on *Pseudo-nitzschia subcurvata* and *Phaeocystis antarctica*, two dominant phytoplankton from the Ross Sea, Antarctica. *Biogeosciences*, 14(23):5281–5295.

Chapter 2

In contrast to diatoms, cryptophytes are susceptible to iron limitation, but not to ocean acidification

Marianne Camoying[1*], Silke Thoms[1], Jana Geuer[1], Boris Koch[1,2], Kai Bischof[3], Scarlett Trimborn[1,3]

[1]Ecological Chemistry, Alfred Wegener Institute, Helmholtz Centre for Polar and Marine Research, Bremerhaven, Germany
[2]Department of Technology, University of Applied Sciences Bremerhaven, Bremerhaven, Germany
[3]Marine Botany and MARUM, University of Bremen, Bremen, Germany

Published in Physiologia Plantarum

Received: 12 October 2021 | Revised: 9 December 2021 | Accepted: 17 December 2021

DOI: 10.1111/ppl.13614

ECOPHYSIOLOGY, STRESS AND ADAPTATION

Physiologia Plantarum

In contrast to diatoms, cryptophytes are susceptible to iron limitation, but not to ocean acidification

Marianne G. Camoying[1] | Silke Thoms[1] | Jana K. Geuer[1] | Boris P. Koch[1,2] | Kai Bischof[3] | Scarlett Trimborn[1,3]

[1]Ecological Chemistry, Alfred Wegener Institute, Helmholtz Centre for Polar and Marine Research, Bremerhaven, Germany

[2]Department of Technology, University of Applied Sciences Bremerhaven, Bremerhaven, Germany

[3]Marine Botany & MARUM, University of Bremen, Bremen, Germany

Correspondence
Marianne G. Camoying, Ecological Chemistry, Alfred Wegener Institute, Helmholtz Centre for Polar and Marine Research, Bremerhaven, Germany.
Email: marianne.camoying@awi.de

Funding information
Alfred Wegener Institute Helmholtz Centre for Polar and Marine Research, AWI Strategy Fund (J. Geuer); Katholischer Akademischer Ausländer-Dienst (KAAD), Phd Fellowship (M. Camoying).

Edited by W.S.(F.). Chow

Abstract

Previous field studies in the Southern Ocean (SO) indicated an increased occurrence and dominance of cryptophytes over diatoms due to climate change. To gain a better mechanistic understanding of how the two ecologically important SO phytoplankton groups cope with ocean acidification (OA) and iron (Fe) availability, we chose two common representatives of Antarctic waters, the cryptophyte *Geminigera cryophila* and the diatom *Pseudo-nitzschia subcurvata*. Both species were grown at 2°C under different pCO_2 (400 vs. 900 µatm) and Fe (0.6 vs. 1.2 nM) conditions. For *P. subcurvata*, an additional high pCO_2 level was applied (1400 µatm). At ambient pCO_2 under low Fe supply, growth of *G. cryophila* almost stopped while it remained unaffected in *P. subcurvata*. Under high Fe conditions, OA was not beneficial for *P. subcurvata*, but stimulated growth and carbon production of *G. cryophila*. Under low Fe supply, *P. subcurvata* coped much better with OA than the cryptophyte, but invested more energy into photoacclimation. Our study reveals that Fe limitation was detrimental for the growth of *G. cryophila* and suppressed the positive OA effect. The diatom was efficient in coping with low Fe, but was stressed by OA while both factors together strongly impacted its growth. The distinct physiological response of both species to OA and Fe limitation explains their occurrence in the field. Based on our results, Fe availability is an important modulator of OA effects on SO phytoplankton, with different implications on the occurrence of cryptophytes and diatoms in the future.

1 | INTRODUCTION

The Southern Ocean (SO) is considered as a High-Nutrient, Low-Chlorophyll (HNLC) region, wherein primary productivity is mainly influenced by the availability of the trace metal iron (Fe; Martin et al., 1990; De Baar et al., 1995; Smetacek et al., 2012). Fe plays a major role in various cellular processes such as photosynthesis, respiration, and carbon and nitrogen fixation. Fe-limited phytoplankton cells normally exhibit lowered photochemical quantum efficiency (Greene et al., 1991, 1992; Marchetti et al., 2006, 2017) and reduced cellular pigment concentrations (van Leeuwe et al., 2014), leading to less-efficient electron transport (Greene et al., 1991). Fe limitation also results in reduced growth and particulate organic carbon (POC) production (Alderkamp et al., 2012; Koch et al., 2018; Petrou et al., 2014; Trimborn et al., 2019a). To deal with low Fe availability, SO phytoplankton were also found to lower their Fe requirement by replacing the Fe-rich electron transporter cytochrome c6 with the Cu-containing plastocyanin (Peers & Price, 2006).

Due to ongoing CO_2 emissions into the atmosphere, SO phytoplankton will be affected by ocean acidification (OA), which is the decrease in ocean pH due to the oceanic absorption of atmospheric CO_2. Hence, the current partial pressure of CO_2 (pCO_2) in seawater of ca. 410 μatm is projected to double by the end of this century (IPCC, 2014). In response to OA, changes in community structure and/or productivity of SO natural phytoplankton assemblages were found (Davidson et al., 2016; Donahue et al., 2019; Feng et al., 2010; Hancock et al., 2018; Heiden et al., 2019; Hoppe et al., 2013; Thomson et al., 2016; Tortell et al., 2008; Trimborn et al., 2017a). Only a few studies (Coad et al., 2016; McMinn et al., 2014; Young et al., 2015) have reported no OA effect on SO phytoplankton. At present, studies looking at the combined effects of OA and Fe availability on the ecophysiology of SO phytoplankton are limited (Hoppe et al., 2013; Koch et al., 2018), which could be attributed to the difficulty in conducting experiments under trace metal clean conditions. In combination with Fe limitation, OA was shown to promote species shifts and/or hamper primary production of natural SO phytoplankton assemblages (Feng et al., 2010; Hoppe et al., 2013; Tortell et al., 2008; Trimborn et al., 2017b). It was observed that growth of the diatoms *Chaetoceros* (Feng et al., 2010; Hoppe et al., 2013; Tortell et al., 2008) and *Fragilariopsis* (Davidson et al., 2016; Heiden et al., 2019) or of the prymnesiophyte *Phaeocystis antarctica* (Trimborn et al., 2017b) was promoted by OA. The tolerance of the genus *Phaeocystis* to OA in combination with different environmental factors such as light and Fe was previously reported (Feng et al., 2010; Hancock et al., 2018; Heiden et al., 2019; Hoogstraten et al., 2012; Koch et al., 2018; Thoisen et al., 2015; Tortell et al., 2008; Trimborn et al., 2017b; Trimborn et al., 2019a; Young et al., 2015; Zhu et al., 2017). While a specific strain of the diatom *Pseudo-nitzschia subcurvata* showed no susceptibility to OA (even up to 1730 ppm pCO_2; Zhu et al., 2017), other studies reported an OA-dependent decline in the growth of several *Pseudo-nitzschia* species (another *P. subcurvata* strain, *Pseudo-nitzschia turgiduloides*, *Pseudo-nitzschia turgiduloides prolongatoides*) regardless of Fe availability (Hancock et al., 2018; Hoppe et al., 2013; Trimborn et al., 2017b). It is evident from these observations that different taxa have specific CO_2-tolerance levels. However, a mechanistic understanding of these responses is still lacking, specifically for the genus *Pseudo-nitzschia*, which contributes significantly to the total diatom blooms in the SO (Almandoz et al., 2008; Garibotti et al., 2003).

The effects of climate change in different regions of the SO are now becoming more evident. The Western Antarctic Peninsula (WAP), for example, has been experiencing rapid warming over the past decades (Henley et al., 2019; Kerr et al., 2018; Moffat & Meredith, 2018), which has led to changes in the observed occurrence and distribution of various phytoplankton groups of this region (Garibotti & Ferrario, 2005; Montes-Hugo et al., 2009). It is now widely recognized that next to diatoms, cryptophytes also significantly contribute to phytoplankton biomass in the coastal regions of the WAP (Moline & Prézelin, 1996; Moline et al., 2004; Mendes et al., 2013, 2017; Schofield et al., 2017; Brown et al., 2021). Previous studies have shown that diatoms and cryptophytes have distinct ecological niches and typically do not co-occur spatially and temporally (Garibotti et al., 2003; Schofield et al., 2017). Since the dominance of cryptophytes in the field are associated with lower temperature and salinity brought by the increase in sea ice retreat and glacial melting (Moline et al., 2004; Mendes et al., 2013; Schofield et al., 2017), cryptophytes may thus appear to be the winners of the ongoing climatic changes in the SO. However, studies looking at the effects of different environmental factors (OA, Fe, light) on the ecophysiology of this group are still limited. To date, only two studies are available on Antarctic cryptophytes, which show that OA and high light promoted growth and POC production of *Geminigera cryophila* (Trimborn et al., 2019b) while Fe limitation, on the other hand, strongly impacted its growth and photophysiology (Koch et al., 2018). Our study aims to gain a better understanding of the ecophysiology of two key Antarctic phytoplankton species, the cryptophyte *G. cryophila* and the diatom *Pseudo-nitzschia subcurvata*, in response to OA and Fe limitation.

2 | MATERIALS AND METHODS

2.1 | Culture conditions

Prior to the initiation of the experiment, the Antarctic diatom *Pseudo-nitzschia subcurvata* (isolated by P. Assmy, Polarstern expedition ANT-XXI/4) and the Southern Ocean cryptophyte *G. cryophila* (CCMP 2564), were kept for more than a year in stock cultures with Fe-deplete and -replete natural Antarctic seawater medium. Before the start of the main experiment, both species were pre-acclimated for at least 2 weeks under the target experimental conditions (CO_2 and Fe), which will be described below. The sterile-filtered (0.2 μm), Fe-poor (0.12 nmol L^{-1}) Antarctic seawater collected during the Antarctic Circumpolar Expedition (59°S) was enriched with macronutrients (100 μmol L^{-1} Si, 100 μmol L^{-1} NO_3^-, and 6.25 μmol L^{-1} PO_4^{3-}) and vitamins (30 nmol L^{-1} B_1, 23 nmol L^{-1} B_7, and 0.228 nmol L^{-1} B_{12}), which were chelated (Chelex® 100, Sigma Aldrich, Merck) to remove any trace metals present. Nitrate and phosphate were added following the Redfield N:P ratio of 16:1 (Redfield, 1958). For the pre-acclimation phase and the main experiment, dilute batch cultures of both species were grown in this seawater, to which either a trace metal (TM) mix containing no Fe (i.e. Control treatment) or 0.5 nmol L^{-1} Fe ($FeCl_3$, ICP-MS standard, TraceCERT, Fluka; i.e. +Fe treatment) was added. The TM mixture contained zinc (0.16 nmol L^{-1}), copper (0.08 nmol L^{-1}), cobalt (0.09 nmol L^{-1}), molybdenum (0.05 nmol L^{-1}), and manganese (1.9 nmol L^{-1}). These TM additions were adjusted to maintain the ratio of the original F/2 recipe and represent trace metal concentrations typical for SO waters. The total dissolved Fe concentration [dFe] of our Control treatments represents the [dFe] values measured in the upper surface mixed layer of SO waters (0.1–0.3 nM Fe, Klunder et al., 2011). On the other hand, +Fe treatments mimic [dFe] values representative for coastal regions of the SO or during natural Fe supply events (e.g. vertical mixing, upwelling) (1–2 nM Fe, Klunder et al., 2014). As suggested by Gerringa et al. (2000), in an effort to minimize the alteration of the natural seawater trace metal chemistry and ligands, no ethylenediaminetetraacetic acid (EDTA) was added. Due to the presence of natural ligands, it is expected that the added Fe was buffered rather than bound in complexed inorganic colloids. TM clean techniques were employed throughout the whole experiment. 4 L polycarbonate (PC) incubation bottles, tubings, and all

other equipment were TM cleaned according to the Geotraces cookbook (Cutter et al., 2017), as previously described in Koch et al. (2018). All sampling and handling of the incubation bottles were conducted under the laminar flow hood (US class 100, Opta). Both species were also grown under the target pCO_2 levels of 400 and 900 μatm (i.e. 400 and 900 treatment, respectively). Only *P. subcurvata* was additionally grown at 1400 μatm pCO_2 (i.e. 1400 treatment). The three different pCO_2 levels were attained by gentle bubbling of the culture bottles with humidified CO_2 air. A mixture of CO_2-free air (<1 ppmv CO_2; Dominic Hunter) and pure CO_2 (Air Liquide Deutschland Ltd.) was used and controlled through a gas flow controller (CGM 2000, MCZ Umwelttechnik) to generate the three target pCO_2 treatments. Triplicates of each experimental treatment were grown at 2°C and exposed to 100 μmol photons m^{-2} s^{-1} under a light/dark cycle of 16/8 h using light-emitting diodes (LED) lamps (SolarStinger LED SunStrip Daylight, Econlux).

2.1.1 | Carbonate chemistry determination

To ensure that there would be no pH drift (≤ 0.06 pH units) in cultures, the pH (NBS) was measured regularly in all incubation and culture medium bottles throughout the whole experiment. The pH was measured using a pH meter (826 pH mobile, Metrohm), calibrated (3-point calibration) prior to usage. The pH of all treatments was stable (Table 1). At the end of the experiment, samples for total alkalinity (TA) analysis were collected from all incubations and culture medium bottles by filtering a sample through a glass fiber filter (GF/F, Whatman) and placing the filtrate into 200-ml borosilicate flasks. TA samples were measured by potentiometric titrations via a TW alpha plus (SI Analytics). Systematic errors were corrected with a certified reference material (from A. Dickson; batch no. 161). TA, pH, silicate, phosphate, temperature, and salinity measurements were used to determine the seawater carbonate chemistry using the CO2Sys program (Pierrot et al., 2006), wherein the equilibrium constant of Mehrbach et al. (1973) refitted by Dickson and Millero (1987) was used.

2.1.2 | Concentrations of total dissolved Fe in seawater, domoic acid, and cellular trace metal quotas

To determine the concentration of total Fe dissolved [dFe] in seawater, all culture medium and incubation bottles were sampled at the end of the experiments. To this end, 100 ml of each sample was filtered (HCl-cleaned 0.2 μm PC filters, 47 mm, Nuclepore, Whatman, GE Healthcare) under a laminar flow hood and stored in TM cleaned PE bottles. Total dissolved Fe (dFe) concentrations of all seawater samples and process blanks were determined as previously described in Koch and Trimborn (2019). Results of the analysis were validated by analyzing a NASS-7 (National Research Council of Canada) reference standard in a 1:10 dilution, which was done at the beginning and end of each batch run. Measured dFe values (361 ± 16 ng L^{-1}, $n = 12$) did not vary from the certified reference (351 ± 26 ng L^{-1}).

Intracellular TM (Fe, Zn, Mn, Zn, and Co) quotas were determined by collecting phytoplankton cells onto 0.2 μm acid-cleaned PC filters (EMD Millipore). To remove the trace metals attached to the cell surface, the filters were rinsed (15 min) with 0.1 M oxalic acid wash (Hassler & Schoemann, 2009), followed by a filtered seawater rinse before finally storing them into TM-cleaned 30-ml polytetrafluoroethylene vials. Intracellular TM contents were analyzed via ICP-MS (Attom, Nu Instruments) following digestion with HNO_3 and HF, as previously described in Koch and Trimborn (2019). To ensure low background TM values and good digestion quality, acid (5 ml of subboiled HNO_3, 0.5 ml HF) and two filter blanks, as well as the BCR-414 (Plankton reference material, Sigma Aldrich) samples, were also processed and analyzed via ICP-MS (Table S1).

We also examined whether our *P. subcurvata* strain can produce domoic acid (DA) since it has been reported that under low Fe supply, many temperate *Pseudo-nitzschia* species produce DA, which can act as an Fe-binding ligand (Maldonado et al., 2002; Rue & Bruland, 2001). Moreover, it has also been shown that DA production in *Pseudo-nitzschia multiseries* can be influenced by pH (Lundholm et al., 2004; Trimborn et al., 2008). Hence, we collected samples for DA (dissolved and particulate forms) measurements as described in Geuer et al. (2020). In contrast to the study by Olesen et al. (2021), which reported the presence of DA in several *P. subcurvata* strains, no DA was extracted from the cells and the culture medium of all our treatments, indicating that our *P. subcurvata* strain was unable to produce DA (data not shown).

2.1.3 | Cell density and volume

During the pre-acclimation period, as well as during the main experiments, we regularly monitored the cell density of both species to ensure that exponential growth was reached and maintained for all treatments. To avoid any changes in carbonate chemistry, we diluted our culture bottles before cell densities reached ca. 15,000 cells/ml for *G. cryophila* and

TABLE 1 The CO2Sys program (Pierrot et al., 2006) was used to calculate the dissolved inorganic carbon (DIC) concentrations and partial pressure of CO_2 (pCO_2) from the measured total alkalinity (TA), pH, silicate, phosphate, salinity, and temperature. For all parameters, values are given for all culture bottles of each pCO_2 treatment at the end of the experiment, representing the means and SD ($n = 6$). Significant differences between treatments (post hoc tests) are indicated by varying lower case letters in superscript ($P < 0.05$)

Target pCO_2 (μatm)	Calculated pCO_2 (μatm)	Calculated DIC (μmol kg^{-1})	Measured pH (NBS)	Measured TA (μmol kg^{-1})
400	405 ± 56^a	2342 ± 35^a	8.14 ± 0.06^a	2492 ± 41^a
900	868 ± 33^b	2426 ± 17^b	7.82 ± 0.02^b	2467 ± 22^a
1400	1387 ± 64^c	2507 ± 18^c	7.65 ± 0.02^c	2488 ± 13^a

150,000 cells ml^{-1} for *P. subcurvata*. The main experiments were started only when the cultures maintained exponential growth. The initial cell density of the main experiment was ca. 500 cells ml^{-1} for *G. cryophila* and 5,000 cells ml^{-1} for *P. subcurvata*. The main experiment lasted between 5 and 7 days for *P. subcurvata* and between 10 and 15 days for *G. cryophila*, depending on the treatment. The final cell density of the main experiment was ca. 3000–9000 cells ml^{-1} for *G. cryophila* and 100,000–140,000 cells ml^{-1} for *P. subcurvata*. Samples for cell density and size determination were collected at the same time of the day at the start, during, and at the end of the main experiment. For *P. subcurvata*, samples were fixed with 10% acidic Lugol's solution and stored in the dark at 2°C. Utermöhl chambers (Hydrobios) were prepared and allowed to settle for 24 h before counting at least 400 cells under an inverted microscope (Axio Observer D1; Zeiss). For *G. cryophila*, a Beckman Multisizer™ 3 Coulter Counter® was used to determine cell density immediately after sampling. For both species, growth rates (d^{-1}), denoted by the growth rate coefficient (μ), were calculated using the formula:

$$\mu = \ln(N_t : N_0)/t$$

where N_t refers to the cell density during the final harvest and N_0 to the one at the start of the experiment. The duration between both sampling points is represented by t. According to Hillebrand et al. (1999), cell volume was estimated for each species.

2.1.4 | Elemental carbon and nitrogen composition

Samples for POC and nitrogen (PON) were collected by gently filtering (<20 mm Hg) cultures onto precombusted glass fiber filters (15 h, 200°C, GF/F, ~0.6 μm, 25 mm, Whatman). Filters were acidified with 200 μl of 0.2 M HCl and oven-dried (> 12 h, 60°C) before analyzing them on an automated carbon nitrogen elemental analyzer (EURO EA-CN Elemental Analyzer, HEKAtech GmbH). The blank-corrected quotas were normalized with the filtered volume and cell volume. To calculate daily production rates, cellular quotas were multiplied by the corresponding growth rate of the respective treatment.

2.1.5 | Pigments

Pigment samples were collected by filtering the cultures onto GF/F filters (~0.6 μm, 25 mm, Whatman) and directly frozen in liquid nitrogen. As previously described in Trimborn et al. (2019b), the concentrations of chlorophyll *a* (Chl *a*) and c_2 (Chl c_2), fucoxanthin (Fuco), diatoxanthin (Dt), diadinoxanthin (Dd), and alloxanthin (Allo) were measured on a reversed phase high-performance liquid chromatography on a LaChromEliteR system equipped with a chilled autosampler L-2200 and a DAD detector L-2450 (VWR-Hitachi International GmbH). Peak detection, identification, and quantification were made with pigment standards (DHI Lab Products) using the EZChrom Elite software version 3.1.3. (Agilent Technologies).

2.1.6 | Photophysiological parameters

A Fast Repetition Rate fluorometer (FastOcean PTX) coupled with a FastAct Laboratory system (both from Chelsea Technologies Group Ltd.) was used to assess the photophysiological response of *P. subcurvata* and *G. cryophila* under all pCO_2-Fe treatments at the end of the experiment. After dark-adaption for 10 min at 2°C, the minimum Chl *a* fluorescence (F_0) was recorded. To gradually saturate photosystems II (PSII), a single turnover flashlet of 1.2×10^{22} photons m^{-2} s^{-1} and a wavelength of 450 nm was applied, consisting of 100 flashlets on a 2 μs pitch. Subsequently, a relaxation phase of 40 flashlets on a 50 μs pitch was applied. This combination of saturation-relaxation phases was reiterated six times for every acquisition. To determine the maximum (F_m) Chl *a* fluorescence, the saturation phase of the single turnover was fitted according to Kolber et al. (1998). The dark-adapted maximum quantum yield of photosynthesis of PSII (F_v/F_m) was then calculated using the equation:

$$F_v/F_m = (F_m - F_0)/F_m$$

Fluorescence light curves (FLC) were also recorded, exposing cells to increasing light intensities for 5 min. After each light intensity, six Chl *a* fluorescence measurements were carried out. The light–adapted minimum (F') and maximum (F_m') Chl *a* fluorescence of the single turnover acquisition was estimated from these measurements. The effective PSII quantum yield under ambient light (F_q'/F_m') was calculated according to the equation ((F_m' – F')/F_m') (Genty et al., 1989). The electron transport rates (ETR) were calculated following Suggett et al. (2004, 2009):

$$\mathrm{ETR} = \sigma_{\mathrm{PSII}} \times \left[(F_q'/F_m')/(F_v/F_m)\right] \times \mathrm{E}$$

where E is the instantaneous irradiance (photons m^{-2} s^{-1}). Irradiance-dependent ETRs were curve-fitted according to Ralph and Gademann (2005) to determine maximum ETR (ETR_{max}), minimum saturating irradiance (I_k) and maximum light utilization efficiency (α). Non-photochemical quenching (NPQ) was calculated using the Stern–Volmer equation:

$$\mathrm{NPQ} = F_m/F_m' - 1.$$

2.1.7 | Statistical analysis

A two-way analysis of variance (ANOVA) (SigmaPlot 12.3, SysStat Software Inc.) was used to evaluate the combined effects of pCO_2 and Fe availability on each physiological parameter. Standard *t*-tests were performed to determine direct effects between two specific treatments. Test for normality (Shapiro–Wilk) and post hoc tests (Holm–Sidak method) were also conducted ($\alpha = 0.05$), and in cases wherein datasets were not normally distributed, Mann–Whitney rank sum test was used.

2.2 | Results

2.2.1 | Seawater chemistry

At the end of the experiment, TA remained the same, while DIC increased and pH decreased with increasing pCO_2 ($P = 0.002$, Table 1). In the +Fe culture medium bottles (without cells), [dFe] of the 400 was higher compared to the 900 ($P = 0.001$) and 1400 ($P < 0.001$) treatments, with the latter two pCO_2 treatments exhibiting no difference in dFe values (Figure 1A). The concentrations of dFe in the Control culture medium bottles were not affected by increasing pCO_2. For all pCO_2 levels, the Control culture medium bottles had significantly lower dFe concentration than the Fe-enriched treatments ($P < 0.001$). For all incubation bottles of both species, increasing pCO_2 had no effect on dFe concentrations (Figure 1B,C). In *P. subcurvata*, significantly higher dFe values were seen in the +Fe compared to the Control treatments under all pCO_2 levels ($P < 0.001$). For *G. cryophila*, no differences in dFe concentrations were observed between the Control and +Fe at 400, while at 900 the +Fe had 81% higher dFe than the Control ($P = 0.02$).

2.2.2 | Photosynthetic yield

For *P. subcurvata* (Figure 2A), the increase in pCO_2 did not influence F_v/F_m of +Fe cells, whereas, in the Control, F_v/F_m remained unaltered

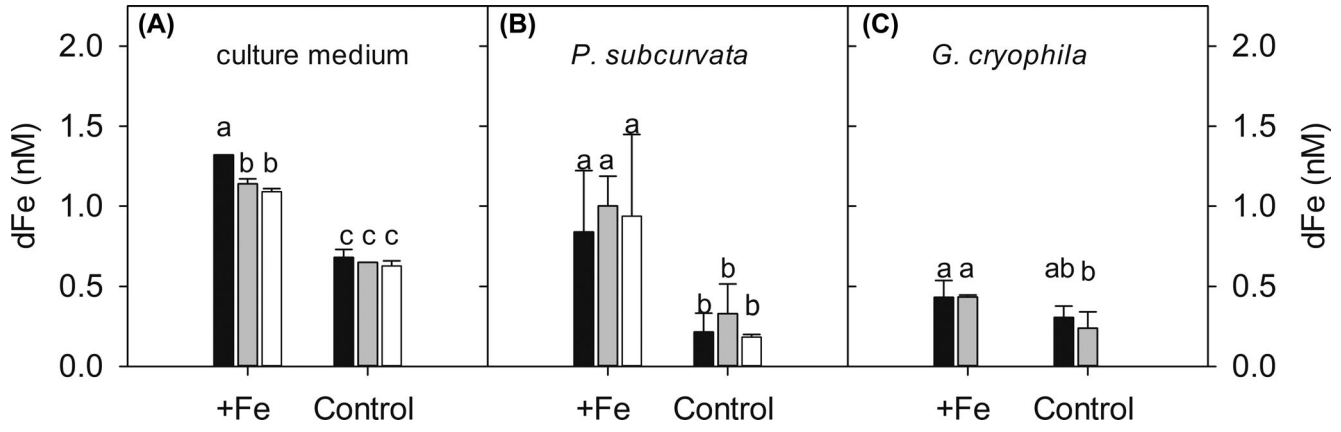

FIGURE 1 Total dissolved Fe (dFe) concentrations of the culture media (A) of the different pCO_2 treatments (400, 900, and 1400) without (Control) and with Fe enrichment (+Fe). Concentrations of dFe were also determined in all incubation bottles of *Pseudo-nitzschia subcurvata* (B) and *Geminigera cryophila* (C) at the end of the experiment. Both cultures were grown under Fe-deplete (Control) and Fe-enriched (+Fe) conditions in combination with 400 (black) or 900 µatm (gray) pCO_2. An additional pCO_2 treatment of 1400 µatm (white) was grown for *P. subcurvata*. Values represent the mean and SD (culture medium, $n = 2$; incubation bottles, $n = 3$). Significant differences between treatments are indicated by varying lower case letters (post hoc tests, $P < 0.05$)

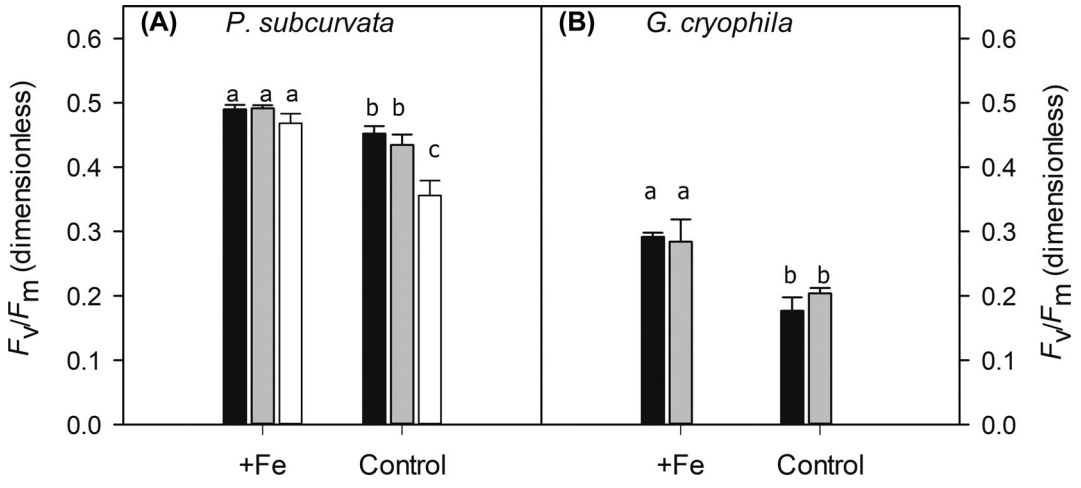

FIGURE 2 The dark-adapted maximum photosystem II quantum yield F_v/F_m for *Pseudo-nitzschia subcurvata* (A) and *Geminigera cryophila* (B) grown under Fe-deplete (Control) and Fe-enriched (+Fe) conditions at different pCO_2 levels: 400 µatm (black), 900 µatm (gray) and 1400 µatm (white, for *P. subcurvata* only). Values represent the mean and SD ($n = 3$). Significant differences between treatments are indicated by varying lower case letters (post hoc tests, $P < 0.05$)

between 400 and 900, but was significantly reduced by 21% toward 1400 ($P < 0.001$). Lower [dFe] strongly decreased the F_v/F_m for all pCO_2 levels in the diatom (400: $P = 0.01$; 900: $P < 0.001$; 1400: $P < 0.001$). For the diatom, there was a significant interactive effect of CO_2 and Fe on F_v/F_m, with the lowest value encountered in the 1400-Control treatment ($P = 0.003$). For *G. cryophila* (Figure 2B),

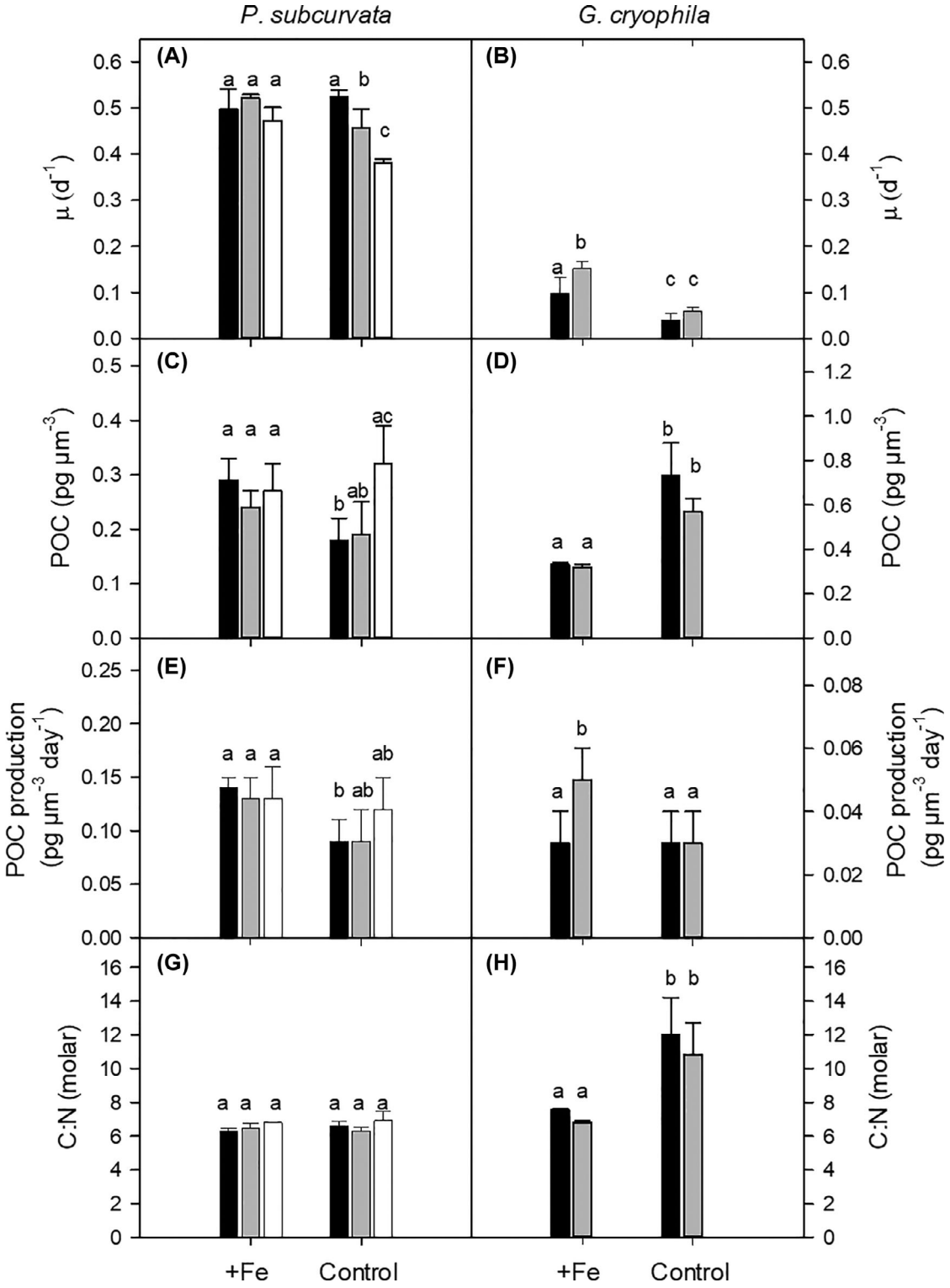

FIGURE 3 Growth rates (A, B), cellular particulate organic carbon (POC) quota normalized to cell volume (C, D), POC production rate normalized to cell volume (E, F) and molar carbon:nitrogen (C:N) ratios (G, H) of *Pseudo-nitzschia subcurvata* (A, C, E, and G) and *Geminigera cryophila* (B, D, F, and H) grown under Fe-deplete (Control) and Fe-enriched (+Fe) conditions at different pCO_2 levels: 400 (black), 900 (grey) and 1400 μatm (white, for *P. subcurvata* only). Values represent the mean and SD ($n = 3$). Significant differences between treatments are indicated by varying lower case letters (post hoc tests, $P < 0.05$)

increasing pCO_2 had no effect on the F_v/F_m for both Fe treatments. A negative Fe-effect was, however, observed for the cryptophyte, wherein F_v/F_m of Control cells was significantly lowered by 40% and 28% in the 400 ($P < 0.001$) and 900 ($P = 0.003$) treatment, respectively.

2.2.3 | Growth and elemental composition

For the +Fe treatments of *P. subcurvata*, no CO_2-effect was observed (Figure 3A), whereas increasing pCO_2 significantly decreased the

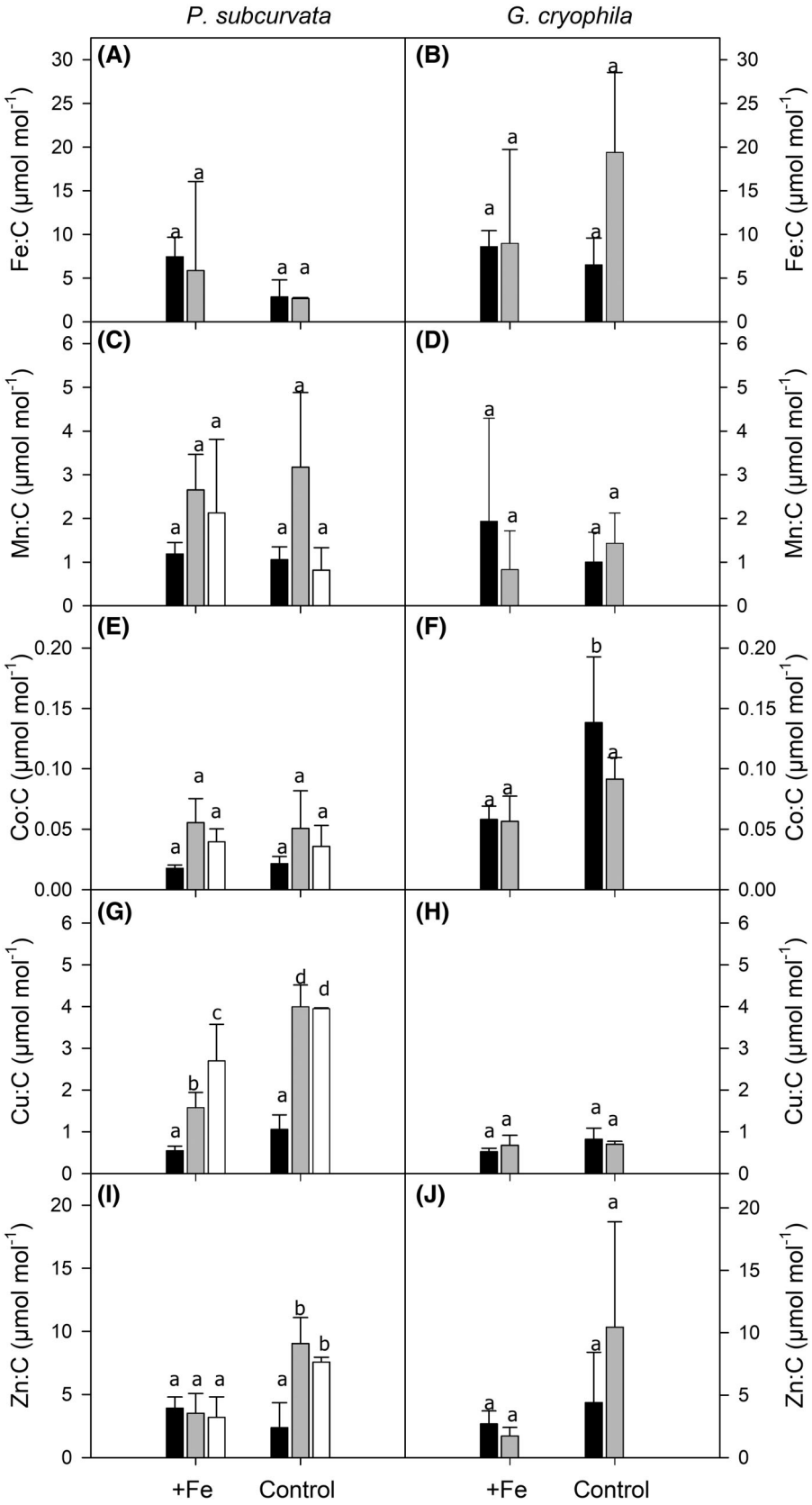

FIGURE 4 Molar trace metal to carbon (TM:C) ratios of *Pseudo-nitzschia subcurvata* (A, C, E, G, and I) and *Geminigera cryophila* (B, D, F, H, and J) grown under Fe-deplete (Control) and Fe-enriched (+Fe) conditions at different pCO_2 levels: 400 (black) and 900 (grey). No Fe quota was measured for the 1400 µatm pCO_2 treatment of *P. subcurvata*. Values represent the mean and SD ($n = 3$). Significant differences between treatments are indicated by varying lower case letters (post hoc tests, $P < 0.05$)

growth rates of the Control cells ($P < 0.001$). Lower [dFe] decreased the growth of *P. subcurvata* by 13% ($P = 0.02$) and 19% ($P = 0.002$) at 900 and 1400, respectively, but not at 400. Hence, there was a significant interactive effect of CO_2 and Fe on the growth rate of *P. subcurvata* ($P = 0.01$). For *G. cryophila* (Figure 3B), both significant OA and Fe effects were observed, while the interaction between both factors had no effect on growth. Increasing pCO_2 significantly promoted higher growth rates in the +Fe (54%, $P = 0.012$) but had no

TABLE 2 Cellular quotas (normalized to cell volume) of chlorophyll a (Chl *a*), chlorophyll c_2 (Chl c_2), fucoxanthin (Fuco), diadinoxanthin (Dd) and alloxanthin (Allo) were measured for *Pseudo-nitzschia subcurvata* and *Geminigera cryophila* grown at 400 and 900 µatm pCO_2 in combination with Fe-deplete (Control) or Fe-enriched (+Fe) conditions. An additional pCO_2 treatment of 1400 µatm was grown for *P. subcurvata*. Significant differences between treatments (post hoc tests) are indicated by varying lower case letters in superscript ($P < 0.05$). Values represent the mean and SD ($n = 3$)

Species	Fe	pCO_2	Chl *a* (fg µm^{-3})	Chl c_2 (fg µm^{-3})	Fuco (fg µm^{-3})	Dd (fg µm^{-3})	Allo (fg µm^{-3})
P. subcurvata	+ Fe	400	4.6 ± 0.7^{a}	0.4 ± 0.1^{a}	2.3 ± 0.3^{a}	0.7 ± 0.1^{a}	
P. subcurvata	+ Fe	900	3.1 ± 0.5^{b}	0.3 ± 0.0^{a}	1.6 ± 0.3^{b}	0.4 ± 0.0^{b}	
P. subcurvata	+ Fe	1400	3.2 ± 0.7^{b}	0.3 ± 0.1^{a}	1.8 ± 0.4^{ab}	0.4 ± 0.1^{b}	
P. subcurvata	Control	400	2.7 ± 0.5^{b}	0.3 ± 0.0^{a}	1.5 ± 0.3^{b}	0.3 ± 0.1^{b}	
P. subcurvata	Control	900	2.6 ± 0.2^{b}	0.2 ± 0.0^{a}	1.4 ± 0.0^{b}	0.3 ± 0.1^{b}	
P. subcurvata	Control	1400	3.2 ± 0.3^{b}	0.3 ± 0.1^{a}	1.8 ± 0.2^{b}	0.5 ± 0.1^{b}	
G. cryophila	+ Fe	400	2.3 ± 0.2^{a}	0.4 ± 0.0^{a}			1.3 ± 0.1^{a}
G. cryophila	+ Fe	900	2.4 ± 0.2^{a}	0.3 ± 0.1^{a}			1.3 ± 0.1^{a}
G. cryophila	Control	400	1.5 ± 0.0^{b}	0.2 ± 0.0^{b}			1.0 ± 0.0^{b}
G. cryophila	Control	900	1.9 ± 0.1^{c}	0.3 ± 0.0^{ab}			1.2 ± 0.0^{c}

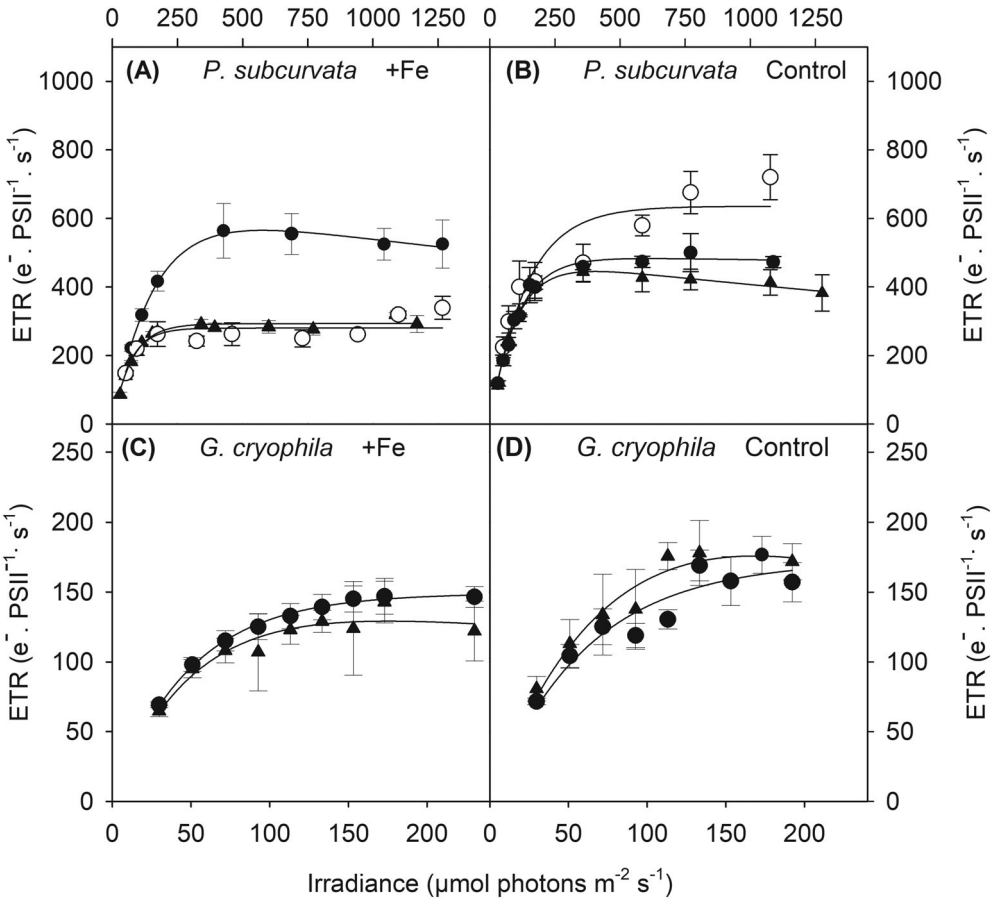

FIGURE 5 Absolute electron transport rates (ETR) were measured in response to increasing irradiance in *Pseudo-nitzschia subcurvata* (A, B) and *Geminigera cryophila* (C, D) grown under Fe-deplete (Control) and Fe-enriched (+Fe) conditions at different pCO_2 levels: 400 µatm (filled circle), 900 µatm (filled triangle) and 1400 µatm (open circle, for *P. subcurvata* only). ETR values show the mean and SD ($n = 3$)

effect in the Control. Lower [dFe] strongly decreased the growth of *G. cryophila* in both pCO_2 treatments ($P < 0.01$).

POC quotas of *P. subcurvata* cells in the +Fe were not affected by OA (Figure 3C). In the Control, POC was similar between 400 and 900, but was enhanced toward 1400. Lower [dFe] decreased the POC quota of *P. subcurvata* by 40% at 400 ($P = 0.015$), while no Fe-effect was observed at 900 and 1400. For *G. cryophila*, no CO_2 effect was evident in both +Fe and Control treatments (Figure 3D). Lower [dFe], however, resulted in a significant increase of the POC quotas by 120% and 75% in the 400 ($P < 0.001$) and 900 treatments ($P = 0.001$), respectively.

In all treatments of the diatom (Figure 3E), no CO_2 effect on POC production rates was observed. Lower [dFe] significantly decreased the POC production rates of *P. subcurva*ta by 36% in the 400 treatment ($P = 0.018$) while it had no effect on the other two pCO_2 treatments. In *G. cryophila* (Figure 3F), increasing pCO_2 enhanced the POC production of +Fe cells by 53% ($P = 0.023$), but remained constant in Control cells. With lower [dFe], POC production remained unchanged in the 400 treatment but was decreased by 32% in the 900 treatment ($P = 0.033$).

Compared to *P. subcurvata*, higher C:N ratios were generally determined for *G. cryophila* (Figure 3G, H). Neither CO_2 nor Fe affected C:N ratios of *P. subcurvata*. For *G. cryophila*, increasing pCO_2 did not change the C:N ratio in any Fe treatments, while lower [dFe] resulted in a significant increase in the C:N ratios of the cryptophyte in both pCO_2 treatments ($P = 0.01$).

2.2.4 | Trace metal quotas

Neither OA nor Fe had an effect on the Fe:C, Mn:C, and Co:C ratios of *P. subcurvata* (Figure 4). However, with increasing pCO_2, there was a significant enhancement in the Cu:C ratio of the diatom in both Fe treatments. With lower [dFe], Cu:C ratios increased at 900 ($P < 0.001$) and 1400 ($P = 0.015$), while no change at 400. Zn:C ratios of *P. subcurvata* in the +Fe were not affected by OA, but it was significantly increased in the Control cells between 400 and 900 ($P = 0.003$), but not toward 1400. With lower [dFe], Zn:C ratios of the diatom increased by 150% and 138% at 900 ($P = 0.004$) and 1400 ($P = 0.019$), respectively. In *G. cryophila*, TM:C ratios were more variable than that of the diatom, thus differences between treatments were not significant and difficult to interpret. It was only for the Co:C ratio at 400 pCO_2 that we observed a significant increase in response to lower [dFe] ($P = 0.013$).

2.2.5 | Pigment quotas

In *P. subcurvata*, except for Chl c_2, all pigment quotas of the +Fe cells were decreased from 400 to 900, but with no further change toward 1400 (Table 2). In general, no OA effect was found for the Control. The lowered Fe concentration significantly reduced quotas of Chl *a* (41%: $P = 0.001$), Fuco (35%: $P = 0.005$), and Dd (52%: $P > 0.001$) when grown at 400 while no Fe-effect was found at 900 and 1400. For *G. cryophila*, with increasing pCO_2, concentrations of Chl *a* ($P = 0.016$) and Allo ($P = 0.007$) were significantly enhanced, but only in the Control (Table 2). In general, lower [dFe] decreased the pigment concentrations of the cryptophyte at 400 and 900, except for the Chl c_2 quota of cells grown at 900.

2.2.6 | Photophysiological characteristics

The two species showed distinct FLC in response to the different CO_2–Fe treatments (Figure 5). For *P. subcurvata*, a significant interactive effect between CO_2 and Fe on ETR_{max} was found ($P < 0.001$). In the +Fe treatment, ETR_{max} decreased between 400 and 900 ($P = 0.01$), but remained unchanged toward 1400 (Table 3). For the Control, a significant CO_2-dependent increase in ETR_{max} was only observed between 900 and 1400 ($P = 0.006$). Lower [dFe] did not alter the ETR_{max} of *P. subcurvata* cells grown at 400, whereas a strong increase was seen at 900 ($P = 0.003$) and 1400 ($P < 0.001$). In

TABLE 3 Maximum electron transport rates (ETR_{max}), minimum saturating irradiance (I_k), and maximum light utilization efficiency (α) were determined for *Pseudo-nitzschia subcurvata* and *Geminigera cryophila*. Both species were grown under Fe-deplete (Control) and Fe-enriched (+Fe) conditions in combination with 400 and 900 µatm pCO_2. An additional pCO_2 treatment of 1400 µatm was grown for *P. subcurvata*. Values represent the mean and SD ($n = 3$). Significant differences between treatments (post hoc tests) are indicated by varying lower case letters in superscript ($P < 0.05$)

Species	Fe	pCO_2	ETR_{max} ($e^- PSII^{-1} s^{-1}$)	I_k (µmol photons $m^{-2} s^{-1}$)	α (rel. unit)
P. subcurvata	+ Fe	400	565 ± 68^a	140 ± 15^a	4.1 ± 0.2^a
P. subcurvata	+ Fe	900	293 ± 6^b	73 ± 5^b	4.0 ± 0.2^a
P. subcurvata	+ Fe	1400	275 ± 18^b	59 ± 7^b	4.7 ± 0.9^a
P. subcurvata	Control	400	519 ± 63^a	114 ± 9^c	4.6 ± 0.2^a
P. subcurvata	Control	900	445 ± 33^a	90 ± 2^b	4.9 ± 0.4^a
P. subcurvata	Control	1400	673 ± 74^c	142 ± 24^d	5.0 ± 1.4^a
G. cryophila	+ Fe	400	147 ± 8^a	49 ± 2^a	3.0 ± 0.1^a
G. cryophila	+ Fe	900	137 ± 8^a	46 ± 7^a	3.0 ± 0.4^a
G. cryophila	Control	400	170 ± 18^{ab}	62 ± 5^b	2.8 ± 0.2^a
G. cryophila	Control	900	175 ± 18^b	54 ± 4^{ab}	3.3 ± 0.6^a

G. cryophila, increasing pCO_2 had no effect on ETR_{max} in both Fe treatments. Lower [dFe], however, led to a 28% increase in ETR_{max}, but only when grown at 900 ($P = 0.009$). Similar to ETR_{max}, I_k in *P. subcurvata* was strongly influenced by the different CO_2–Fe treatments (Table 3). In the +Fe, I_k was highest in the 400 treatment, while no significant difference in I_k was observed between 900 and 1400. In the Control, there was a decrease of I_k (21%) from 400 to 900 ($P = 0.04$), while from 900 to 1400, a 58% increase was observed ($P < 0.001$). In *P. subcurvata*, lower [dFe] caused a minor decrease in I_k at 400 ($P = 0.028$), had no effect at 900 and enhanced I_k at 1400 ($P < 0.001$). For the cryptophyte, no CO_2-dependent effects on I_k were observed. In response to lower [dFe], I_k increased by 27% at 400 ($P = 0.012$) while there was no change at 900. For both species, α was neither altered by CO_2 nor by Fe availability (Table 3).

During the FLC, both species exhibited higher NPQ values with increasing irradiance in all treatments (Figure 6). For the +Fe treatment of *P. subcurvata*, no CO_2-dependent differences were seen in NPQ. In the Control, a CO_2-effect was observed wherein at irradiances >1000 μmol photons m^{-2} s^{-1}, lowest and highest NPQ values were encountered in the 400 and 1400 treatments, respectively. Again, at irradiances >1000 μmol photons m^{-2} s^{-1}, lower [dFe] resulted in an increase in NPQ but only for the 1400 treatment of the diatom. In the case of *G. cryophila*, neither a CO_2 nor Fe effect on NPQ was observed.

3 | DISCUSSION

3.1 | Compared to the diatom, growth of the cryptophyte was drastically impacted by low Fe supply at ambient pCO_2

The Control treatments of both species displayed common photophysiological characteristics of Fe-stressed cells (Alderkamp et al., 2012; Koch et al., 2018; Strzepek et al., 2011, 2012; Trimborn et al., 2019a) such as reduced F_v/F_m values (Figure 2A, B) accompanied by enhanced functional absorption cross-section of PSII (σ_{PSII}; Table S2). The increase in σ_{PSII} enabled the Fe-limited cells to ensure similar light usage (Ryan-Keogh et al., 2012). In contrast, the low Fe supply differently affected the growth of the two species under ambient pCO_2, as growth remained the same in *P. subcurvata* while it was significantly reduced in *G. cryophila*.

Although F_v/F_m was decreased in the Control relative to the +Fe under ambient pCO_2 (Figure 2A), the diatom maintained similar high growth rates (0.52±0.01 d^{-1}, Figure 3A). Similarly, for various temperate oceanic *Pseudo-nitzschia* isolates, substantial reductions in the photochemical yield were found despite having little or no change in growth (Marchetti et al., 2006). The authors explained that growth and photophysiology are usually decoupled in oceanic *Pseudo-nitzschia* species and that under Fe limitation, oceanic species have a low Fe requirement to achieve rapid growth. Indeed, our *P. subcurvata*

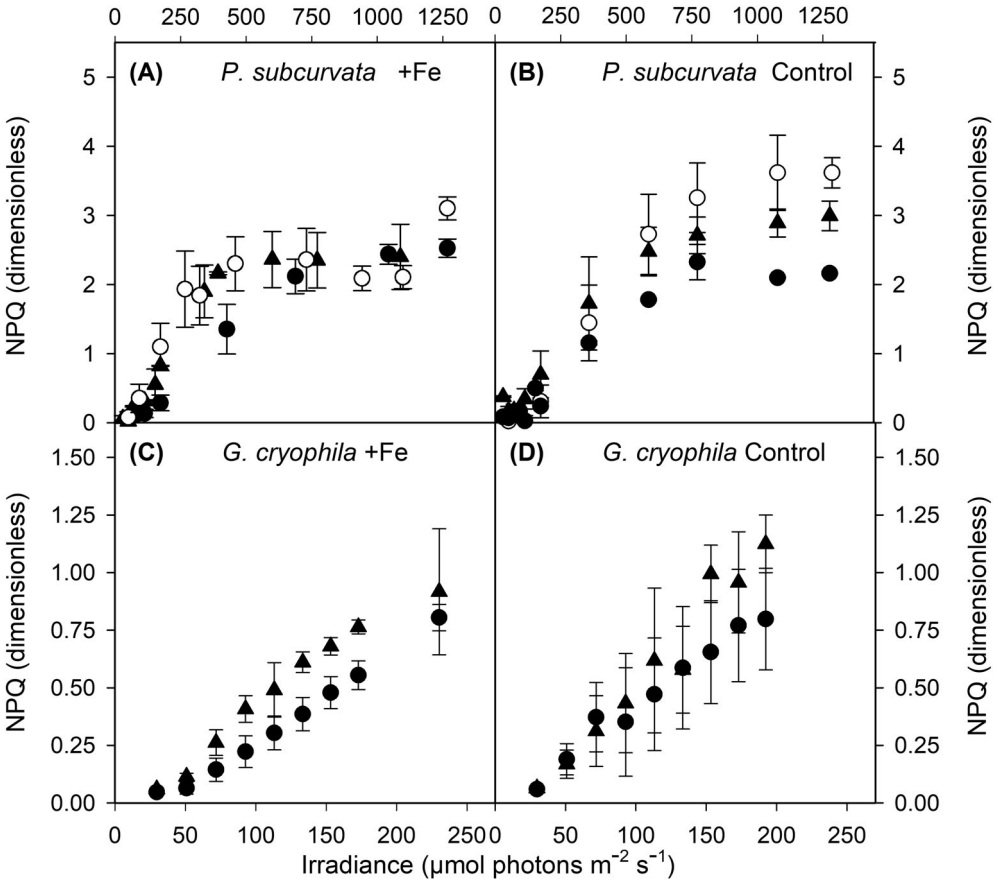

FIGURE 6 Nonphotochemical quenching (NPQ) was measured in response to increasing irradiance in *Pseudo-nitzschia subcurvata* (A, B) and *Geminigera cryophila* (C, D) grown under Fe-deplete (Control) and Fe-enriched (+Fe) conditions at different pCO_2 levels: 400 μatm (filled circle), 900 μatm (filled triangle) and 1400 μatm (open circle, for *P. subcurvata* only). NPQ values show the mean and SD ($n = 3$)

was isolated from open waters of the Southern Ocean (49° S) and exhibited lower Fe:C ratios (2.85 μmol mol^{-1}, Figure 4A) compared to that of the *P. subcurvata* strain isolated from the sea ice edge in the Ross Sea (10-50 Fe:C μmol mol^{-1}; Zhu et al., 2016) and the ones measured in temperate coastal *Pseudo-nitzschia* species (5-11 Fe:C μmol mol^{-1}; Marchetti et al., 2006). Oceanic *Pseudo-nitzschia* species also have the ability to carry out luxury Fe uptake and store this surplus in the Fe storage protein ferritin (Cohen et al., 2018; Lampe et al., 2018; Marchetti et al., 2006, 2017; Sunda & Huntsman, 1995). Although not statistically significant, our Control cells had a lower intracellular Fe content than the +Fe cells under ambient pCO_2 (Figure 4A). This may suggest that the Control cells may have used their internal Fe pool, allowing them to keep growth constant relative to the +Fe cells. When comparing the growth rate of our *P. subcurvata* in both Fe treatments under ambient pCO_2 (+Fe: 0.50 ± 0.04 d^{-1}; Control: 0.52 ± 0.01 d^{-1}, Figure 3A) with the one reported in the same strain grown under ample supply of Fe ($\mu = 0.9$ d^{-1}; 12 μM Fe, Trimborn et al., 2013) and that in the study of Moreno et al. (2018) ($\mu = 0.6$ d^{-1}; 2.7 nM Fe), it becomes evident that our *P. subcurvata* cultures were already experiencing Fe stress in our +Fe treatments. Hence, the +Fe conditions applied here (1.2 nM Fe) were already Fe-limiting for *P. subcurvata*.

Compared to the diatom, F_v/F_m and growth of the cryptophyte *G. cryophila* were much more strongly affected by lower [dFe] under ambient pCO_2. The cryptophyte almost stopped growing in our Control treatments, dividing only at 0.05 d^{-1}. Comparing our growth rate of *G. cryophila* under ambient pCO_2 in the +Fe treatment (1.2 nM Fe, $\mu = 0.10 \pm 0.03$ d^{-1}, Figure 3B) with the values determined in the same strain under high (Aquil medium, 2 μM Fe, Koch and Trimborn (2019) and very high (12 μM, Trimborn et al., 2019b) Fe concentrations, in this study growth was already strongly reduced. To verify this, we grew the cryptophyte at 2 nM Fe, and indeed, we found a significant enhancement in growth (0.24 d^{-1}, data not shown). In fact, the exposure of *G. cryophila* to our Control conditions (0.6 nM Fe, Figure 1A) strongly amplified the effect of Fe limitation, with the Control cells exhibiting stronger reductions in F_v/F_m, growth and cellular pigment concentrations (Chl *a*, Chl c_2, and Allo) as well as higher I_k (Figures 2B and 3B, Tables 2 and 3). Indeed, the Control conditions were more stressful for the cryptophyte than the +Fe conditions under ambient pCO_2.

Fe has a crucial role in the electron transport chain as it is an important component of the photochemical reaction centers (Behrenfeld & Milligan, 2012; Strzepek & Harrison, 2004). It is a common response of phytoplankton to reduce its maximum quantum yield (F_v/F_m) as well as its photosynthetic ETRs under Fe limitation (Koch & Trimborn, 2019; Petrou et al., 2014). In this study, while the maximum ETRs and NPQ of the diatom remained the same between the +Fe and Control (Table 3, Figures 5 and 6), POC production was, however, significantly reduced in the Control cells (Figure 3E), suggesting the utilization of alternative electron sinks other than solely undergoing photosynthetic carbon assimilation. Lower [dFe] also caused an earlier onset of light saturation in the diatom, as indicated by the decrease in I_k in the Control relative to the +Fe treatment (Table 3). To potentially counteract this and diminish light absorption, the concentration of light harvesting pigments (Chl *a* and Fuco) (Table 2), as well as the cellular concentration of functional PSII reaction centers ([RCII]) and the connectivity between PSII (*P*) were reduced in the Control (Table S2). These adjustments enabled *P. subcurvata* to cope well with short-term light stress, as shown by the similar high F_v/F_m recovery (% of the ratio of F_v/F_m determined before and after the FLC) between the +Fe and Control treatments. Overall, even though fast growth was achieved in both Control and +Fe cells, all results together (F_v/F_m, σ_{PSII}, POC, PON, pigments) point toward the fact that the Control conditions were more stressful for the diatom than the +Fe conditions under ambient pCO_2.

Similar to *P. subcurvata*, the cryptophyte also exhibited high tolerance to short-term light stress as it had similar high F_v/F_m recovery values in both Control and +Fe cells (Table S2). Moreover, *G. cryophila* maintained similar POC production rates between the +Fe and Control under ambient pCO_2 (Figure 3F). This unchanged POC production of the Control cells was a consequence of a more enhanced cellular POC buildup while cell division almost stopped (Figure 3B, D, F). At the same time, PON quota remained unchanged in Control versus +Fe cells (Figure S1B). Consequently, the C:N ratio was enhanced in the cryptophyte Control (Figure 3H), which was likely the result of the Fe-limited cells acquiring excess carbon, as evident in the significant increase of POC quota of the Control (Figure 3D). Hence, the Control cells of *G. cryophila* may have prioritized carbon fixation over cell division, as previously observed for the same species under Fe limitation (Koch & Trimborn, 2019) and the Fe-limited diatom *Thalassiosira antarctica* (Andrew et al., 2019). All these photophysiological adjustments of the cryptophyte suggest that Control cells became saturated at higher light intensities, thus requiring higher light to sustain the same rate of POC production (Figure 3F).

Previous studies have shown an increase in cellular Cu concentration of several phytoplankton species in response to Fe limitation (Annett et al., 2008; Guo et al., 2012; Koch & Trimborn, 2019; Maldonado et al., 2006; Semeniuk et al., 2009; Wells et al., 2005). This is because Cu is needed in Fe-reductases and multicopper oxidases, being thus important components of the high-affinity Fe uptake system (Behnke & LaRoche, 2020; Maldonado et al., 2006). This increase in Cu quotas with low Fe supply was, however, not found in *G. cryophila* (Figure 4H) since the Cu:C ratio remained unchanged irrespective of Fe availability under ambient pCO_2. This agrees with the observations of Koch and Trimborn (2019), and further fits well with the observation that the marine cryptophyte *Guillardia theta* did not possess the gene encoding for the Cu-containing enzyme plastocyanin (Blaby-Haas & Merchant, 2017). Under Fe limitation, oceanic diatoms (Peers & Price, 2006) are commonly observed to substitute the Fe-requiring cytochrome c6 with plastocyanin in the electron transport chain (Behrenfeld & Milligan, 2012; Castell et al., 2021; Raven et al., 1999). Moreover, similar to *P. subcurvata* (Moreno et al., 2018), two different cryptophyte species did not have genes encoding Fe-reductases and multicopper oxidases (Behnke & LaRoche, 2020; Curtis et al., 2012), indicating the inability of both species for Cu-dependent high-affinity Fe uptake (Behnke &

LaRoche, 2020; Moreno et al., 2018). Taken together these observations may explain why the cryptophyte was more drastically impacted than the diatom under low Fe supply.

Overall, our results clearly show that under ambient pCO_2, low Fe supply was stressful for both the diatom and the cryptophyte, but with the diatom coping much better with these conditions. The diatom underwent physiological adjustments, which on the one hand, led to reduced carbon buildup and the need for dissipation of excess light energy, but enabling it to sustain high growth rates on the other hand. In contrast, low Fe was highly detrimental for the cryptophyte as it almost stopped dividing.

3.2 | OA together with Fe supply was beneficial for *G. cryophila*, but not for *P. subcurvata*

A meta-analysis on OA effects on SO phytoplankton (Hancock et al., 2018) revealed that Antarctic phytoplankton is generally unaffected by pCO_2 levels below 1000 μatm, with negative effects on physiology becoming evident only at higher pCO_2 levels. In line with the results for the same (Trimborn et al., 2013) and another (Zhu et al., 2017) *P. subcurvata* strain, an increase in pCO_2 up to 1400 μatm did not alter growth or POC production of *P. subcurvata* under +Fe conditions (Figure 3A,E). We observed, however, OA-dependent changes in its photoacclimation. Even though F_v/F_m and σ_{PSII} remained the same between 400 and 900 μatm pCO_2 (Figure 2A, Table S2), [RCII] (Table S2), ETR_{max}, I_k and pigment concentration (Chl *a*, Fuco and Dd) were significantly reduced (Tables 2 and 3, Figure 5), suggesting that electron transport was downregulated, as previously observed (Trimborn et al., 2017a). Calculations of photosynthetic electron transport using the model by Kroon and Thoms (2006) revealed that the higher the rates of electron consumption in upstream metabolic reactions, such as CO_2 fixation by RubisCO, the more pronounced is the decline of the ATP synthesis rate relative to the rate of NADPH synthesis (Trimborn et al., 2017a). Consequently, in this study, downregulation of ETRs can preclude ATP limitation under OA and Fe-enrichment. Furthermore, we observed a highly significant OA-dependent increase in the Cu:C ratio of *P. subcurvata* cells in the +Fe treatments (390 vs. 900: 187%; 390 vs. 1400: 391%, Figure 4G). This was unexpected, as enhanced Cu:C ratios are usually found only in response to Fe limitation and not to OA. For diatoms, the low carbonate concentration present under high pCO_2 was identified to hamper the phytotransferrin-dependent high-affinity Fe uptake (McQuaid et al., 2018). Indeed, the gene encoding for the ferric Fe-concentrating protein ISIP2a (phytotransferin) was found in *P. subcurvata* (Moreno et al., 2018). Perhaps, due to the hampered Fe uptake under increasing pCO_2, the diatom may have potentially switched from using cytochrome c6 to plastocyanin instead, thus increasing the Cu:C ratios. The potentially impacted phytotransferrin-based Fe uptake pathway of the diatom under OA (i.e. low carbonate concentration) may explain why *P. subcurvata* did not benefit from OA even under higher Fe supply, as growth and POC production remained unchanged.

In comparison to the diatom, growth and POC production of the cryptophyte were significantly promoted between 400 and 900 μatm pCO_2 under +Fe, suggesting that *G. cryophila* benefitted from lower energy requirements under OA. Similar observations were made for the same cryptophyte strain grown under OA and high light (200 μmol photons m^{-2} s^{-1}, Trimborn et al., 2019b). In contrast to the diatom, OA did not alter the photoacclimation status of the cryptophyte under +Fe conditions, with no changes in cellular concentrations of the light harvesting pigments (Chl *a*, Chl c_2, and Allo) and photophysiolgy (F_v/F_m, σ_{PSII}, ETR_{max}, and I_k). The slight increase in NPQ (Figure 6C) suggests that excess light energy was dissipated as heat to prevent overexcitation, enabling the cryptophyte to cope well with high light stress in the short term (F_v/F_m recovery of >90%, Table S2). Moreover, ratios of Fe:C as well as of the other TMs (Mn, Co, Cu, and Zn) remained constant between 400 and 900 μatm pCO_2 (Figure 4), which may indicate that TM requirements of the cryptophyte did not change under OA and high Fe supply. As in Trimborn et al.(2019b), *G. cryophila* benefited from OA under higher Fe availability.

3.3 | The diatom coped better with low Fe supply and OA than the cryptophyte, but required adjustments in its photophysiology

For *G. cryophila*, in contrast to the +Fe treatment, Control cells were so strongly Fe limited that increasing pCO_2 did no longer have any effect in most of the investigated physiological parameters (growth, POC production, TM:C ratios, photophysiology, Figures 3 and 4, Table 3). This indicates that Fe limitation alone was the main controlling factor on the cryptophyte. In comparison to the cryptophyte, increasing pCO_2 in combination with low Fe supply synergistically reduced the growth rates of *P. subcurvata* (Figure 3A). Simultaneously, POC production rates, cellular pigment pools (Chl *a*, Chl c_2, Fuco, and Dd) (Figure 3E, Table 2) and the number of functional RCII remained the same (Table S2). However, ETR_{max} was significantly enhanced under these conditions, which may suggest saturation of the Calvin Cycle and the need for alternative electron cycling. Accordingly, we observed highest NPQ values in the 1400 pCO_2-Control treatment (Figure 6B), indicating that not all light energy was channeled downstream and partially dissipated as heat. Control cells may have also operated alternative electron pathways (Behrenfeld & Milligan, 2012) such as cyclic electron transport around PSII (Prasil et al., 1996) and plastid terminal oxidases (Mackey et al., 2008). In previous studies, exposure to either OA or Fe limitation alone was found to increase the production of reactive oxygen species in some phytoplankton species (Allen et al., 2008; Wu et al., 2021). For *P. subcurvata*, one may speculate whether the combined effect of OA and low Fe supply may have also led to higher oxidative stress, most pronounced in the 1400 pCO_2-Control treatment. In line with this, highest Cu:C and Zn:C ratios were observed in the 900 and 1400 pCO_2-Control treatments (Figure 4G), indicating that the diatom may have utilized Cu/Zn superoxide dismutase (Cu/Zn SOD) to counteract the formation of reactive oxygen species (Alscher et al., 2002). Hence, the low Fe availability amplified the negative effects of OA in *P. subcurvata*, hampering linear electron transport and thus increasing the need to dissipate the excess light energy (NPQ, alternative electron sinks). The latter

mechanisms were probably insufficient and potentially increased the formation of reactive oxygen species, impacting the physiological performance of the diatom.

3.4 | Ecological implications

While diatoms form blooms in both open ocean and coastal regions of the SO (Smetacek et al., 2012), high abundances of cryptophytes are mainly observed in coastal SO waters (Brown et al., 2021; Moline et al., 2004; Montes-Hugo et al., 2009). In this study, we provide evidence that cryptophytes such as *G. cryophila* cannot cope well with low Fe concentrations, which are typical for open SO waters. Our findings suggest that low Fe conditions are detrimental for *G. cryophila*, as it almost stopped growing. The reason for this could be that cryptophytes lack the Cu-dependent high-affinity Fe uptake (Behnke & LaRoche, 2020) as well as the capability to substitute cytochrome c6 with plastocyanin. This could explain why cryptophytes mainly occur in coastal waters, which have an ample supply of Fe. In comparison, the oceanic diatom *P. subcurvata* relied on an efficient physiological machinery to cope with low Fe concentration, including low Fe requirements and potentially substituting cytochrome c6 with plastocyanin.

In the future, both groups will need to deal with high CO_2 conditions, with different consequences for their occurrence in Fe-poor and -rich SO waters. In regions with high Fe supply, such as coastal SO waters, high pCO_2 levels could be beneficial for the cryptophyte, displaying elevated rates of growth and POC production, while the diatom would not benefit from OA. The reason for this could be the impacted phytotransferrin-based Fe uptake pathway of the diatom under OA (i.e. low carbonate concentration). In future acidified Fe-poor waters, the overall physiological performance of *P. subcurvata* would be strongly compromised as the low Fe availability amplified the negative effects of OA, in particular impacting its photoacclimation. Overall, our study indicates that Fe availability is a strong modulator of the overall effect imposed by OA on SO phytoplankton, with different implications on the occurrence of cryptophytes and diatoms in the future.

ACKNOWLEDGMENTS

We are grateful to T. Brenneis for lab assistance, B. Meier-Schlosser for pigment analysis, M. Machnik for POC analysis, and C. Völkner for ICP-MS measurements. We thank the members of the EcoTrace and Marine Biogeosciences Section at the AWI for the diverse logistical support. We also thank M. Maldonado for helpful discussions on Cu:C ratio as well as A. Pagnone for the insightful discussions on *P. subcurvata*. We extend our gratitude to the reviewers for their comments and suggestions, which greatly helped in improving our manuscript. Marianne G. Camoying was supported by the Katholischer Akademischer Ausländerdienst (KAAD) through a PhD fellowship. Jana K. Geuer was funded by the AWI strategy fund (IP76010001).

Open access funding enabled and organized by Projekt DEAL.

AUTHOR CONTRIBUTION

Scarlett Trimborn conceived and designed the research. Marianne G. Camoying performed the research. Jana K. Geuer analyzed the DA samples and assisted during harvests. Marianne G. Camoying analyzed the data as well as performed the interpretation of data together with Scarlett Trimborn and Silke Thoms. Boris P. Koch contributed lab materials/reagents and analysis tools needed in the study. Marianne G. Camoying, Scarlett Trimborn and Silke Thoms wrote the manuscript with critical feedback from Jana K. Geuer, Kai Bischof and Boris P. Koch. All authors approved the submitted version.

DATA AVAILABILITY STATEMENT

The data that support the findings of this study will be available at PANGAEA after publication (https://www.pangaea.de).

ORCID

Marianne G. Camoying https://orcid.org/0000-0002-4180-7850

REFERENCES

Alderkamp, A.C., Kulk, G., Buma, A.G.J., Visser, R.J., Van Dijken, G.L., Mills, M. et al. (2012) The effect of iron limitation on the photophysiology of *Phaeocystis antarctica* (Prymnesiophyceae) and *Fragilariopsis cylindrus* (Bacillariophyceae) under dynamic irradiance. *Journal of Phycology*, 48, 45–59.

Allen, A., LaRoche, J., Maheswari, U., Lommer, M., Schauer, N., Lopez, P. et al. (2008) Whole-cell response of the pennate diatom *Phaeodactylum tricornutum* to iron starvation. *Proceedings of the National Academy of Sciences of the United States of America*, 105, 10438–10443.

Almandoz, G.O., Ferreyra, G.A., Schloss, I.R., Dogliotti, A.I., Rupolo, V., Paparazzo, F.E. et al. (2008) Distribution and ecology of *Pseudo-nitzschia* species (Bacillariophyceae) in surface waters of the Weddell Sea (Antarctica). *Polar Biology*, 31, 429–442.

Alscher, R.G., Erturk, N. & Heath, L.S. (2002) Role of superoxide dismutases (SODs) in controlling oxidative stress in plants. *Journal of Experimental Botany*, 53, 1331–1341.

Andrew, S.M., Morell, H.T., Strzepek, R.F., Boyd, P.W. & Ellwood, M.J. (2019) Iron availability influences the tolerance of Southern Ocean phytoplankton to warming and elevated irradiance. *Frontiers in Marine Science*, 6, 1–12.

Annett, A.L., Lapi, S., Ruth, T.J. & Maldonado, M.T. (2008) The effects of Cu and Fe availability on the growth and Cu:C ratios of marine diatoms. *Limnology and Oceanography*, 53, 2451–2461.

de Baar, H.J.W., Bathmannt, U., Smetacek, V., Löscher, B.M. & Veth, C. (1995) Importance of iron for plankton blooms and carbon dioxide drawdown in the Southern Ocean. *Nature*, 373, 412–415.

Behnke, J. & LaRoche, J. (2020) Iron uptake proteins in algae and the role of Iron Starvation-Induced Proteins (ISIPs). *European Journal of Phycology*, 55, 339–360.

Behrenfeld, M.J. & Milligan, A.J. (2012) Photophysiological expressions of iron stress in phytoplankton. *Annual Review of Marine Science*, 5, 217–246.

Blaby-Haas, C.E. & Merchant, S.S. (2017) Regulating cellular trace metal economy in algae. *Current Opinion in Plant Biology*, 39, 88–96.

Brown, M.S., Bowman, J.S., Lin, Y., Feehan, C.J., Moreno, C.M., Cassar, N. et al. (2021) Low diversity of a key phytoplankton group along the West Antarctic Peninsula. *Limnology and Oceanography*, 66, 2470–2480.

Castell, C., Bernal-bayard, P. & Hervás, M. (2021) The heterologous expression of a plastocyanin in the diatom *Phaeodactylum tricornutum* improves cell growth under iron- deficient conditions. *Physiologia Plantarum*, 171, 277–290.

Coad, T., McMinn, A., Nomura, D. & Martin, A. (2016) Effect of elevated CO_2 concentration on microalgal communities in Antarctic pack ice. *Deep Sea Research Part II: Topical Studies in Oceanography*, 131, 160–169.

Cohen, N.R., Mann, E., Stemple, B., Moreno, C.M., Rauschenberg, S., Jacquot, J. et al. (2018) Iron storage capacities and associated ferritin gene expression among marine diatoms. *Limnology and Oceanography*, 63, 1677–1691.

Curtis, B.A., Tanifuji, G., Burki, F., Gruber, A., Irimia, M., Maruyama, S. et al. (2012) Algal genomes reveal evolutionary mosaicism and the fate of nucleomorphs. *Nature*, 492, 59–65.

Cutter, G.A., Casciotti, K., Croot, P., Geibert, W., Heimbürger, L.E., Lohan, M. et al. (2017) *Sampling and Sample-handling Protocols for GEOTRACES Cruises*. Toulouse, France: GEOTRACES International Project Office, 139 pp.

Davidson, A.T., McKinlay, J., Westwood, K., Thomson, P., van den Enden, R., de Salas, M. et al. (2016) Enhanced CO_2 concentrations change the structure of Antarctic marine microbial communities. *Marine Ecology Progress Series*, 552, 93–113.

Dickson, A.G. & Millero, F.J. (1987) A comparison of the equilibrium constants for the dissociation of carbonic acid in seawater media. *Deep Sea Research Part A: Oceanographic Research Papers*, 34, 1733–1743.

Donahue, K., Klaas, C., Dillingham, P.W. & Hoffmann, L.J. (2019) Combined effects of ocean acidification and increased light intensity on natural phytoplankton communities from two Southern Ocean water masses. *Journal of Plankton Research*, 41, 30–45.

Feng, Y., Hare, C.E., Rose, J.M., Handy, S.M., DiTullio, G.R., Lee, P.A. et al. (2010) Interactive effects of iron, irradiance and CO_2 on Ross Sea phytoplankton. *Deep Sea Research Part I: Oceanographic Research Papers*, 57, 368–383.

Garibotti, I.A. & Ferrario, M.E. (2005) Annually recurrent phytoplanktonic assemblages during summer in the seasonal ice zone west of the Antarctic Peninsula (Southern Ocean). *Deep-Sea Research*, 52, 1823–1841.

Garibotti, I.A., Vernet, M., Kozlowski, W.A. & Ferrario, M.E. (2003) Composition and biomass of phytoplankton assemblages in coastal Antarctic waters: a comparison of chemotaxonomic and microscopic analyses. *Marine Ecology Progress Series*, 247, 27–42.

Genty, B., Briantais, J.M. & Baker, N.R. (1989) The relationship between the quantum yield of photosynthetic electron transport and quenching of chlorophyll fluorescence. *Biochimica et Biophysica Acta*, 990, 87–92.

Gerringa, L.J.A., De Baar, H.J.W. & Timmermans, K.R. (2000) A comparison of iron limitation of phytoplankton in natural oceanic waters and laboratory media conditioned with EDTA. *Marine Chemistry*, 68, 335–346.

Geuer, J.K., Trimborn, S., Koch, F., Brenneis, T., Krock, B. & Koch, B.P. (2020) Dissolved domoic acid does not improve growth rates and iron content in iron-stressed *Pseudo-Nitzschia subcurvata*. *Frontiers in Marine Science*, 7, 478.

Greene, R.M., Geider, R.J. & Falkowski, P.G. (1991) Effect of iron limitation on photosynthesis in a marine diatom. *Limnology and Oceanography*, 36, 1772–1782.

Greene, R.M., Geider, R.J., Kolber, Z. & Falkowski, P.G. (1992) Iron-induced changes in light harvesting and photochemical energy conversion processes in eukaryotic marine algae. *Plant Physiology*, 100, 565–575.

Guo, J., Lapi, S., Ruth, T.J. & Maldonado, M.T. (2012) The effects of iron and copper availability on the copper stoichiometry of marine phytoplankton. *Journal of Phycology*, 48, 312–325.

Hancock, A.M., Davidson, A.T., Mckinlay, J., Mcminn, A., Schulz, K.G. & van den Enden, R.L. (2018) Ocean acidification changes the structure of an Antarctic coastal protistan community. *Biogeosciences*, 15, 2393–2410.

Hassler, C.S. & Schoemann, V. (2009) Discriminating between intra- and extracellular metals using chemical extractions: an update on the case of iron. *Limnology and Oceanography: Methods*, 7, 479–489.

Heiden, J.P., Völkner, C., Jones, E.M., van de Poll, W.H., Buma, A.G., Meredith, M. et al. (2019) Impact of ocean acidification and high solar radiation on productivity and species composition of a late summer phytoplankton community of the coastal Western Antarctic Peninsula. *Limnology and Oceanography*, 64, 1716–1736.

Henley, S.F., Schofield, O.M., Hendry, K.R., Schloss, I., Steinberg, D., Moffat, C. et al. (2019) Variability and change in the west Antarctic Peninsula marine system: research priorities and opportunities. *Progress in Oceanography*, 173, 208–237.

Hillebrand, H., Dürselen, C.D., Kirschtel, D., Pollingher, U. & Zohary, T. (1999) Biovolume calculation for pelagic and benthic microalgae. *Journal of Phycology*, 35, 403–424.

Hoogstraten, A., Peters, M., Timmermans, K.R. & De Baar, H.J.W. (2012) Combined effects of inorganic carbon and light on *Phaeocystis globosa* Scherffel (Prymnesiophyceae). *Biogeosciences*, 9, 1885–1896.

Hoppe, C.J.M., Hassler, C.S., Payne, C.D., Tortell, P.D., Rost, B. & Trimborn, S. (2013) Iron limitation modulates ocean acidification effects on Southern Ocean phytoplankton communities. *PLoS One*, 8, e79890. https://doi.org/10.1371/journal.pone.0079890

Intergovernmental Panel on Climate Change. (2014) In: Pachauri, R.K. & Meyer, L.A. (Eds.) *Synthesis Report. Contribution of Working Groups I, II and III to the Fifth Assessment Report of the Intergovernmental Panel on Climate Change*. Geneva, Switzerland: Intergovernmental Panel on Climate Change.

Kerr, R., Goyet, C., da Cunha, L.C., da Cunha, L., Orselli, I., Lencina-Avila, J. et al. (2018) Carbonate system properties in the Gerlache Strait, Northern Antarctic Peninsula (February 2015): II. Anthropogenic CO_2 and seawater acidification. *Deep Sea Research Part II: Topical Studies in Oceanography*, 149, 182–192.

Klunder, M.B., Laan, P., Middag, R., De Baar, H.J.W. & Van Ooijen, J.C. (2011) Dissolved iron in the Southern Ocean (Atlantic sector). *Deep Sea Research Part II: Topical Studies in Oceanography*, 58, 2678–2694.

Klunder, M.B., Laan, P., De Baar, H.J.W., Middag, R., Neven, I. & Van Ooijen, J.C. (2014) Dissolved Fe across the Weddell Sea and Drake Passage: Impact of DFe on nutrient uptake. *Biogeosciences*, 11, 651–669.

Koch, F. & Trimborn, S. (2019) Limitation by Fe, Zn, Co, and B_{12} results in similar physiological responses in two Antarctic phytoplankton species. *Frontiers in Marine Science*, 6, 514.

Koch, F., Beszteri, S., Harms, L. & Trimborn, S. (2018) The impacts of iron limitation and ocean acidification on the cellular stoichiometry, photophysiology, and transcriptome of *Phaeocystis antarctica*. *Limnology and Oceanography*, 64, 357–375.

Kolber, Z.S., Prášil, O. & Falkowski, P.G. (1998) Measurements of variable chlorophyll fluorescence using fast repetition rate techniques: Defining methodology and experimental protocols. *Biochimica et Biophysica Acta*, 1367, 88–106.

Kroon, B.M.A. & Thoms, S. (2006) From electron to biomass: A mechanistic model to describe phytoplankton photosynthesis and steady-state growth rates. *Journal of Phycology*, 42, 593–609.

Lampe, R.H., Mann, E.L., Cohen, N.R., Till, C.P., Thamatrakoln, K., Brzenzinski, M.A. et al. (2018) Different iron storage strategies among bloom-forming diatoms. *Proceedings of the National Academy of Sciences of the United States of America*, 115, E12275–E12284.

van Leeuwe, M.A., Visser, R.J.W. & Stefels, J. (2014) The pigment composition of *Phaeocystis antarctica* (Haptophyceae) under various conditions of light, temperature, salinity, and iron. *Journal of Phycology*, 50, 1070–1080.

Lundholm, N., Hansen, P.J. & Kotaki, Y. (2004) Effect of pH on growth and domoic acid production by potentially toxic diatoms of the genera *Pseudo-nitzschia* and *Nitzschia*. *Marine Ecology Progress Series*, 273, 1–15.

Mackey, K.R.M., Paytan, A., Grossman, A.R. & Bailey, S. (2008) A photosynthetic strategy for coping in a high-light, low-nutrient environment. *Limnology and Oceanography*, 53, 900–913.

Maldonado, M.T., Hughes, M.P., Rue, E.L. & Wells, M.L. (2002) The effect of Fe and Cu on growth and domoic acid production by *Pseudo-*

nitzschia multiseries and *Pseudo-nitzschia australis*. *Limnology and Oceanography*, 47, 515–526.

Maldonado, M.T., Allen, A.E., Chong, J.S., Lin, K., Leus, D., Karpenko, N. et al. (2006) Copper-dependent iron transport in coastal and oceanic diatoms. *Limnology and Oceanography*, 51, 1729–1743.

Marchetti, A., Maldonado, M.T., Lane, E.S. & Harrison, P.J. (2006) Iron requirements of the pennate diatom *Pseudo-nitzschia* Comparison of oceanic (high-nitrate, low-chlorophyll waters) and coastal species. *Limnology and Oceanography*, 51, 2092–2101.

Marchetti, A., Moreno, C.M., Cohen, N.R., Oleinikov, I., DeLong, K., Twining, B. et al. (2017) Development of a molecular-based index for assessing iron status in bloom-forming pennate diatoms. *Journal of Phycology*, 53, 820–832.

Martin, J.H., Gordon, R.M. & Fitzwater, S.E. (1990) Iron in Antarctic waters. *Nature*, 345, 156–158.

McMinn, A., Müller, M.N., Martin, A. & Ryan, K.G. (2014) The response of Antarctic sea ice algae to changes in pH and CO_2. *PLoS One*, 28, e86984. https://doi.org/10.1371/journal.pone.0086984

McQuaid, J.B., Kustka, A.B., Oborník, M., Horák, A., McCrow, J.P., Karas, B. et al. (2018) Carbonate-sensitive phytotransferrin controls high-affinity iron uptake in diatoms. *Nature*, 555, 534–537.

Mehrbach, C., Culberson, C., Hawley, J. & Pytkowicx, R. (1973) Measurements of the apparent dissociation constants of carbonic acid in seawater at atmospheric pressure. *Limnology and Oceanography*, 18, 897–907.

Mendes, C.R.B., Tavano, V.M., Leal, M.C., de Souza, M.S., Brotas, V. & Garcia, C.A.E. (2013) Shifts in the dominance between diatoms and cryptophytes during three late summers in the Bransfield Strait (Antarctic Peninsula). *Polar Biology*, 36, 537–547.

Mendes, C.R.B., Tavano, V.M., Dotto, T.S., Kerr, R., de Souza, M.S., CAE, G. et al. (2017) New insights on the dominance of cryptophytes in Antarctic coastal waters: a case study in Gerlache Strait. *Deep Sea Research Part II: Topical Studies in Oceanography*, 149, 161–170.

Moffat, C. & Meredith, M. (2018) Shelf-ocean exchange and hydrography west of the Antarctic Peninsula: A review. *Philosophical Transactions of the Royal Society A - Mathematical Physical and Engineering Sciences*, 376, 20170164.

Moline, M.A. & Prézelin, B.B. (1996) Long-term monitoring and analyses of physical factors regulating variability in coastal Antarctic phytoplankton biomass, in situ productivity and taxonomic composition over subseasonal, seasonal and interannual time scales. *Marine Ecology Progress Series*, 145, 143–160.

Moline, M.A., Claustre, H., Frazer, T.K., Schofield, O. & Vernet, M. (2004) Alteration of the food web along the Antarctic Peninsula in response to a regional warming trend. *Global Change Biology*, 10, 1973–1980.

Montes-Hugo, M., Doney, S., Ducklow, H., Fraser, W., Martinson, D., Stammerjohn, S. et al. (2009) Recent changes in phytoplankton communities associated with rapid regional climate change along the Western Antarctic Peninsula. *Science*, 323, 1470–1473.

Moreno, C.M., Lin, Y., Davies, S., Monbureau, E., Cassar, N. & Marchetti, A. (2018) Examination of gene repertoires and physiological responses to iron and light limitation in Southern Ocean diatoms. *Polar Biology*, 41, 679–696. https://doi.org/10.1007/s00300-017-2228-7

Olesen, A.J., Leithoff, A., Altenburger, A., Krock, B., Beszteri, B., Eggers, S. L. et al. (2021) First evidence of the toxin domoic acid in antarctic diatom species. *Toxins*, 13, 93. https://doi.org/10.3390/toxins13020093

Peers, G. & Price, N.M. (2006) Copper-containing plastocyanin used for electron transport by an oceanic diatom. *Nature*, 441, 341–344.

Petrou, K., Trimborn, S., Rost, B., Ralph, P.J. & Hassler, C.S. (2014) The impact of iron limitation on the physiology of the Antarctic diatom *Chaetoceros simplex*. *Marine Biology*, 161, 925–937.

Pierrot, D., Lewis, E., Wallace, D. (2006) MS excel program developed for CO_2 system calculations. ORNL/ CDIAC-105. U.S. Department of Energy

Prasil, O., Kolber, Z., Berry, J.A. & Falkowski, P.G. (1996) Cyclic electron flow around photosystem II in vivo. *Photosynthesis Research*, 48, 395–410.

Ralph, P.J. & Gademann, R. (2005) Rapid light curves: a powerful tool to assess photosynthetic activity. *Aquatic Botany*, 82, 222–237.

Raven, J.A., Evans, M.C.W. & Korb, R.E. (1999) The role of trace metals in photosynthetic electron transport in O_2-evolving organisms. *Photosynthesis Research*, 60, 111–149.

Redfield, A. (1958) The biological control of chemical factors in the environment. *American Scientist*, 46, 230A–221A.

Rue, E. & Bruland, K. (2001) Domoic acid binds iron and copper: a possible role for the toxin produced by the marine diatom *Pseudo-nitzschia*. *Marine Chemistry*, 76, 127–134.

Ryan-Keogh, T.J., Macey, A.I., Cockshutt, A.M., Moore, C.M. & Bibby, T.S. (2012) The cyanobacterial chlorophyll-binding-protein IsiA acts to increase the in vivo effective absorption cross-section of PSI under iron limitation. *Journal of Phycology*, 48, 145–154.

Schofield, O., Saba, G., Coleman, K., Carvalho, F., Couto, N. & Ducklow, H. (2017) Decadal variability in coastal phytoplankton community composition in a changing West Antarctic Peninsula. *Deep Sea Research Part I: Oceanographic Research Papers*, 124, 42–54. http://dx.doi.org/10.1016/j.dsr.2017.04.014

Semeniuk, D.M., Cullen, J.T., Johnson, W.K., Gagnon, K., Ruth, T.J. & Maldonado, M.T. (2009) Plankton copper requirements and uptake in the subarctic Northeast Pacific Ocean. *Deep-Sea Research Part I: Oceanography Research Papers*, 56, 1130–1142.

Smetacek, V., Klaas, C., Strass, V.H., Assmy, P., Montresor, M., Cisewski, B. et al. (2012) Deep carbon export from a Southern Ocean iron-fertilized diatom bloom. *Nature*, 487, 313–319.

Strzepek, R.F. & Harrison, P.J. (2004) Photosynthetic architecture differs in coastal and oceanic diatoms. *Nature*, 431, 689–692.

Strzepek, R.F., Maldonado, M.T., Hunter, K.A., Frew, R.D. & Boyd, P.W. (2011) Adaptive strategies by Southern Ocean phytoplankton to lessen iron limitation: uptake of organically complexed iron and reduced cellular iron requirements. *Limnology and Oceanography*, 56, 1983–2002.

Strzepek, R.F., Hunter, K.A., Frew, R.D., Harrison, P.J. & Boyd, P.W. (2012) Iron –light interactions differ in Southern Ocean phytoplankton. *Limnology and Oceanography*, 57, 1182–1200.

Suggett, D.J., MacIntyre, H.L. & Geider, R.J. (2004) Evaluation of biophysical and optical determinations of light absorption by photosystem II in phytoplankton. *Limnology and Oceanography*, 2, 316–332.

Suggett, D.J., Moore, C.M., Hickman, A.E. & Geider, R.J. (2009) Interpretation of fast repetition rate (FRR) fluorescence: Signatures of phytoplankton community structure versus physiological state. *Marine Ecology Progress Series*, 376, 1–19.

Sunda, W.G. & Huntsman, S.A. (1995) Iron uptake and growth limitation in oceanic and coastal phytoplankton. *Marine Chemistry*, 50, 189–206.

Thoisen, C., Riisgaard, K., Lundholm, N., Nielsen, T.G. & Hansen, P.J. (2015) Effect of acidification on an Arctic phytoplankton community from Disko Bay, West Greenland. *Marine Ecology Progress Series*, 520, 21–34.

Thomson, P.G., Davidson, A.T. & Maher, L. (2016) Increasing CO_2 changes community composition of pico- and nano-sized protists and prokaryotes at a coastal Antarctic site. *Marine Ecology Progress Series*, 554, 51–69.

Tortell, P.D., Payne, C.D., Li, Y., Trimborn, S., Rost, B., Smith, W.O. et al. (2008) CO_2 sensitivity of Southern Ocean phytoplankton. *Geophysical Research Letters*, 35, L04605.

Trimborn, S., Lundholm, N., Thoms, S., Richter, K., Krock, B., Hansen, P.J. et al. (2008) Inorganic carbon acquisition in potentially toxic and non-toxic diatoms: The effect of pH-induced changes in seawater carbonate chemistry. *Physiologia Plantarum*, 133, 92–105.

Trimborn, S., Brenneis, T., Sweet, E. & Rost, B. (2013) Sensitivity of Antarctic phytoplankton species to ocean acidification: growth, carbon acquisition, and species interaction. *Limnology and Oceanography*, 58, 997–1007.

Trimborn, S., Thoms, S., Brenneis, T., Heiden, J.P., Beszteri, S. & Bischof, K. (2017a) Two Southern Ocean diatoms are more sensitive to ocean acidification and changes in irradiance than the prymnesiophyte *Phaeocystis antarctica*. *Physiologia Plantarum*, 160, 155–170.

Trimborn, S., Brenneis, T., Hoppe, C.J.M., Laglera, L., Norman, L., Santos-Echeandía, J. et al. (2017b) Iron sources alter the response of Southern Ocean phytoplankton to ocean acidification. *Marine Ecology Progress Series*, 578, 35–50.

Trimborn, S., Thoms, S., Bischof, K. & Beszteri, S. (2019a) Susceptibility of two Southern Ocean phytoplankton key species to iron limitation and high light. *Frontiers in Marine Science*, 6, 1–17.

Trimborn, S., Thoms, S., Karitter, P. & Bischof, K. (2019b) Ocean acidification and high irradiance stimulate the photo-physiological fitness, growth and carbon production of the Antarctic cryptophyte *Geminigera cryophila*. *Biogeosciences*, 16, 2997–3008.

Wells, M.L., Trick, C.G., Cochlan, W.P., Hughes, M.P. & Trainer, V.L. (2005) Domoic acid: The synergy of iron, copper, and the toxicity of diatoms. *Limnology and Oceanography*, 50, 1908–1917.

Wu, S., Mi, T., Zhen, Y., Yu, K., Wang, F. & Yu, Z. (2021) A rise in ROS and EPS production: new insights into the *Trichodesmium erythraeum* response to ocean acidification. *Journal of Phycology*, 57, 172–182.

Young, J.N., Kranz, S.A., Goldman, J.A.L., Tortell, P.D. & Morel, F.M.M. (2015) Antarctic phytoplankton down-regulate their carbon-concentrating mechanisms under high CO_2 with no change in growth rates. *Marine Ecology Progress Series*, 532, 13–28.

Zhu, Z., Xu, K., Fu, F., Spackeen, J.L., Bronk, D.A. & Hutchins, D.A. (2016) A comparative study of iron and temperature interactive effects on diatoms and *Phaeocystis antarctica* from the Ross Sea, Antarctica. *Marine Ecology Progress Series*, 550, 39–51.

Zhu, Z., Qu, P., Gale, J., Fu, F. & Hutchins, D.A. (2017) Individual and interactive effects of warming and CO_2 on *Pseudo-nitzschia subcurvata* and *Phaeocystis antarctica*, two dominant phytoplankton from the Ross Sea, Antarctica. *Biogeosciences*, 14, 5281–5295.

SUPPORTING INFORMATION

Additional supporting information may be found in the online version of the article at the publisher's website.

How to cite this article: Camoying, M.G., Thoms, S., Geuer, J. K., Koch, B.P., Bischof, K. & Trimborn, S. (2022) In contrast to diatoms, cryptophytes are susceptible to iron limitation, but not to ocean acidification. *Physiologia Plantarum*, 174(1), e13614. Available from: https://doi.org/10.1111/ppl.13614

Chapter 3

Physiological response of an Antarctic cryptophyte to increasing temperature, CO_2, and irradiance

Marianne Camoying[1*], Scarlett Trimborn[1]

[1]Ecological Chemistry, Alfred Wegener Institute,
Helmholtz Centre for Polar and Marine Research, Bremerhaven, Germany

Published in Limnology and Oceanography

LIMNOLOGY and OCEANOGRAPHY

ASLO

Limnol. Oceanogr. 9999, 2023, 1–15

doi: 10.1002/lno.12392

Physiological response of an Antarctic cryptophyte to increasing temperature, CO_2, and irradiance

Marianne G. Camoying ,* **Scarlett Trimborn**
Ecological Chemistry, Alfred Wegener Institute, Helmholtz Centre for Polar and Marine Research, Bremerhaven, Germany

Abstract

The Southern Ocean, a globally important CO_2 sink, is one of the most susceptible regions in the world to climate change. Phytoplankton of the coastal shelf waters around the Western Antarctic Peninsula have been experiencing rapid warming over the past decades and current ongoing climatic changes will expose them to ocean acidification and high light intensities due to increasing stratification. We conducted a multiple-stressor experiment to evaluate the response of the still poorly studied key Antarctic cryptophyte species *Geminigera cryophila* to warming in combination with ocean acidification and high irradiance. Based on the thermal growth response of *G. cryophila*, we grew the cryptophyte at suboptimal (2°C) and optimal (4°C) temperatures in combination with two light intensities (medium light: 100 μmol photons m^{-2} s^{-1} and high light [HL]: 500 μmol photons m^{-2} s^{-1}) under ambient (400 μatm pCO_2) and high pCO_2 (1000 μatm pCO_2) conditions. Our results reveal that *G. cryophila* was not susceptible to high pCO_2, but was strongly affected by HL at 2°C, as both growth and carbon fixation were significantly reduced. In comparison, warming up to 4°C stimulated the growth of the cryptophyte and even alleviated the previously observed negative effects of HL at 2°C. When grown, however, at temperatures above 4°C, the cryptophyte already reached its maximal thermal limit at 8°C, pointing out its vulnerability toward even higher temperatures. Hence, our results clearly indicate that warming and high light and not pCO_2 control the growth of *G. cryophila*.

The Southern Ocean is reported to have stored not only large quantities of atmospheric carbon dioxide (CO_2) but also a significant amount of heat associated with climate change (Frölicher et al. 2015). The coastal waters of the Western Antarctic Peninsula (WAP), for example, has been experiencing rapid warming for the past several decades (Jones et al. 2019). Climate model projections show that the Southern Ocean would experience between a ~2°C up to ~6°C increase in temperature by 2100 and 2300, respectively (Boyd et al. 2015; Moore et al. 2018; IPCC 2019). In fact, an unprecedented mean temperature anomaly of +4.5°C has just been reported in the WAP coastal waters in February 2020 (González-Herrero et al. 2022). In this region, previous warming events have been associated with the increasing dominance of cryptophytes over diatoms under conditions of lowered salinity due to the increased sea ice retreat and glacial melting as a result of warming (Mendes et al. 2013; Schofield et al. 2017). As cryptophytes are not the preferred food of krill, the increasing dominance of cryptophytes over diatoms would potentially also alter the Antarctic marine food web (Meyer and El-Sayed 1983). The shift from diatoms to cryptophytes could also result in a reduced drawdown of atmospheric CO_2 in the WAP (Brown et al. 2019). Coastal shelf phytoplankton communities along the WAP are also projected to be more prone to high light exposure due to warming and the subsequently increased freshwater input from the sea-ice melt. The latter potentially enhances vertical stratification and thus results in shoaling of the mixed layer depth and thus more illuminated surface waters (Boyd et al. 2015). At present, studies looking at the effects of high irradiances on Antarctic phytoplankton are still scarce. In addition, due to anthropogenic emissions, the present-day CO_2 level of 413 ppm is going to increase at an unprecedented rate (Hoegh-Guldberg and Bruno 2010) and is projected to reach 936 ppm by 2100 (IPCC 2014). The implications of increased pCO_2 levels in particular on Antarctic cryptophytes is only poorly understood, with the few studies available pointing toward a high pCO_2 tolerance of this group

*Correspondence: marianne.camoying@awi.de

Additional Supporting Information may be found in the online version of this article.

Author Contribution Statement: M.C. and S.T. designed the research. M.C. performed the research and analyzed the data. M.C. and S.T. interpreted the data and wrote the manuscript.

(Schulz et al. 2017; Donahue et al. 2019). Overall, studies looking at the effects of future climate change scenarios such as warming, ocean acidification, and high light on Antarctic cryptophytes are at present still lacking.

Along the WAP, the cryptophyte *Geminigera* is the most abundant genus observed in coastal shelf waters (Brown et al. 2021). In response to warming, laboratory experiments have shown that the Antarctic *Geminigera cryophila* exhibited enhanced growth up to the highest temperature treatment of 4°C (Wang and Smith 2021). Whether the cryptophyte would be able to outcompete other phytoplankton groups at much higher temperatures still yet remains unknown. In response to high irradiances (500 μmol photons m^{-2} s^{-1}), *G. cryophila* was strongly negatively impacted (Trimborn et al. 2019). The reasons for this are not yet clear. On the other hand, it was reported that *G. cryophila* was not negatively affected by high pCO_2 (Trimborn et al. 2019; Camoying et al. 2022), similar to what has been observed for cryptophytes in general when natural phytoplankton were grown under elevated pCO_2 levels (Sommer et al. 2015; Schulz et al. 2017; Donahue et al. 2019). This is in line with the findings that cryptophytes are able to grow within a broad pH range (i.e., at both lower and upper extreme of the pH spectrum, Weisse and Stadler 2006; Gaillard et al. 2020).

As *G. cryophila* represents an important and abundant species in coastal shelf waters along the WAP (Brown et al. 2021), we investigated the combined effects of warming, ocean acidification (high pCO_2) and high light on its physiology. It still remains unexplored how all three environmental factors will influence the ecophysiology of the cryptophyte. Hence, it was the objective of our study to (1) characterize its thermal performance and to (2) identify its physiological strategies to cope with future climate change conditions such as warming in conjunction with high pCO_2 and increasing light.

Methods

Experimental design and culture conditions

We examined the interactive effects of increasing pCO_2, temperature and light on growth, carbon fixation, and photophysiology of the Antarctic cryptophyte *G. cryophila* (CCMP 2564, isolated from McMurdo Sound, Ross Sea, Antarctica). All *G. cryophila* cells grew at 2°C and 100 μmol photons m^{-2} s^{-1} under a 16 : 8 h light–dark cycle. The species was grown in sterile-filtered (0.2 μm) unbuffered natural Antarctic seawater, which was enriched with macronutrients (100 μmol L^{-1} NO_3^- and 6.25 μmol L^{-1} PO_4^{-3}), vitamins (30 nmol L^{-1} B_1, 23 nmol L^{-1} B_7, and 0.228 nmol L^{-1} B_{12}) and trace metals according to $F/2_R$ medium (Guillard and Ryther 1962). Nitrate and phosphate were added following the Redfield N : P ratio of 16 : 1 (Redfield 1958).

To determine the thermal functional response curve of *G. cryophila*, experiments were done at 100 μmol photons m^{-2} s^{-1} under a 16 : 8 light–dark cycle and 400 μatm pCO_2 (bubbled). All *G. cryophila* cultures were grown in triplicate 1 L custom-made cylindrical glass bottles under a range of temperatures, starting at 2°C and then gradually transferred to 4°C, 6°C, 7°C, and 8°C (Fig. 1). More specifically, we followed the methods of Zhu et al. (2017) and did a series of step-wise transfers, making sure that *G. cryophila* cultures were well-acclimated to the lower temperature before exposing them to a higher temperature (Fig. 1). Please note that at 8°C *G. cryophila* died.

For the main temperature-CO_2-light experiment, we chose the temperature treatments based on the outcome of the experiment on the thermal functional response curve of *G. cryophila* (Fig. 2). As 4°C was identified to be the optimal growth of this species based on Fig. 2, we wanted to investigate the response of *G. cryophila* under suboptimal (2°C), optimal (4°C), and supraoptimal (6°C) temperatures (Fig. 1).

Next to the different temperature conditions, *G. cryophila* cells were further grown under two light intensities (*medium light treatment*: 100 μmol photons m^{-2} s^{-1}; *high light treatment*: 500 μmol photons m^{-2} s^{-1}) in combination with two pCO_2 levels (*400 treatment*: 400 μatm pCO_2; *1000 treatment*: 1000 μatm pCO_2). The light intensities of the medium light treatment chosen mimic realistic average daily irradiances of surface coastal waters of the WAP ($\sim$ 100 up to 570 μmol photons m^{-2} s^{-1}; Young et al. 2015*a*; Heiden et al. 2019) while the elevated mean irradiance of the high light treatment simulates future light conditions. Moreover, *G. cryophila* was also grown under pCO_2 levels representing values of present-day ($\sim$ 410 ppm), and those projected for the year 2100 ($\sim$ 1000 μatm, RCP8.5 scenario; IPCC 2014). The two different pCO_2 levels were achieved by gentle bubbling of each culture bottle with humidified air of the respective pCO_2 level. To this end, a mixture of CO_2-free air (< 1 ppmv CO_2; Dominic Hunter) and pure CO_2 (Air Liquide Deutschland Ltd.) was used and controlled through a gas flow controller (CGM 2000; MCZ Umwelttechnik) to generate the two target pCO_2 treatments. A non-dispersive infrared analyzer system (LI6252; Li-Cor Biosciences), which was calibrated with CO_2-free air and purchased gas mixtures of 150 $\pm$ 10 and 1000 $\pm$ 20 ppmv CO_2 (Air Liquide, Deutschland), was utilized regularly to monitor the different CO_2 gas mixtures. Light-emitting diodes (LED) lamps (SolarStinger LED SunStrip Marine Daylight, Econlux) were used as light source and light intensities were set and monitored using an LI-1400 data logger (Li-Cor) with a 4π-sensor (Walz). Water temperature of the aquaria was also regularly checked to make sure that the cultures were grown under stable temperature.

Prior to the start of the main experiment, cultures were pre-acclimated to each temperature-light-pCO_2 treatment for at least 15 d. During both the preacclimation period and the main experiment, cultures were diluted semi-continuously (before cell density reached 15,000 cells mL^{-1}) with preconditioned media to keep cells in exponential growth, thus ensuring that cells were in the same physiological state

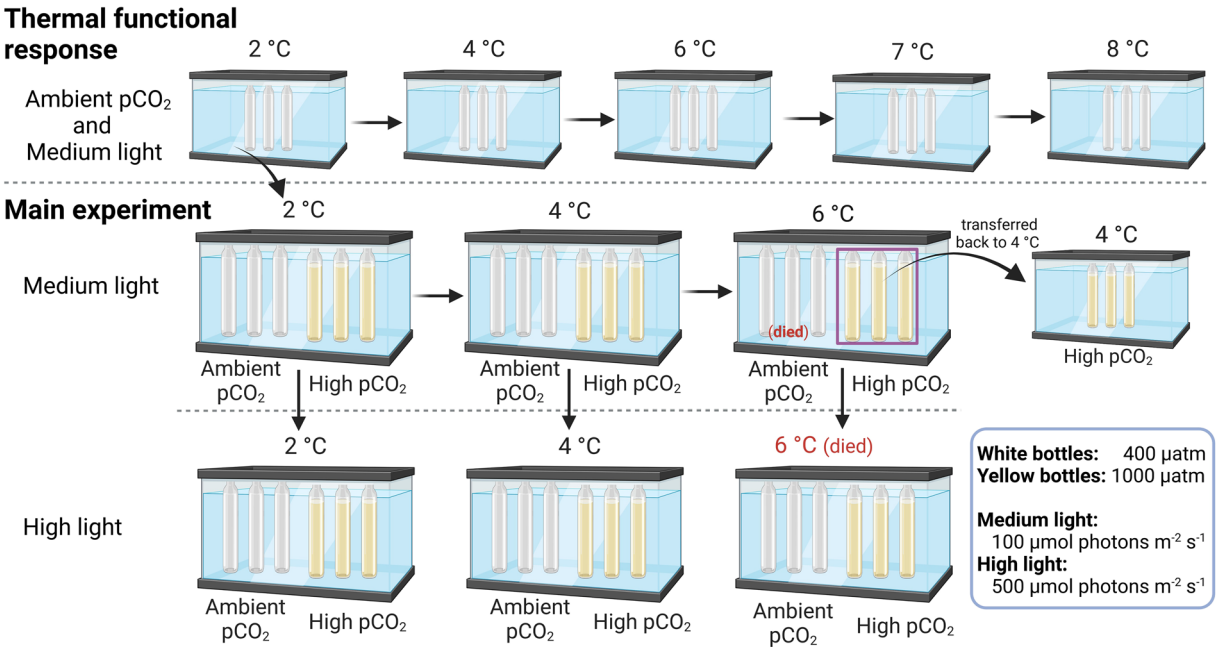

Fig. 1. Overview of the experimental setup (illustration created with BioRender.com). To determine the thermal response curve of *Geminigera cryophila*, cultures were grown at the medium light (ML) intensity of 100 μmol photons m^{-2} s^{-1} and at the ambient pCO_2 of 400 μatm in triplicate 1 L custom-made cylindrical glass bottles under a range of temperatures, starting at 2°C and then gradually transferred to 4°C, 6°C, 7°C, and 8°C. At 8°C *G. cryophila* died. Based on the thermal response, for the main experiment *G. cryophila* was grown at 2°C, 4°C, and 6°C. Each temperature treatment was then combined with two pCO_2 levels (white color: ambient pCO_2 of 400 μatm; yellow: high pCO_2 of 1000 μatm) and two light intensities (medium light and high light). Except for the 6°C-1000-ML treatment, all other 6°C treatments died. To test whether the 6°C-1000-ML treatment could recover from warming stress, it was transferred back to 4°C.

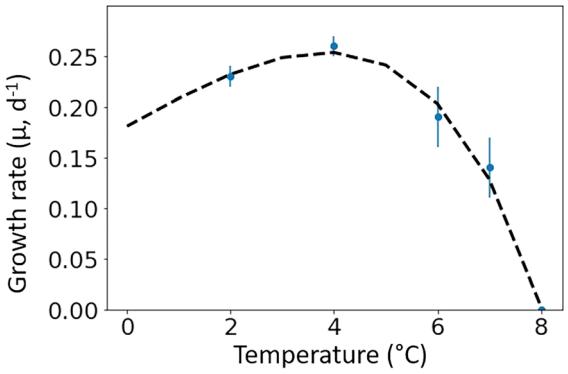

Fig. 2. Thermal functional response curve showing the specific growth rates (μ) of *Geminigera cryophila* at 400 μatm pCO_2 and 100 μmol photons m^{-2} s^{-1} across a range of temperatures from 2°C to 8°C. Values represent the mean and standard deviation ($n = 3$).

during sampling. The starting cell density of cultures in the main experiment was ca. 1000 cells mL^{-1} and final sampling was conducted when densities reached ca. 15,000–20,000 cells mL^{-1}, this ensured a stable carbonate chemistry over the whole experimental time (Table 1).

Due to the small volume of the incubation bottles (ca. 1 L), dilutions were done and final sampling were conducted in batches. This was to make sure that we have enough biomass for each parameter and cell densities are not too high, thus avoiding a shift in the carbonate chemistry as well as potential cell self-shading. In total, the main experiment lasted ca. 10–20 d depending on the treatments. Please note that apart from the medium light-high pCO_2 treatment, in all other 6°C treatments *G. cryophila* was not able to maintain exponential growth and stopped growing after ca. 4 weeks (Fig. 3). To test whether the 6°C-1000-medium light treatment of *G. cryophila* would be able to recover from warming, after 11 weeks of incubation we transferred the 6°C-1000-medium light treatment back to 4°C (ca. 2 weeks preacclimation and 1 week in main experiment) (Fig. 1). From this treatment, we collected triplicate samples for particulate organic carbon (POC), pigments, and conducted chlorophyll *a* (Chl *a*) fluorescence measurements, as will be described later. Hence, the main experiment includes 2°C and 4°C treatments and findings from the 6°C-high pCO_2-medium light treatment.

Carbonate chemistry

To ensure that there would be no pH drift (≤ 0.06 pH units) in cultures, the pH (NBS) was measured regularly in all incubation and culture medium bottles over the duration of the whole experiment (Table 1). Measurements were done with a pH meter (826 pH mobile; Metrohm), which was calibrated (3-point calibration) prior to usage with the National Institute of Standards and Technology-certified buffer systems. At the

Table 1. The CO2Sys program (Pierrot et al. 2006) was used to calculate the dissolved inorganic carbon (DIC) concentrations and the partial pressure of CO_2 (pCO_2) from the measured total alkalinity (TA), pH, silicate, phosphate, salinity, and temperature sampled at the end of the experiment. Values represent mean and SD of each pCO_2 level for both light (medium light and high light) and temperature (2°C and 4°C) treatments (incubation, $n = 12$; medium, $n = 8$). Significant differences between the two pCO_2 treatments (post hoc tests) are indicated by varying lower case letters in superscript ($p < 0.05$).

	Target pCO_2 (μatm)	Calculated pCO_2 (μatm)	Measured pH (NBS)	Measured TA (μmol kg^{-1})	Calculated DIC (μmol kg^{-1})
Geminigera incubations	400	430 ± 60^{a}	8.09 ± 0.05^{a}	2314 ± 27^{a}	2192 ± 28^{a}
Medium (no cells)	400	429 ± 68^{a}	8.08 ± 0.05^{a}	2294 ± 51^{ab}	2173 ± 56^{a}
Geminigera incubations	1000	1035 ± 99^{b}	7.73 ± 0.04^{b}	2319 ± 22^{a}	2307 ± 27^{b}
Medium (no cells)	1000	1060 ± 66^{b}	7.72 ± 0.03^{b}	2282 ± 8^{b}	2275 ± 14^{b}

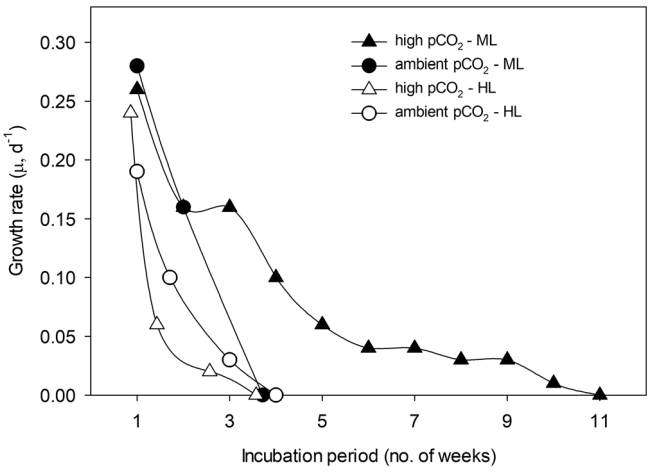

Fig. 3. Growth rates (μ) of *Geminigera cryophila* at 6°C under ambient pCO_2 (400 μatm, filled symbols) and high pCO_2 (1000 μatm, open symbols) in combination with different light intensity (medium light, ML: 100 μmol photons m^{-2} s^{-1}; high light, HL: 500 μmol photons m^{-2} s^{-1}) treatments. All high light treatments and the ambient pCO_2-medium light cultures died after 4 weeks of incubation. Main experiment for the high pCO_2-medium light treatment was aborted as growth stopped.

end of the experiment, samples for total alkalinity (TA) analysis were collected from all incubation and medium bottles by filtering a sample through a glass fiber filter (GF/F; Whatman) and placing the filtrate into 200 mL borosilicate flasks. TA samples were measured in duplicates by potentiometric titrations via a TW alpha plus (SI Analytics). Systematic errors were corrected with certified reference material (from Prof. A Dickson, Scripps, USA; batch no. 161). TA, pH, silicate, phosphate, temperature, and salinity measurements were used to determine the seawater carbonate chemistry using the CO2Sys program (Pierrot et al. 2006), wherein the equilibrium constant of Mehrbach et al. (1973) refitted by Dickson and Millero (1987) was utilized.

Cell density and thermal functional response curve

Cell densities were regularly monitored and samples were taken at the same time of the day at the start, during, and the end of both the thermal functional response experiment and the main experiment. To this end, a Beckman Multisizer 3 Coulter Counter with a 100 μm aperture was used to determine cell density immediately after sampling. Growth rates (μ; d^{-1}) of *G. cryophila* under all experimental treatments were determined and were calculated using the formula:

$$\mu = \frac{\ln\left(\frac{N_t}{N_0}\right)}{t}, \quad (1)$$

where N_t refers to the cell density during the final harvest and N_0 to the one at the start of the experiment. The duration between both sampling points is represented by t. To describe the thermal growth response curve of *G. cryophila*, a modified Ratkowsky equation (Ratkowsky et al. 1983; Zwietering et al. 1991) was used:

$$\mu_{max} = [b(T - T_{min})]^2 \times \left\{1 - e^{[c(T - T_{max})]}\right\} \quad (2)$$

where μ_{max} is the maximum specific growth rate, T_{min} and T_{max} are the minimum and maximum temperatures, respectively, at which the growth rate is zero, while b and c are Ratkowsky parameters that possess no specific biological meaning. The optimum temperature for growth (T_{opt}) was derived from the fitted curve as the temperature at which the growth rate was the highest.

Pigments

At the end of the experiment, pigment samples were collected by filtering the cultures onto GF/F filters (~ 0.6 μm, 25 mm; Whatman) and directly freezing them in liquid nitrogen. After storage at −80°C, the extraction and Chl *a* and chlorophyll c_2 (Chl c_2) analysis was done as described in Camoying et al. (2022). To calculate cellular quotas, Chl *a* and Chl c_2 contents were normalized to filtered volume and cell densities.

POC and particulate organic nitrogen quotas

At the end of the experiment, samples for POC and particulate organic nitrogen (PON) were collected by gently filtering (< 20 mmHg) cultures onto precombusted glass fiber filters

(15 h, 200°C, GF/F, ~ 0.6 μm, 25 mm; Whatman). Filters were then stored at −20°C and were oven-dried first overnight (> 12 h, 60°C) before acidifying them with 200 μL of 0.2 N HCl. The acidified filters were again oven-dried (> 12 h, 60°C) and analyzed on an automated carbon nitrogen elemental analyzer (EURO EA-CN Elemental Analyzer; HEKAtech GmbH). Samples for blank measurements were also prepared. In order to determine cellular quotas, the blank-corrected POC/PON values were normalized with the filtered volume and cell densities. To calculate cellular daily production rates of POC and PON, cellular quotas were multiplied by the corresponding growth rate of the respective treatment. Molar ratios of carbon to nitrogen (C : N) were also calculated.

Photophysiology

A Fast Repetition Rate fluorometer (FastOcean PTX; Chelsea Technologies Group Ltd.) coupled with a FastAct Laboratory system (Chelsea Technologies Group Ltd.) was used to assess the photophysiological response of *G. cryophila* under all pCO_2-temperature-light treatments at the end of the experiment. Prior to the Chl *a* fluorescence measurements, cells were dark-adapted for 10 min at the respective growth temperature to ensure open photosystem II (PSII) reaction centers and no occurrence of non-photochemical quenching. The minimum Chl *a* fluorescence (F_0) was recorded immediately after the dark-acclimation phase. To gradually saturate PSII, a single turnover flashlet of 1.2×10^{22} photons $m^{-2}\,s^{-1}$ and a wavelength of 450 nm was applied consisting of 100 flashlets on a 2 μs pitch. A relaxation phase of 40 flashlets on a 50 μs pitch was subsequently done. This combination of saturation-relaxation phases was reiterated 6 times for every acquisition. To determine the maximum (F_m) Chl *a* fluorescence, the saturation phase of the single turnover was fitted according to Kolber et al. (1998). The dark-adapted maximum quantum yield of photosynthesis of PSII (F_v/F_m) was then calculated using the equation:

$$F_v/F_m = \frac{(F_m - F_0)}{F_m}. \quad (3)$$

The energy transfer between PSII units (i.e., connectivity, *P*), the functional absorption of PSII photochemistry (σ_{PSII}) and the concentration of functional PSII reaction centers ([RCII]) were also determined from the single turnover measurement of the dark-adapted cells.

Fluorescence light curves were also done, which lasted in total for ca. 1 h. During the fluorescence light curves, cells were exposed to increasing light intensities (30–900 μmol photons $m^{-2}\,s^{-1}$) for 5 min per light step. After each light intensity, six Chl *a* fluorescence measurements were carried out. The light-adapted minimum (F') and maximum (F_m') Chl *a* fluorescence of the single turnover acquisition were estimated from these measurements. The effective PSII quantum yield under ambient light (F_q'/F_m') was calculated according to the equation $(F_m' - F')/F_m'$ (Genty et al. 1989). The absolute electron transport rates (ETR) were calculated following Suggett et al. (2004, 2009):

$$\mathrm{ETR} = \sigma_{PSII} \times \left(\frac{F_{q'}/F_{m'}}{F_v/F_m}\right) \times E, \quad (4)$$

where σ_{PSII} is the functional absorption cross-section of PSII's photochemistry (nm^2) and *E* the instantaneous irradiance (photons $m^{-2}\,s^{-1}$). Irradiance-dependent ETRs were curve-fitted according to Ralph and Gademann (2005) to determine maximum ETR (ETR_{max}), minimum saturating irradiance (I_k) and maximum light utilization efficiency (α).

Statistical analyses

A three-way ANOVA with Tukey's multiple comparison post hoc tests was done using Graphpad Prism 9 Statistical Software. The independent variables consisted of two temperatures (2°C and 4°C), two light intensities (100 and 500 μmol photons $m^{-2}\,s^{-1}$) and two pCO_2 levels (400 and 1000 μatm). The interactive effects of the three factors temperature, light, and pCO_2 were examined on all parameters. Graphs were created using SigmaPlot 12.0 (Systat Software, Inc.). All statistical tests were done at the 95% confidence interval. Python 3.8 was used to generate the corresponding thermal response curve by performing curve fitting on the measured growth rates with the modified Ratkowsky equation (using *scipy* curve fit function).

Results

Seawater carbonate chemistry

A stable carbonate chemistry was maintained throughout the course of the experiment (Table 1). For both *G. cryophila* incubations (containing cells) and culture medium (without cells) bottles, pCO_2, pH, and DIC values were significantly different between all ambient pCO_2 and OA treatments ($p < 0.0001$). Among the incubation bottles, TA remained the same irrespective of the applied pCO_2 level (Table 1).

Thermal functional response curve

Growth of *G. cryophila* was strongly influenced by increasing temperature (Fig. 2). Measured growth rate increased from 2°C to 4°C and started to decline at 6°C until growth stopped at 8°C. Based on the thermal response curve of *G. cryophila*, the optimum temperature (T_{opt}) for maximum growth ($\mu_{max} = 0.25$) of the cryptophyte was at 3.80°C. The maximum (T_{max}) temperature, wherein positive growth could still be maintained, was 8.02°C.

Growth, carbon production, and pigment cellular concentration

High pCO_2 did not affect the growth of *G. cryophila* in all treatments (Fig. 4A). In response to increasing temperature up to 4°C, growth was generally significantly enhanced

irrespective of the applied light intensity and pCO_2 level ($p < 0.0001$). Only under medium light and high pCO_2 conditions, increasing temperature did not alter growth. A significant medium light effect ($p < 0.01$) on growth was evident, as growth rates were significantly reduced in the 2°C treatment under each pCO_2 level. At 4°C, growth remained unchanged with increasing irradiance. A significant interactive effect was observed only between temperature and light ($p < 0.05$; Table 2).

For the 6°C-medium light-400 treatment, growth was reduced by 73% after 2 weeks of incubation (Fig. 3; Table 3) relative to the 4°C-medium light-400 treatment (Fig. 4A). After 4 weeks of incubation, the 6°C-400-medium light cells stopped growing. Only under high pCO_2, the medium light treatment grew very slowly at 6°C, and finally stopped growing after 11 weeks (Fig. 3; Table 3). Moreover, the latter exhibited morphological changes typical for unhealthy cells such as compromised cell membrane (i.e., bubble-like formation) and the appearance of hair-like projections (Supporting Information Fig. S1). When the 6°C-medium light-1000 treatment was transferred back to 4°C, it recovered and exhibited growth rates ($\mu = 0.27 \pm 0.01$ d^{-1}; Table 3) comparable to the 4°C-medium light-400 treatment ($\mu = 0.26 \pm 0.01$ d^{-1}; Fig. 4A).

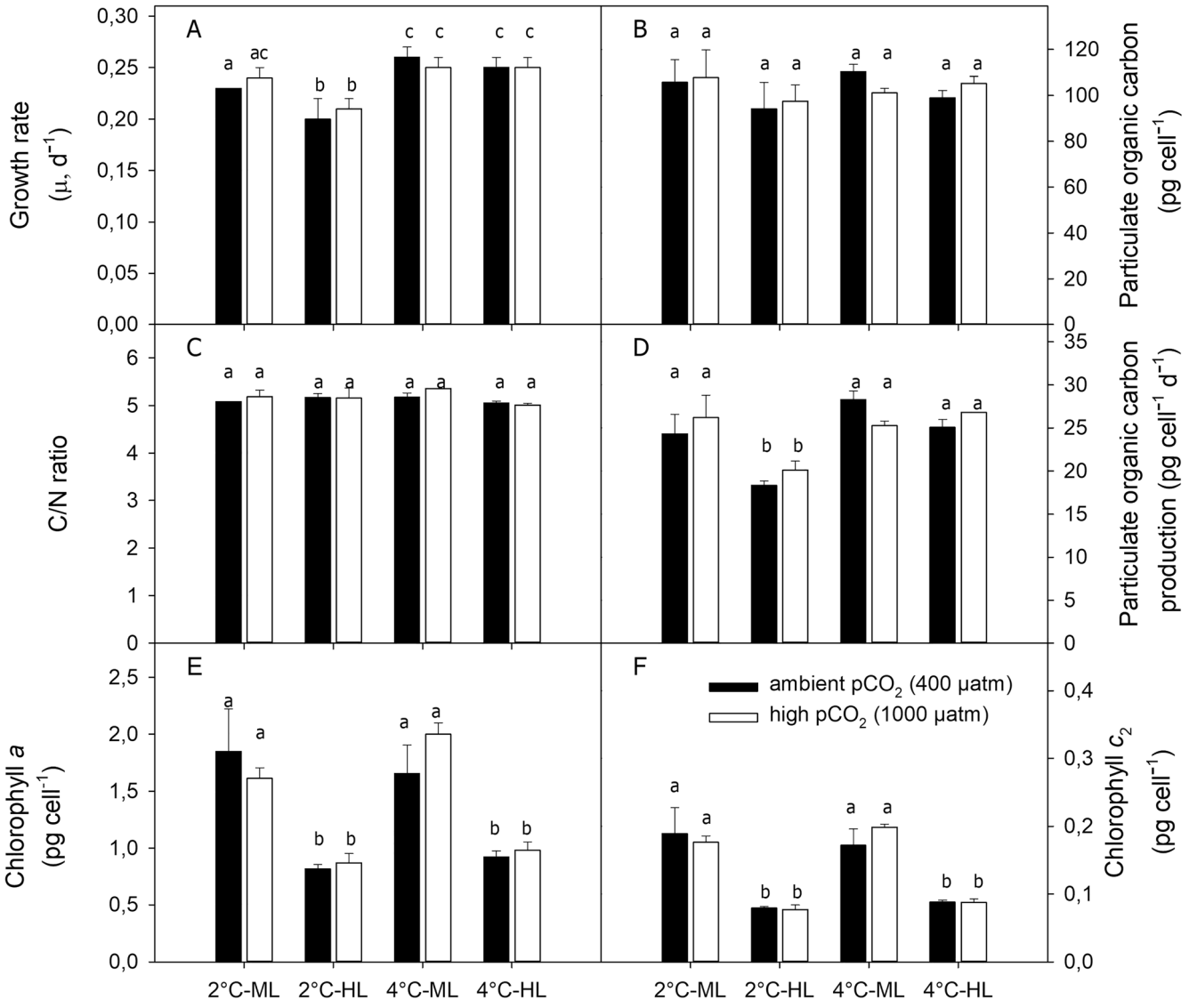

Fig. 4. Growth rates (**A**), cellular particulate organic carbon (POC) contents (**B**), molar carbon to nitrogen (C/N) ratios (**C**), POC production rates (**D**), and cellular concentrations of chlorophyll *a* (**E**) and chlorophyll c_2 (**F**) of *Geminigera cryophila* were determined under ambient pCO_2 (400 μatm, dark bars) and high pCO_2 (1000 μatm, white bars) in combination with different temperature (2°C and 4°C) and light (medium light, ML: 100 μmol photons m^{-2} s^{-1}; high light, HL: 500 μmol photons m^{-2} s^{-1}) treatments at the end of the experiments. Values represent the mean and standard deviation ($n = 3$). Significant differences between the two pCO_2 treatments (post hoc tests) are indicated by varying lower case letters ($p < 0.05$).

Table 2. Significance of interactive effects of pCO_2, light and temperature ($p < 0.05$) on the growth rate (μ), particulate organic carbon (POC) quota and production, C : N ratio, cellular chlorophyll *a* (Chl *a*) and chlorophyll c_2 (Chl c_2) concentrations, as well as the dark-adapted maximum photosystem II quantum yield (photosynthetic yield, F_v/F_m), yield recovery (F_v/F_m recovery), energy transfer between photosystem II units (connectivity, *P*), functional absorption cross-section of PSII (σ_{PSII}), reoxidation times of the primary electron acceptor Q_a (τ_{Qa}), cellular concentration of functional PSII reaction centers ([RCII]), maximum electron transport rates (ETR_{max}), minimum saturating irradiance (I_k), and the maximum light utilization efficiency (α) of *Geminigera cryophila*. Statistically insignificant effects ($p > 0.05$) are denoted by n.s.

Parameters	pCO_2	Light	Temperature	Temperature and light	Temperature and pCO_2	Light and pCO_2	Temperature, light, and pCO_2
Growth	n.s.	<0.05	<0.0001	<0.05	n.s.	n.s.	n.s.
POC content	n.s.	n.s.	n.s.	n.s.	n.s.	n.s.	n.s.
POC production	n.s.	0.0001	<0.0001	<0.05	n.s.	n.s.	n.s.
C : N	n.s.	n.s.	n.s	<0.05	n.s.	n.s.	n.s.
Chl *a*	n.s.	<0.0001	n.s.	n.s.	n.s.	n.s.	n.s.
Chl c_2	n.s.	<0.0001	n.s.	n.s.	n.s.	n.s.	n.s.
F_v/F_m	<0.05	<0.0001	0.0001	<0.05	<0.05	<0.05	n.s.
F_v/F_m recovery	n.s.	<0.0001	n.s.	<0.05	n.s.	n.s.	n.s.
P	<0.05	<0.0001	<0.05	n.s.	<0.05	n.s.	n.s.
σ_{PSII}	<0.05	<0.05	<0.05	n.s.	n.s.	n.s.	<0.05
τ_{Qa}	<0.05	<0.0001	n.s.	n.s.	n.s.	n.s.	n.s.
[RCII]	<0.05	<0.0001	<0.05	<0.05	<0.05	<0.05	n.s.
ETR_{max}	n.s.	<0.0001	<0.05	<0.05	n.s.	n.s.	n.s.
I_k	n.s.	<0.0001	<0.05	<0.05	n.s.	n.s.	n.s.
α	<0.05	<0.05	n.s.	n.s.	n.s.	n.s.	n.s.

Table 3. Growth rate (μ), particulate organic carbon (POC) quota and production, as well as cellular chlorophyll *a* (Chl *a*) and chlorophyll c_2 (Chl c_2) concentrations of *Gemingera cryophila* were determined after 2, 8, and 11 weeks of incubation at 6°C and medium light (ML) in conjunction with ambient pCO_2 (400) and high pCO_2 (1000). Please note that after 11 weeks, the 6°C-medium light-1000 was transferred back to 4°C, referred here as the recovered 6°C-ML-1000 treatment. After 4 weeks of incubation at 4°C, the same physiological parameters were also determined for the recovered 6°C-ML-1000 cells. Values represent the mean and standard deviation ($n = 3$).

Treatment	Incubation period	μ (d^{-1})	POC (pg $cell^{-1}$)	POC production (pg $cell^{-1}$ d^{-1})	Chl *a* (pg $cell^{-1}$)	Chl c_2 (pg $cell^{-1}$)
6°C-ML-400	2 weeks	0.19 ± 0.01	121 ± 1	23 ± 1	1.85 ± 0.04	0.17 ± 0.03
6°C-ML-1000	8 weeks	0.03 ± 0.01	231 ± 4	7 ± 2	No data	No data
6°C-ML-1000	11 weeks	0.00 ± 0.00	No data	No data	1.14 ± 0.04	0.15 ± 0.03
Recovered 6°C-ML-1000	4 weeks	0.27 ± 0.01	121 ± 16	33 ± 4	1.78 ± 0.25	0.17 ± 0.02

The cellular POC contents and C/N ratios remained unchanged in all treatments irrespective of the applied environmental factor (Fig. 4B,C). While pCO_2 did not affect the POC production of the cryptophyte, temperature ($p < 0.0001$) and high light ($p < 0.0001$) alone strongly altered POC production (Table 2). There was a significant interaction between temperature and light on POC production of the cryptophyte ($p < 0.05$; Fig. 4D; Table 2), with the lowest POC production rates observed in the two 2°C-high light treatments, whereas values were similar in all other treatments. For the 6°C-medium light-400 treatment, growth continuously decreased and cellular POC quotas were enhanced compared to the 2°C- and 4°C-medium light-400 treatments after just 2 weeks of incubation (Fig. 4B; Table 3). Although POC quota were highest in the 6°C-medium light-1000 treatment at 8-week incubation (Table 3), the latter had the lowest POC production among all treatments (Fig. 4D; Table 3). However, when transferred back to 4°C after 11 weeks of incubation under 6°C-medium light-400 treatment, cells exhibited similar high POC production rates (Table 3) as cells grown at 4°C-medium light-400 (Fig. 4D).

Cellular Chl *a* and Chl c_2 quotas of *G. cryophila* were only influenced by high light alone ($p < 0.0001$; Fig. 4E,F). In response to increasing irradiance ($p < 0.0001$), cellular pigment concentrations were reduced regardless of the applied temperature or pCO_2 level. As for the 6°C-medium light-400 treatment

after 2-week incubation, pigment concentrations were comparable to that of the 2°C and 4°C at medium light (Fig. 4E,F; Table 3). The 6°C-medium light-1000 lowered its Chl *a* concentration after 11 weeks of incubation (1.14 ± 0.04 pg cell^{-1}), but increased its Chl *a* content again (1.78 ± 0.25 pg cell^{-1}) after transferring it back to 4°C (Table 3).

Photophysiology

The dark-adapted maximum quantum yield of PSII (photosynthetic yield, F_v/F_m) was similarly influenced by high pCO_2 temperature and irradiance (Fig. 5A). A significant pCO_2 effect on photosynthetic yield ($p < 0.05$) was observed only in the 2°C-medium light treatment, wherein values increased in response to high pCO_2.

No temperature effect was observed in the yield across all high light treatments, while at medium light increasing temperature (4°C) led to a significant increase in photosynthetic yield ($p < 0.0001$) only under ambient pCO_2, but had no effect under high pCO_2. Hence, there was a significant interaction between temperature and pCO_2 on photosynthetic yield ($p < 0.05$; Fig. 5A). Increasing irradiance had a negative effect on the yield in all treatments ($p < 0.0001$) except for the 2°C-400 treatment, wherein values remained unchanged (Fig. 5A). Cellular concentrations of functional PSII reaction centers ([RCII]) were affected by each environmental factor alone (light: $p < 0.0001$; pCO_2: $p < 0.05$; temperature: $p < 0.05$) as well as their combination in that highest [RCII] was seen in the 2°C-400-medium light treatment (Fig. 5B; Table 2). In response to high pCO_2, [RCII] in the 2°C-medium light treatment was reduced by 33% ($p < 0.05$) while it remained the same in all other treatments. Increasing temperature (up to 4°C) significantly reduced the concentration of reaction centers under medium light-400 while a negative high light effect was observed only in the 2°C-400 treatment (Fig.5B). Different from increasing temperature, high light ($p < 0.0001$) alone significantly influenced the reoxidation times of the primary electron acceptor Qa (τ_{Qa}), with high irradiance significantly reducing τ_{Qa} in both temperature treatments irrespective of pCO_2 level ($p < 0.0001$) (Fig. 5C).

The 6°C-medium light-400 (2-week incubation) exhibited comparable photosynthetic yield, *P*, [RCII], and τ_{Qa} values to that of the 2°C- and 4°C-medium light treatments (Fig. 5; Tables 4). However, the 6°C-medium light-1000 treatment decreased its photosynthetic yield while increasing the number of PSII reaction centers after 11 weeks of incubation. When the latter was transferred back to 4°C, cells fully recovered and shared the same photophysiological characteristics (photosynthetic yield, *P*, σ_{PSII}, τ_{Qa}; Table 4**)** with that of the 4°C-400-medium light treatment (Fig. 5; Supporting Information Table S1).

The different treatments distinctively affected the magnitude and shape of absolute ETRs (Fig. 6A,B). While light ($p < 0.0001$) and temperature ($p < 0.05$) alone and their combination ($p < 0.05$) had a significant effect, pCO_2 had no influence on ETR_{max} (Supporting Information Table S1). Increasing

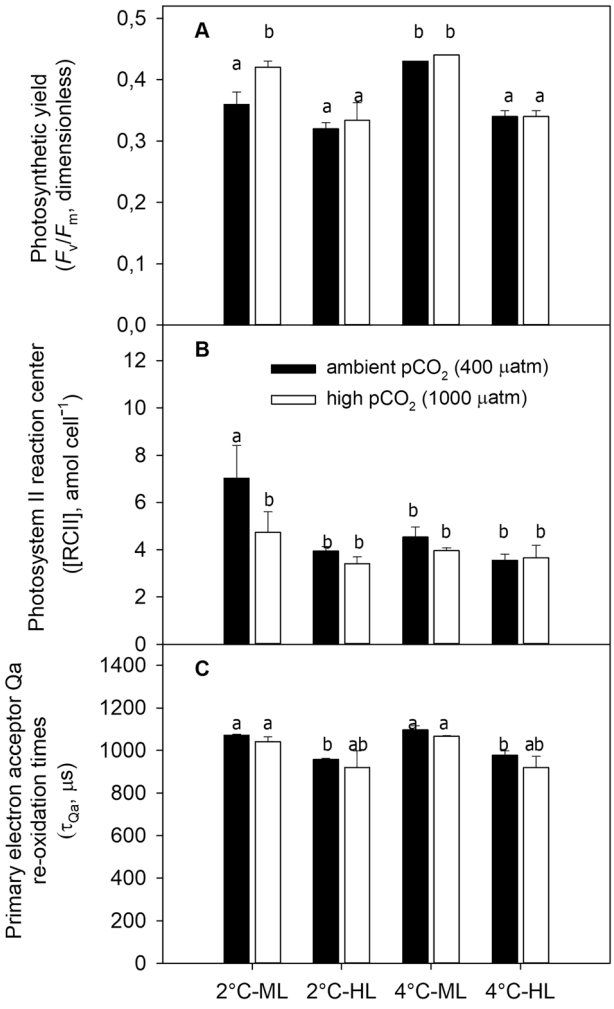

Fig. 5. The dark-adapted maximum photosystem II quantum yield (photosynthetic yield, F_v/F_m) (**A**), cellular concentration of functional PSII reaction centers ([RCII]) (**B**), and reoxidation times of the primary electron acceptor Qa (τ_{Qa}) of *Geminigera cryophila* were determined under ambient pCO_2 (400 μatm, dark bars) and high pCO_2 (1000 μatm, white bars) in combination with different temperature (2°C and 4°C) and light intensity (medium light, ML: 100 μmol photons m^{-2} s^{-1}; high light, HL: 500 μmol photons m^{-2} s^{-1}) treatments at the end of the experiments. Values represent the mean and standard deviation ($n = 3$). Significant differences between the two pCO_2 treatments (post hoc tests) are indicated by varying lower case letters ($p < 0.05$).

temperature decreased ETR_{max} in the high light-400 treatment (Table 4). High light resulted in higher ETR_{max} values relative to medium light irrespective of temperature and pCO_2. ETRs of the 6°C treatments (400 and 1000 pCO_2 at medium light) were significantly reduced (Fig. 6C).

Discussion

The single effect of high pCO_2 on *G. cryophila*

Previous studies have reported no stimulatory effect of high pCO_2-alone on growth of several Antarctic phytoplankton

Table 4. The dark-adapted maximum photosystem II quantum yield (photosynthetic yield, F_v/F_m), energy transfer between photosystem II units (connectivity, *P*), cellular concentration of functional PSII reaction centers ([RCII]), the functional absorption cross-section of PSII (σ_{PSII}), reoxidation times of the primary electron acceptor Q_a (τ), maximum electron transport rates (ETR_{max}), minimum saturating irradiance (I_k), and the maximum light utilization efficiency (α) of *Geminigera cryophila* were determined after 2 and 11 weeks of incubation at 6°C and medium light in conjunction with 400 μatm (400) and 1000 μatm (1000) pCO_2. Please note that after 11 weeks, the 6°C-medium light-1000 treatment was transferred back to 4°C, referred here as the recovered 6°C-medium light-1000 treatment. After 4 weeks of incubation at 4°C, the same photophysiological parameters were also determined for the recovered 6°C-medium light-1000 cells. Values represent the mean and standard deviation ($n = 3$).

Treatment	Incubation period	F_v/F_m (dimensionless)	*P* (dimensionless)	[RCII] (amol cell^{-1})	σ_{PSII} nm^2 PSII^{-1}	τ_{Qa} (μs)	ETR_{max} (e$^-$ PSII^{-1} s^{-1})	I_k (μmol photons m^{-2} s^{-1})	α (rel. unit)
6°C-medium light-400	2 weeks	0.40 ± 0.04	0.40 ± 0.07	6.12 ± 0.38	3.76 ± 0.27	1280 ± 156	56 ± 0	19 ± 5	3.12 ± 0.70
6°C-medium light-1000	11 weeks	0.30 ± 0.04	0.24 ± 0.04	8.57 ± 0.13	3.65 ± 0.38	1049 ± 55	70 ± 5	28 ± 11	2.65 ± 0.75
Recovered 6°C-medium light-1000	4 weeks	0.45 ± 0.01	0.44 ± 0.01	3.45 ± 0.20	4.29 ± 0.18	1065 ± 32	120 ± 26	49 ± 24	2.68 ± 0.67

species, in particular, even negative high pCO_2 effects were found for Antarctic diatoms in conjunction with high irradiance (Trimborn et al. 2013, 2017*a*; Hoppe et al. 2015; Heiden et al. 2016, 2018). Different to diatoms, flagellates such as *Phaeocystis antarctica* (Trimborn et al. 2017*a*,*b*; Koch et al. 2019) and cryptophytes (Domingues et al. 2014; Sommer et al. 2015; Schulz et al. 2017) seem to be tolerant to ocean acidification even in combination with other environmental factors including high irradiance, iron or warming. Our results are in line with this, as we also show here that growth and POC production of *G. cryophila* were not influenced by increasing pCO_2 under any of the applied light levels (Fig. 4A,D). Our observations are consistent with the results from the same *G. cryophila* strain showing either no (20 and 200 μmol photons m^{-2} s^{-1}, respectively; Trimborn et al. 2019) or a modest stimulatory (100 μmol photons m^{-2} s^{-1}; Camoying et al. 2022) high pCO_2 effect in conjunction with low and medium irradiance.

Previous studies have reported the increased susceptibility of temperate phytoplankton (Chen and Gao 2011; Li and Campbell 2013) and several Antarctic diatoms (e.g., Trimborn et al. 2017*b*; Heiden et al. 2018) to photodamage as a result from high pCO_2. In fact, diatoms were found to be prone to PSII photoinactivation in particular under high pCO_2 and high irradiance (Chen and Gao 2011; Li and Campbell 2013; Trimborn et al. 2017*a*) which may be attributed to the decreased PSII D2 protein turnover rate caused by high pCO_2 (Gao et al. 2018). Indeed, in our study, the number of functional PSII was significantly reduced under high pCO_2 and medium light in *G. cryophila* (Fig. 5B), but this was efficiently counteracted by an increased connectivity between photosystems (*P*) (Supporting Information Table S1), thus ensuring a more efficient distribution of photons among PSII preventing thereby photodamage (Fig. 5C). As in Trimborn et al. (2019), our results indicate that *G. cryophila* was not stressed by high pCO_2 at medium light and 2°C as no further photophysiological adjustments were required (Fig. 5; Supporting Information Table S1).

The single effect of high light on *G. cryophila*

In our study, under ambient pCO_2 and 2°C, increasing light intensity (between 100 and 500 μmol photons m^{-2} s^{-1}) led to a significant reduction in growth of the cryptophyte (Fig. 4A). This is consistent with the previously reported sensitivity of the same strain of *G. cryophila* to high irradiance, where under ambient pCO_2, it was even unable to grow at the highest irradiance of 500 μmol photons m^{-2} s^{-1} (Trimborn et al. 2019). As a common photoacclimation response of phytoplankton to increasing irradiance (Kropuenske et al. 2010; Trimborn et al. 2019), the cryptophyte reduced the cellular concentration of the light-harvesting pigments (Fig. 4E,F) and the number of functional PSII reaction centers (Fig. 5B). POC production rates of the cryptophyte were also strongly reduced (Fig. 4D) which could be due to potential oxidative

stress in the cells from high light exposure (Häder et al. 2015). Higher ETR_{max}, minimum saturating irradiance (I_k), as well as lower light utilization efficiency, were found (Supporting Information Table S1), which suggests a saturation of the Calvin cycle and therewith the need for alternative electron cycling to dissipate the excessive light energy. There was also faster reoxidation of the primary electron acceptor Q_a (τ_{Qa}; Fig. 5C), potentially indicating that the cryptophyte depended on additional electron acceptors such as the Mehler reaction, which is a commonly observed photoprotective mechanism of phytoplankton when exposed to high light intensities (Kranz et al. 2010; Roberty et al. 2014). Under stressful conditions such as suboptimal temperatures and high irradiances, phytoplankton were also reported to enhance lipid production (e.g., Dong et al. 2016; Jaussaud et al. 2020) as lipids are good energy sinks, in particular under excess light (Klok et al. 2013). It could be that the excess light energy was used by the cryptophyte for lipid anabolism, which requires large quantities of ATP and NADPH (Jónasdóttir 2019). In fact, we observed the presence of lipid droplets on *G. cryophila* cells at 2°C (Supporting Information Fig. S2A). Apparently, these photoacclimation characteristics ensured that high light-acclimated cells were able to cope well with short-term high light stress as they had higher yield recovery values compared with the cells grown in medium light under ambient pCO_2 and 2°C (Supporting Information Table S1).

Overall, our results are in line with the observation of Trimborn et al. (2019) that growth and carbon fixation of *G. cryophila* are greatly reduced by high light under ambient pCO_2.

The single effect of high temperature on *G. cryophila*

Aside from iron availability, increasing temperature has been reported to strongly affect phytoplankton productivity in the Southern Ocean under ambient pCO_2 (e.g., Rose et al. 2009; Boyd et al. 2015; Spackeen et al. 2018) and was found to stimulate growth of various Antarctic diatoms (Fiala and Oriol 1990), even under low iron concentrations (Hutchins and Boyd 2016; Zhu et al. 2016). Indeed, the increased temperature was beneficial for *G. cryophila* as its growth and photochemical efficiency were enhanced under ambient pCO_2 and medium light (Figs. 4A, 5A), similar to observations in other Antarctic phytoplankton (e.g., Cheah et al. 2013; Andrew et al. 2019). The higher temperature decreased the appearance of lipid droplets on *G. cyophila* cells (Supporting Information Fig. S2B). Lipid droplets are commonly observed for this cryptophyte species (Deane et al. 2002), and the decrease in the lipid content of *G. cryophila* in response to warming may influence its biochemical composition, which in turn could influence the Antarctic marine food web.

Antarctic phytoplankton usually grows under suboptimal temperatures (~ 0–2°C) and have their calculated optimal growth temperature (T_{opt}) at 5.2°C (Coello-Camba and Agustí 2017). In our study, under ambient pCO_2 and medium light, the calculated T_{opt} for *G. cryophila* was 3.8°C (Fig. 2). This temperature is indeed lower than the calculated value for Antarctic phytoplankton in general (Coello-Camba and Agustí 2017) and fits well the observations of Wang and Smith (2021), which reported a T_{opt} of 4°C for another *G. cryophila* strain. Different to *G. cryophila*, the Antarctic haptophyte *P. antarctica* (Zhu et al. 2017; Andrew et al. 2019) and the diatoms *Chaetoceros flexuosus* and *Thalassiosira antarctica* showed enhanced growth in response to increased temperature up to 5°C (Andrew et al. 2019) while the diatom *Pseudo-nitzschia subcurvata* exhibited highest growth at 8°C (Zhu et al. 2017). Moreover, *G. cryophila* had the lowest maximal thermal limit (T_{maxlim}) at 8°C compared to *P. antarctica* and *P. subcurvata*,

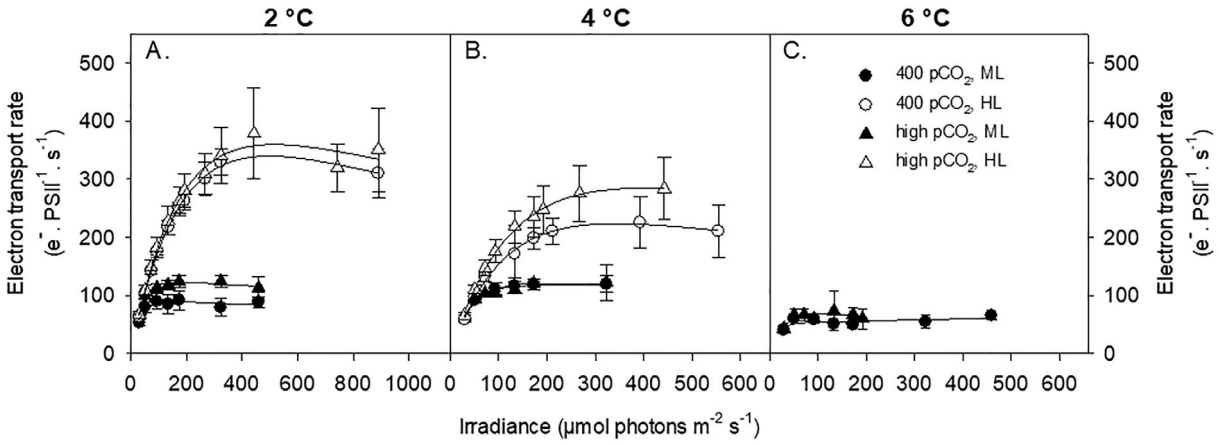

Fig. 6. Absolute electron transport rates were measured in *Geminigera cryophila* grown under ambient pCO_2 (400 μatm, circle) and high pCO_2 (1000 μatm, triangle) in combination with different temperature (2°C (**A**), 4°C (**B**), and 6°C (**C**)) and light intensities (filled symbols, ML, 100 μmol photons m^{-2} s^{-1}; open symbols; HL, 500 μmol photons m^{-2} s^{-1}) at the end of the experiments. Please note that for the 6°C treatment, after 11 weeks of incubation, the unhealthy 6°C-medium light-1000 cells (filled triangle) were transferred back to 4°C to test whether they would be able to recover from exposure to temperature above T_{opt}. Values represent the mean and standard deviation ($n = 3$).

which had their T_{maxlim} at 10°C and 14°C, respectively (Buma et al. 1991; Zhu et al. 2017). Hence, in comparison to other species, the cryptophyte *G. cryophila* had a narrow thermal limit. This indicates that the cryptophyte *G. cryophila* may be less competitive to haptophytes and diatoms under future increased temperatures in the Southern Ocean.

The combined effects of increased temperature, light, and pCO_2

Interestingly, the previously observed negative effects of high light on growth and POC production at 2°C were alleviated at 4°C, as at T_{opt} growth and POC production remained unchanged between medium light and high light under ambient pCO_2 (Fig. 4A,D). This may indicate that at T_{opt}, the generally faster enzymatic reactions might have enabled the cryptophyte to keep up with the high excitation pressure from exposure to high light. Indeed, faster carboxylation rates of RubisCO were previously observed in Antarctic phytoplankton under warming (Young et al. 2015*b*). Increasing temperature in combination with high pCO_2 even promoted the growth of the cryptophyte under high light (Fig. 4A). Under these conditions, to reduce HL stress the cryptophyte rearranged its photophysiological machinery to capture less light. As a consequence, it had less pigments and PSII (Figs. 4E,F, 5B), lowering thereby its light saturation point (Supporting Information Table S1). Still, this did not prevent ETR_{max} to be increased (Supporting Information Table S1). Hence, the excess light energy was potentially drained via additional electron acceptors such as Mehler, as indicated by the faster τ_{Qa} (Fig. 5C). Similar to the temperate cryptophyte *Teleaulax amphioxeia* (Gaillard et al. 2020), *G. cryophila* was mainly influenced by temperature and irradiance and not by high pCO_2. Based on our results, it becomes evident that the previously observed negative effects of high light alone on growth of the cryptophyte were alleviated by warming. This suggests that under future climatic condition, where both warming as well as higher light availability are expected, both environmental factors (warming up to 4°C and light intensities up to 500 μmol photons m^{-2} s^{-1}) together could stimulate growth of *G. cryophila* in the future.

Exposure to 6°C impacts the growth of *G. cryophila*

Temperatures between 6°C and 9°C were reported to be already lethal to several Antarctic diatoms (i.e., *Corethron criophila*, *Nitzschia* spp., *Synedra* sp.) (Fiala and Oriol 1990). Results of our study are in line with this previous finding as we also observed that growth and POC production of *G. cryophila* were severely impacted at 6°C (Fig. 3; Table 3). Compared to the 2°C- and 4°C-medium light-400 treatments, POC quotas of the 6°C-medium light-400 (2-week incubation time; Table 3) were enhanced but this did not lead to increased POC production due to the lowered growth. In fact, ETRs were dramatically reduced under this treatment relative to the 4°C-400-medium light treatment (60 e^- $PSII^{-1}$ s^{-1} [2-week incubation time; Table 4] and 130 e^- $PSII^{-1}$ s^{-1} [Supporting Information Table S1], respectively). After 4 weeks of incubation, the 6°C-medium light-400 already stopped growing, indicating that *G. cryophila* was unable to survive at 6°C under ambient pCO_2. It was only the 6°C-medium light-1000 which was able to somehow sustain a very minimal growth until ca. 10 weeks of incubation (Fig. 3). As for the photophysiological response, the unhealthy cells of the 6°C-medium light-1000 treatment (11 weeks incubation) showed reduced photosynthetic yield, as indicated by the lower F_v/F_m values (0.30 ± 0.04; Table 4) relative to the ones of the 4°C-medium light-1000 treatment (0.44 ± 0.00) (Fig. 5A). This in line with the observation that thermal stress can also cause physical dissociation of the PSII reaction centers and the light-harvesting complex (Armond et al. 1980). In addition, the 6°C-medium light-1000 (11-week incubation) also had the highest concentration of PSII reaction centers (Table 4) among all other experimental treatments (Fig. 5B). As observed in the cyanobacteria *Synechocystis* sp. (Ueno et al. 2016), exposure to temperatures above T_{opt} might have led to more efficient PSII repair in *G. cryophila*, potentially resulting from supposedly enhanced production of the D1 protein, which is a key subunit of PSII. Overall, our results suggest that although growth of the cryptophyte was strongly impacted at 6°C, the high pCO_2-medium light treatment was able to maintain functional reaction centers, enabling it to still fix carbon. But clearly, these results further show that the cells were unable to keep this physiological state as after 11 weeks of incubation at the growth temperature of 6°C, *G. cryophila* did not survive.

In summary, *G. cryophila* was drastically impacted by 6°C warming as growth of this treatment stopped after several weeks of incubation. This indicates the inability of the cryptophyte to tolerate supraoptimal temperatures over a longer period. Interestingly, similar to the observation of Trimborn et al. (2019), high pCO_2 somehow had also a beneficial effect on *G. cryophila* under heat stress exposure as it fully recovered once it was transferred back to 4°C. This may be an important finding given that heat waves are becoming more frequent in the Southern Ocean (González-Herrero et al. 2022).

Implications

Consistent with the results of previous studies (Trimborn et al. 2019; Camoying et al. 2022), the Antarctic cryptophyte *G. cryophila* was not affected by high pCO_2. In line with the observations of Trimborn et al. (2019) at ambient temperature (2°C), exposure to high light irrespective of the applied pCO_2 impacted growth and POC production of *G. cryophila*. As in most Antarctic phytoplankton studied so far (e.g., Rose et al. 2009; Zhu et al. 2017; Andrew et al. 2019), a projected 2°C increase in the Southern Ocean temperature would be beneficial for the growth of *G. cryophila*. In fact, increasing temperature up to 4°C even alleviated the negative effects of

high light on the physiology of the cryptophyte. It is interesting to note that under high pCO_2, the cryptophyte was able to fully recover from heat stress (6°C) after transferring it back to 4°C (T_{opt}). This may indicate that *G. cryophila* may have a competitive advantage when exposed to more frequent heat waves (e.g., González-Herrero et al. 2022). However, on a longer term, in a future warming scenario when grown under temperatures higher than 4°C, *G. cryophila* would, however, be outcompeted by other Antarctic phytoplankton groups such as diatoms due to its narrower thermal limit. Hence, similar to the study of Zhu et al. (2017) on Antarctic diatoms and prymnesiophytes, our results indicate that while pCO_2 may not be a major controlling factor for the distribution of cryptophytes in the Southern Ocean, primarily warming and increasing irradiance will control the growth of *G. cryophila* in the future.

Data availability statement

The data that support the findings of this study will be available at PANGAEA after publication (https://www.pangaea.de).

References

Andrew, S. M., H. T. Morell, R. F. Strzepek, P. W. Boyd, and M. J. Ellwood. 2019. Iron availability influences the tolerance of Southern Ocean phytoplankton to warming and elevated irradiance. Front. Mar. Sci. **6**: 681. doi:10.3389/fmars.2019.00681

Armond, P. A., O. Björkman, and L. A. Staehelin. 1980. Dissociation of supramolecular complexes in chloroplast membranes a manifestation of heat damage to the photosynthetic apparatus. Biochim. Biophys. Acta **601**: 433–442. doi:10.1016/0005-2736(80)90547-7

Boyd, P. W., T. L. Sinikka, D. M. Glover, and S. C. Doney. 2015. Biological ramifications of climate-change-mediated oceanic multi-stressors. Nat. Clim. Change **5**: 71–79. doi:10.1038/nclimate2441

Brown, M. S., D. R. Munro, C. J. Feehan, C. Sweeney, H. W. Ducklow, and O. M. Schofield. 2019. Enhanced oceanic CO_2 uptake along the rapidly changing West Antarctic peninsula. Nat. Clim. Change **9**: 678–683. doi:10.1038/s41558-019-0552-3

Brown, M. S., J. S. Bowman, Y. Lin, C. J. Feehan, C. M. Moreno, N. Cassar, A. Marchetti, and O. M. Schofield. 2021. Low diversity of a key phytoplankton group along the West Antarctic peninsula. Limnol. Oceanogr. **66**: 2470–2480. doi:10.1002/lno.11765

Buma, A. G. J., N. Bano, M. J. W. Veldhuis, and G. W. Kraay. 1991. Comparison of the pigmentation of two strains of the prymnesiophyte *Phaeocystis* sp. Neth. J. Sea Res. **27**: 173–182. doi:10.1016/0077-7579(91)90010-X

Camoying, M. G., K. Bischof, J. K. Geuer, B. P. Koch, and S. Trimborn. 2022. In contrast to diatoms, cryptophytes are susceptible to iron limitation, but not to ocean acidification. Physiol. Plant. **174**: e13614. doi:10.1111/ppl.13614

Cheah, W., A. McMinn, F. B. Griffiths, K. J. Westwood, S. W. Wright, and L. A. Clementson. 2013. Response of phytoplankton photophysiology to varying environmental conditions in the sub-Antarctic and polar frontal zone. PLoS One **8**: e72165. doi:10.1371/journal.pone.0072165

Chen, S., and K. S. Gao. 2011. Solar ultraviolet radiation and CO_2-induced ocean acidification interacts to influence the photosynthetic performance of the red tide alga *Phaeocystis globosa* (Prymnesiophyceae). Hydrobiologia **675**: 105–117. doi:10.1007/s10750-011-0807-0

Coello-Camba, A., and S. Agustí. 2017. Thermal thresholds of phytoplankton growth in polar waters and their consequences for a warming polar ocean. Front. Mar. Sci. **4**: 168. doi:10.3389/fmars.2017.00168

Deane, J. A., I. M. Strachan, G. W. Saunders, D. R. A. Hill, and G. I. McFadden. 2002. Cryptomonad evolution: Nuclear 18S rDNA phylogeny versus cell morphology and pigmentation. J. Phycol. **38**: 1236–1244. doi:10.1046/j.1529-8817.2002.01250.x

Dickson, A. G., and F. J. Millero. 1987. A comparison of the equilibrium constants for the dissociation of carbonic acid in seawater media. Deep-Sea Res. A: Oceanogr. Res. Pap. **34**: 1733–1743. doi:10.1016/0198-0149(87)90021-5

Domingues, R. B., C. C. Guerra, A. B. Barbosa, V. Brotas, H. M. Galvao, and A. Notes. 2014. Effects of ultraviolet radiation and CO_2 increase on winter phytoplankton assemblages in a temperate coastal lagoon. J. Plankton Res. **36**: 672–684. doi:10.1093/plankt/fbt135

Donahue, K., C. Klaas, P. W. Dillingham, and L. J. Hoffmann. 2019. Combined effects of ocean acidification and increased light intensity on natural phytoplankton communities from two Southern Ocean water masses. J. Plankton Res. **41**: 30–45. doi:10.1093/plankt/fby048

Dong, H. P., Y. L. Dong, L. Cui, S. Balamurugan, J. Gao, S. H. Lu, and T. Jiang. 2016. High light stress triggers distinct proteomic responses in the marine diatom *Thalassiosira pseudonana*. BMC Genomics **17**: 994. doi:10.1186/s12864-016-3335-5

Fiala, M., and L. Oriol. 1990. Light-temperature interactions on the growth of Antarctic diatoms. Polar Biol. **10**: 629–636. doi:10.1007/BF00239374

Frölicher, T. L., J. L. Sarmiento, D. J. Paynter, J. P. Dunne, J. P. Krasting, and M. Winton. 2015. Dominance of the Southern Ocean in anthropogenic carbon and heat uptake in CMIP5 models. J. Climate **28**: 862–886. doi:10.1175/JCLI-D-14-00117.1

Gaillard, S., and others. 2020. Combined effects of temperature, irradiance, and pH on *Teleaulax amphioxeia* (Cryptophyceae) physiology and feeding ratio for its predator *Mesodinium rubrum* (Ciliophora). J. Phycol. **56**: 775–783. doi:10.1111/jpy.12977

Gao, G., Z. Xu, Q. Shi, and H. Wu. 2018. Increased CO_2 exacerbates the stress of ultraviolet radiation on photosystem II function in the diatom *Thalassiosira weissflogii*. Environ. Exp. Bot. **156**: 96–105. doi:10.1016/j.envexpbot.2018.08.031

Genty, B., J. M. Briantais, and N. R. Baker. 1989. The relationship between the quantum yield of photosynthetic electron transport and quenching of chlorophyll fluorescence. Biochim. Biophys. Acta **990**: 87–92. doi:10.1016/S0304-4165(89)80016-9

González-Herrero, S., D. Barriopedro, R. M. Trigo, J. López-Bustins, and M. Oliva. 2022. Climate warming amplified the 2020 record-breaking heatwave in the Antarctic Peninsula. Commun. Earth Environ. **3**: 122. doi:10.1038/s43247-022-00450-5

Guillard, R. R., and J. H. Ryther. 1962. Studies of marine planktonic diatoms. 1. *Cyclotella nana* (Hustedt) and *Detonula confervacea* (Cleve) gran. Can. J. Microbiol. **8**: 229–239. doi:10.1139/m62-029

Häder, D. P., and others. 2015. Effects of UV radiation on aquatic ecosystems and interactions with other environmental factors. Photochem. Photobiol. Sci. **14**: 108–126. doi:10.1039/c4pp90035a

Heiden, J. P., K. Bischof, and S. Trimborn. 2016. Light intensity modulates the response of two Antarctic diatom species to ocean acidification. Front. Mar. Sci. **3**: 260. doi:10.3389/fmars.2016.00260

Heiden, J. P., S. Thoms, K. Bischof, and S. Trimborn. 2018. Ocean acidification stimulates particulate organic carbon accumulation in two Antarctic diatom species under moderate and high solar radiation. J. Phycol. **54**: 505–517. doi:10.1111/jpy.12753

Heiden, J. P., and others. 2019. Impact of ocean acidification and high solar radiation on productivity and species composition of a late summer phytoplankton community of the coastal Western Antarctic Peninsula. Limnol. Oceanogr. **64**: 1716–1736. doi:10.1002/lno.11147

Hoegh-Guldberg, O., and J. F. Bruno. 2010. The impact of climate change on the world's marine ecosystem. Science **328**: 1523–1528. doi:10.1126/science.118993

Hoppe, C. J. M., L. Holtz, S. Trimborn, and B. Rost. 2015. Ocean acidification decreases the light-use efficiency in an Antarctic diatom under dynamic but not constant light. New Phytol. **207**: 159–171. doi:10.1111/nph.13334

Hutchins, D. A., and P. W. Boyd. 2016. Marine phytoplankton and the changing ocean iron cycle. Nat. Clim. Change **6**: 1072–1079. doi:10.1038/nclimate3147

IPCC. 2014. *In* R. K. Pachauri and L. A. Meyer [eds.], Climate change 2014: Synthesis report. Contribution of working groups I, II and III to the fifth assessment report of the intergovernmental panel on climate change. IPCC.

IPCC. 2019. *In* H.-O. Pörtner and others [eds.], IPCC special report on the ocean and cryosphere in a changing climate. IPCC.

Jaussaud, A., J. Lupette, J. Salvaing, J. Jouhet, O. Bastien, M. Gromova, and E. Maréchal. 2020. Stepwise biogenesis of subpopulations of lipid droplets in nitrogen starved *Phaeodactylum tricornutum* cells. Front. Plant Sci. **11**: 48. doi:10.3389/fpls.2020.00048

Jónasdóttir, S. H. 2019. Fatty acid profiles and production in marine phytoplankton. Mar. Drugs **17**: 151. doi:10.3390/md17030151

Jones, M. E., D. H. Bromwich, J. P. Nicolas, J. Carrasco, E. Plavcová, X. Zou, and S.-H. Wang. 2019. Sixty years of widespread warming in the southern middle and high latitudes (1957–2016). J. Climate **32**: 6875–6898. doi:10.1175/JCLI-D-18-0565.1

Klok, A. J., D. E. Martens, R. H. Wijffels, and P. P. Lamers. 2013. Simultaneous growth and neutral lipid accumulation in microalgae. Bioresour. Technol. **134**: 233–243. doi:10.1016/j.biortech.2013.02.006

Koch, F., S. Beszteri, L. Harms, and S. Trimborn. 2019. The impacts of iron limitation and ocean acidification on the cellular stoichiometry, photophysiology and transcriptome of *Phaeocystis antarctica*. Limnol. Oceanogr. **64**: 357–375. doi:10.1002/lno.11045

Kolber, Z. S., O. Prášil, and P. G. Falkowski. 1998. Measurements of variable chlorophyll fluorescence using fast repetition rate techniques: Defining methodology and experimental protocols. Biochim. Biophys. Acta **1367**: 88–106. doi:10.1016/S0005-2728(98)00135-2

Kranz, S. A., O. Levitan, K. Richter, O. Prasil, I. Berman-Frank, and B. Rost. 2010. Combined effects of CO_2 and light on the N_2-fixing cyanobacterium *Trichodesmium* IMS101: Physiological responses. Plant Physiol. **154**: 334–345. doi:10.1104/pp.110.159145

Kropuenske, L. R., M. M. Mills, G. L. van Dijken, A. C. Alderkamp, G. Mine Berg, D. H. Robinson, N. A. Welschmeyer, and K. R. Arrigo. 2010. Strategies and rates of photoacclimation in two major Southern Ocean phytoplankton taxa: *Phaeocystis antarctica* (Haptophyta) and *Fragilariopsis cylindrus* (Bacillariophyceae). J. Phycol. **46**: 1138–1151. doi:10.1111/j.1529-8817.2010.00922.x

Li, G., and D. A. Campbell. 2013. Rising CO_2 interacts with growth light and growth rate to alter photosystem II photoinactivation of the coastal diatom *Thalassiosira pseudonana*. PLoS One **8**: e55562. doi:10.1371/journal.pone.0055562

Mehrbach, C., C. Culberson, J. Hawley, and R. Pytkowicx. 1973. Measurements of the apparent dissociation constants of carbonic acid in seawater at atmospheric pressure. Limnol. Oceanogr. **18**: 897–907. doi:10.4319/lo.1973.18.6.0897

Mendes, C. R. B., V. M. Tavano, M. C. Leal, M. S. de Souza, V. Brotas, and C. A. E. Garcia. 2013. Shifts in the dominance between diatoms and cryptophytes during three late summers in the Bransfield Strait (Antarctic peninsula). Polar Biol. **36**: 537–547. doi:10.1007/s00300-012-1282-4

Meyer, M. A., and S. Z. El-Sayed. 1983. Grazing of *Euphausia superba* Dana on natural phytoplankton populations. Polar Biol. **1**: 193–197. doi:10.1007/BF00443187

Moore, J. K., and others. 2018. Sustained climate warming drives declining marine biological productivity. Science **359**: 1139–1143. doi:10.1126/science.aao6379

Pierrot, D., E. Lewis, and D. Wallace. 2006. MS excel program developed for CO_2 system calculations. ORNL/CDIAC-105. U.S. Department of Energy.

Ralph, P. J., and R. Gademann. 2005. Rapid light curves: A powerful tool to assess photosynthetic activity. Aquat. Bot. **82**: 222–237. doi:10.1016/j.aquabot.2005.02.006

Ratkowsky, D. A., R. K. Lowry, T. A. McMeekin, A. N. Stokes, and R. E. Chandler. 1983. Model for bacterial culture growth rate throughout the entire biokinetic temperature range. J. Bacteriol. **154**: 1222–1226. doi:10.1128/jb.154.3.1222-1226.1983

Redfield, A. C. 1958. The biological control of chemical factors in the environment. Am. Sci. **64**: 205–221.

Roberty, S., B. Bailleul, N. Berne, F. Franck, and P. Cardol. 2014. PSI Mehler reaction is the main alternative photosynthetic electron pathway in *Symbiodinium* sp., symbiotic dinoflagellates of cnidarians. New Phytol. **204**: 81–91. doi:10.1111/nph.12903

Rose, J. M., and others. 2009. Synergistic effects of iron and temperature on Antarctic phytoplankton and microzooplankton assemblages. Biogeosciences **6**: 3131–3147. doi:10.5194/bg-6-3131-2009

Schofield, O., G. Saba, K. Coleman, F. Carvalho, N. Couto, and H. Ducklow. 2017. Decadal variability in coastal phytoplankton community composition in a changing West Antarctic Peninsula. Deep-Sea Res. I: Oceanogr. Res. Pap. **124**: 42–54. doi:10.1016/j.dsr.2017.04.014

Schulz, K. G., and others. 2017. Phytoplankton blooms at increasing levels of atmospheric carbon dioxide: Experimental evidence for negative effects on prymnesiophytes and positive on small picoeukaryotes. Front. Mar. Sci. **4**: 64. doi:10.3389/fmars.2017.00064

Sommer, U., C. Paul, and M. Moustaka-Gouni. 2015. Warming and ocean acidification effects on phytoplankton—From species shifts to size shifts within species in a mesocosm experiment. PLoS One **10**: e0125239. doi:10.1371/journal.pone.0125239

Spackeen, J. L., and others. 2018. Impact of temperature, CO_2, and iron on nutrient uptake by a late-season microbial community from the Ross Sea, Antarctica. Aquat. Microb. Ecol. **82**: 145–159. doi:10.3354/ame01886

Suggett, D. J., H. L. MacIntyre, and R. J. Geider. 2004. Evaluation of biophysical and optical determinations of light absorption by photosystem II in phytoplankton. Limnol. Oceanogr.: Methods **2**: 316–332. doi:10.4319/lom.2004.2.316

Suggett, D. J., C. M. Moore, A. E. Hickman, and R. J. Geider. 2009. Interpretation of fast repetition rate (FRR) fluorescence: Signatures of phytoplankton community structure versus physiological state. Mar. Ecol. Prog. Ser. **376**: 1–19. doi:10.3354/meps07830

Trimborn, S., T. Brenneis, E. Sweet, and B. Rost. 2013. Sensitivity of Antarctic phytoplankton species to ocean acidification: Growth, carbon acquisition and species interaction. Limnol. Oceanogr. **58**: 997–1007. doi:10.4319/lo.2013.58.3.0997

Trimborn, S., S. Thoms, T. Brenneis, J. P. Heiden, S. Beszteri, and K. Bischof. 2017*a*. Two Southern Ocean diatoms are more sensitive to ocean acidification and changes in irradiance than the prymnesiophyte *Phaeocystis antarctica*. Physiol. Plant. **160**: 155–170. doi:10.1111/ppl.12539

Trimborn, S., T. Brenneis, C. J. M. Hoppe, L. Norman, J. Santos, L. Laglera, D. Wolf-Gladrow, and C. Hassler. 2017*b*. Iron sources alter the response of Southern Ocean phytoplankton to ocean acidification. Mar. Ecol. Prog. Ser. **578**: 35–50. doi:10.3354/meps12250

Trimborn, S., S. Thoms, P. Karitter, and K. Bischof. 2019. Ocean acidification and high irradiance stimulate the photo-physiological fitness, growth and carbon production of the Antarctic cryptophyte *Geminigera cryophila*. Biogeosciences **16**: 2997–3008. doi:10.5194/bg-16-2997-2019

Ueno, M., P. Sae-Tang, Y. Kusama, Y. Hihara, M. Matsuda, T. Hasunuma, and Y. Nishiyama. 2016. Moderate heat stress stimulates repair of photosystem II during photoinhibition in *Synechocystis* sp. PCC 6803. Plant Cell Physiol. **57**: 2417–2426. doi:10.1093/pcp/pcw153

Wang, X., and W. O. Smith. 2021. Phytoplankton growth at low temperatures: Results from low temperature incubations. J. Plankton Res. **43**: 633–641. doi:10.1093/plankt/fbab054

Weisse, T., and P. Stadler. 2006. Effect of pH on growth, cell volume, and production of freshwater ciliates, and implications for their distribution. Limnol. Oceanogr. **51**: 1708–1715. doi:10.4319/lo.2006.51.4.1708

Young, J. N., S. A. Kranz, J. A. L. Goldman, P. D. Tortell, and F. M. M. Morel. 2015*a*. Antarctic phytoplankton down-regulate their carbon-concentrating mechanisms under high CO_2 with no change in growth rates. Mar. Ecol. Progr. Ser. **532**: 13–28. doi:10.3354/meps11336

Young, J. N., J. A. L. Goldman, S. A. Kranz, P. D. Tortell, and F. M. M. Morel. 2015*b*. Slow carboxylation of rubisco constrains the rate of carbon fixation during Antarctic phytoplankton blooms. New Phytol. **205**: 172–181. doi:10.1111/nph.13021

Zhu, Z., K. Xu, F. Fu, J. L. Spackeen, D. A. Bronk, and D. A. Hutchins. 2016. A comparative study of iron and temperature interactive effects on diatoms and *Phaeocystis antarctica* from the Ross Sea, Antarctica. Mar. Ecol. Prog. Ser. **550**: 39–51. doi:10.3354/meps11732

Zhu, Z., P. Qu, J. Gale, F. Fu, and D. A. Hutchins. 2017. Individual and interactive effects of warming and CO_2 on *Pseudo-nitzschia subcurvata* and *Phaeocystis Antarctica*, two dominant

phytoplankton from the Ross Sea, Antarctica. Biogeosciences **14**: 5281–5295. doi:10.5194/bg-14-5281-2017

Zwietering, M. H., J. T. de Koos, B. E. Hasenack, J. C. de Wit, and K. van't Riet. 1991. Modeling of bacterial growth as a function of temperature. Appl. Environ. Microbiol. **57**: 1094–1101. doi:10.1128/aem.57.4.1094-1101.1991

Acknowledgments

We thank B. Meier-Schlosser and Kai Bischof for pigment analysis, S. Murawski for POC analysis, and A. Cayetano for his help in the data analysis using Python. We are grateful to A. Kraberg for her technical assistance in scanning electron microscopy observations, and S. Rokitta for the insightful discussions on the thermal functional response of phytoplankton. We also thank the members of the EcoTrace Group and the Marine Biogeosciences Section (especially L. Rehder) at the AWI for the diverse logistical support. M. Camoying was supported by the Katholischer Akademischer Ausländerdienst (KAAD) through a PhD fellowship. Open Access funding enabled and organized by Projekt DEAL.

Conflict of Interest

None declared.

Submitted 29 July 2022
Revised 27 February 2023
Accepted 15 June 2023

Associate editor: Bingzhang Chen

Chapter 4

Distinct responses of diatom- and flagellate-dominated Antarctic phytoplankton communities to altered iron and light supply

Marianne Camoying[1*], Florian Koch[1], Jasmin Stimpfle[1], Franziska Pausch[1], Christel Hassler[2,3], Scarlett Trimborn[1]

[1]Ecological Chemistry, Alfred Wegener Institute, Helmholtz Centre for Polar and Marine Research, Bremerhaven, Germany
[2]Department F.-A. Forel for Environmental and Aquatic Science, University of Geneva, Geneva, Switzerland
[3]Ecole Polytechnique Fédérale de Lausanne, Alpoles, Sion, Switzerland

Published in Frontiers in Marine Science – Global Change and the Future Ocean

frontiers | Frontiers in Marine Science

TYPE Original Research
PUBLISHED 04 November 2024
DOI 10.3389/fmars.2024.1441087

OPEN ACCESS

EDITED BY
Christopher Edward Cornwall,
Victoria University of Wellington,
New Zealand

REVIEWED BY
Wei Liu,
Shanghai University, China
Kristian Spilling,
Finnish Environment Institute (SYKE), Finland

*CORRESPONDENCE
Marianne Camoying
marianne.camoying@awi.de

RECEIVED 30 May 2024
ACCEPTED 09 October 2024
PUBLISHED 04 November 2024

CITATION
Camoying M, Koch F, Stimpfle J, Pausch F, Hassler C and Trimborn S (2024) Distinct responses of diatom- and flagellate-dominated Antarctic phytoplankton communities to altered iron and light supply. *Front. Mar. Sci.* 11:1441087. doi: 10.3389/fmars.2024.1441087

Distinct responses of diatom- and flagellate-dominated Antarctic phytoplankton communities to altered iron and light supply

Marianne Camoying[1*], Florian Koch[1], Jasmin Stimpfle[1], Franziska Pausch[1], Christel Hassler[2,3] and Scarlett Trimborn[1]

[1]EcoTrace, Alfred Wegener Institute, Helmholtz Centre for Polar and Marine Research, Bremerhaven, Germany, [2]Department F.-A. Forel for Environmental and Aquatic Science, University of Geneva, Geneva, Switzerland, [3]Ecole Polytechnique Fédérale de Lausanne, Sion, Switzerland

Primary production in the Southern Ocean is strongly influenced by the availability of light and iron (Fe). To examine the response of two distinct natural Antarctic phytoplankton communities (diatom vs. flagellates) to increasing light and Fe availability, we conducted two shipboard incubation experiments during late summer and exposed each community to increasing light intensities (30, 80, and 150 µmol photons m^{-2} s^{-1}) with or without Fe amendment. Our results show clearly that both communities were Fe-limited since Fe addition resulted in higher particulate organic carbon (POC) production rates. The magnitude of the Fe-dependent increase in POC production, however, varied between the two stations being higher in the diatom-dominated community relative to the flagellate-dominated community. This differential response to increasing Fe supply could be attributed to the higher Fe requirement of the flagellate-dominated assemblage relative to the diatom-dominated assemblage. Irrespective of Fe availability, light also strongly stimulated the POC production of both communities between low and medium light supply (30 versus 80 µmol photons m^{-2} s^{-1}), indicating that both assemblages were light-limited *in situ*. However, since POC production of both communities did not increase further at the highest light intensity (150 µmol photons m^{-2} s^{-1}) even under high Fe supply, this suggests that light supply was saturated or that other conditions must be fulfilled (e.g., availability of trace metals other than Fe) in order for the communities to benefit from the higher light and Fe conditions.

KEYWORDS

Southern Ocean, diatoms, flagellates, light, iron, photoacclimation, ecophysiology, Fe demand

Introduction

Primary production in the Southern Ocean (SO) is mainly constrained by the availability of light and the trace metal iron (Fe; Martin et al., 1990; Mitchell et al., 1991; Strzepek et al., 2019). As Fe plays an important role in the cellular process of photosynthesis (Behrenfeld and Milligan, 2013), several studies have already established the positive effects of Fe addition on the growth and carbon production of SO phytoplankton (Boyd et al., 2000; Blain et al., 2007; Moore et al., 2007). The effect of Fe on SO phytoplankton is, however, influenced by light availability. An antagonistic relationship between Fe and light has been observed in temperate phytoplankton (Sunda and Huntsman, 1997; Maldonado et al., 1999) wherein the Fe demand is said to increase under low light conditions, amplifying thereby Fe limitation. In particular, at low irradiance, phytoplankton cells would require more Fe for the synthesis of chlorophyll *a* (Chl *a*) and light-harvesting complexes (Raven, 1990). SO phytoplankton have been shown, however, to employ a different strategy in dealing with low light availability by not increasing their Fe requirement, as they can enhance the size of their light-harvesting antennae instead of increasing the number of their Fe-rich photosystem units (Strzepek et al., 2012, 2019). This finding is supported by several studies reporting larger photosystem II (PSII) absorption cross-section (σ_{PSII}) of SO phytoplankton, especially under low light and Fe-depleted conditions (e.g., Ryan-Keogh et al., 2017; Alderkamp et al., 2019; Trimborn et al., 2019). While larger σ_{PSII} may be advantageous under low Fe and low light conditions, this may, however, be stressful when SO phytoplankton are exposed to high light intensities. Due to the larger antenna size, the efficiency of energy transfer from the light-harvesting complexes to the photosynthetic reaction centers may be reduced (Raven, 1990), thereby causing cellular stress. Indeed, previous shipboard incubation experiments have shown a higher susceptibility of SO phytoplankton to photoinhibition and decreased photosynthetic efficiency when cells are exposed to high light in conjunction with low Fe conditions (Alderkamp et al., 2010; Petrou et al., 2011). The susceptibility of Fe-limited SO phytoplankton to high light cannot be generalized because some field studies also reported that natural SO phytoplankton assemblages coped well with high irradiances even under Fe-limited conditions. For instance, in spring–summer field experiments in the Ross Sea, both the Fe-limited diatom- and *Phaeocystis*-dominated phytoplankton communities did not exhibit any photoinhibitory response even when exposed to high irradiances of up to 550 µmol photons m^{-2} s^{-1} for over 6 days (Alderkamp et al., 2019). A similar capability to cope with high light stress (765 µmol photons m^{-2} s^{-1}) under low Fe supply was also reported for a subantarctic nanoflagellate-dominated phytoplankton community sampled during summer (Petrou et al., 2011). This could be attributed to the ability of Antarctic phytoplankton to photoacclimate such as by decreasing the concentration of its light-harvesting pigments (Van Leeuwe and Stefels, 1998; Luxem et al., 2017) and/or by releasing excess energy through non-photochemical quenching (NPQ; Falkowski and Raven, 2007).

The capability of SO phytoplankton to deal with varying light intensities greatly depends on their cellular Fe requirement, which has been reported to be species-specific. For example, a laboratory Fe–light incubation experiment by Trimborn et al. (2019) revealed that an Fe-limited flagellate *Phaeocystis antarctica* was able to maintain similar high growth rates irrespective of the light intensity, while another flagellate, the cryptophyte *Geminigera cryophila*, exhibited reduced carbon production at high light even when Fe supply was high (500 µmol photons m^{-2} s^{-1}; Camoying and Trimborn, 2023). In contrast, under low Fe supply, the Antarctic diatom *Chaetoceros debilis* was not able to grow at 500 µmol photons m^{-2} s^{-1} (Trimborn et al., 2019). In line with the observations from these laboratory experiments, the spring *Phaeocystis*-dominated phytoplankton communities along the Western Antarctic Peninsula (WAP) also exhibited a strong positive response to light regardless of Fe availability (Joy-Warren et al., 2022). However, the summer diatom-dominated assemblage sampled in East Antarctica displayed the highest growth and biomass production only under Fe-replete conditions in combination with high light intensities (Vives et al., 2022). While there are already available studies that looked at the effects of Fe and light on diatom- and *Phaeocystis*-dominated natural SO assemblages, the response of communities dominated by other flagellates such as cryptophytes and dinoflagellates still remains less studied.

Climate change models project that net primary production in the SO would be enhanced as a whole due to a potential increase in Fe input and light availability in the future (Henley et al., 2020). Granted that this would be the case, it is crucial, however, to determine whether the magnitude of the projected increase in carbon production would be similar among SO phytoplankton assemblages dominated by different taxonomic groups. Hence, our study aims to address this knowledge gap by conducting field incubation experiments on the effects of Fe and light availability on the growth, carbon production, and photophysiology of two distinct natural Antarctic phytoplankton communities. Here, we compared the ecophysiological responses of the open ocean diatom-dominated assemblage and the coastal flagellate-dominated community to the increase in light and Fe supply.

Materials and methods

Field sampling and setup of two Fe–light shipboard phytoplankton incubation experiments

Two Fe–light shipboard bottle-incubation experiments were conducted during the *RV Polarstern* expedition PS97 (February–March 2016) to investigate the response of natural phytoplankton communities from two distinct environments in the Atlantic sector of the SO to increasing light and Fe availability. Both sampling locations, where the initial seawater was collected, had high macronutrients but different trace metal concentrations (Table 1). BIO 1, sampled on March 2, 2016, at 25-m depth in the Drake

10.3389/fmars.2024.1441087

TABLE 1 Initial conditions of BIO 1 and BIO 2 stations.

		BIO 1	BIO 2
Latitude	min^{-1}	60° 24.78′ S	60° 29.94′ S
Longitude	min^{-1}	66° 21.85′ W	55° 29.70′ W
dFe	nM	0.05	2.89
dMn	nM	0.15	1.00
dCu	nM	1.05	1.37
dZn	nM	3.21	11.11
dCo	nM	0.03	0.05
dFe:dMn	nM:nM	0.33	2.89
dFe:dCu	nM:nM	0.05	2.11
dFe:dZn	nM:nM	0.02	0.26
dFe:dCo	nM:nM	1.67	58
NO_x	µM	24	25
PO_4	µM	1.50	1.49
$SiOH_4$	µM	17	59
Chl *a*	µg L^{-1}	0.05	1.04
LH: LP	ng ng^{-1}	8.94	12.84

Coordinates, concentrations of total dissolved iron (dFe), dissolved manganese (dMn), dissolved copper (dCu), dissolved zinc (dZn), dissolved cobalt (dCo), macronutrients (NO_x = NO_3 (nitrate) and NO_2 (nitrite), PO_4 = phosphate, $SiOH_4$ = silicate), chlorophyll *a* (Chl *a*) and ratios of light-harvesting (LH: sum of chlorophyll *a*, chlorophyll c_{1+2}, and fucoxanthin) to light-protective pigments (LP: sum of diadinoxanthin and diatoxanthin; LH:LP, ng ng^{-1}) are shown for the initial seawater sampled at BIO 1 and BIO 2 stations.

Passage (60° 24.78′ S, 66° 21.85′ W, 25 m), had very low concentrations of both total dissolved Fe (0.05 nM) and manganese (dMn; 0.15 nM), while station BIO 2, sampled on March 13, 2016, at 25-m depth and located close to the Antarctic Peninsula (60° 29.94′ S, 55° 29.70′ W, 25 m), had higher dFe (2.89 nM) and dMn (1.0 nM) values. Trace metal clean (TMC) techniques were employed for all seawater sampling of each incubation experiment according to the GEOTRACES guidelines (Cutter et al., 2017). Prior to the expedition, all bottles, tubing, and other labware were acid-cleaned in the laboratory, as previously described in Balaguer et al. (2022) and Pausch et al. (2022). At both stations, seawater was directly pumped into a clean container (US class 100, Opta, Bensheim, Germany) using a Teflon membrane pump (Almatec, Futur 50) and pre-filtered with a 200-µm mesh to remove mesozooplankton before filling the incubation bottles inside a laminar flow hood. Before sampling, the pump and tubing were flushed for at least 1 h with seawater at each location.

For the two shipboard incubation experiments, each natural phytoplankton community was exposed to three light levels—low light (LL; 30 µmol photons m^{-2} s^{-1}), medium light (ML; 80 µmol photons m^{-2} s^{-1}), and high light (HL; 150 µmol photons m^{-2} s^{-1})—in combination with *in situ* Fe concentrations (Control: no Fe addition) and after Fe addition (+Fe: addition of 0.9 nM $FeCl_3$). Light-emitting diode (LED) daylight lamps (SolarStinger LED Sun Strip Marine Daylight, Econlux, Cologne, Germany) were used as light sources and were set to the target light intensities. For each light treatment, six incubation bottles (three Control and three +Fe) were aligned horizontally in front of the light source (Supplementary Figure 1). The incubation bottles were gently turned and shaken daily to prevent cells from settling at the bottom. To address potential "spatial effects" due to the arrangement of the bottles, their positions in front of the light source were also interchanged daily. Since the *in situ* concentrations of macronutrients were also high (Table 1), no additional macronutrient amendment was necessary. All treatments were conducted in triplicate TMC 2.5-L polycarbonate (PC) bottles and maintained under the above-described light intensities and a 16:8 (light:dark) hour cycle at 1°C simulating typical natural conditions of the sampling region and time. Depending on the Fe treatment, incubation experiments lasted 10–14 days. During the experiment, the photosynthetic efficiency of the community was monitored every 2–4 days after 1-h dark-acclimation via a Fast Repetition Rate Fluorometer [FRRf; Fast Ocean PTX sensor, Chelsea Technologies Group (CTG) Ltd., West Molesey, UK] at 1°C. At the start and end of each experiment, samples were collected to determine changes in phytoplankton community composition, photophysiology, elemental composition, and seawater chemistry.

Seawater chemistry

The concentration of the dissolved trace metals (TMs) (Fe, Mn, Cu, Zn, and Co) *in situ* was determined by filtering 100 mL of seawater through HCl-cleaned polycarbonate filters (0.2-µm pore size) using a TMC Nalgene filtration system. The filtrate was then collected into a PE bottle and stored triple-bagged at 2°C until analysis. As described in Balaguer et al. (2022), dTM concentrations were determined on a SeaFast system (Elemental Scientific, Omaha, NE, USA) (Hathorne et al., 2012; Rapp et al., 2017), coupled to an inductively coupled plasma–mass spectrometer (ICP-MS; Element2, resolution of R = 2000, Thermo Fisher Scientific, Waltham, MA, USA). An imino-diacetate (IDA) chelation column (part number CF-N-0200, Elemental Scientific) was used in the pre-concentration step. To minimize the adsorption of TMs onto the bottle walls and to reduce the formation of hydroxides during storage, the pre-filtered seawater samples were acidified to pH = 1.7 with a double-distilled nitric acid (HNO_3) and were UV-treated using a 450-W photo-chemical UV power supply (ACE GLASS Inc., Vineland, NJ, USA). Two blanks were taken during each digestion step, and daily optimization of the ICP-MS was performed to maintain oxide-forming rates below 0.3%.

Seawater samples were analyzed via external calibration to minimize any matrix effect, which could affect the quality of the analysis. The accuracy and precision of the method were assessed by analyzing a NASS-7 (National Research Council of Canada) reference standard in a 1:10 dilution (corresponding to environmentally representative concentrations) at the beginning and at the end of each run. All measured values were within the limits of the certified NASS-7 reference material with an average recovery rate of 97% for Fe, 91% for Mn, 98% for Cu, 94% for Zn, and 100% for Co.

10.3389/fmars.2024.1441087

Samples for the initial and final macronutrient concentrations for each experiment were filtered through a 0.2-µm filter and stored in a Falcon tube at −20°C. The concentration of dissolved macronutrients [total nitrate (nitrite + nitrate), phosphate, and silicate] was measured colorimetrically in the home laboratory on a QuAATro autoanalyzer (SEAL Analytical).

Pigments

Samples for photosynthetic pigment analyses were collected by filtering seawater onto 25-mm glass fiber filters (GF/F, Whatman). Filters were directly flash-frozen in liquid nitrogen and stored at −80°C. Concentrations of the pigments Chl *a*, chlorophyll *c*1 + 2 (Chl *c*1 + 2), fucoxanthin, diadinoxanthin, alloxanthin, peridinin, and 19′-hexanoyloxyfucoxanthin were measured by high-performance liquid chromatography (HPLC). As described in detail in Pausch et al. (2022), pigments were extracted from the filters using acetone (>99.9% HPLC grade; Merck, Darmstadt, Germany), and the synthetic pigment canthaxanthin (≥95% HPLC grade, Sigma-Aldrich, St. Louis, MO, USA) was used as an internal standard. Pigment samples were analyzed using an HPLC system consisting of a Waters 600 controller (Waters Corporation, Milford, MA, USA) combined with a refrigerated autosampler (Waters 717 plus), a photodiode array detector (Waters 2996), and a fluorescence detector (Waters 2475). Pigments were then identified and quantified using the EMPOWER software (Waters). Specifically, pigments were identified by comparing their retention time to those of the standards, and concentrations were determined based on peak areas of external standards. Pigment concentrations were normalized to the extraction volume using the internal standard canthaxanthin. The ratio of light-harvesting (LH) pigments to light-protecting (LP) pigments was calculated by dividing the sum of the concentration of Chl *a*, Chl *c*1+*c*2, and fucoxanthin by the sum of the concentration of diadinoxanthin (DD) and diatoxanthin (DT) (Pausch et al., 2022).

Phytoplankton community composition

To determine the taxonomic composition of the natural phytoplankton community of both stations, unfiltered seawater samples were collected at the start and the end of the incubation experiments. For the BIO 1 experiment, samples were fixed with 1% (final v:v) Lugol's solution right after sampling and were allowed to settle in 10 mL Utermöhl sedimentation chambers (Hydro-Bios GmbH, Altenholz, Germany) for at least 24 h before counting them under an inverted microscope (Axio Observer D1, Carl Zeiss AG, Oberkochen, Germany). Phytoplankton were classified into four major groups of diatoms (*Fragilariopsis*, *Pseudo-nitzschia*, *Chaetoceros*, and other diatoms) and two flagellate groups (large, >5 µm; small, <5 µm). Cell growth rate (µ, d^{-1}) was calculated according to the following:

$$\mu = (\ln N_{T2} - \ln N_{T1})/\Delta T$$

where N_{T1} and N_{T2} represent cell densities (cell mL^{-1}) at the start and the end of the experiment, respectively, and ΔT denotes the duration of the incubation (in days).

For the BIO 2 experiment, as it was not possible to identify the flagellates, which dominated the station, using microscopy, the phytoplankton community composition for this station was inferred from the HPLC pigment data. Specifically, the pigment fucoxanthin was used as a proxy for diatoms, peridinin for dinoflagellates, alloxanthin for cryptophytes, and 19′-hexanoyloxyfucoxanthin for haptophytes (Feng et al., 2010; Wright and Van den Enden, 2000; Mackey et al., 1996). Marker pigment to Chl *a* ratios were calculated for the initial community and at the end of the experiments to assess the percentage decrease or increase of the relative abundance of each phytoplankton group for the BIO 2 experiment. The following equation was used to calculate the change in the relative abundance (ΔRA, %) of target phytoplankton groups:

$$\Delta RA = [(PM:Chl\ a)_{T2}/(PM:Chl\ a)_{T1}] * 100$$

where (PM: Chl $a)_{T1}$ and (PM: Chl $a)_{T2}$ denote the ratio of specific pigment marker to Chl *a* at the start and end, respectively, of the BIO 2 incubation experiment.

Net particulate organic carbon production rates

For particulate organic carbon (POC) analysis, water was filtered for each replicate bottle onto pre-combusted (500°C, 15 h) 25-mm GF/F filters (Whatman). A filter blank was also taken as a blank sample for each bottle. All filters were placed in pre-combusted glass Petri dishes and were stored at −20°C. In the lab, filters were first dried at 50°C for >12 h and then acidified with 200 µL of 0.2 M HCl before samples were analyzed on an automated carbon nitrogen elemental analyzer (Euro EA–CN Elemental Analyzer, HEKAtech GmbH, Wegberg, Germany). Net daily POC production rates were calculated based on the difference between the initial and final POC concentrations over the duration of the incubation in days. To examine whether the phytoplankton assemblages of the two stations would increase their Fe demand with decreasing light (Fe–light antagonism; Sunda and Huntsman, 1997), the ratio of POC-based growth rate (µPOC) under Control (μPOC_{Con}) to the µPOC under +Fe (μPOC_{+Fe}) ($\mu POC_{Con}/\mu POC_{+Fe}$) was calculated for each light treatment. Based on Latour et al. (2023), the following equation was used to calculate the $\mu POC_{Con}/\mu POC_{+Fe}$ ratio:

$$\mu POC_{Con}/\mu POC_{+Fe} = \frac{\{[\ln (POC_{Con})_{T2} - \ln (POC_{Con})_{T1}]/\Delta T\}}{\{[\ln (POC_{+Fe})_{T2} - \ln (POC_{+Fe})_{T1}]/\Delta T\}}$$

where (POC_{Con}) and (POC_{+Fe}) represent the POC concentration (µmol L^{-1}) of the Control and +Fe treatments, respectively, at the start (T1) and the end (T2) of the experiment, and ΔT denotes the duration of the incubation (in days).

Photophysiology

An FRRf (FastOcean PTX sensor, CTG Ltd., West Molesey, UK) connected with a FastAct Laboratory system (CTG Ltd.) was used to measure Chl *a* fluorescence at the start, during, and end of the experiments of both stations. The fluorometer's LED had

excitation wavelengths of 450 nm, 530 nm, and 624 nm, and the light intensity was automatically adjusted. As in Balaguer et al. (2022) and Pausch et al. (2022), the single turnover mode was set with a saturation phase of 100 flashlets on a 2-µs pitch followed by a relaxing phase of 40 flashlets on a 50-µs pitch. In order to allow full oxidation of all PSII reaction centers, samples were dark-acclimated for 1 h before each measurement. The minimum (F_0) and maximum (F_m) Chl *a* fluorescence of PSII were measured six times with the use of the FastPro8 software (Version 1.0.55, Kevin Oxborough, CTG Ltd.). The maximum quantum yield of photochemistry in PSII (F_v/F_m, rel. unit) was then calculated using the following equation:

$$F_v/F_m = (F_m - F_0)/F_m$$

Using the single turnover measurements of the dark-acclimated community, the functional absorption cross-section of PSII (σ_{PSII}, nm^2 $PSII^{-1}$), the time constant for electron transport at the acceptor side of PSII (τ_{Qa}, µs), and the connectivity factor (P, dimensionless) were derived as in Oxborough et al. (2012). Electron transport rate (ETR)–irradiance curves were performed, and the ETRs (e^- $PSII^{-1}$ s^{-1}) were calculated using the following formula (Suggett et al., 2004, 2009; Huot and Babin, 2010; Schuback et al., 2015):

$$ETR = \sigma_{PSII} * ((F'_q/F'_m) / (F_v/F_m)) * E$$

where (F'_q/F'_m) denotes the effective PSII quantum yield under ambient light and E is the irradiance level (photons m^{-2} s^{-1}). The maximum ETR (ETR_{max}, e^- $PSII^{-1}$ s^{-1}), maximum light utilization efficiency (α, rel. unit), and minimum saturation irradiance (I_k, µmol photons m^{-2} s^{-1}) were calculated from the ETR–irradiance curve based on Ralph and Gademann (2005). The Stern–Volmer equation was used to calculate the NPQ:

$$NPQ = F_m/F'_m - 1$$

Statistics

Two-way analysis of variance (ANOVA) with Tukey's multiple comparison *post-hoc* tests was used to statistically analyze the interactive effects of the two Fe (Control and +Fe) and three light (LL, ML, and HL) treatments on all experimental parameters. Due to the nature of the light source used in the experiments as well as the specific spatial arrangement of the incubation bottles, any test of light effects is a test of both light and spatial effects. All statistical analyses were performed using the program GraphPad Prism (Version 10.1.0 (316) for Windows, GraphPad Software, San Diego, CA, USA), and the significance testing was conducted at the $p < 0.05$ level.

Results

Initial chemical and biological characteristics of both sampling stations

Shipboard Fe–light incubation experiments were conducted with phytoplankton communities sampled in two distinct environments. The phytoplankton community collected at station BIO 1 was located in the open waters of the Drake Passage. Here, macronutrient concentrations were high (Table 1), while only low levels of chlorophyll *a* (Chl *a*) and the trace metals Fe and Mn were found (Table 1). The initial phytoplankton community of BIO 1 also exhibited very low photosynthetic efficiency (F_v/F_m) together with large functional absorption cross-sections of PSII (σ_{PSII}) (Table 2). The initial micro-phytoplankton community of station BIO 1 was dominated by diatoms composed mainly of the genera *Fragilariopsis*, *Chaetoceros*, and *Pseudo-nitzschia*, while the nanoflagellate group was present only in smaller numbers. Based on Balaguer et al. (2022), the most abundant phytoplankton group *Fragilariopsis* was FeMn-co-limited, while the other phytoplankton groups (*Chaetoceros*, *Pseudo-nitzschia*, and *Phaeocystis*) were only Fe-limited. The initial BIO 1 phytoplankton community was also found to be light-limited based on the observations of Pausch et al. (2022).

In contrast, the BIO 2 station was located close to the WAP and had way higher concentrations of dFe (2.89 nM) and dMn (1.0 nM) than BIO 1 (Table 1). In line with this, F_v/F_m (0.38 ± 0.01) and Chl *a* (1.04 µg L^{-1}) values of the initial community of the BIO 2 station were also much higher compared to the initial community of BIO 1. Based on Blanco-Ameijeiras et al. (2020), the BIO 2 phytoplankton community was dominated by flagellates represented by prymnesiophytes, choanoflagellates, dinoflagellates, and cryptophytes, while diatoms were observed only in low concentrations. The authors also reported that the BIO 2 initial assemblage was only mildly Fe-limited.

BIO 1: POC production, phytoplankton community structure, and photoacclimation

At the end of the experiment (Control, 11-day duration; +Fe, 10-day duration), POC production of the phytoplankton community sampled in BIO 1 was significantly influenced by Fe ($p < 0.0001$) and light alone ($p < 0.0001$) as well as their interaction ($p < 0.0043$) (Figure 1A; Table 3). Fe addition significantly increased POC production rates in all light treatments (Figure 1). For the Control treatments, POC production increased with increasing light intensity. In the +Fe treatments, POC production was strongly stimulated between LL and ML, while no further stimulation was observed between ML and HL (Figure 1). Looking at the POC-based growth rates (µPOC) of the BIO 1 assemblage, the ratio of µPOC in the Control (μPOC_{Con}) to µPOC in the +Fe (μPOC_{+Fe}) was similar between LL and ML and increased at HL ($\mu POC_{Con}/\mu POC_{+Fe}$; Table 4).

Growth rates of each counted phytoplankton group (Figure 2) were significantly influenced by both Fe (diatoms and nano- and small flagellates, $p < 0.0001$; big flagellates, $p = 0.0224$) and light (diatoms and nano- and small flagellates, $p < 0.000$; big flagellates, $p = 0.0006$) alone, but no interactive effects between the two factors were observed (Table 3). Irrespective of the light level, Fe enrichment enhanced the growth of all phytoplankton groups except for the large-sized flagellates, for which a significant increase in growth was observed only at ML. In response to

TABLE 2 The dark-adapted maximum photosystem II quantum yield (F_v/F_m), the functional absorption cross-section of PSII (σ_{PSII}), energy transfer between photosystem II units (connectivity, *P*), re-oxidation times of the primary electron acceptor Qa (τ_{Qa}), maximum electron transport rates (ETR_{max}), minimum saturating irradiance (I_k), and the maximum light utilization efficiency (α) of the natural phytoplankton communities sampled in BIO 1 and BIO 2 stations after growing them at low light (LL; 30 µmol photons m^{-2} s^{-1}), middle light (ML; 80 µmol photons m^{-2} s^{-1}), and high light (HL; 150 µmol photons m^{-2} s^{-1}) under *in situ* iron concentrations (Con) and after Fe addition (+Fe) conditions.

Station	Fe	Light	F_v/F_m (dimensionless)	σ_{PSII} (nm^2 $PSII^{-1}$)	*P* (dimensionless)	τ_{Qa} (µs)	ETR_{max} (e^- $PSII^{-1}$ s^{-1})	I_k (µmol photons m^{-2} s^{-1})	α (rel. unit)
BIO 1 initial			*0.16 ± 0.03*	*5.3 ± 0.37*	*0.23 ± 0.03*	*619 ± 76*	*408*	*118*	*3.45*
BIO 1	Con	LL	0.34 ± 0.07^{a}	3.2 ± 0.5^{a}	0.34 ± 0.03^{ac}	603 ± 49^{a}	159 ± 18^{a}	87 ± 18^{a}	1.84 ± 0.17^{a}
Bio 1	Con	ML	0.24 ± 0.06^{a}	3.8 ± 0.5^{a}	0.22 ± 0.07^{b}	502 ± 65^{b}	334 ± 57^{ab}	166 ± 25^{b}	2.02 ± 0.21^{a}
Bio 1	Con	HL	0.30 ± 0.06^{a}	3.7 ± 1.4^{a}	0.28 ± 0.07^{ab}	590 ± 30^{a}	404 ± 206^{b}	220 ± 46^{c}	1.76 ± 0.52^{a}
Bio 1	+Fe	LL	0.43 ± 0.01^{b}	2.5 ± 0.08^{ab}	0.41 ± 0.01^{c}	610 ± 19^{ac}	134 ± 4^{ac}	70 ± 6^{a}	1.93 ± 0.14^{a}
Bio 1	+Fe	ML	0.34 ± 0.02^{b}	2.7 ± 0.19^{ab}	0.33 ± 0.01^{ac}	574 ± 18^{c}	177 ± 8^{c}	105 ± 5^{a}	1.68 ± 0.06^{a}
Bio 1	+Fe	HL	0.34 ± 0.05^{ab}	2.5 ± 0.15^{b}	0.28 ± 0.01^{a}	586 ± 17^{ac}	184 ± 19^{ac}	118 ± 15^{a}	1.56 ± 0.06^{a}
BIO 2 initial			*0.38 ± 0.01*	*6.0 ± 0.26*	*0.39 ± 0.01*	*679 ± 35*	*221*	*144*	*1.53*
BIO 2	Con	LL	0.31 ± 0.00^{a}	3.0 ± 0.63^{ab}	0.23 ± 0.04^{a}	644 ± 42^{a}	91 ± 18^{a}	61 ± 3^{a}	1.50 ± 0.38^{a}
Bio 2	Con	ML	0.31 ± 0.00^{a}	3.5 ± 0.06^{a}	0.22 ± 0.03^{a}	603 ± 20^{a}	186 ± 13^{b}	106 ± 7^{b}	1.76 ± 0.06^{a}
Bio 2	Con	HL	0.30 ± 0.01^{a}	2.6 ± 0.25^{b}	0.20 ± 0.01^{a}	613 ± 28^{a}	146 ± 6^{c}	102 ± 10^{b}	1.44 ± 0.13^{a}
Bio 2	+Fe	LL	0.40 ± 0.01^{b}	2.3 ± 0.12^{c}	0.35 ± 0.04^{b}	660 ± 23^{ab}	89 ± 6^{a}	59 ± 3^{a}	1.51 ± 0.04^{a}
Bio 2	+Fe	ML	0.38 ± 0.05^{b}	3.3 ± 0.24^{a}	0.29 ± 0.06^{b}	611 ± 23^{ab}	197 ± 15^{b}	127 ± 13^{c}	1.56 ± 0.09^{a}
Bio 2	+Fe	HL	0.38 ± 0.00^{b}	2.2 ± 0.05^{bc}	0.31 ± 0.03^{b}	661 ± 8^{b}	124 ± 8^{d}	97 ± 9^{b}	1.29 ± 0.06^{a}

Values represent the means (± SD) of triplicate incubations. Significant differences between treatments are indicated by varying lowercase letters (*post-hoc* tests, $p < 0.05$).

increasing light under Control conditions, the growth of *Fragilariopsis* was stimulated, while that of all other phytoplankton groups remained the same between LL and ML and increased only at HL. In response to increasing light under +Fe conditions, the growth of most groups was stimulated but depended on the applied light intensity. For instance, the growth of *Chaetoceros* was stimulated across all light levels, while the growth of *Pseudo-nitzschia*, *Fragilariopsis*, and the large-sized flagellates increased only from LL to ML with no further change at HL. In comparison, the growth of the other diatoms and the small flagellates was enhanced only between ML and HL (Figure 2).

At the end of the experiment, the ratio of LH to light-protective pigments (LP; LH: LP, ng ng^{-1}) of the BIO 1 phytoplankton community was influenced by both light ($p < 0.0001$) and Fe ($p < 0.0001$) alone, but not by their interaction (Table 3). An Fe-dependent stimulation of LH: LP ratios was observed in all light treatments (Figure 3). Irrespective of Fe availability, the LH: LP ratio decreased from LL to ML and remained unchanged toward HL (Figure 3).

The F_v/F_m and the connectivity between adjacent photosystems (*P*) were influenced by both Fe (F_v/F_m, $p = 0.0053$; *P*, $p = 0.0102$) and light (F_v/F_m, $p = 0.0137$; $p = 0.0024$) alone. Fe addition led to higher F_v/F_m values except at HL. In response to increasing irradiance, F_v/F_m remained the same regardless of Fe availability (Table 2). *P* generally increased with Fe addition, but the change was significant only at ML. Irrespective of Fe availability, *P* decreased from LL to ML and remained the same at HL. The functional absorption cross-sections of PSII (σ_{PSII}) were influenced only by Fe ($p = 0.0057$) whereby a decrease was observed in the HL and +Fe treatments. The time constant for electron transfer at PSII (τ_{QA}) responded to light alone ($p = 0.0239$), decreasing from LL to ML and increasing again between ML and HL in the Control (Table 2). No interactive effect of Fe and light on all photophysiological parameters (F_v/F_m, σ_{PSII}, *P*, and τ_{QA}) of the phytoplankton assemblage in BIO 1 was observed (Table 3).

The maximum electron transport rates (ETR_{max}) and minimum saturating irradiances (I_k) of the BIO 1 phytoplankton assemblage were influenced by both Fe (ETR_{max}, $p = 0.0071$; I_k, $p = 0.0002$) and light alone (ETR_{max}, $p = 0.0343$; I_k, $p < 0.0001$), while a significant interactive Fe–light effect ($p = 0.0283$) was evident only for I_k (Table 3). Fe addition resulted in lower ETR_{max} and I_k values, but this effect was only significant for ML and HL. Increasing irradiance led to higher ETR_{max} for ML compared to LL but not HL, and I_k values, but only in the Control treatment (Table 2; Figures 4A, B). The maximum light utilization efficiency (α), however, was affected by neither light nor Fe (Table 2). NPQ values of the final communities in BIO 1 were enhanced with increasing irradiance during the fluorescence light curve (FLC) in all treatments (Figure 5A). While lower NPQ values were observed in +Fe compared to the Control treatments, light availability in all cases did not have an influence on NPQ.

BIO 2: POC production, phytoplankton community structure, and photoacclimation

For the BIO 2 station, at the end of the experiment (Control: 14-day duration; +Fe: 11-day duration), POC production was positively

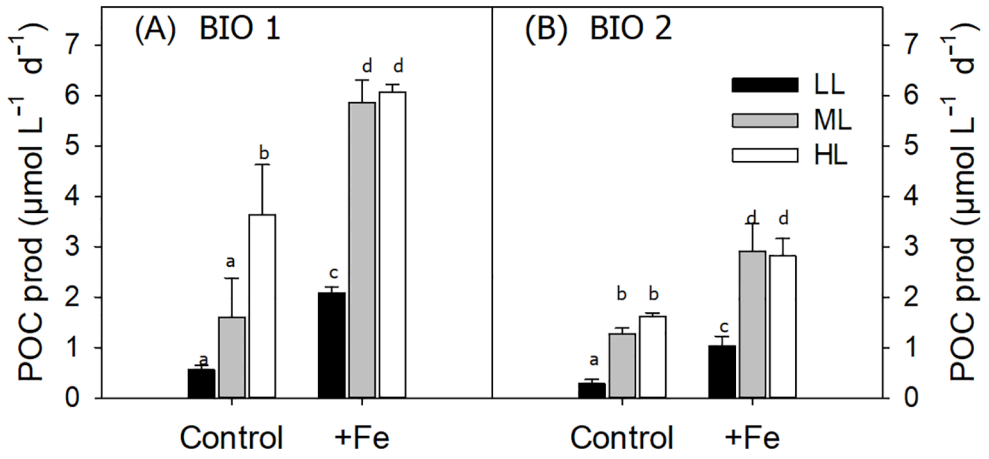

FIGURE 1
Daily particulate organic carbon (POC) production rates of the phytoplankton communities sampled at stations BIO 1 **(A)** and BIO 2 **(B)** after growing them at low light (LL; 30 µmol photons m^{-2} s^{-1}), middle light (ML; 80 µmol photons m^{-2} s^{-1}), and high light (HL; 150 µmol photons m^{-2} s^{-1}) in conjunction with *in situ* iron concentrations (Control) or after iron addition (+Fe). Values represent the means (± SD) of triplicate incubations. Significant differences between treatments are indicated by varying lowercase letters (*post-hoc* tests, $p < 0.05$).

influenced by both Fe ($p < 0.0001$) and light ($p < 0.0001$) alone, but not their interaction (Table 3). In response to Fe addition, POC production increased significantly in all light treatments. Irrespective of Fe availability, increasing light intensity stimulated POC production rates between LL and ML, while values remained unchanged between ML and HL (Figure 1B). The $\mu POC_{Con}/\mu POC_{+Fe}$ ratios increased from LL to ML and remained the same at HL (Table 4).

Since it was not feasible to count the flagellate groups using microscopy for the BIO 2 samples, the ratio of pigment marker to Chl *a* was used instead as a proxy to assess the relative changes of the major phytoplankton taxa [fucoxanthin (Fuco): diatoms; peridinin (Peri): dinoflagellates; alloxanthin (Allo): cryptophytes; 19′-hexanoyloxyfucoxanthin (19′-hexa): haptophytes] over the course of the BIO 2 experiment (Figure 6). In all incubation bottles, among the four taxa, only the haptophyte group exhibited an overall decrease (~60%) in its abundance relative to their number at the start of the experiment. In contrast, at the end of the incubation, the relative abundance of diatoms either remained unchanged or increased slightly, while dinoflagellates and cryptophytes exhibited up to a twofold increase in abundance depending on the treatment. In all light treatments, Fe addition had no effect on the relative abundance of the cryptophytes and haptophytes, while a decrease in diatoms was observed at LL, and there was higher dinoflagellate abundance in both the LL and ML treatments in +Fe compared to Control. In response to increasing light intensity, diatom abundance represented by Fuco concentrations did not change except under the Control treatment where their relative abundance decreased from LL to ML. Dinoflagellate abundance was only influenced by light under the +Fe treatment, being decreased from ML to HL. In both the Control and +Fe treatments, the abundance of cryptophytes was enhanced at HL relative to LL. However, increasing light only had a positive effect on the abundance of haptophytes under the Control, while values remained unchanged in the +Fe (Figure 6).

Fe addition did not have any effect on the LH: LP ratios. Increasing light, however, negatively influenced LH: LP ratios ($p < 0.0001$) except when Fe was added, and the ratio remained the same between ML and HL (Figure 3B). In general, the F_v/F_m and *P* values of the final BIO 2 phytoplankton assemblage were influenced only by Fe alone ($p < 0.0001$), while light and the combination of both factors had no effect. Accordingly, only the addition of Fe significantly increased F_v/F_m and *P* in all light treatments (Table 2). Both single Fe ($p = 0.0054$) and light ($p = 0.0003$) effects were observed in σ_{PSII} (Table 3). Fe addition decreased σ_{PSII} only at LL. In the Control, increasing irradiance resulted in similar σ_{PSII} between LL and ML but was decreased at HL, while in the +Fe, σ_{PSII} was enhanced from LL to ML and decreased at HL. τ_{QA} was affected by neither light nor Fe except at HL where it was significantly increased after Fe addition (Table 2).

Fe addition did not influence ETR_{max} of LL and ML treatments but significantly reduced ETR_{max} of the HL treatment (Table 2). Increasing light intensity led to an increase in ETR_{max} values ($p < 0.0001$) in all treatments (Figures 4C, D). I_k remained unchanged with Fe addition except in the ML, which exhibited higher I_k values. I_k was altered in response to increasing irradiance ($p < 0.0001$) but differently affected depending on the Fe availability. Both the Control and +Fe treatments exhibited an increase in I_k from LL to ML, but in the Control, I_k did not change between ML and HL, while it was reduced from ML to HL in the +Fe. Neither light nor Fe had an influence on α of the phytoplankton communities in BIO 2 (Table 2). In all treatments, NPQ values were enhanced with increasing actinic irradiance during the fluorescence light curve runs but unaffected by Fe availability. Interestingly, the Control ML had the highest NPQ values in response to varying light, while values were relatively similar among the three light treatments under +Fe (Figures 5C, D).

10.3389/fmars.2024.1441087

TABLE 3 Significance of the single effects of light and Fe as well as their interactive effects effects on the different physiological parameters.

Parameter	Light	Fe	Interaction
BIO 1			
POC production	<0.0001	<0.0001	0.0043
Fragilariopsis, μ	<0.0001	<0.0001	No
Pseudo-nitzschia, μ	<0.0001	<0.0001	No
Chaetoceros, μ	<0.0001	<0.0001	No
Other diatoms, μ	<0.0001	<0.0001	No
Nanoflagellates, μ	<0.0001	<0.0001	No
Big flagellates, μ	0.0006	0.0224	No
Small flagellates, μ	<0.0001	<0.0001	No
LH: LP ratio	<0.0001	<0.0001	No
F_v/F_m	0.0137	0.0053	No
σ_{PSII}	No	0.0057	No
P	0.0024	0.0102	No
τ_{Qa}	0.0239	No	No
ETR_{max}	0.0343	0.0071	No
I_k	<0.0001	0.0002	0.0283
α	No	No	No
BIO 2			
POC production	<0.0001	<0.0001	No
LH: LP ratio	<0.0001	No	No
F_v/F_m	No	<0.0001	No
σ_{PSII}	0.0003	0.0054	No
P	No	0.0001	No
τ_{Qa}	0.0310	No	No
ETR_{max}	<0.0001	No	No
I_k	<0.0001	No	0.0366
α	0.0369	No	No
Fucoxanthin	No	0.0140	No
Peridinin	0.0213	0.0310	0.0142
Alloxanthin	0.0039	0.0135	No
19′-Hexanoyloxyfucoxanthin	0.0253	No	No

Discussion

Our study shows that both Fe addition and increasing light stimulated the POC production of the two phytoplankton communities. The degree of POC production increase, however, varied between the two wherein it was slightly higher in the diatom-dominated BIO 1 assemblage compared to the flagellate-dominated BIO 2 community. This differential response to Fe could be attributed to the species-specific cellular Fe demand and the Fe uptake capabilities of the dominant phytoplankton groups in each station. While SO phytoplankton commonly increase their σ_{PSII} under Fe limitation, we did not observe such physiological adjustment in most of our treatments. Accordingly, both communities increased their Fe demand with decreasing light availability. We also show here that POC production was not enhanced further between ML and HL even when Fe was added, potentially indicating that both communities had additional requirements, which were not fulfilled (e.g., availability of other trace metals such as Mn).

Fe addition stimulated the POC production of the phytoplankton community at both stations and in all light treatments

In line with the observations of previous studies with SO natural phytoplankton assemblages (e.g., Feng et al., 2010; Alderkamp et al., 2015; Balaguer et al., 2022; Joy-Warren et al., 2022; Pausch et al., 2022; Vives et al., 2022) and laboratory cultures (e.g., Andrew et al., 2019; Koch et al., 2019; Koch and Trimborn, 2019; Camoying et al., 2022), POC production rates of both stations were stimulated after Fe addition relative to the Control, indicating Fe limitation of both communities. However, the degree of the limitation differed between the two stations (Figure 1). The diatom-dominated BIO 1 station had a very low dFe concentration and a low F_v/F_m value *in situ*; hence, Fe addition resulted in a 100% increase of F_v/F_m values in the +Fe treatments relative to the initial. In addition, σ_{PSII} values of the +Fe treatments were reduced by 50% after Fe addition compared to the initial value (Table 2). However, different from the observations of other studies showing a decrease in σ_{PSI} in response to Fe enrichment (Petrou et al., 2014; Strzepek et al., 2019), we only observed an Fe-dependent decrease in σ_{PSI} at HL (Table 2). Similarly, the initial LH: LP ratio of BIO 1 was also low, with Fe amendment leading to much higher LH: LP ratios in the +Fe treatments (Figure 3). As Fe is required in chlorophyll synthesis, it is a common response of SO phytoplankton to increase the concentration of light-harvesting pigments after Fe enrichment (Van Leeuwe and Stefels, 1998; Moore et al., 2007; Alderkamp et al., 2012). The above observations indicate that the *in situ* BIO 1 community was severely Fe-limited, in line with the findings of Blanco-Ameijeras et al. (2020) and Pausch et al. (2022). By contrast, the flagellate-dominated BIO 2 station had a high dFe concentration together with a high F_v/F_m value *in situ*. This is similar to observations for the BIO 2 community by Blanco-Ameijeiras et al. (2020), who also demonstrated in their Fe addition experiments that the BIO 2 community was mildly Fe-limited. Based on our data, the BIO 2 flagellate-dominated community exhibited lower F_v/F_m values in all of its Control treatments compared to the initial (Table 2). It could be that Fe was depleted over the incubation period due to the high cellular Fe requirement of flagellates. In line with this, open ocean nanophytoplankton was found to acquire both new and recycled Fe compared to large-sized diatoms, which are not able to utilize the latter (Boyd et al., 2012). Moreover, Twining et al. (2004) reported higher Fe:C ratios in SO flagellates than diatoms, suggesting a higher Fe demand of the former in sustaining growth as has been observed for the cryptophyte *G. cryophila* (Camoying et al., 2022).

TABLE 4 Particulate organic carbon-based growth rates (μPOC, d^{-1}) of the natural phytoplankton communities sampled in BIO 1 and BIO 2 stations after growing them at low light (LL; 30 μmol photons m^{-2} s^{-1}), middle light (ML; 80 μmol photons m^{-2} s^{-1}), and high light (HL; 150 μmol photons m^{-2} s^{-1}) under *in situ* iron concentrations (Con) and after Fe addition (+Fe) conditions.

Station	POC-based growth rate (μPOC, d^{-1})						$\mu POC_{Con}/\mu POC_{+Fe}$		
	LL		ML		HL		LL	ML	HL
	μPOC_{Con}	μPOC_{+Fe}	μPOC_{Con}	μPOC_{+Fe}	μPOC_{Con}	μPOC_{+Fe}			
BIO 1	0.08 ± 0.01	0.18 ± 0.00	0.12 ± 0.01	0.27 ± 0.01	0.21 ± 0.02	0.27 ± 0.00	0.45 ± 0.07[a]	0.47 ± 0.05[a]	0.77 ± 0.07[b]
BIO 2	0.03 ± 0.01	0.07 ± 0.01	0.08 ± 0.00	0.14 ± 0.01	0.09 ± 0.00	0.13 ± 0.01	0.35 ± 0.09[a]	0.57 ± 0.06[b]	0.67 ± 0.05[b]

Values represent the means (± SD) of triplicate incubations. Significant differences between light treatments are indicated by varying lowercase letters (*post-hoc* tests, $p < 0.05$).

The distinct phytoplankton community composition of each station and their differential Fe uptake capabilities as well as Fe demand most likely influenced the overall POC production in BIO 1 and BIO 2. The degree of Fe-dependent increase in POC production varied between the two stations, being slightly higher in BIO 1 than in BIO 2. In BIO 1, POC production in the +Fe was on average two times higher than in the Control, while it was only 1.6 times higher in BIO 2. In line with this, growth rates of all phytoplankton groups in BIO 1 were also strongly promoted after Fe addition (Figure 2), while Fe enrichment, except for the dinoflagellate group, had no effect on the relative abundances of the other phytoplankton groups in BIO 2 (Figure 6). The high resource uptake capabilities of diatoms as *r* strategists (Arrigo et al., 2005) as well as their low Fe demand (Sunda et al., 1991; Marchetti et al., 2006) could be the reason for the sustained dominance of diatoms over flagellates in BIO 1, being, therefore, the primary drivers of enhanced POC production at this station. However, the higher Fe requirement of flagellates (high Fe:C ratios; Twining et al., 2004; Camoying et al., 2022) could be responsible for the smaller degree of increase in POC production of the BIO 2 community and the absence of positive Fe effects on the growth of almost all BIO 2 phytoplankton groups, despite the high *in situ* dFe concentration.

BIO 1: The Fe-enriched BIO 1 community required medium irradiance to yield highest POC production rates

Even though increasing light enhanced the overall growth of the Fe-enriched BIO 1 assemblage, similar photophysiological characteristics were maintained between light treatments (Table 2), indicating optimal photoacclimation of the diatom-dominated communities. The growth of various phytoplankton groups was, however, differentially affected by increasing light levels (Figure 2). *Fragilariopsis*, *Chaetoceros*, *Pseudo-nitzschia*, and the large-sized flagellates, among them *P. antarctica*, increased their growth rates from LL to ML. Similar light-dependent stimulation in the growth of Fe-replete *Fragilariopsis* was already previously observed for *Fragilariopsis curta* (Heiden et al., 2016), *Fragilariopsis cylindrus* (Ye et al., 2023), and *Fragilariopsis pseudonana* (Heiden et al., 2019). As in this study, previous studies have reported a positive effect of increasing light on the growth of *Chaetoceros lineola* (Feng et al., 2010), *C. debilis* (Trimborn et al., 2019), and *Pseudo-nitzschia prolongatoides/subcurvata* (Lee et al., 2022) as well as the flagellate *P. antarctica* (Feng et al., 2010; Strzepek et al., 2012; Lee et al., 2022). From ML to HL, *Chaetoceros* showed even further light-dependent growth stimulation, as previously observed in other studies (Feng et al., 2010; Trimborn et al., 2019). In addition to *Chaetoceros*, the other diatoms and small-sized flagellates also exhibited the highest growth rates at HL. This suggests that Fe addition allowed them to take advantage of the HL availability. Based on our results, the growth of the BIO 1 community was clearly limited by Fe and light.

As observed in other field studies with natural SO phytoplankton communities (Viljoen et al., 2018; Alderkamp et al., 2019; Joy-Warren et al., 2022; Latour et al., 2023), the increasing light intensity from LL to ML promoted a strong enhancement in POC production (181%) of the Fe-enriched BIO 1 community (Figure 1A). However, no further increase in POC production was observed from ML to HL in spite of the increase in growth of *Chaetoceros*, the other diatoms, and the small flagellate group at HL. This suggests that these three groups were not the main drivers of POC production at HL in BIO 1, but instead, production rates were more strongly influenced by *Fragilariopsis*, which dominated the initial BIO 1 community. In fact, in the +Fe treatment, the growth of *Fragilariopsis* was enhanced between LL and ML but remained the same at HL. *Fragilariopsis* of the BIO 1 community was identified to suffer from FeMn-co-limitation *in situ*, as it yielded the highest growth rates only when both Fe and Mn were supplied (Balaguer et al., 2022). Since Mn is a crucial component of the PSII water-splitting center (Raven, 1990), it could be that the HL conditions in our study triggered a higher Mn demand for *Fragilariopsis*, which was, however, not fulfilled, as only Fe was supplied in this study, preventing thus its growth stimulation from ML to HL under high Fe conditions. Indeed, an increased Mn demand under HL conditions (>120 μmol photons m^{-2} s^{-1} PAR; Joy-Warren et al., 2022) was reported for the springtime phytoplankton community from the WAP region of the SO. It could also be that due to the unfulfilled high Mn demand of *Fragilariopsis*, the HL exposure led potentially to higher oxidative stress. The cells may have prioritized the allocation of the available Fe for the production of Fe superoxide dismutase (FeSOD) to reduce the formation of reactive oxygen species (ROS) (Peers and Price, 2004). Hence, as a consequence, no further increase in carbon production was observed between ML and HL treatments of the BIO 1 community under high Fe supply.

BIO 1: The Fe-limited BIO 1 community required high light to achieve maximum POC production

Comparing the F_v/F_m and LH: LP ratios of the Control LL to those of the initial community, it can be seen that both parameters increased at the end of the incubation (Table 2; Figure 3). This indicates the relief of light limitation and photoacclimation of the Fe-limited community to a constant and stable light supply over the course of the experiments. In line with the observations of other studies (Vives et al., 2022; Alderkamp et al., 2019; Viljoen et al., 2018), the exposure of the BIO 1 Control community to increasing light levels did not alter F_v/F_m and σ_{PSII} (Table 2). While previous studies have found that HL conditions (>300 µmol photons m^{-2} s^{-1}) can induce additional light stress in Fe-limited phytoplankton (Moore et al., 2007; Alderkamp et al., 2010, 2019), this was not the case here, probably due to the fact that the applied HL treatment of 150 µE was not high enough. As in Petrou et al. (2011), LH: LP ratios (Figure 3A) and the connectivity

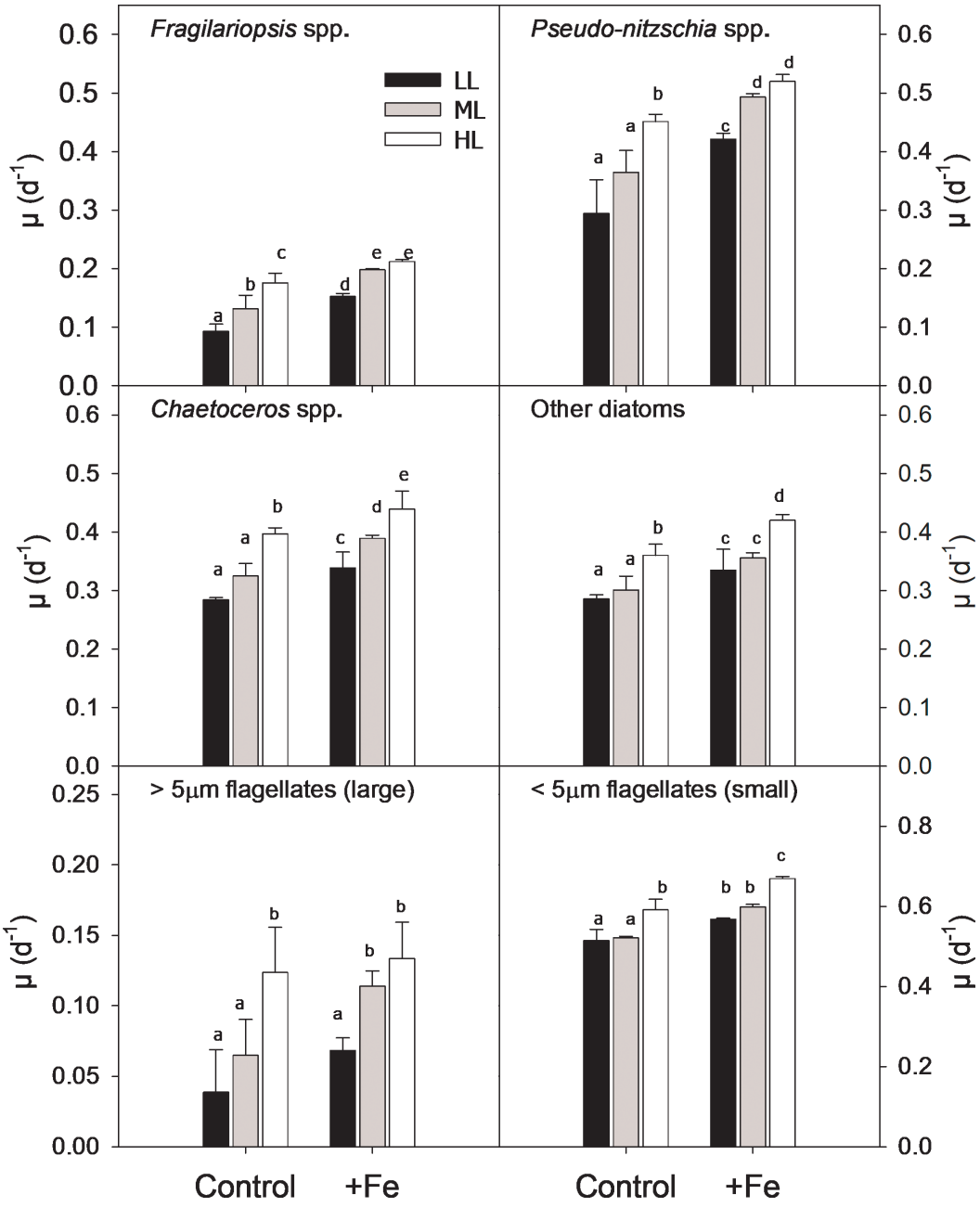

FIGURE 2
Growth rates of the different phytoplankton groups [*Fragilariopsis* spp. **(A)**, *Pseudo-nitzschia* spp. **(B)**, *Chaetoceros* spp. **(C)**, other diatoms **(D)**, large flagellates **(E)**, and small flagellates **(F)**] from BIO 1 station after growing at low light (LL; 30 µmol photons m^{-2} s^{-1}), middle light (ML; 80 µmol photons m^{-2} s^{-1}), and high light (HL; 150 µmol photons m^{-2} s^{-1}) in conjunction with *in situ* iron concentrations (Control) and after iron addition (+Fe). Values represent the means (± SD) of triplicate incubations. Significant differences between treatments are indicated by varying lowercase letters (*post-hoc* tests, $p < 0.05$).

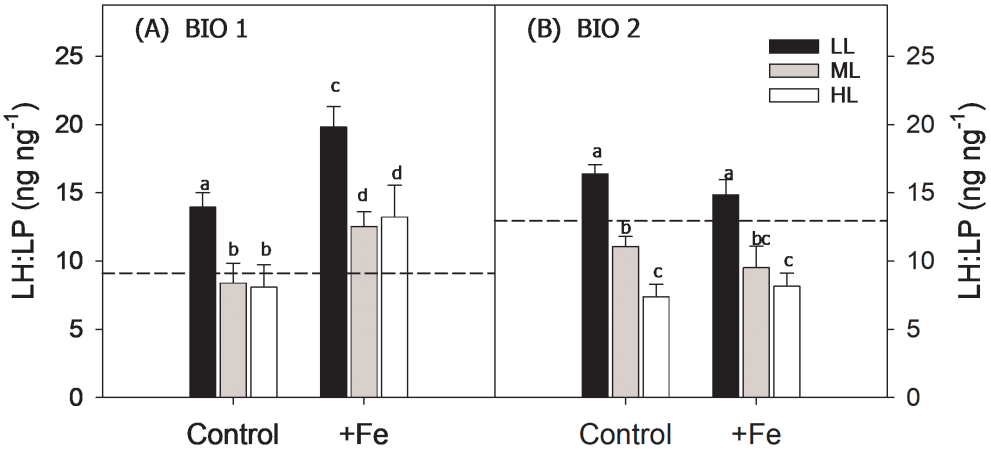

FIGURE 3
Ratios of light-harvesting (LH; sum of chlorophyll *a*, chlorophyll c_{1+2}, and fucoxanthin) to light-protective pigments (LP; sum of diadinoxanthin and diatoxanthin; LH: LP, ng ng^{-1}) of the phytoplankton communities sampled in BIO 1 **(A)** and BIO 2 **(B)** stations after growing them at low light (LL; 30 µmol photons m^{-2} s^{-1}), middle light (ML; 80 µmol photons m^{-2} s^{-1}), and high light (HL; 150 µmol photons m^{-2} s^{-1}) in conjunction with *in situ* iron concentrations (Control) and after iron addition (+Fe). The initial LH: LP ratios of the starting communities of each station are presented as black dashed lines. Values represent the means (± SD) of triplicate incubations. Significant differences between treatments are indicated by varying lowercase letters (*post-hoc* tests, $p < 0.05$).

between photosystems (*P*; Table 2) were reduced between LL and ML, indicating active photoacclimation to absorb less light under ML by the Fe-limited BIO 1 community. As a consequence, I_k significantly increased between LL and ML (Table 2), indicating that more light was required to saturate photosynthesis. In fact, the re-oxidation time of Qa (τ_{QA}) was much shorter (Table 2), yet this did not translate into more efficient electron cycling (Table 2) and POC production (Figure 1A), suggesting that the Calvin cycle was not saturated.

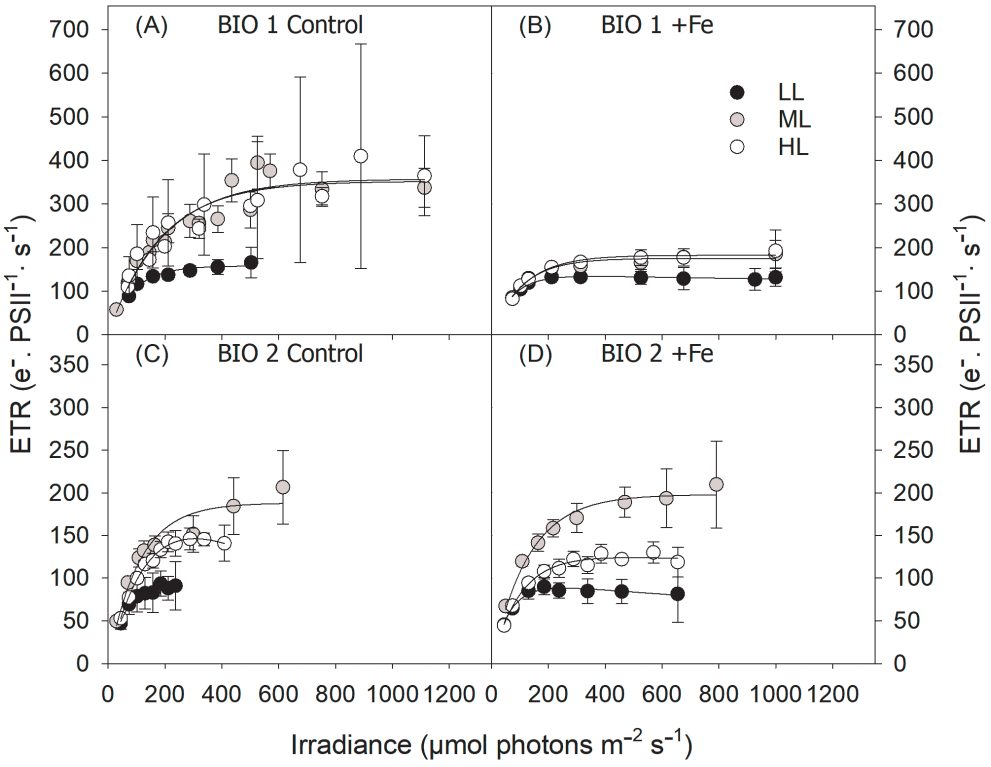

FIGURE 4
Absolute electron transport rates (ETRs) of the final phytoplankton communities sampled in BIO 1 **(A, B)** and BIO 2 **(C, D)** stations were measured in response to increasing irradiance (LL: 30 µmol photons m^{-2} s^{-1}; ML: 80 µmol photons m^{-2} s^{-1}; HL: 150 µmol photons m^{-2} s^{-1}) in conjunction with *in situ* iron concentrations (Control) **(A, C)** and after Fe addition (+Fe) **(B, D)**. Values represent the means (± SD) of triplicate incubations.

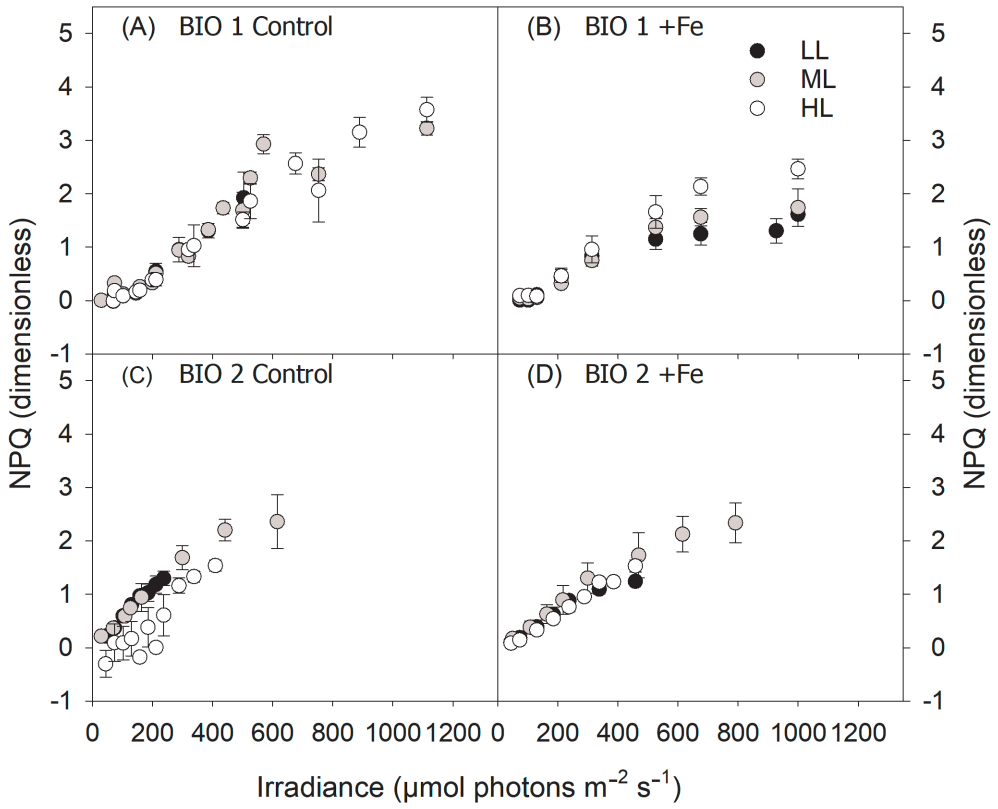

FIGURE 5
Non-photochemical quenching (NPQ) of the final phytoplankton communities sampled in BIO 1 **(A, B)** and BIO 2 **(C, D)** stations were measured in response to increasing irradiance (LL: 30 µmol photons m^{-2} s^{-1}; ML: 80 µmol photons m^{-2} s^{-1}; HL: 150 µmol photons m^{-2} s^{-1}) in conjunction with *in situ* iron concentrations (Control) **(A, C)** and after Fe addition (+Fe) **(B, D)**. Values represent the means (± SD) of triplicate incubations.

Only when exposed to HL were ETR_{max} and POC production in the Control treatment of the BIO 1 community significantly increased (Table 2; Figure 1). In fact, POC production yielded maximum rates of 3.64 µmol L^{-1} d^{-1} under Control HL conditions, being 74% higher than the rate of the +Fe LL treatment (2.09 µmol L^{-1} d^{-1}; Figure 1A). Even without the addition of Fe, the combination of the Control treatment of the BIO 1 community with HL resulted in 5.6 times higher POC production rates than the Control LL treatment (0.55 µmol L^{-1} d^{-1}; Figure 1A). This clearly shows that HL neither led to light stress nor had a negative impact on the photosynthetic performance of the BIO 1 community. This is similar to the response of other natural phytoplankton communities (Joy-Warren et al., 2022; Vives et al., 2022; Latour et al., 2023) showing stimulation of POC rates with increasing light intensity even under low Fe availability. Hence, compared to the Fe-enriched community that yielded maximum POC production rates at ML, the Fe-limited BIO 1 phytoplankton community achieved maximum POC fixation rates only at HL (Figure 1A). Thus, only the supply of HL was able to alleviate the negative impact of Fe limitation on the BIO 1 community, demonstrating clearly that the BIO 1 community was limited by both Fe and light.

We also tested whether there was an increase in Fe demand at LL relative to the HL treatments, particularly under low Fe availability (Fe–light antagonism) as suggested by Sunda and Huntsman (1997). The observed lower $\mu POC_{Con}/\mu POC_{+Fe}$ ratios at LL suggest a higher Fe requirement of the BIO 1 community (Table 4), which is consistent with the observations of previous studies (Viljoen et al., 2018; Joy-Warren et al., 2022), but in contrast to other Fe–light studies with Antarctic phytoplankton assemblages (Alderkamp et al., 2019; Vives et al., 2022; Latour et al., 2023). The reason for this discrepancy among studies could be the chosen light treatments since LL conditions were comparably high in our study (30 µmol photons m^{-2} s^{-1}), while our ML and HL treatments represented rather moderate light conditions (80 and 150 µmol photons m^{-2} s^{-1}, respectively). In comparison, the studies that did not find this antagonistic relationship applied either very low light intensities (2–6 µmol photons m^{-2} s^{-1}: Latour et al., 2023) or very high irradiances (331–512 µmol photons m^{-2} s^{-1}, Alderkamp et al., 2019; 370–926 µmol photons m^{-2} s^{-1}, Vives et al., 2022). Perhaps the larger light range that the phytoplankton was exposed to in the latter studies required potentially even stronger photoacclimation strategies, which, in contrast, lowered their Fe demand.

In our study, except for *Fragilariopsis*, which exhibited a light-dependent growth stimulation at each light level, growth of all other phytoplankton groups was enhanced only at HL (150 µmol photons m^{-2} s^{-1}) in the Control treatment of the BIO 1 community (Figure 2). Hoffmann et al. (2008) reported a negative impact on the growth of the SO diatoms *Chaetoceros dichaeta* and *Actinocyclus* sp. in response to increasing light up to a moderate light level of 90 µmol photons m^{-2} s^{-1}, while the growth of *C. debilis*

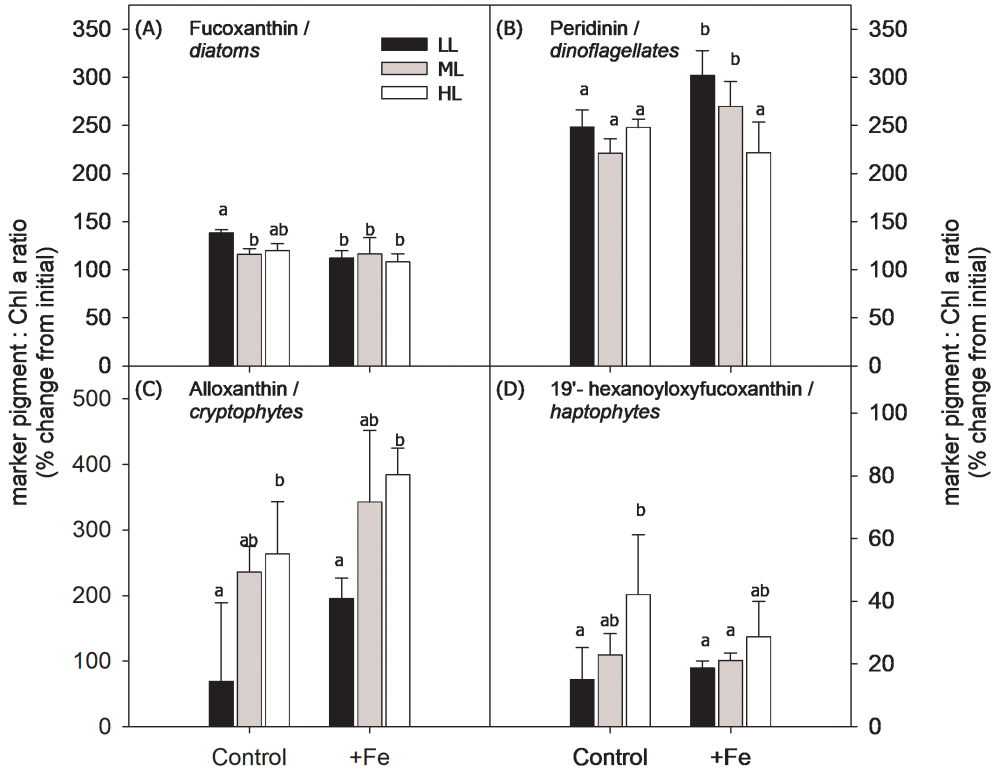

FIGURE 6
Ratio of marker pigment [fucoxanthin: diatoms **(A)**; peridinin: dinoflagellates **(B)**; alloxanthin: cryptophytes **(C)**; 19′-hexanoyloxyfucoxanthin: haptophytes **(D)**] relative to Chl *a* was used as proxy to assess relative changes in the abundance of the major phytoplankton taxa in BIO 2 at the end of the incubation experiment. Using the calculated marker pigment to Chl *a* ratio of the initial community and at the end of the incubation, changes in the relative abundance of the target phytoplankton groups were calculated and given as % change from the marker pigment to Chl *a* ratio at the start of the experiment (>100% indicates positive growth). The phytoplankton community was grown at low light (LL; 30 µmol photons m^{-2} s^{-1}), middle light (ML; 80 µmol photons m^{-2} s^{-1}), and high light (HL; 150 µmol photons m^{-2} s^{-1}) in conjunction with *in situ* iron concentrations (Control) and after iron addition (+Fe). Values represent the means (± SD) of triplicate incubations. Significant differences between treatments are indicated by varying lowercase letters (*post-hoc* tests, $p < 0.05$).

remained unaffected. Moreover, Strzepek et al. (2012) showed either no or positive high light effects (ranging from 100 up to 280 µmol photons m^{-2} s^{-1}) on the growth of two Fe-limited Antarctic diatoms (*Proboscia inermis* and *Eucampia antarctica*, respectively). In contrast to ML, our study showed that the growth of all phytoplankton groups strongly benefitted from the HL supply, indicating that light limitation could be relieved under low Fe supply, as previously observed for Antarctic phytoplankton assemblages (Viljoen et al., 2018; Joy-Warren et al., 2022; Vives et al., 2022; Latour et al., 2023). It appears that the HL treatment of 150 µmol photons m^{-2} s^{-1} provided optimal growth conditions for all community members. Based on our results, the growth of most members of the BIO 1 community was clearly Fe–light co-limited.

BIO 2: ML successfully relieved light limitation of the Fe-enriched BIO 2 community and promoted the highest POC production

Similar to the BIO 1 phytoplankton assemblage, positive light effects between LL and ML on POC production were found in the +Fe treatments of the BIO 2 community (Figure 1B). Between LL and ML, the ratio of LH: LP declined, shifting the pigment ratio from a light absorption toward a more light-protective state (Figure 3B). Furthermore, σ_{PSII} and I_k increased between LL and ML (Table 2), indicating that more light was required for photosynthesis to become saturated. This photophysiological adjustment, however, allowed the cells to achieve higher ETR_{max} (Table 2) and POC production rates (Figure 1B) between LL and ML, indicating efficient linear electron cycling. Overall, this study shows that, as for the BIO 1 community, ML successfully relieved the light limitation of the BIO 2 community. With Fe enrichment, ML promoted the highest growth and POC fixation rates. In contrast to the diatom-dominated BIO 1 assemblage, the flagellate-dominated BIO 2 community underwent various photophysiological adjustments even after Fe addition under ML, corresponding to Fe-limiting conditions such as the increase in σ_{PSII} and more photoprotective pigments (Petrou et al., 2014; Vives et al., 2022; Alderkamp et al., 2019). This points toward the higher Fe requirement of SO flagellates than diatoms (Twining et al., 2004), as previously shown for the Antarctic cryptophyte *G. cryophila* relative to the diatom *Pseudo-nitzschia subcurvata* (Camoying et al., 2022).

When exposed to even higher irradiance (HL), POC production remained constant in the Fe-enriched BIO 2 community, with σ_{PSII}, I_k, and ETR_{max} being lowered between ML and HL (Table 2; Figure 4). The relative abundance of cryptophytes, however, was enhanced between LL and HL, suggesting that the higher light supply was beneficial for this group. Such positive light effects, especially of moderate light intensities under Fe-replete conditions on cryptophytes, have been observed before, both in laboratory studies with the cryptophyte *G. cryophila* (Trimborn et al., 2019; Camoying and Trimborn, 2023) and in field studies showing that cryptophytes are often associated with illuminated and stratified waters (Mendes et al., 2018; 2023). In contrast to the beneficial HL effects on cryptophytes, relative abundances of the dinoflagellates of the BIO 2 community declined from ML to HL under +Fe conditions, as indicated by the lowered peridinin:Chl *a* ratio (Figure 6B). This suggests that dinoflagellates benefit more from low and medium irradiances than from HL after Fe addition. Even though species composition was altered in response to the HL supply, this, however, did not change the overall productivity of the BIO 2 community. Hence, the BIO 2 community was most productive when grown in Fe-enriched and medium irradiances, indicating a successful relief of their Fe and light limitation. Similar to the BIO 1 community, the exposure of even higher irradiances did not lead to any further additional positive effects, suggesting light saturation and probably also a higher Fe demand, which potentially needed to be fulfilled in order to achieve even higher POC production by the flagellate-dominated BIO 2 community.

BIO 2: The Control treatment of the BIO 2 community responded to increasing light in the same manner as the Fe-enriched treatment

In contrast to BIO 1, in both the Control and +Fe treatments of the BIO 2 community, the LH: LP ratios decreased, while I_k and ETR_{max} were enhanced from LL to ML (Table 2), which in turn resulted in significantly higher POC production rate at ML (Figure 1B). Moreover, it needs to be noted that the supply of ML alone (without any Fe added) increased the POC production of the Control similarly high as that of the +Fe treatment under LL (Figure 1B). This indicates that the community was not only Fe-limited but light-limited as well and that the higher light availability alleviated the negative effects of Fe limitation in the Control. For BIO 2, σ_{PSII} and ETR_{max} decreased in the Control from ML to HL, but this did not result in reduced POC production, as rates remained the same between ML and HL, similar to the +Fe treatment. Since maximum POC production was achieved at ML after Fe addition, the BIO 2 phytoplankton community was clearly Fe–light co-limited.

As was observed for BIO 1, the BIO 2 assemblage also exhibited an increased demand for Fe at LL as shown by the lower $\mu POC_{Con}/\mu POC_{+Fe}$ ratio of the LL treatment compared to both ML and HL treatments (LL: 0.35 ± 0.09 vs. ML: 0.57 ± 0.06 and HL: 0.67 ± 0.05; Table 4). The $\mu POC_{Con}/\mu POC_{+Fe}$ ratios of the LL treatment of the BIO 2 assemblage were also lower than those of the LL treatment of the BIO 1 community (Table 4), potentially indicating higher Fe requirement of the flagellate-dominated station. While SO phytoplankton are commonly known to increase their σ_{PSII} in response to Fe limitation (Strzepek et al., 2019), both communities in our study did not exhibit a strong Fe-dependent decrease in σ_{PSII} with Fe addition, and values at the end of the incubations were fairly similar between the two stations despite being composed of different phytoplankton assemblages (Table 2). The absence of this photophysiological adjustment may explain the increase in Fe demand of both communities under LL.

With respect to the community composition, aside from the strongly lowered relative abundance of haptophytes at the end of the incubation, the diatoms, cryptophytes, and dinoflagellates maintained positive growth throughout the course of the experiment (% change of pigment marker to Chl *a* ratio from the initial: >100% indicates positive growth; Figure 6). At the end of the incubation, the mixotrophic cryptophytes and dinoflagellates were most abundant, showing up to 300% and 250% increase, respectively. Since in the Control both the cryptophytes and haptophytes exhibited a similar increase in their relative abundance between LL and HL, this suggests that the dinoflagellates most likely were the ones to prey on haptophytes, causing their overall decline at the end of the incubation. In line with this, culture experiments with a novel dinoflagellate isolated from the Ross Sea (Gast et al., 2007) have shown the selective predation of the dinoflagellate on the Antarctic haptophyte *P. antarctica* (Sellers et al., 2014). In addition to potential predation effects, some HL effects were also observed. For instance, the relative abundance of diatoms significantly declined between LL and ML in the Control, indicating a susceptibility of diatoms to higher irradiances under Fe limitation, while positive HL effects were observed for the cryptophytes and haptophytes. Considering that our Fe–light experiments were conducted during late summer, it could also be that grazing of large-sized diatoms occurred prior to sampling and that much of the dFe in BIO 2 was recycled Fe. In the absence of Fe addition, the small-sized diatoms were potentially outcompeted by the flagellates in the Control treatment since regenerated Fe is more easily accessible to the latter (Boyd et al., 2012), in addition to the finding that haptophytes and cryptophytes are well-adapted to high irradiances (Trimborn et al., 2019; Camoying and Trimborn, 2023; Mendes et al., 2023).

Ecological implications

With the ongoing ocean acidification and global warming events, two scenarios are projected for the open ocean regions of the SO. The first scenario predicts the shallowing of the mixed layer depth (MLD) due to sea surface temperature warming and the subsequent melting of sea ice (Meijers, 2014). This would result in increased light availability to phytoplankton (Bopp et al., 2013) but would reduce the input of trace metals from deeper water layers (Bopp et al., 2001). The second scenario, in contrast, projects a poleward shift and strengthening of westerly winds (Meijers, 2014), and this is expected

to result in reduced light availability due to the deepening of the MLD and an increase in Fe input from deeper layers due to stronger water column mixing (Hauck et al., 2015). Based on the response of the diatom-dominated community in the open waters of the Drake Passage (BIO 1), under the first scenario with less Fe, but more light, POC production would only be enhanced when exposed to high light (150 µmol photons m^{-2} s^{-1}), but not at low and medium light (30 and 80 µmol photons m^{-2} s^{-1}, respectively). With the second scenario of high Fe supply, but low light availability, POC production would also be enhanced. Hence, both scenarios would lead to increased growth and carbon production of the open ocean diatom-dominated community.

With regard to the coastal Antarctic region, climate change models project increased stratification due to melting ice and surface water freshening, thereby increasing the light available to phytoplankton together with higher nutrient inputs from the melting glaciers and sea ice (Deppeler and Davidson, 2017). Such a scenario of high light and high Fe availability would also lead to enhanced growth and carbon production of the flagellate-dominated coastal WAP community (BIO 2).

Climate change models predict an enhanced Fe input and light availability in the future SO, which would in turn result in an overall increase in net primary production and growth of SO phytoplankton (Henley et al., 2020). The results of our two field experiments corroborate the simulation outcomes of the SO models since we observed a significant enhancement in the POC production of the two distinct SO phytoplankton assemblages in response to medium irradiance (80 µmol photons m^{-2} s^{-1}) and high Fe supply. However, the degree of POC production increase would be higher in the diatom-dominated than flagellate-dominated community, which could be attributed to the lower Fe requirement of diatoms relative to flagellates. Exposure of SO phytoplankton communities to even higher light (150 µmol photons m^{-2} s^{-1}), however, would not lead to a further increase in POC production. Given the projected dominance of diatoms, carbon export of the open ocean regions of the SO would be enhanced, while that of coastal WAP waters would be reduced since small flagellates are said to be less efficient vectors for carbon export compared to the large, silica-containing diatoms (Armstrong et al., 2009; Ducklow et al., 2001). Moreover, the increase in the abundance of small flagellates could also have an impact on the distribution patterns of key SO grazers (krill and salps). For instance, krill are reported to prefer feeding on large-sized diatoms (Meyer and El-Sayed, 1983; Haberman et al., 2003), while salps, being non-selective feeders, are able to efficiently feed on small flagellates (Pakhomov et al., 2002). The potential shift in the dominance from krill to salps could result in a decreased availability of food to higher trophic organisms (i.e., seals, penguins, and whales; Henley et al., 2020), thus affecting the food web dynamics in the SO. Moreover, while flagellates may not be the preferred food of krill, they may serve as a rich source of recycled Fe due to their high cellular Fe content.

Data availability statement

The raw data supporting the conclusions of this article will be made available by the authors, without undue reservation.

Author contributions

MC: Formal analysis, Visualization, Writing – original draft, Writing – review & editing. FK: Investigation, Writing – review & editing. JS: Methodology, Writing – review & editing. FP: Methodology, Writing – review & editing. CH: Writing – review & editing. ST: Conceptualization, Funding acquisition, Investigation, Supervision, Writing – review & editing.

Funding

The author(s) declare financial support was received for the research, authorship, and/or publication of this article. FK, FP, and ST were funded by the Helmholtz Impulse Fond (HGF Young Investigators Group EcoTrace, VH-NG-901). MC was funded by the Katholischer Akademischer Ausländer-Dienst (KAAD) through a PhD scholarship.

Acknowledgments

We thank T. Brenneis for analyzing the POC samples and C. Völkner and D. Wilhelms-Dick for the ICP-MS measurements. We are grateful to M. Van Leeuwe for the insightful discussions on the interpretation of our HPLC marker pigment data. We acknowledge the support from the Open Access Publication Fund of the Alfred Wegener Institute, Helmholtz Centre for Polar and Marine Research. We also thank J. Heiden, R. Zimmerman, and P. Karitter for their assistance during field sampling. Lastly, we thank the cruise leader, captain, and crew of *RV Polarstern* during the PS97 expedition.

Conflict of interest

The authors declare that the research was conducted in the absence of any commercial or financial relationships that could be construed as a potential conflict of interest.

Publisher's note

Supplementary material

The Supplementary Material for this article can be found online at: https://www.frontiersin.org/articles/10.3389/fmars.2024.1441087/full#supplementary-material

References

Alderkamp, A. C., De Baar, H. J. W., Visser, R. J. W., and Arrigo, K. R. (2010). Can photoinhibition control phytoplankton abundance in deeply mixed water columns of the Southern Ocean? *Limnol. Oceanogr.* 55, 1248–1264. doi: 10.4319/lo.2010.55.3.1248

Alderkamp, A. C., Kulk, G., Buma, A. G. J., Visser, R. J. W., Van Dijken, G. L., Mills, M. M., et al. (2012). The effect of iron limitation on the photophysiology of *Phaeocystis Antarctica* (Prymnesiophyceae) and *Fragilariopsis cylindrus* (Bacillariophyceae) under dynamic irradiance. *J. Phycol.* 48, 45–59. doi: 10.1111/j.1529-8817.2011.01098.x

Alderkamp, A. C., Van Dijken, G. L., and Lowry, K. E. (2015). Fe availability drives phytoplankton photosynthesis rates during spring bloom in the Amundsen Sea Polynya, Antarctica. *Elementa* 3, 1–26. doi: 10.12952/journal.elementa.000043

Alderkamp, A. C., Van Dijken, G. L., and Lowry, K. E. (2019). Effects of iron and light availability on phytoplankton photosynthetic properties in the Ross Sea. *Mar. Ecol. Prog. Ser.* 621, 33–50. doi: 10.3354/meps13000

Andrew, S. M., Morell, H. T., Strzepek, R. F., Boyd, P. W., and Ellwood, M. J. (2019). Iron availability influences the tolerance of Southern Ocean phytoplankton to warming and elevated irradiance. *Front. Mar. Sci.* 6. doi: 10.3389/fmars.2019.00681

Armstrong, R. A., Peterson, M. L., Lee, C., and Wakeham, S. G. (2009). Settling velocity spectra and the ballast ratio hypothesis. *Deep Sea Res. Part II Top. Stud. Oceanogr.* 56, 1470–1478. doi: 10.1016/j.dsr2.2008.11.032

Arrigo, K. R. (2005). Marine microorganisms and global nutrient cycles. *Nature* 437, 349–355.

Balaguer, J., Koch, F., Hassler, C., and Trimborn, S. (2022). Iron and manganese co-limit the growth of two phytoplankton groups dominant at two locations of the Drake Passage. *Commun. Biol.* 5, 1–12. doi: 10.1038/s42003-022-03148-8

Behrenfeld, M. J., and Milligan, A. J. (2013). Photophysiological expressions of iron stress in phytoplankton. *Ann. Rev. Mar. Sci.* 5, 217–246. doi: 10.1146/annurev-marine-121211-172356

Blain, S., Quéguiner, B., Armand, L., Belviso, S., Bombled, B., Bopp, L., et al. (2007). Effect of natural iron fertilization on carbon sequestration in the Southern Ocean. *Nature* 446, 1070–1074. doi: 10.1038/nature05700

Blanco-Ameijeiras, S., Cabanes, D. J. E., Cable, R. N., Trimborn, S., Jacquet, S., Wiegmann, S., et al. (2020). Exopolymeric substances control microbial community structure and function by contributing to both C and Fe nutrition in Fe-limited Southern Ocean provinces. *Microorganisms* 8, 1–21. doi: 10.3390/microorganisms8121980

Bopp, L., Monfray, P., Aumont, O., Dufresne, J.-L., LeTreut, H., Madec, G., et al. (2001). Potential impact of climate change on marine export production. *Glob. Biogeochem. Cyc.* 15, 81–99. doi: 10.1029/1999GB001256

Bopp, L., Resplandy, L., Orr, J. C., Doney, S. C., Dunne, J. P., Gehlen, M., et al. (2013). Multiple stressors of ocean ecosystems in the 21st century: projections with CMIP5 models. *Biogeosciences* 10, 6225–6245. doi: 10.5194/bg-10-6225-2013

Boyd, P. W., Strzepek, R., Chiswell, S., Chang, H., DeBruyn, J. M., Ellwood, M., et al. (2012). Microbial control of diatom bloom dynamics in the open ocean. *Geophys. Res. Lett.* 39, L18601. doi: 10.1029/2012GL053448

Boyd, P. W., Watson, A. J., and Law, C. S. (2000). A mesoscale phytoplankton bloom in the polar Southern Ocean stimulated by iron fertilization. *Nature* 407, 695–702. doi: 10.1038/35037500

Camoying, M. G., Bischof, K., Geuer, J. K., Koch, B. P., and Trimborn, S. (2022). In contrast to diatoms, cryptophytes are susceptible to iron limitation, but not to ocean acidification 174, 1–16. doi: 10.1111/ppl.13614

Camoying, M. G., and Trimborn, S. (2023). Physiological response of an Antarctic cryptophyte to increasing temperature, CO_2, and irradiance. *Limnol. Oceanogr.* 2100, 1–15. doi: 10.1002/lno.12392

Cutter, G., Casciotti, K., Croot, P., Geibert, W., Heimbürger, L.-E., Lohan, M., et al. (2017). *Sampling and Sample-handling Protocols for GEOTRACES Cruises* (Toulouse, France: GEOTRACES International Project Office). Available at: http://www.geotraces.org/images/stories/documents/intercalibration/Cookbook.pdf.

Deppeler, S. L., and Davidson, A. T. (2017). Southern ocean phytoplankton in a changing climate. *Front. Mar. Sci.* 4. doi: 10.3389/fmars.2017.00040

Ducklow, H. W., Steinberg, D. K., and Buesseler, K. O. (2001). Upper ocean carbon export and the biological pump. *Oceanography* 14, 50–58. doi: 10.5670/oceanog.2001.06

Falkowski, P. G., and Raven, J. A. (2007). *Aquatic photosynthesis: (Second edition) (STU-student edition)* (Princeton University Press). Available at: http://www.jstor.org/stable/j.ctt4cgbxs.

Feng, Y., Hare, C. E., Rose, J. M., et al (2010). Interactive effects of iron, irradiance and CO2 on ross sea phytoplankton. *Deep. Res. Part I Oceanogr. Res. Pap.* 57, 368–383. doi: 10.1016/j.dsr.2009.10.013

Gast, R. J., Moran, D. M., Dennett, M. R., and Caron, D. A. (2007). Kleptoplasty in an Antarctic dinoflagellate: caught in evolutionary transition? *Environ. Microbiol.* 9, 39–45. doi: 10.1111/j.1462-2920.2006.01109.x

Haberman, K. L., Ross, R. M., and Quetin, L. B. (2003). Diet of the Antarctic krill (Euphausia superba Dana): II. Selective grazing in mixed phytoplankton assemblages. *J. Exp. Mar. Biol. Ecol.* 283, 97–113. doi: 10.1016/S0022-0981(02)00467-7

Hathorne, E. C., Haley, B., Stichel, T., Grasse, P., Zieringer, M., and Frank, M. (2012). Online preconcentration ICP-MS analysis of rare earth elements in seawater. *Geochemistry Geophysics Geosystems* 13. doi: 10.1029/2011GC003907

Hauck, J., Völker, C., Wolf-Gladrow, D. A., Laufkötter, C., Vogt, M., Aumont, O., et al. (2015). On the Southern Ocean CO2 uptake and the role of the biological carbon pump in the 21st century. *Glob. Biogeochem. Cycles* 29, 1451–1470. doi: 10.1002/2015GB005140

Heiden, J. P., Bischof, K., and Trimborn, S. (2016). Light intensity modulates the response of two Antarctic diatom species to ocean acidification. *Front. Mar. Sci.* 3. doi: 10.3389/fmars.2016.00260

Heiden, J. P., Völkner, C., Jones, E. M., et al (2019). Impact of ocean acidification and high solar radiation on productivity and species composition of a late summer phytoplankton community of the coastal western antarctic peninsula. *Limnol. Oceanogr.* 64, 1716–1736. doi: 10.1002/lno.11147

Henley, S. F., Cavan, E. L., Fawcett, S. E., Kerr, R., Monteiro, T., Sherrell, R. M., et al. (2020). Changing biogeochemistry of the southern ocean and its ecosystem implications. *Front. Mar. Sci.* 7. doi: 10.3389/fmars.2020.00581

Hoffmann, L. J., Peeken, I., and Lochte, K. (2008). Iron, silicate, and light co-limitation of three Southern Ocean diatom species. *Polar Biol.* 31, 1067–1080. doi: 10.1007/s00300-008-0448-6

Huot, Y., and Babin, M. (2010). "Overview of fluorescence protocols: theory, basic concepts, and practice," in *Chlorophyll a fluorescence in aquatic sciences: Methods and applications*. Eds. D. J. Suggett, M. A. Borowitzka and O. Prášil (Berlin: Springer). doi: 10.1007/978-90-481-9268-7

Joy-Warren, H. L., Alderkamp, A. C., and van Dijken, G. L. (2022). Springtime phytoplankton responses to light and iron availability along the western Antarctic Peninsula. *Limnol. Oceanogr.* 67, 1–16. doi: 10.1002/lno.12035

Koch, F., Beszteri, S., Harms, L., and Trimborn, S. (2019). The impacts of iron limitation and ocean acidification on the cellular stoichiometry, photophysiology, and transcriptome of *Phaeocystis Antarctica*. Limnol. *Oceanogr.* 64, 357–375. doi: 10.1002/lno.11045

Koch, F., and Trimborn, S. (2019). Limitation by Fe, Zn, Co, and B_{12} results in similar physiological responses in two Antarctic phytoplankton species. *Front. Mar. Sci.* 6. doi: 10.3389/fmars.2019.00514

Latour, P., Eggins, S., and van der Merwe, P. (2023). Characterization of a Southern Ocean deep chlorophyll maximum: Response of phytoplankton to light, iron, and manganese enrichment. *Limnol. Oceanogr. Lett.* 9, 145–154. doi: 10.1002/lol2.10366

Lee, Y., Jung, T. W., Kim, E. J., and Park, J. (2022). Phytoplankton growth rates in the Amundsen Sea (Antarctica) during summer: The role of light. *Environ. Res.* 207. doi: 10.1016/j.envres.2021.112165

Luxem, K. E., Ellwood, M. J., and Strzepek, R. F. (2017). Intraspecific variability in phaeocystis antarctica's response to iron and light stress. *PloS One* 12 (7), e0179751. doi: 10.1371/journal.pone.0179751

Mackey, M. D., Mackey, D. J., Higgins, H. W., and Wright, S. W. (1996). CHEMTAX - A program for estimating class abundances from chemical markers: Application to HPLC measurements of phytoplankton. *Mar. Ecol. Prog. Ser.* 144, 265–283. doi: 10.3354/meps144265

Maldonado, M. T., Boyd, P. W., Harrison, P. J., and Price, N. M. (1999). Co-limitation of phytoplankton growth by light and fe during winter in the NE subarctic pacific ocean. *Deep. Res. Part II Top. Stud. Oceanogr.* 46, 2475–2485. doi: 10.1016/S0967-0645(99)00072-7

Marchetti, A., Maldonado, M. T., Lane, E. S., and Harrison, P. J. (2006). Iron requirements of the pennate diatom Pseudo-nitzschia Comparison of oceanic (high-nitrate, low-chlorophyll waters) and coastal species. *Limnology Oceanography* 51, 2092–2101. doi: 10.4319/lo.2006.51.5.2092

Martin, J. H., Fitzwater, S. E., and Gordon, R. M. (1990). Iron deficiency limits phytoplankton growth in antarctic waters. *Global Biogeochem. Cycles* 4, 5–12. doi: 10.1029/GB004i001p00005

Meijers, A. J. S. (2014). The Southern Ocean in the coupled model intercomparison project phase 5. *Phil. Trans. R. Soc A* 372, 20130296. doi: 10.1098/rsta.2013.0296

Mendes, C. R. B., Costa, R. R., Ferreira, A., Jesus, B., Tavano, V. M., Dotto, T. S., et al (2023). Cryptophytes: An emerging algal group in the rapidly changing antarctic peninsula marine environments. *Glob. Change Biol.* 29, 1791–1808. doi: 10.1111/gcb.16602

Mendes, C. R. B., Tavano, V. M., Dotto, T. S., Kerr, R., de Souza, M. S., Garcia, C. A. E., et al. (2018). New insights on the dominance of cryptophytes in antarctic coastal waters: A case study in gerlache strait. *Deep. Res. Part II Top. Stud. Oceanogr.* 149, 161–170. doi: 10.1016/j.dsr2.2017.02.010

Meyer, M. A., and El-Sayed, S. Z. (1983). Grazing of *Euphausia superba* Dana on natural phytoplankton populations. *Polar Biol.* 1, 193–197. doi: 10.1007/BF00443187

Mitchell, B. G., Brody, E. A., Holm-Hansen, O., McClain, C., and Bishop, J. (1991).). light limitation of phytoplankton biomass and macro- nutrient utilization in the southern ocean. *Limnology Oceanography* 36 (8), 1662–1677.

Moore, C. M., Seeyave, S., Hickman, A. E., Allen, J. T., Lucas, M. I., Planquette, H., et al. (2007). Iron-light interactions during the CROZet natural iron bloom and EXport experiment (CROZEX) I: phytoplankton growth and photophysiology. *Deep-Sea Res. II Top. Stud. Oceanogr.* 54, 2045–2065. doi: 10.1016/j.dsr2.2007.06.011

Oxborough, K., Moore, C. M., Suggett, D. J., Lawson, T., Chan, H. G., and Geider, R. J. (2012). Direct estimation of functional PSII reaction center concentration and PSII electron flux on a volume basis: A new approach to the analysis of fast repetition rate fluorometry (FRRf) data. *Limnol. Oceanogr. Methods* 10, 142–154. doi: 10.4319/lom.2012.10.142

Pakhomov, E. A., Froneman, P. W., and Perissinotto, R. (2002). Salp/krill interactions in the Southern Ocean: Spatial segregation and implications for the carbon flux. *Deep Sea Res. II* 49, 1881–1907. doi: 10.1016/S0967-0645(02)00017-6

Pausch, F., Koch, F., Hassler, C., Bracher, A., Bischof, K., and Trimborn, S. (2022). Responses of a natural phytoplankton community from the Drake Passage to two predicted climate change scenarios. *Front. Mar. Sci.* 9, 1–18. doi: 10.3389/fmars.2022.759501

Peers, G., and Price, N. M. (2004). A role for manganese in superoxide dismutases and growth of iron-deficient diatoms. *Limnol. Oceanogr.* 49, 1774–1783. doi: 10.4319/lo.2004.49.5.1774

Petrou, K., Hassler, C. S., Doblin, M. A., Shelly, K., Schoemann, V., van den Enden, R., et al. (2011). Iron-limitation and high light stress on phytoplankton populations from the Australian Sub-Antarctic Zone (SAZ). *Deep. Res. Part II Top. Stud. Oceanogr.* 58, 2200–2211. doi: 10.1016/j.dsr2.2011.05.020

Petrou, K., Trimborn, S., Rost, B., Ralph, P. J., and Hassler, C. S. (2014). The impact of iron limitation on the physiology of the Antarctic diatom *Chaetoceros simplex*. *Mar. Biol.* 161, 925–937. doi: 10.1007/s00227-014-2392-z

Ralph, P. J., and Gademann, R. (2005). Rapid light curves: a powerful tool to assess photosynthetic activity. *Aquat. Bot.* 82, 222–237. doi: 10.1016/j.aquabot.2005.02.006

Rapp, I., Schlosser, C., Rusiecka, D., Gledhill, M., and Achterberg, E. P. (2017). Automated preconcentration of Fe, Zn, Cu, Ni, Cd, Pb, Co, and Mn in seawater with analysis using high-resolution sector field inductively-coupled plasma mass spectrometry. *Analytica Chim. Acta* 976, 1–13. doi: 10.1016/j.aca.2017.05.008

Raven, J. A. (1990). Predictions of Mn and Fe use efficiencies of phototrophic growth as a function of light availability for growth and of C assimilation pathway. *New Phytol.* 116, 1–18. doi: 10.1111/j.1469-8137.1990.tb00505.x

Ryan-Keogh, T. J., DeLizo, L. M., Smith, W. O., Sedwick, P. N., McGillicuddy, D. J., Moore, C. M., et al. (2017). Temporal progression of photosynthetic-strategy in phytoplankton in the Ross Sea, Antarctica. *J. Mar. Syst.* 166, 87–96. doi: 10.1016/j.jmarsys.2016.08.014

Sellers, C. G., Gast, R. J., and Sanders, R. W. (2014). Selective feeding and foreign plastid retention in an Antarctic dinoflagellate. *J. Phycol.* 50, 1081–1088. doi: 10.1111/jpy.12240

Strzepek, R. F., Boyd, P. W., and Sunda, W. G. (2019). Photosynthetic adaptation to low iron, light, and temperature in Southern Ocean phytoplankton. *Proc.Natl. Acad. Sci. U.S.A.* 116, 4388–4393. doi: 10.1073/pnas.1810886116

Strzepek, R. F., Hunter, K. A., Frew, R. D., Harrison, P. J., and Boyd, P. W. (2012). Iron-light interactions differ in Southern Ocean phytoplankton. *Limnol. Oceanogr* 57, 1182–1200. doi: 10.4319/lo.2012.57.4.1182

Suggett, D. J., MacIntyre, H. L., and Geider, R. J. (2004). Evaluation of biophysical and optical determinations of light absorption by photosystem II in phytoplankton. *Limnol. Oceanogr. Methods* 2, 316–332. doi: 10.4319/lom.2004.2.316

Sunda, W. G., and Huntsman, S. A. (1997). Interrelated influence of iron, light and cell size on marine phytoplankton growth. *Nature* 390, 389–392. doi: 10.1038/37093

Sunda, W., Swift, D., and Huntsman, S. (1991). Low iron requirement for growth in oceanic phytoplankton. *Nature* 351, 55–57. doi: 10.1038/351055a0

Trimborn, S., Thoms, S., Bischof, K., and Beszteri, S. (2019). Susceptibility of two Southern Ocean phytoplankton key species to iron limitation and high light. *Front. Mar. Sci.* 6. doi: 10.3389/fmars.2019.00167

Twining, B. S., Baines, S. B., Fisher, N. S., and Landry, M. R. (2004). Cellular iron contents of plankton during the Southern Ocean Iron Experiment (SOFeX). *Deep. Res. Part I Oceanogr. Res. Pap.* 51, 1827–1850. doi: 10.1016/j.dsr.2004.08.007

Van Leeuwe, M., and Stefels, J. (1998). Effects of iron and light stress on the biochemical composition of antarctic Phaeocystis sp. (Prymnesiophyceae). II. Pigment composition. *J. Phycol* 503, 496–503. doi: 10.1046/j.1529-8817.1998.340486.x

Viljoen, J. J., Philibert, R., Van Horsten, N., Mtshali, T., Roychoudhury, A. N., Thomalla, S., et al. (2018). Phytoplankton response in growth, photophysiology and community structure to iron and light in the Polar Frontal Zone and Antarctic waters. *Deep Sea Res. Part I Oceanogr. Res. Pap.* 141, 118–129. doi: 10.1016/j.dsr.2018.09.006

Vives, C. R., Schallenberg, C., Strutton, P. G., and Westwood, K. J. (2022). Iron and light limitation of phytoplankton growth off East Antarctica. *J. Mar. Syst.* 234, 103774. doi: 10.1016/j.jmarsys.2022.103774

Wright, S. W., and Van den Enden, R. L. (2000). Phytoplankton community structure and stocks in the East Antarctic marginal ice zone (BROKE survey, January-March 1996) determined by CHEMTAX analysis of HPLC pigment signatures. *Deep. Res. Part II Top. Stud. Oceanogr.* 47, 2363–2400. doi: 10.1016/S0967-0645(00)00029-1

Ye, Y., Sunda, W. G., Hong, H., and Shi, D. (2023). Interrelated influence of iron, light, and CO2 on carbon fixation in a Southern Ocean diatom. *Limnol. Oceanogr.* 68, 1504–1516. doi: 10.1002/lno.12360

Chapter 5

Synthesis

5.1 Discussion of major findings

This chapter summarizes and discusses the major findings of the thesis in a broader context. Specifically, I will discuss the ecophysiology of cryptophytes in today's ocean and will further assess the influence of various environmental drivers such as warming, ocean acidification (OA), varying light and Fe availability on this yet less-studied ecologically important SO phytoplankton group. Their ecophysiological responses and the adaptive mechanisms they employ in dealing with these stressors are compared to that of the extensively studied groups of diatoms and haptophytes. Lastly, the ecological implications of these observations are presented and potential future research directions are proposed to improve our understanding of the ecophysiology of SO cryptophytes.

5.1.1 Increasing temperature alleviates the negative HL effect on growth and carbon production of cryptophytes

Aside from the study of Wang and Smith (2021), which showed an enhanced growth of another *G. cryophila* strain at 4 °C, nothing is known yet about the thermal growth response of *G. cryophila*. In *Publication 2*, it was revealed that the calculated optimal temperature for growth of the cryptophyte at ambient pCO_2 and 100 µmol photons m^{-2} s^{-1} is 3.8 °C (T_{opt}). This is lower compared to the calculated T_{opt} of 5.2 °C by Coello-Camba and Agustí (2017) for Antarctic phytoplankton in general. Moreover, the calculated highest temperature, at which it could maintain positive growth is 8.02 °C (T_{max}). In comparison, *P. antarctica* (Zhu et al., 2017; Andrew et al., 2019) and the diatoms *Chaetoceros flexuosus* and *Thalassiosira antarctica* showed enhanced growth in response to increased temperature up to 5 °C (Andrew et al., 2019). *Pseudo-nitzschia subcurvata* even exhibited highest growth at 8 °C (Zhu et al., 2017), which was already the T_{max} of *G. cryophila*. Hence, cryptophytes may be less competitive than haptophytes and diatoms under a future warming of > 4 °C and may be more susceptible to globally increasing temperatures due to their narrow thermal growth window. Indeed, *G. cryophila* cells eventually stopped dividing when exposed to 6 °C for a longer period (4 weeks). The only exception is when it was grown under OA in combination with medium light (100 µmol photons m^{-2} s^{-1}), wherein it was able

to maintain an efficient photosynthetic machinery as well as positive growth. However, after 10 weeks of incubation, its growth was still continuously decreasing until it stopped dividing after 11 weeks. Interestingly, when this treatment was transferred back to its optimal temperature for growth at 4 °C, it was able to recover and exhibited again high growth rates similar to the original 4 °C treatment. Cells, however, became smaller and the appearance of lipid droplets decreased compared to the 2 °C treatment (Figure 5.1). This observation implies that OA in combinatiom with medium irradiances may potentially increase the ability of the cryptophyte to tolerate short warming episodes or heatwaves, which are becoming more frequent now in the SO (González-Herrero et al., 2022).

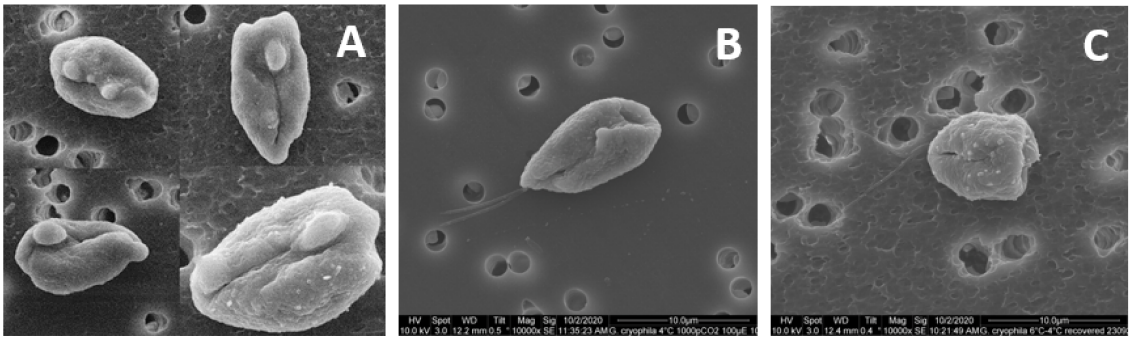

Figure 5.1. Scanning electron microscopy pictures were taken from *G. cryophila* cells grown at 100 µmol photons m^{-2} s^{-1} that were additionally also exposed to increasing pCO_2 and temperature: (A) 2°C-400pCO_2, (B) 4°C-400pCO_2 and (C) cell image of the "recovered" 6°C-1000pCO_2 treatment after transferring it back to 4 °C. Presence of lipid accumulations is indicated by bumps. *Source: Publication 1, Supplementary File*

It was further shown in *Publication 2* that the exposure of the cryptophyte to 500 µmol photons m^{-2} s^{-1} high light under ambient pCO_2 and high Fe supply, resulted in reduced growth and POC production rates compared when it was grown at medium irradiance (100 µmol photons m^{-2} s^{-1}). Combining the growth rate data from *Publication 2* (100 and 500 µmol photons m^{-2} s^{-1}) and from the OA-light experiment of Trimborn et al. (2019) (20 and 200 µmol photons m^{-2} s^{-1}) for the same *G. cryophila* strain, the growth-irradiance curve of the cryptophyte at 2 °C was calculated (Figure 5.2). The figure reveals that growth of *G. cryophila* already starts to plateau at 100 µmol photons m $^{-2}$ s^{-1}, but still no photoinhibition was observed at 500 µmol photons m^{-2} s^{-1}. Indeed, *G. cryophila* was able to tolerate a wide range of light intensities although a negative impact on its physiology emerged when cells were exposed to 500 µmol photons m^{-2} s^{-1} (i.e. reduced growth and carbon production *Publication 2*).

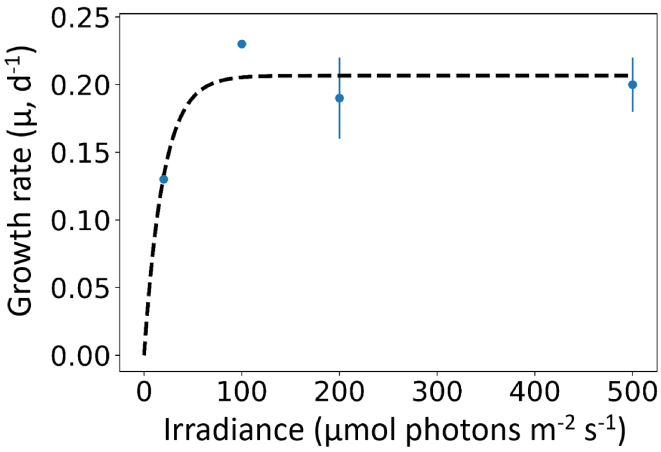

Figure 5.2. Growth-irradiance curve of *Geminigera cryophila* using the growth data from *Publication 1* (100 and 500 µmol photons m^{-2} s^{-1}) and from Trimborn et al. (2019) (20 and 200 µmol photons m^{-2} s^{-1}).

In the study of Trimborn et al. (2019), at ambient pCO_2, the same *G. cryophila* strain was even unable to grow at 500 µmol photons m^{-2} s^{-1}. The discrepancy between this observation of Trimborn et al. (2019) and the results of *Publication 2* could have stemmed from their direct transfer of the culture from 20 to 200 µmol photons m^{-2} s^{-1}. As can be seen in the growth-irradiance curve of *G. cryophila* (Figure 5.2), its growth already becomes saturated at 200 µmol photons m^{-2} s^{-1}. Possibly, the direct transfer of the low light acclimated cultures to saturating light (200 µmol photons m^{-2} s^{-1}) in Trimborn et al. (2019) could have caused too much light stress on the cryptophyte, which then led to the cells' mortality. On the other hand, in *Publication 2*, *G. cryophila* was first acclimated to 100 µmol photons m^{-2} s^{-1} (at which optimal growth was observed) and because cultures were more fit and healthy, they were then able tolerate the high light treatment (500 µmol photons m^{-2} s^{-1}) although growth and carbon production were compromised. It was also observed in *Publication 3* that the growth of the cryptophyte group increased from 30 to 80 µmol photons m^{-2} s^{-1} but no further enhancement at 150 µmol photons m^{-2} s^{-1} (Figure 6). The results of this thesis indicate that under ambient pCO_2 and high Fe supply, cryptophytes benefit from moderate irradiances (e.g. 100 – 150 µmol photons m^{-2} s^{-1}). They are also able to tolerate low and high irradiances, specifically at higher temperatures (500 µmol photons m^{-2} s^{-1} at 4 °C, *Publication 2*; Mendes et al., 2023) by undergoing important physiological adjustments. For instance, *G. cryophila* reduced the concentration of its light harvesting pigments in response to 500 µmol photons m^{-2} s^{-1} (*Publication 2*, Fig. 4). Upon exposure to short-term light stress, *G. cryophila* cells also employed non-photochemical quenching (NPQ) to dissipate the excess light energy. Surprisingly, the cultures acclimated to 100 µmol photons m^{-2} s^{-1} exhibited higher NPQ values compared to the ones grown under 500 µmol photons m^{-2} s^{-1} (*Synthesis*, Figure 5.3). Probably, the medium light-acclimated cultures had to deal with more excess light energy due to their high cellular concentration of light harvesting pigments (*Publication 2*, Fig. 4), which potentially led to earlier saturation of the Calvin cycle (indicated by lowered I_k and ETR_{max}, *Publication 2*, Fig. 6) and in turn activated NPQ. Such enhanced NPQ response upon saturation of the Calvin Cycle was

also observed in the cryptophyte *Rhodomonas salina* (Kaňa et al., 2012).

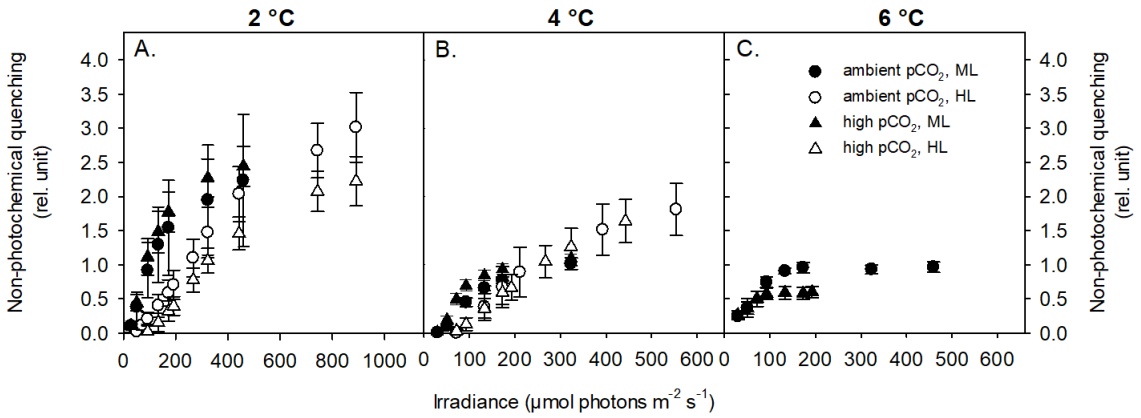

Figure 5.3. Non-photochemical quenching was measured in response to increasing irradiance in *Geminigera cryophila* grown under ambient pCO_2 (400 µatm, circle) and high pCO_2 (1000 µatm, triangle) in combination with different temperature (2 (A), 4 (B) and 6 °C (C)) and light intensities (filled symbols, ML, 100 µmol photons m^{-2} s^{-1}; open symbols; HL, 500 µmol photons m^{-2} s^{-1}) at the end of the experiments. Please note that for the 6 °C treatment, after 11 weeks of incubation, the unhealthy 6 °C-ML-1000 cells (filled triangle) were transferred back to 4 °C to test whether they would be able to recover from exposure to temperature above T_{opt}. Values represent the mean and standard deviation (n=3). *Source: Publication 1, Supplementary File*

In line with this, a different strain of *G. cryophila* was shown to maintain similar growth rates between 72 to 535 µmol photons m^{-2} s^{-1} (Mendes et al., 2023). Different to *Publication 2* and Trimborn et al. (2019), where *G. cryophila* was grown at 2 °C, Mendes et al. (2023) conducted their laboratory experiments at 3 °C. Based on the latter, one can hypothesize that the exposure of *G. cryophila* to a higher temperature, close to the T_{opt} of the species (3.8 °C), provided more favorable growth conditions, hence a decrease in growth was not observed even under the highest light treatment of 535 µmol photons m^{-2} s^{-1} by Mendes et al. (2023). Indeed, based on the results of *Publication 2*, increasing temperature (from 2 up to 4 °C) alleviated the negative effect of 500 µmol photons m^{-2} s^{-1} on the growth and carbon production of *G. cryophila*. The enhanced enzymatic reactions at 4 °C might have enabled the cryptophyte to efficiently deal with high light. In contrast to the 2 °C treatment, no lipid droplet appearance was observed in cells grown at T_{opt} (*Synthesis*, Figure 5.1), which may indicate that the available high energy was balanced by faster enzymatic rates. In fact, increasing temperature from 0 to 10 °C resulted in the enhanced carboxylation rates of the enzyme RuBisCO of the Antarctic phytoplankton *Fragilariopsis cylindrus* (Young et al., 2015a), something that may apply for cryptophytes as well. This could provide an explanation for the finding that *G. cryophila* benefited only from high light (500 µmol photons m^{-2} s^{-1}) when grown at a higher temperature (4 °C, *Publication 2*).

5.1.2 Cryptophytes benefit slightly from OA under high Fe

Field studies on natural phytoplankton communities have shown that cryptophytes are less susceptible to changes in pCO_2 (Sommer et al., 2015; Young et al., 2015b; Schulz et al., 2017; Donahue et al., 2019). This is in line with observations from laboratory experiments, which showed the ability of several cryptophyte species to grow in a wide range of pH (Weisse and Stadler, 2006; Gaillard et al., 2020). The findings of this thesis corroborate the observations of previous studies as *Publications 1 and 2* revealed that *G. cryophila* was not negatively affected by OA under high Fe conditions. While Trimborn et al. (2019) reported no significant OA-effects on the growth of *G. cryophila* in their 20 and 200 µmol photons m^{-2} s^{-1} light treatments under high Fe supply, *Publication 1* showed a slight increase in growth and carbon production of the cryptophyte in response to OA without exhibiting changes in its photophysiology (maintained similar F_v/F_m, σ_{PSII}, ETR_{max}, and I_k). How exactly cryptophytes benefit from OA at a mechanistic level still remains unexplained and further studies are required. Currently, we also still lack information on the efficiency and regulative capacity of the carbon concentrating mechanism (CCM) of cryptophytes. Van de Waal et al. (2019), however, revealed that phytoplankton groups that evolved earlier (i.e. cyanobacteria and dinoflagellates) have been observed to possess more active and plastic CCMs compared to the recently evolved haptophytes and diatoms. Since cryptophytes also belong to a primitive group (Stiller et al., 2014; Kim et al., 2017), one can hypothesize that cryptophytes also possess highly plastic CCMs. The down-regulation of their potential CCM under OA may allow the cryptophytes to use the extra energy for nutrient acquisition or other cellular processes (van de Waal and Litchman, 2020) as has been suggested for cyanobacteria and dinoflagellates which evolved earlier (Van de Waal et al., 2019). This could potentially explain the modest positive effect of OA on the growth and carbon production of *G. cryophila* under the +Fe treatment (*Publication 1*, Fig. 3).

In contrast to the cryptophyte, growth and carbon production of the diatom *P. subcurvata* remained the same in response to increasing pCO_2 under +Fe conditions (*Publication 1*, Fig. 3), in line with the results of previous studies (Trimborn et al., 2013; Zhu et al., 2017). However, while the cryptophyte did not undergo photo-physiological adjustments, the Fe-replete diatom cultures exhibited photoacclimation strategies such as lowered cellular concentrations of light harvesting pigments and decreased ETR_{max} and I_k, in response to OA which may indicate an onset of Fe stress. Since genes encoding phytotransferrin was found in *P. subcurvata* (Moreno et al., 2018), it could be that the diatom is dependent on the phytotransferrin-based Fe uptake which was potentially impacted due to the low carbonate concentration under OA (McQuaid et al., 2018). To potentially lower its Fe demand under OA, *P. subcurvata*, could have replaced the Fe-requiring cytochrome c_6 with the Cu-containing plastocyanin thereby increasing the Cu:C ratio of the diatom under the +Fe treatment as observed in *Publication 1*. Based on the results of *Publications 1 and 2*, OA is more beneficial to cryptophytes than diatoms, specifically under high Fe supply.

5.1.3 Cryptophytes are highly susceptible to Fe limitation at ambient pCO_2

Fe is required in several cellular processes such as in the photosynthetic transport chain wherein Fe forms an integral component of photosystems I and II as well as in the electron

carriers cytochrome c_6 and cytochrome *b6f* (Raven et al., 1999; Behrenfeld and Milligan, 2013; Schoffman et al., 2016). Fe is also required in the synthesis of chlorophyll and in nitrogen acquisition and assimilation. The exposure of SO phytoplankton to low Fe conditions normally results in reduced photosynthetic efficiency, growth and carbon production, as observed in several laboratory experiments with Antarctic diatoms and *P. antarctica* (e.g. Strzepek et al., 2012; Petrou et al., 2014; Koch and Trimborn, 2019; Koch et al., 2019; Andrew et al., 2019) and natural Antarctic phytoplankton assemblages (Hoppe et al., 2013; Alderkamp et al., 2015; Trimborn et al., 2015; Balaguer et al., 2022). Hence, the susceptibility of SO phytoplankton to Fe limitation greatly depends on the cellular requirement, the bioavailability of Fe *in situ* and the efficiency of the Fe uptake strategy of the phytoplankton.

In *Publication 1*, at ambient pCO_2 under low Fe supply (Control treatment, 0.6 nM Fe), growth of *G. cryophila* almost stopped. Under these conditions, the photosynthetic efficiency of the cryptophyte was strongly reduced (*Publication 1*, Fig. 2). Comparing the growth of the cryptophyte under the +Fe treatment (high Fe supply, 1.2 nM Fe, *Publication 1*) to the growth values determined in Koch and Trimborn (2019) (Aquil medium, 2 µM) and Trimborn et al. (2019) (12 µM) for the same strain, it is apparent that even in the +Fe treatment, the cryptophyte was already experiencing Fe stress since its growth (0.10 ± 0.03 d^{-1}) was lower compared to the latter studies. Indeed, when it was separately grown at 2 nM, *G. cryophila* increased its growth up to 0.24 d^{-1}. In contrast, the diatom *P. subcurvata* maintained similar high growth rates between the Control and the +Fe treatments. *G. cryophila* also exhibited higher Fe:C ratios (6.5 µmol mol^{-1}, *Publication 1*) relative to *P. subcurvata* (2.85 µmol mol^{-1}, *Publication 1*), albeit not statistically significant (*Publication 1*, Fig. 4). It can be seen from the results of the Fe-CO_2 laboratory incubation experiment in *Publication 1* that the cryptophyte *G. cryophila* has a higher Fe requirement than the diatom *Pseudo-nitzschia subcurvata*.

This finding on the higher Fe demand of cryptophytes was also reflected in the field experiments in *Publication 3*. The mildly Fe-limited flagellate-dominated phytoplankton community of the coastal WAP waters, where a significant number of cryptophytes was encountered (Blanco-Ameijeiras et al., 2020; *Publication 3*, Fig. 6), also exhibited lower F_v/F_m values in all of its Control treatments (no Fe addition) relative to *in situ* conditions. This may indicate that Fe was used up over the course of the incubation period potentially due to the high cellular Fe demand of the flagellates. This is in line with the observations of Twining et al. (2004) which also revealed higher Fe:C ratios of SO flagellates compared to diatoms. Indeed, in response to Fe addition, the flagellate-dominated community also exhibited a lower magnitude of POC production increase compared to the diatom-dominated open ocean assemblage (*Publication 3*).

In contrast to diatoms, which rely on chlorophyll *a* and *c* harvesting complexes, cyanobacteria and cryptophytes possess an additional nitrogen-rich light harvesting complex containing phycobiliproteins (Bryant and Gisriel, 2024). The synthesis of phycobiliproteins requires a significant amount of nitrogen, potentially leading to an increase in the Fe requirement of cryptophytes. In connection to this, Maldonado and Price (1996) reported that higher Fe is required by phytoplankton when assimilating NO_3 than when acquiring NH_4^+. In a laboratory culture experiment, *Rhodomonas salina* exhibited higher growth rates

when grown in a NH_4^+-enriched medium than when nitrate is used (Jepsen et al., 2019). All the laboratory experiments conducted in this thesis used nitrate as the nitrogen source. This could have probably increased even more the demand for Fe of the cryptophyte and consequently, growth rates were low. Moreover, while oceanic diatoms (Peers and Price, 2006) and the haptophyte *P. antarctica* (Rizkallah et al., 2020) have been reported to reduce their Fe demand by replacing the Fe-requiring cytochrome c_6 with plastocyanin in the electron transport chain (Behrenfeld and Milligan, 2013; Castell et al., 2021; Raven et al., 1999), cryptophytes may not have the same capability. Genes encoding the Cu-containing enzyme plastocyanin were not observed in the marine cryptophyte *Guillardia theta* (Blaby-Haas and Merchant, 2017). Perhaps, this might also be the case for *G. cryophila*. In fact, *Publication 1* shows that Fe limitation did not trigger any change in the Cu:C ratio of the cryptophyte, as opposed to *P. subcurvata*, which exhibited a higher Cu:C ratio under the Control treatment relative to the +Fe conditions (Fig. 4). These observations indicate that cryptophytes may be at a disadvantage under conditions of low Fe supply.

Besides their potentially higher cellular Fe demand, it can be hypothesized that the susceptibility of cryptophytes to Fe limitation could also be due to their inefficient Fe uptake strategy or that they are only able to perform a limited suite of Fe uptake strategies compared to other phytoplankton groups such as diatoms. For instance, the diatom *Fragilariopsis cylindrus* has been reported to have the protein building blocks for all the Fe acquisition mechanisms (i.e. siderophore-mediated uptake, reductive high-affinity uptake; phytotransferrin-mediated and divalent metal uptake proteins, Behnke and LaRoche, 2020), indicating the ability of diatoms to thrive under extremely low Fe conditions (Mock et al., 2017). Indeed, in the Fe-light experiment in *Publication 3*, *Fragilariopsis* was the most dominant diatom species in the natural open ocean diatom-dominated assemblage that was sampled from very low *in situ* dFe concentrations (0.05 nM dFe; Table 1), potentially providing it a competitive advantage to acquire Fe. Indeed, several diatom species such as *Thalassiosira oceanica* (Lommer et al., 2012) and *T. pseudonana* (Kustka et al., 2007) have been shown to possess Fe reductase genes. *P. antarctica* has also been reported to utilize a Cu-dependent ferric reductase under low Fe supply (Rizkallah et al., 2020). In contrast to diatoms and haptophytes, Behnke and LaRoche (2020) suggested that cryptophytes may not be capable of performing Cu-dependent high-affinity Fe uptake since genes encoding for Fe-reductases and multicopper oxidases were not observed in the cryptophyte *Guillardia theta* and another unidentified cryptophyte species. Again, in support for this, the Cu quotas of *G. cryophila* was not enhanced under low Fe supply (*Publication 1*, Fig, 4). Moreover, iron starvation-induced proteins (ISIPs) have been observed to be strongly upregulated in several phytoplankton species in response to Fe limitation (Behnke and LaRoche, 2020). For example, the gene encoding the ISIP2 protein (phytotransferrin) has been detected in *Phaeodactylum tricornutum* (Morrissey et al., 2015; McQuaid et al., 2018), *P. subcurvata* (Moreno et al., 2018) and also in some cryptophyte species (Curtis et al., 2012). As already discussed in the preceding subsection, unlike *P. subcurvata*, *G. cryophila* is less likely dependent on the phytotransferrin-mediated Fe uptake strategy since its growth was not negatively affected by lower carbonate concentrations under the OA treatment (*Publication 1*, Fig. 3). Perhaps, cryptophytes more likely rely on divalent metal uptake proteins since genes encoding several Zinc-Regulated Transporter (ZRT)- Iron-Regulated Transporter (IRT)-like proteins (ZIP), capable of transporting Fe^{2+}

and Zn^{2+}, have been detected in a number of cryptophyte species (Behnke and LaRoche, 2020).

Overall, findings from *Publications 1 and 3* highlight that in contrast to diatoms, cryptophytes could not cope well with Fe limitation. This could be due to their high Fe requirement, which potentially is not fulfilled because of their less efficient Fe acquisition strategies, thus making them less efficient in taking up Fe relative to diatoms.

Furthermore, in *Publication 1* it was found that the Zn:C and Co:C ratios of the cryptophyte were generally higher in the Control than the +Fe treatment, irrespective of the pCO_2 treatment. Although not all of these observed trends were statistically significant, it might still be worth exploring plausible reasons behind these observations and to try linking them to the physiology of the cryptophyte. Aside from its role in DNA/RNA replication, Zn, which can also be replaced by Co (Morel et al., 2020), is also needed in carbonic anhydrase (CA), an enzyme that accelerates the interconversion of CO_2 and bicarbonate intra- and extracellularly. In connection to this observation, the extremely Fe-limited cyanobacterium *Synechococcus* sp. was found to up-regulate the gene encoding internal carbonic anhydrase and RubisCO oxidase (Blanco-Ameijeiras et al., 2017) to increase the CO_2 concentration close to the RuBisCO carboxylation site and to reduce thereby photorespiration. Considering the possibility that cryptophytes possess a similar CCM with cyanobacteria and dinoflagellates (Van de Waal et al., 2019), increasing internal CA activity, in this case, could then be a potential reason for the observed higher cellular Zn requirement of the cryptophyte under very low Fe conditions (Control treatment, *Publication 1*). The Fe-dependent CCM up-regulation might have allowed the cryptophyte to maintain similar high carbon production rates even under low Fe supply (*Publication 1*, Fig. 3). The laboratory incubation experiment of Koch and Trimborn (2019) revealed that Zn limitation posed a strong impact on the growth of *G. cryophila*, which may also support the idea that Zn plays an important role in the physiology of the cryptophyte (i.e. CCM operation). In fact, Zn has also been shown to regulate the full induction of Fe uptake in the green alga *Ostreococcus tauri* under Fe limitation (Lelandais et al., 2016). This might also be plausible in the case of cryptophytes given the fact that genes from green algae have been detected in the cryptophyte *Guillardia theta* (Curtis et al., 2012).

In conclusion, this thesis highlights that cryptophytes have a high Fe requirement and that Fe limitation potentially induces an increase in their cellular demand for Zn (i.e. potentially for CCM operation, induction of Fe uptake). These findings may explain why cryptophytes are commonly found in the coastal regions of the SO, which are typically characterized by both high macronutrient and trace metal (i.e. Fe and Zn) availabilities.

5.1.4 OA has no influence on the physiology of Fe-limited cryptophytes, but poses negative effects on diatoms

Under low Fe supply, the stimulatory effect of OA on the cryptophyte vanished, as growth and carbon production of *G. cryophila* remained unchanged between ambient and high pCO_2 (*Publication 1*, Fig. 3). Apart from this, no major physiological adjustments were found. In contrast to the cryptophyte, the Fe-limited *P. subcurvata* exhibited decreased growth rates in response to increasing pCO_2, indicating that OA amplified the impact of

Fe limitation. Indeed, *Pseudo-nitzschia* did not benefit from OA, as previously observed in OA-experiments with an Fe-limited open ocean phytoplankton community from the Weddell Sea (Hoppe et al., 2013), the Atlantic sector of the SO (Trimborn et al., 2017) and the Ross Sea (Tortell et al., 2008). It could be that, in *Publication 1*, the potential phytotransferrin-based Fe uptake in *P. subcurvata* was even further impacted under low Fe condition in combination with OA, and led to the formation of reactive oxygen species (ROS) (Alscher et al., 2002). The diatom might have utilized Cu/Zn superoxide dismutase (Cu/Zn SOD) to deal with ROS, hence an enhancement in both Cu:C and Zn:C ratios were observed for the Fe-limited diatom under OA. To clarify this aspect, future studies are needed.

Interestingly, the Fe-limited cryptophyte *G. cryophila* exhibited an increase in its cellular Fe quota in response to OA, although not statistically significant (*Publication 1*, Fig. 4). Since the Fe:C ratio of the cryptophyte did not change between the Control and +Fe treatment under ambient pCO_2 (*Publication 1*, Fig. 4), it may be reasonable to assume that Fe-limitation in combination with OA induced Fe uptake in *G. cryophila*. Such response has been observed in the marine green alga *Chlorococcum littorale*, where the combination of high-CO_2 and Fe-deficient conditions resulted in enhanced cellular Fe accumulation and induced the expression of the high-CO_2 response (HCR) gene which has been shown to have a similar sequence to the yeast ferric reductase proteins (Sasaki et al., 1998a,b). The authors proposed that Fe uptake by *C. littorale* consists of two steps: first is the reduction of extracellular Fe^{3+}, potentially being carried out by the HCR protein (ferric reductase), and the subsequent incorporation of Fe^{2+} into the cells by high-affinity Fe uptake mechanism (Sasaki et al., 1998b). There is currently no available study on the Fe uptake strategy of cryptophytes and the presence of the said high-CO_2 response genes has never been reported in any of the cryptophyte species that has been studied so far. Nevertheless, since cryptophytes (a red algal lineage) and chlorophytes (green algae) are also both ancient groups that are believed to have evolved earlier than diatoms (cf. Tortell, 2000), the possibility of these two groups sharing similar Fe uptake mechanisms is plausible and warrants further investigation.

5.1.5 Compared to diatoms, cryptophytes are less able to take advantage of HL availability under low Fe supply

Besides the on-going OA, SO phytoplankton are also projected to be exposed to varying light intensities under low Fe availability. It is well-established that low Fe supply constraints the growth of SO phytoplankton (Martin, 1990; Boyd et al., 2007). Fe limitation also impacts phytoplankton photosynthesis since Fe is an integral component of reaction centers and the electron transport chain (Raven, 1990). Phytoplankton are expected to increase their Fe requirement under low light conditions in order to increase the number of their reaction centers and thus enhance light capture (Maldonado et al., 1999). This may, however, not the case for SO phytoplankton as some species have been observed to adapt to the low Fe supply *in situ* by increasing the size of their light harvesting antennae, without increasing their Fe demand (Strzepek et al., 2012). In *Publication 3*, an antagonistic relationship between low light and low Fe supply was observed in both incubation experiments. Despite being dominated by different phytoplankton groups,

both assemblages exhibited a higher Fe demand under the low light intensity of 30 µmol photons m^{-2} s^{-1}. This is in line with the results of other Fe-light studies with Antarctic phytoplankton assemblages (Alderkamp et al., 2019; Vives et al., 2022), but differed from those studies which exposed the communities to very low light intensities (2-6 µmol photons m^{-2} s^{-1}: Latour et al., 2023) or very high irradiances (331-512 µmol photons m^{-2} s^{-1}: Alderkamp et al., 2019; 370-926 µmol photons m^{-2} s^{-1}: Vives et al., 2022). Perhaps, it could be hypothesized that the decrease in the Fe demand of SO phytoplankton is more likely induced only when they are acclimated to extremely low and high light intensities, something that requires further investigation.

The Fe-light field incubation experiments in *Publication 3* revealed, however, that the two distinct communities responded differently to increasing light under low Fe supply. In line with the findings of *Publication 1*, which highlighted the low Fe demand of oceanic diatoms, the diatom-dominated community was indeed able to take advantage of the highest light treatment of 150 µmol photons m^{-2} s^{-1} despite being Fe-limited. Accordingly, the diatom assemblage reached maximum POC production only at the highest light intensity, whereas rates did not differ between 30 and 80 µmol photons m^{-2} s^{-1} under low Fe supply. Hence, increasing light availability alleviated the negative effects of Fe limitation in the open ocean diatom-dominated phytoplankton assemblage. In comparison, the carbon production of the flagellate-dominated coastal community as well as the abundance of the cryptophyte group were not further enhanced from 80 to 150 µmol photons m^{-2} s^{-1}. This suggests that the community required more Fe to enable them to take advantage of higher irradiances (*Publication 3*, Figs. 1 and 6).

Clearly, the differential response of phytoplankton communities to increasing light under low Fe supply strongly depends on the species-specific Fe requirement of the major phytoplankton groups in the assemblage.

5.2 Ecological implications

5.2.1 Factors influencing the distribution of cryptophytes in the field

It is not well-understood yet as to what drives the dominance and distribution of cryptophytes in the field. Previous studies have linked the cryptophytes' occurrence to lower salinity and to warm, stratified and well-illuminated surface waters specifically when sea ice and glacial melting progresses in summer (e.g. Moline et al., 2004; Mendes et al., 2013, 2018). Although data on Fe concentration in the field were not provided in these previous studies, it could be hypothesized that sea ice and glacial melts bring in a high supply of Fe (Lannuzel et al., 2016; Monien et al., 2017) and potentially fuels the high Fe requirement of cryptophytes, as shown in *Publication 1*. Cryptophytes may further be able to take advantage of the increasing light availability during summer (*Publication and 3*) or perhaps, they resort to mixotrophy when ideal conditions are not met (i.e. low Fe supply). As it is proposed in *Publication 1* that cryptophytes tend to have a less efficient Fe uptake mechanism and a high Fe demand, it could be that due to their mixotrophic nature, it was not necessary for them to evolve and develop highly efficient Fe uptake

strategies. Hence, they are less competitive than diatoms in coping with low Fe conditions. This could potentially be related to their dominance in high Fe coastal regions, and not in open ocean waters characterized by low Fe supply. Moreover, based on the results of this thesis, cryptophytes appear to prefer medium irradiances (80-150 µmol photons m^{-2} s^{-1}, *Publication 1 and 3*). Nevertheless, they were also able to tolerate low (30 µmol photons m^{-2} s^{-1}, *Publication 3*) and high (500 µmol photons m^{-2} s^{-1}, *Publication 2*) although growth and carbon production were compromised. Their occurrence in summer (e.g. Moline et al., 2004; Mendes et al., 2013, 2018), when temperature is higher, also coincides with the results of *Publication 2*, wherein *G. cryophila* benefited from 4 °C warming.

Overall, the results of this thesis point toward the idea that Fe availability, temperature, and light, but not CO_2, strongly influence the ecophysiology of cryptophytes and may play an important role in shaping the occurrence and distribution pattern of cryptophytes in the field.

5.2.2 Projected changes in the distribution of cryptophytes in SO coastal waters and its impacts

In conjunction with OA and warming, coastal WAP waters are also projected to experience freshening, increased stratification and melting of glaciers and sea ice (Deppeler and Davidson, 2017). Glacial and sea ice melting would result in enhanced Fe supply (Monien et al., 2017) while increased stratification would expose coastal phytoplankton communities to higher light intensities (Deppeler and Davidson, 2017). *Publications 1 and 2* revealed that OA and an increase in temperature up to 4 °C would be beneficial to cryptophytes. Hence, under this future OA and warming scenario combined with high Fe availability, growth and carbon production of cryptophytes would be enhanced. Although cryptophytes are better suited in growing under medium light irradiances (e.g. 80-150 µmol photons m^{-2} s^{-1}, *Publication 2 and 3*), exposure to higher temperatures would enable them to deal with potential high-light stress (i.e. exposure to 500 µmol photons m^{-2} s^{-1}, *Publications 2*) brought by enhanced stratification of surface waters. The findings of this thesis point toward the potential positive effects of future climatic changes (i.e. warming, OA, high Fe availability) on the increased abundance of cryptophytes in coastal WAP waters.

As also proposed by Trimborn et al. (2019), the increase in the dominance of flagellates such as cryptophytes under future climate change scenario could weaken the biological carbon pump in the WAP since small flagellates such as cryptophytes are generally considered to be less efficient in exporting carbon compared to diatoms (Brown et al., 2019). Some cryptophyte species, however, have been shown to produce mucus and form cell aggregates (Klaveness, 1988), which on the other hand, could enhance their role in the export of carbon into ocean depths.

The shift in the dominance from diatoms to cryptophytes would also have an impact on the trophic food web dynamics in the WAP (Deppeler and Davidson, 2017; Henley et al., 2020). In fact, changes in the distribution patterns of the two key dominant grazers in the SO, the krill *Euphausia superba* and the tunicate *Salpa thompsoni* have already been observed in the field (Pakhomov et al., 2002; Bernard et al., 2012). Besides the direct impact

of reduced sea ice coverage on the spatial distribution of these two grazers, the shift in the size spectrum of dominant phytoplankton groups from the large-sized diatoms to the small-sized cryptophytes, is also hypothesized to potentially lead to a decrease in krill abundance and the dominance of salps (Moline et al., 2004). This is because krill are said to be selective feeders and prefer to feed on large-sized diatoms over small flagellates (Meyer and El-Sayed, 1983; Haberman et al., 2003) while salps appear to be non-selective in their diet (Pakhomov et al., 2002). The decrease in the abundance of krill would also potentially lead to a reduced availability of food to higher trophic organisms such as seals, penguins and whales (Pakhomov et al., 2002; Henley et al., 2020).

In contrast to previous studies (Meyer and El-Sayed, 1983; Pakhomov et al., 2002; Haberman et al., 2003), the recent field incubation experiment of Pauli et al. (2021) showed, however, that krill and salps in the WAP were both selective feeders and interestingly, the two grazers were even observed to specifically avoid feeding on cryptophytes. Since cryptophytes have flagella which allow them to move very fast (> 100 µm s^{-1} velocity, Kaňa et al., 2019), it could also be that they are able to get away from predators as no cryptophyte DNA were detected in the gut of both grazers (Pauli et al., 2021). Based on this finding of Pauli et al. (2021), it could also hypothesized that cryptophytes would not have a direct influence on the nutrition of higher trophic organisms in the WAP. However, they would be an important part of the microbial loop and given their high Fe:C ratio (*Publication 1*), they could also serve as a good source of recycled Fe for the next algal bloom events.

5.3 Perspectives for future research

A number of new insights have emerged from the findings of this thesis. It is shown here that higher dFe concentration did not always lead to an increase in growth and carbon production of the cryptophyte. Hence, this thesis highlights the importance of conducting future experiments looking at the preferred Fe source of cryptophytes as well as the Fe uptake mechanisms they employ. Other suggested research topics to explore include the potential operation of highly plastic carbon concentrating mechanism in cryptophytes as well as understanding and determining the factors that induce mixotrophy in this phytoplankton group.

5.3.1 Fe requirement and Fe uptake strategies of cryptophytes and the role of other trace metals

Publications 1 and 3 revealed that Fe strongly influenced the ecophysiology of cryptophytes. Identifying the factors that increase the cellular Fe demand of cryptophytes is therefore imperative. It has been proposed in this thesis that the high Fe demand of *G. cryophila* could be due in part to its high nitrogen requirement. Since all of the laboratory experiments conducted in this thesis used nitrate as the nitrogen source, it would be useful to conduct laboratory experiments on the influence of different nitrogen substrates or sources and examine how this modulates the Fe requirement of cryptophytes.

To date, no study has been done yet on the Fe uptake strategies employed by cryptophytes. Combining the observations from this thesis (i.e. unchanged Cu:C ratio in *G. cryophila*, absence of OA effects) and the limited Fe-uptake related genes found in cryptophytes (e.g. absence of MCO and FRE genes, Behnke and LaRoche, 2020), this thesis proposes the potential dependence of cryptophytes on divalent metal transporters (i.e. ZIP proteins) for acquiring Fe. It would also be interesting to investigate the role of OA in the Fe uptake of cryptophytes under Fe limitation and determine whether they also possess the High-CO_2-response (HCR) protein involved in Fe^{2+} uptake as observed in the green alga *Chlorococcum littorale* (Sasaki et al., 1998a,b). To unravel this knowledge gap on the Fe uptake mechanism of cryptophytes, gene expression studies as well as gene knockout experiments, similar to the phytotransferrin study of McQuaid et al. (2018), should be conducted.

Moreover, when conducting field studies, it would be important to characterize not only the total dFe concentration *in situ*, but also the bioavailability of Fe to cryptophytes. It would be imperative to determine the different ligands present and also the speciation of Fe in the field since all these factors influence the efficiency of the Fe acquisition of phytoplankton in general.

5.3.2 Potential operation of highly plastic CCM in cryptophytes

This thesis showed that cryptophytes are able to tolerate and even benefit from OA conditions in line with the observations of Trimborn et al. (2019). It would be interesting then to further test its tolerance to very high (>1000 µatm) and very low (< 400 µatm) CO_2 concentrations as well as to investigate and characterize whether cryptophytes operate a carbon concentrating mechanism (CCM). Phytoplankton groups that evolved earlier (i.e. cyanobacteria and dinoflagellates) have been shown to possess a more active and plastic CCMs compared to the recently evolved haptophyte and diatom groups (Van de Waal et al., 2019). Perhaps, this would also be the case for *G. cryophila*. Conducting such CO_2 studies may provide answers as to why and how cryptophytes benefit from OA.

5.3.3 Potential induction of mixotrophy in cryptophytes under heat stress

In the warming experiment in *Publication 2*, it has been shown that the cryptophyte *G. cryophila* (under 1000 µatm pCO_2 and 100 µmol photons m^{-2} s^{-1}) was able to survive and maintain photosynthetically viable cells even after 10 weeks of exposure under supra-optimal temperature (6 °C). Although growth rates were gradually decreasing and cells eventually stopped dividing, the unhealthy cells were still able to fully recover when transferred back to a lower temperature (4 °C). The mechanisms behind this observed ability of *G. cryophila* to survive under long-term heat stress still need to be investigated.

In response to unfavorable conditions (i.e. high light, nutrient limitation), some cryptophyte species have been reported to form resting cysts or palmellae (an aggregation of cells in mucus) (Lichtlé, 1979, 1980; Hoef-Emden and Melkonian, 2003). So far, no study has reported the occurrence of a resting cyst stage in *G. cryophila*. Previous laboratory experiments, however, have shown the ability of *G. cryophila* to feed on bacteria (Gast

et al., 2014) which would be advantageous under growth limiting conditions.

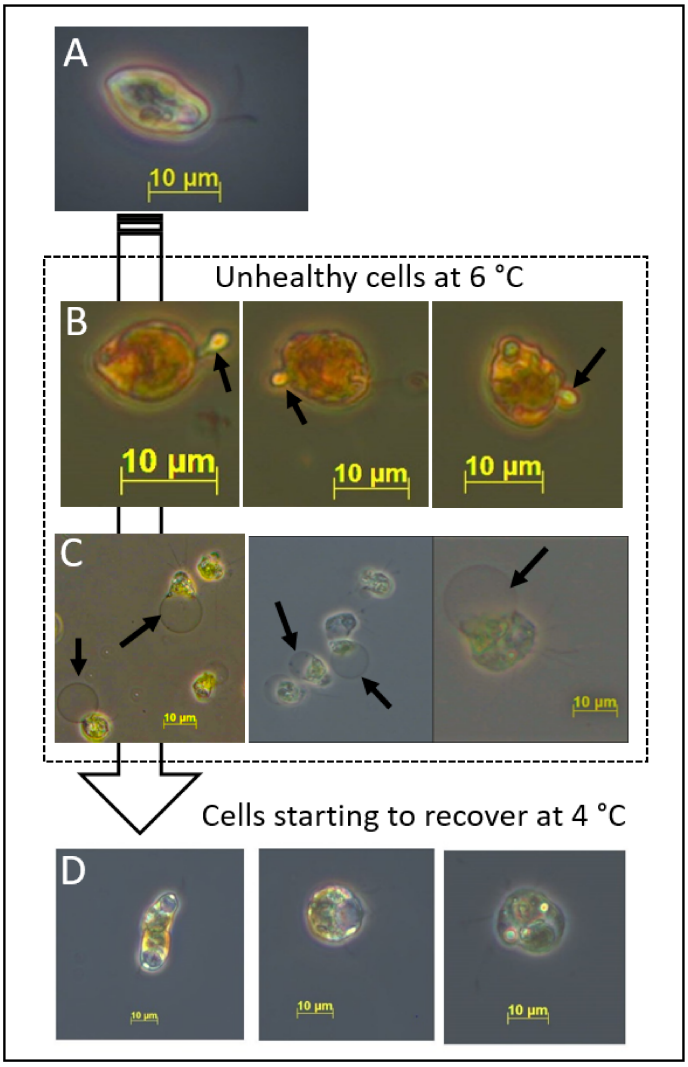

Figure 5.4. Microscope images of *Geminigera cryophila* grown at 6 °C (100 µmol photons m^{-2} s^{-1}, 1000 µatm pCO_2). ***Panel A*** shows an image of a healthy cell at the start of the incubation. ***Panel B*** shows images of *G. cryophila* cells after 8 weeks of incubation at 6 °C wherein small membrane protusions can be seen (indicated by black arrows). ***Panel C*** shows images of the unhealthy cells after 11 weeks of incubation at 6 °C. It can be seen here that cells underwent further morphological modifications such as the formation of "transparent spherical membrane extensions (mucus-like appearance)" (indicated by black arrows). Since these unhealthy cells still exhibited relatively high F_v/F_m values (0.30), they were transferred back to 4 °C to test whether they would be able to recover from the heat stress exposure. ***Panel D*** shows images of the cells which were starting to recover at 4 °C.

In *Publication 2*, changes in the morphology of *G. cryophila* cells were observed upon exposure to 6 °C warming. For the 6°C-1000pCO_2-100light treatment, the healthy cells (Figure 5.4**A**) gradually changed in appearance where cellular small membrane protrusions

were observed at 8 weeks incubation (Figure 5.4**B**). After 11 weeks of incubation, it can be seen in (Figure 5.4**C**) that the small membrane protrusion disappeared and "transparent spherical membrane extensions (mucus-like appearance)" became visible (Figure 5.4**C**).

Shown in Figure 5.5 is a screenshot of the video of the unhealthy 6 °C *G. cryophila* cultures (F_v/F_m = 0.30 ± 0.04) where small moving particles (which could be bacteria) were observed to be trapped in the "mucus-like" structures (Figure 5.5). Although axenic cultures were used in all experiments conducted in this thesis, it is plausible that in the case of the 6 °C incubation, the decay of some unhealthy cells could have potentially led to the growth of bacteria. Although highly speculative, it could be hypothesized that the heat stress exposure induced mixotrophy in *G. cryophila*, allowing it to capture bacteria and organic matter from the decaying cells. This could have allowed the unhealthy cells to maintain certain cellular processes, hence it was able to fully recover when transferred back to 4 °C.

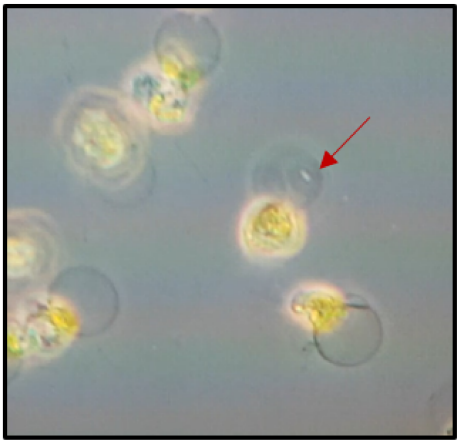

Figure 5.5. A screenshot of the video of the unhealthy 6 °C culture at 11 weeks incubation where small moving particles (potentially bacteria, indicated by the red arrow) were observed to be trapped in the transparent mucus-like structures.

Building upon these initial findings, it would be worthwhile to conduct studies which aim at understanding how mixotrophy or the shift between autotrophic and heterotrophic nutrition is induced in cryptophytes. If cryptophytes are highly dependent on this mode of nutrition, perhaps, this could explain why its Fe uptake strategies are less diverse compared to that of diatoms. Their ability to feed on bacteria may also be associated with their occurrence after diatom bloom decays (van Leeuwe et al., 2020) wherein an increase in the abundance of heterotrophic bacteria would be expected. Indeed, there is now an increasing need in studying the ecophysiology of mixotrophs as it is hypothesized that they may have a significant role in controlling biogeochemical cycles and carbon export (Cohen, 2022).

5.4 Conclusion

Based on the findings of this thesis and in line with the results of previous studies, cryptophytes would more likely be able to take advantage of the on-going ocean acidification and warming events in the WAP region of the Southern Ocean, especially when there is high availability of Fe and in conjunction with moderate irradiances. The new insights gained from this thesis further emphasize the need for conducting studies that aim to determine the Fe uptake strategies of cryptophytes as well as their ability to undergo mixotrophy. Such studies are required to gain a deeper understanding of the cryptophytes' ecophysiology and to better ascertain its influence on the overall carbon production and export in the Sothern Ocean and its role in shaping the Antarctic food web.

5.5 References

Alderkamp, A. C., Van Dijken, G. L., Lowry, K. E., Connelly, T. L., Lagerström, M., Sherrell, R. M., Haskins, C., Rogalsky, E., Schofield, O., Stammerjohn, S. E., Yager, P. L., and Arrigo, K. R. (2015). Fe availability drives phytoplankton photosynthesis rates during spring bloom in the Amundsen Sea Polynya, Antarctica. *Elementa*, 3(April).

Alderkamp, A. C., Van Dijken, G. L., Lowry, K. E., Lewis, K. M., Joy-Warren, H. L., Van De Poll, W., Laan, P., Gerringa, L., Delmont, T. O., Jenkins, B. D., and Arrigo, K. R. (2019). Effects of iron and light availability on phytoplankton photosynthetic properties in the Ross Sea. *Marine Ecology Progress Series*, 621:33–50.

Alscher, R. G., Erturk, N., and Heath, L. S. (2002). Role of superoxide dismutases (SODs) in controlling oxidative stress in plants. *Journal of Experimental Botany*, 53(372):1331–1341.

Andrew, S. M., Morell, H. T., Strzepek, R. F., Boyd, P. W., and Ellwood, M. J. (2019). Iron availability influences the tolerance of Southern Ocean phytoplankton to warming and elevated irradiance. *Frontiers in Marine Science*, 6(November):1–12.

Balaguer, J., Koch, F., Hassler, C., and Trimborn, S. (2022). Iron and manganese co-limit the growth of two phytoplankton groups dominant at two locations of the Drake Passage. *Communications Biology*, 5(1):1–12.

Behnke, J. and LaRoche, J. (2020). Iron uptake proteins in algae and the role of Iron Starvation-Induced Proteins (ISIPs). *European Journal of Phycology*, 55(3):339–360.

Behrenfeld, M. J. and Milligan, A. J. (2013). Photophysiological expressions of iron stress in phytoplankton. *Annual Review of Marine Science*, 5(1):217–246.

Bernard, K. S., Steinberg, D. K., and Schofield, O. M. (2012). Summertime grazing impact of the dominant macrozooplankton off the Western Antarctic Peninsula. *Deep-Sea Research Part I: Oceanographic Research Papers*, 62:111–122.

Blaby-Haas, C. E. and Merchant, S. S. (2017). Regulating cellular trace metal economy in algae. *Current Opinion in Plant Biology*, 39:88–96.

Blanco-Ameijeiras, S., Cabanes, D. J., Cable, R. N., Trimborn, S., Jacquet, S., Wiegmann, S., Völkner, C., Lelchat, F., Bracher, A., Duhaime, M. B., and Hassler, C. S. (2020). Exopolymeric substances control microbial community structure and function by contributing to both C and Fe nutrition in Fe-limited Southern Ocean provinces. *Microorganisms*, 8(12):1–21.

Blanco-Ameijeiras, S., Cosio, C., and Hassler, C. S. (2017). Long-term acclimation to iron limitation reveals new insights in metabolism regulation of *Synechococcus* sp. pcc7002. *Frontiers in Marine Science*, 4.

Boyd, P. W., Jickells, T., Law, C. S., Blain, S., Boyle, E. A., Buesseler, K. O., Coale, K. H., Cullen, J. J., De Baar, H. J., Follows, M., Harvey, M., Lancelot, C., Levasseur, M., Owens, N. P., Pollard, R., Rivkin, R. B., Sarmiento, J., Schoemann, V., Smetacek, V., Takeda, S., Tsuda, A., Turner, S., and Watson, A. J. (2007). Mesoscale iron enrichment experiments 1993-2005: Synthesis and future directions. *Science*, 315(5812):612–617.

Brown, M. S., Munro, D. R., Feehan, C. J., Sweeney, C., Ducklow, H. W., and Schofield, O. M. (2019). Enhanced oceanic CO_2 uptake along the rapidly changing West Antarctic Peninsula. *Nature Climate Change*, 9(9):678–683.

Bryant, D. A. and Gisriel, C. J. (2024). The structural basis for light harvesting in organisms producing phycobiliproteins. *The Plant Cell*, 00(0):1–29.

Castell, C., Rodríguez-Lumbreras, L. A., Hervás, M., Fernández-Recio, J., and Navarro, J. A. (2021). New Insights into the evolution of the electron transfer from cytochrome f to Photosystem I in the green and red branches of photosynthetic eukaryotes. *Plant and Cell Physiology*, 0(March):1–12.

Coello-Camba, A. and Agustí, S. (2017). Thermal thresholds of phytoplankton growth in polar waters and their consequences for a warming polar ocean. *Frontiers in Marine Science*, 4.

Cohen, N. R. (2022). Mixotrophic plankton foraging behaviour linked to carbon export. *Nature Communications*, 13(1):1–3.

Curtis, B. A., Tanifuji, G., Burki, F., Gruber, A., Irimia, M., Maruyama, S., Arias, M. C., Ball, S. G., Gile, G. H., Hirakawa, Y., Hopkins, J. F., Kuo, A., et al. (2012). Algal genomes reveal evolutionary mosaicism and the fate of nucleomorphs. *Nature*, 492(7427):59–65.

Deppeler, S. L. and Davidson, A. T. (2017). Southern Ocean phytoplankton in a changing climate. *Frontiers in Marine Science*, 4(FEB).

Donahue, K., Klaas, C., Dillingham, P. W., and Hoffmann, L. J. (2019). Combined effects of ocean acidification and increased light intensity on natural phytoplankton communities from two Southern Ocean water masses. *Journal of Plankton Research*, 41:30–45.

Gaillard, S., Charrier, A., Malo, F., Carpentier, L., Bougaran, G., Hégaret, H., Réveillon, D., Hess, P., and Séchet, V. (2020). Combined effects of temperature, irradiance, and pH on *Teleaulax amphioxeia* (Cryptophyceae) physiology and feeding ratio for its predator *Mesodinium rubrum* (Ciliophora). *Journal of Phycology*, 56(3):775–783.

Gast, R. J., McKie-Krisberg, Z. M., Fay, S. A., Rose, J. M., and Sanders, R. W. (2014). Antarctic mixotrophic protist abundances by microscopy and molecular methods. *FEMS Microbiology Ecology*, 89(2):388–401.

González-Herrero, S., Barriopedro, D., Trigo, R. M., López-Bustins, J. A., and Oliva, M. (2022). Climate warming amplified the 2020 record-breaking heatwave in the Antarctic Peninsula. *Communications Earth and Environment*, 3(1):1–9.

Haberman, K. L., Ross, R. M., and Quetin, L. B. (2003). Diet of the Antarctic krill (*Euphausia superba* Dana): II. Selective grazing in mixed phytoplankton assemblages. *Journal of Experimental Marine Biology and Ecology*, 283(1):97–113.

Henley, S. F., Cavan, E. L., Fawcett, S. E., Kerr, R., Monteiro, T., Sherrell, R. M., Bowie, A. R., Boyd, P. W., Barnes, D. K., Schloss, I. R., Marshall, T., Flynn, R., and Smith, S. (2020). Changing biogeochemistry of the Southern Ocean and its ecosystem implications. *Frontiers in Marine Science*, 7:1–31.

Hoef-Emden, K. and Melkonian, M. (2003). Revision of the genus *Cryptomonas* (Cryptophyceae): A combination of molecular phylogeny and morphology provides insights into a long-hidden dimorphism. *Protist*, 154(3):371–409.

Hoppe, C. J. M., Hassler, C. S., Payne, C. D., Tortell, P. D., Rost, B., and Trimborn, S. (2013). Iron limitation modulates ocean acidification effects on Southern Ocean phytoplankton communities. *PLOS ONE*, 8(11):e79890.

Jepsen, P. M., Thoisen, C. V., Carron-Cabaret, T., Pinyol-Gallemí, A., Nielsen, S. L., and Hansen, B. W. (2019). Effects of salinity, commercial salts, and water type on cultivation of the cryptophyte microalgae *Rhodomonas salina* and the calanoid copepod *Acartia tonsa*. *Journal of the World Aquaculture Society*, 50(1):104–118.

Kaňa, R., Kotabová, E., Šedivá, B., and Kuthanová Trsková, E. (2019). Photoprotective strategies in the motile cryptophyte alga *Rhodomonas salina* —role of non-photochemical quenching, ions, photoinhibition, and cell motility. *Folia Microbiologica*, 64(5):691–703.

Kaňa, R., Kotabová, E., Sobotka, R., and Prášil, O. (2012). Non-photochemical quenching in cryptophyte alga *Rhodomonas salina* is located in chlorophyll *a*/*c* antennae. *PLoS ONE*, 7(1).

Kim, J. I., Moore, C. E., Archibald, J. M., Bhattacharya, D., Yi, G., Yoon, H. S., and Shin, W. (2017). Evolutionary dynamics of cryptophyte plastid genomes. *Genome Biology and Evolution*, 9(7):1859–1872.

Klaveness, D. (1988). Ecology of the Cryptomonadida: A first review. in C. D. Sandgren (ed.), Growth and reproductive strategies of freshwater phytoplankton. *Cambridge: Cambridge University Press.*, pages 105–133.

Koch, F., Beszteri, S., Harms, L., and Trimborn, S. (2019). The impacts of iron limitation and ocean acidification on the cellular stoichiometry, photophysiology, and transcriptome of *Phaeocystis antarctica*. *Limnology and Oceanography*, 64(1):357–375.

Koch, F. and Trimborn, S. (2019). Limitation by Fe, Zn, Co, and B_{12} results in similar physiological responses in two Antarctic phytoplankton species. 6:514.

Kustka, A. B., Allen, A. E., and Morel, F. M. (2007). Sequence analysis and transcriptional regulation of iron acquisition genes in two marine diatoms. *Journal of Phycology*, 43(4):715–729.

Lannuzel, D., Vancoppenolle, M., Van Der Merwe, P., De Jong, J., Meiners, K. M., Grotti, M., Nishioka, J., and Schoemann, V. (2016). Iron in sea ice: Review and new insights. *Elementa*, 4:1–19.

Latour, P., Eggins, S., van der Merwe, P., Bach, L. T., Boyd, P. W., Ellwood, M. J., Bowie, A. R., Wuttig, K., and Strzepek, R. F. (2023). Characterization of a Southern Ocean deep chlorophyll maximum: Response of phytoplankton to light, iron, and manganese enrichment. *Limnology and Oceanography Letters*.

Lelandais, G., Scheiber, I., Paz-Yepes, J., Lozano, J. C., Botebol, H., Pilátová, J., Žárský, V., Léger, T., Blaiseau, P. L., Bowler, C., Bouget, F. Y., Camadro, J. M., Sutak, R., and Lesuisse, E. (2016). *Ostreococcus tauri* is a new model green alga for studying iron metabolism in eukaryotic phytoplankton. *BMC Genomics*, 17(1):1–23.

Lichtlé, C. (1979). Effects of nitrogen deficiency and light of high intensity on *Cryptomonas rufescens* (Cryptophyceae). *Protoplasma*, 101(4):283–299.

Lichtlé, C. (1980). Effects of nitrogen deficiency and light of high intensity on Cryptomonas rufescens (Cryptophyceae). *Protoplasma*, 102:11–19.

Lommer, M., Specht, M., Roy, A. S., Kraemer, L., Andreson, R., Gutowska, M. A., Wolf, J., Bergner, S. V., Schilhabel, M. B., Klostermeier, U. C., Beiko, R. G., Rosenstiel, P., Hippler, M., and LaRoche, J. (2012). Genome and low-iron response of an oceanic diatom adapted to chronic iron limitation. *Genome Biology*, 13(7):R66.

Maldonado, M. T., Boyd, P. W., Harrison, P. J., and Price, N. M. (1999). Co-limitation of phytoplankton growth by light and Fe during winter in the NE subarctic Pacific Ocean. *Deep-Sea Research Part II: Topical Studies in Oceanography*, 46(11-12):2475–2485.

Maldonado, M. T. and Price, N. M. (1996). Influence of N substrate on Fe requirements of marine centric diatoms. *Marine Ecology Progress Series*, 141(1-3):161–172.

Martin, J. H. (1990). Glacial-interglacial CO_2 change: The Iron Hypothesis. *Paleoceanography*, 5(1):1–13.

McQuaid, J. B., Kustka, A. B., Oborník, M., Horák, A., McCrow, J. P., Karas, B. J., Zheng, H., Kindeberg, T., Andersson, A. J., Barbeau, K. A., and Allen, A. E. (2018). Carbonate-sensitive phytotransferrin controls high-affinity iron uptake in diatoms. *Nature*, 555(7697):534–537.

Mendes, C. R. B., Costa, R. R., Ferreira, A., Jesus, B., Tavano, V. M., Dotto, T. S., Leal, M. C., Kerr, R., Islabão, C. A., Franco, A. d. O. d. R., Mata, M. M., Garcia, C. A. E., and Secchi, E. R. (2023). Cryptophytes: an emerging algal group in the rapidly changing Antarctic Peninsula marine environments. *Global Change Biology*, (January):1–18.

Mendes, C. R. B., Tavano, V. M., Dotto, T. S., Kerr, R., de Souza, M. S., Garcia, C. A. E., and Secchi, E. R. (2018). New insights on the dominance of cryptophytes in Antarctic coastal waters: A case study in Gerlache Strait. *Deep-Sea Research Part II: Topical Studies in Oceanography*, 149:161–170.

Mendes, C. R. B., Tavano, V. M., Leal, M. C., de Souza, M. S., Brotas, V., and Garcia, C. A. E. (2013). Shifts in the dominance between diatoms and cryptophytes during three late summers in the Bransfield Strait (Antarctic Peninsula). *Polar Biology*, 36(4):537–547.

Meyer, M. A. and El-Sayed, S. Z. (1983). Grazing of *Euphausia superba* Dana on natural phytoplankton populations. *Polar Biology*, 1(4):193–197.

Mock, T., Otillar, R. P., Strauss, J., McMullan, M., Paajanen, P., Schmutz, J., Salamov, A., Sanges, R., Toseland, A., Ward, B. J., Allen, A. E., Dupont, C. L., Frickenhaus, S., Maumus, F., Veluchamy, A., Wu, T., Barry, K. W., Falciatore, A., Ferrante, M. I., Fortunato, A. E., Glöckner, G., Gruber, A., Hipkin, R., Janech, M. G., Kroth, P. G., Leese, F., Lindquist, E. A., Lyon, B. R., Martin, J., Mayer, C., Parker, M., Quesneville, H., Raymond, J. A., Uhlig, C., Valas, R. E., Valentin, K. U., Worden, A. Z., Armbrust, E. V., Clark, M. D., Bowler, C., Green, B. R., Moulton, V., van Oosterhout, C., and Grigoriev, I. V. (2017). Evolutionary genomics of the cold-adapted diatom *Fragilariopsis cylindrus*. *Nature*, 541(7638):536–540.

Moline, M. A., Claustre, H., Frazer, T. K., Schofield, O., and Vernet, M. (2004). Alteration of the food web along the Antarctic Peninsula in response to a regional warming trend. *Global Change Biology*, 10(12):1973–1980.

Monien, D., Monien, P., Brünjes, R., Widmer, T., Kappenberg, A., Silva Busso, A. A., Schnetger, B., and Brumsack, H.-J. (2017). Meltwater as a source of potentially bioavailable iron to Antarctica waters. *Antarctic Science*, 29(3):277–291.

Morel, F. M., Lam, P. J., and Saito, M. A. (2020). Trace metal substitution in marine phytoplankton. *Annual Review of Earth and Planetary Sciences*, 48:491–517.

Moreno, C. M., Lin, Y., Davies, S., Monbureau, E., Cassar, N., and Marchetti, A. (2018). Examination of gene repertoires and physiological responses to iron and light limitation in Southern Ocean diatoms. *Polar Biology*, 41(4):679–696.

Morrissey, J., Sutak, R., Paz-Yepes, J., Tanaka, A., Moustafa, A., Veluchamy, A., Thomas, Y., Botebol, H., Bouget, F. Y., McQuaid, J. B., Tirichine, L., Allen, A. E., Lesuisse, E., and Bowler, C. (2015). A novel protein, ubiquitous in marine phytoplankton, concentrates iron at the cell surface and facilitates uptake. *Current Biology*, 25(3):364–371.

Pakhomov, E. A., Froneman, P. W., and Perissinotto, R. (2002). Salp/krill interactions in the Southern Ocean: Spatial segregation and implications for the carbon flux. *Deep-Sea Research Part II: Topical Studies in Oceanography*, 49(9-10):1881–1907.

Pauli, N. C., Metfies, K., Pakhomov, E. A., Neuhaus, S., Graeve, M., Wenta, P., Flintrop, C. M., Badewien, T. H., Iversen, M. H., and Meyer, B. (2021). Selective feeding in Southern Ocean key grazers—diet composition of krill and salps. *Communications Biology*, 4(1):1–12.

Peers, G. and Price, N. M. (2006). Copper-containing plastocyanin used for electron transport by an oceanic diatom. *Nature*, 441(7091):341–344.

Petrou, K., Trimborn, S., Rost, B., Ralph, P. J., and Hassler, C. S. (2014). The impact of iron limitation on the physiology of the Antarctic diatom *Chaetoceros simplex*. *Marine Biology*, 161(4):925–937.

Raven, J. A. (1990). Predictions of Mn and Fe use efficiencies of phototrophic growth as a function of light availability for growth and of C assimilation pathway. *New Phytologist*, 116(1):1–18.

Raven, J. A., Evans, M. C., and Korb, R. E. (1999). The role of trace metals in photosynthetic electron transport in O_2-evolving organisms. *Photosynthesis Research*, 60(2-3):111–149.

Rizkallah, M. R., Frickenhaus, S., Trimborn, S., Harms, L., Moustafa, A., Benes, V., Gäbler-Schwarz, S., and Beszteri, S. (2020). Deciphering patterns of adaptation and acclimation in the transcriptome of *Phaeocystis antarctica* to changing iron conditions. *Journal of Phycology*, 56(3):747–760.

Sasaki, T., Kurano, N., and Miyachi, S. (1998a). Cloning and characterization of high-CO_2-specific cdnas from a marine microalga, *Chlorococcum littorale*, and effect of CO_2 concentration and iron deficiency on the gene expression. *Plant and Cell Physiology*, 39(2):131–138.

Sasaki, T., Kurano, N., and Miyachi, S. (1998b). Induction of ferric reductase activity and of iron uptake capacity in *Chlorococcum littorale* cells under extremely high-CO_2 and iron-deficient conditions. *Plant and Cell Physiology*, 39(4):405–410.

Schoffman, H., Lis, H., Shaked, Y., and Keren, N. (2016). Iron-nutrient interactions within phytoplankton. *Frontiers in Plant Science*, 7:1–12.

Schulz, K. G., Bach, L. T., Bellerby, R. G. J., Bermúdez, R., Büdenbender, J., Boxhammer, T., Czerny, J., Engel, A., Ludwig, A., Meyerhöfer, M., Larsen, A., Paul, A. J., Sswat, M., and Riebesell, U. (2017). Phytoplankton blooms at increasing levels of atmospheric carbon dioxide: Experimental evidence for negative effects on prymnesiophytes and positive on small picoeukaryotes. *Frontiers in Marine Science*, 4.

Sommer, U., Paul, C., and Moustaka-Gouni, M. (2015). Warming and ocean acidification effects on phytoplankton - From species shifts to size shifts within species in a mesocosm experiment. *PLoS ONE*, 10(5):1–17.

Stiller, J. W., Schreiber, J., Yue, J., Guo, H., Ding, Q., and Huang, J. (2014). The evolution of photosynthesis in chromist algae through serial endosymbioses. *Nature Communications*, 5:1–7.

Strzepek, R. F., Hunter, K. A., Frew, R. D., Harrison, P. J., and Boyd, P. W. (2012). Iron-light interactions differ in Southern Ocean phytoplankton. *Limnology and Oceanography*, 57(4):1182–1200.

Tortell, P. D. (2000). Evolutionary and ecological perspectives on carbon acquisition in phytoplankton. *Limnology and Oceanography*, 45(3):744–750.

Tortell, P. D., Payne, C. D., Li, Y., Trimborn, S., Smith, W. O., Riesselman, C., Dunbar, R. B., Sedwick, P., and Ditullio, G. R. (2008). CO_2 sensitivity of Southern Ocean phytoplankton. 35:1–5.

Trimborn, S., Brenneis, T., Hoppe, C. J., Laglera, L. M., Norman, L., Santos-Echeandía, J., Völkner, C., Wolf-Gladrow, D., and Hassler, C. S. (2017). Iron sources alter the response of Southern Ocean phytoplankton to ocean acidification. *Marine Ecology Progress Series*, 578:35–50.

Trimborn, S., Brenneis, T., Sweet, E., and Rost, B. (2013). Sensitivity of Antarctic phytoplankton species to ocean acidification: Growth, carbon acquisition, and species interaction. *Limnology and Oceanography*, 58(3):997–1007.

Trimborn, S., Hoppe, C. J., Taylor, B. B., Bracher, A., and Hassler, C. (2015). Physiological characteristics of open ocean and coastal phytoplankton communities of Western Antarctic Peninsula and Drake Passage waters. *Deep-Sea Research Part I: Oceanographic Research Papers*, 98:115–124.

Trimborn, S., Thoms, S., Karitter, P., and Bischof, K. (2019). Ocean acidification and high irradiance stimulate the photo-physiological fitness, growth and carbon production of the Antarctic cryptophyte *Geminigera cryophila*. *Biogeosciences*, 16(15):2997–3008.

Twining, B. S., Baines, S. B., Fisher, N. S., and Landry, M. R. (2004). Cellular iron contents of plankton during the Southern Ocean Iron Experiment (SOFeX). *Deep-Sea Research Part I: Oceanographic Research Papers*, 51(12):1827–1850.

Van de Waal, D. B., Brandenburg, K. M., Keuskamp, J., Trimborn, S., Rokitta, S., Kranz, S. A., and Rost, B. (2019). Highest plasticity of carbon-concentrating mechanisms in earliest evolved phytoplankton. *Limnology and Oceanography Letters*.

van de Waal, D. B. and Litchman, E. (2020). Multiple global change stressor effects on phytoplankton nutrient acquisition in a future ocean. *Philosophical Transactions of the Royal Society B: Biological Sciences*, 375(1798):1–8.

van Leeuwe, M. A., Webb, A. L., Venables, H. J., Visser, R. J., Meredith, M. P., Elzenga, J. T. M., and Stefels, J. (2020). Annual patterns in phytoplankton phenology in Antarctic coastal waters explained by environmental drivers. *Limnology and Oceanography*, 65(7):1651–1668.

Vives, C. R., Schallenberg, C., Strutton, P. G., and Westwood, K. J. (2022). Iron and light limitation of phytoplankton growth off East Antarctica. *Journal of Marine Systems*, 234:103774.

Wang, X. and Smith, W. O. (2021). Phytoplankton growth at low temperatures: results from low temperature incubations. *Journal of Plankton Research*, 43(5):633–641.

Weisse, T. and Stadler, P. (2006). Effect of pH on growth, cell volume, and production of freshwater ciliates, and implications for their distribution. *Limnology and Oceanography*, 51(4):1708–1715.

Young, J. N., Goldman, J. A., Kranz, S. A., Tortell, P. D., and Morel, F. M. (2015a). Slow carboxylation of Rubisco constrains the rate of carbon fixation during Antarctic phytoplankton blooms. *New Phytologist*, 205(1):172–181.

Young, J. N., Kranz, S. A., Goldman, J. A., Tortell, P. D., and Morel, F. M. (2015b). Antarctic phytoplankton down-regulate their carbon-concentrating mechanisms under high CO_2 with no change in growth rates. *Marine Ecology Progress Series*, 532:13–28.

Zhu, Z., Qu, P., Gale, J., Fu, F., and Hutchins, D. A. (2017). Individual and interactive effects of warming and CO_2 on *Pseudo-nitzschia subcurvata* and *Phaeocystis antarctica*, two dominant phytoplankton from the Ross Sea, Antarctica. *Biogeosciences*, 14(23):5281–5295.

Acknowledgments

The completion of this PhD thesis would not have been possible without the help and support of many people.

First and foremost, I would like to express my deepest gratitude to my PhD supervisor, Dr. Scarlett Trimborn. I will always be grateful for her unwavering support from helping me acquire a Phd scholarship, supporting my University admission, visa extensions, to funding applications, and most especially, for giving me the opportunity to conduct my Phd research at the Alfred Wegener Institute (AWI). I am thankful for her guidance and the time and effort she invested in mentoring me and for sharing her knowledge and expertise which ultimately honed my skills and capabilities and become a better person. It has been a great privilege.

I am extremely grateful to Prof. Dr. Sven Kranz and Prof. Dr. Natalie Cohen for agreeing to review my thesis as well as to Prof. Dr. Christian Wild and Prof. Dr. Tilmann Harder for accepting my request to serve as examiners during my thesis defense. I sincerely thank them for their time and expertise.

I owe an immense debt of gratitude to the German Katholischer Akademischer Ausländer-Dienst (KAAD) for providing me with a scholarship funding which enabled me to pursue this PhD degree. Special thanks to Dr. Heinrich Geiger and Frau Karin Bialas of KAAD for their endless support and assistance. I hope to pay it forward.

I would also like to thank my thesis advisory committee – Dr. Maite Maldonado, Dr. Kai Bischof, Dr. Silke Thoms, and Dr. Florian Koch, and my collaborators – Dr. Boris Koch, Dr. Jana Geuer and Dr. Christel Hassler, for providing critical feedback. I also wish to extend my appreciation to Dr. Maria van Leeuwe for her time and for sharing insightful and helpful comments on my Study 3.

To the members of the EcoTrace Group during the time I was doing my Phd: Franziska Pausch, Sebastian Boeckmann, Jenna Balaguer, Jasmin Stimpfle, Christian Voelkner, Florian, Silke, Doro as well as Anna Pagnone, you are all brilliant and nice people, I feel very fortunate to be part of the group. Thank you very much for all your support and for always making me feel welcome and at home – your kindness means a lot to me. A very special thanks to my officemate Franzi who has been instrumental in helping me integrate smoothly and adjust to the workplace at AWI. She is always very willing to help, and I am very lucky to have known such a beautiful soul. I also thank her for her significant support during the last phase of my Phd, I very much appreciate her feedback on my thesis and helping me with language translations. A huge thank you as well to Christian for the analysis of my trace metal samples and for helping me during experiment harvests.

I thank also all the friendly and helpful members of the Marine Biogeosciences and Ecological Chemistry sections. I am especially grateful to Tina Brenneis for training and assisting me during my first laboratory experiments. Thanks as well to Ulli and Klaus-Uwe Richter for always being available to help and assist me with the set-up of the CO_2 gas lines for my experiments. Thanks also to Alex Kraberg for assisting me with the SEM; to Christine K., Sebastian R., Linda R., Nancy K. and Annegret M. for the various help they have provided; and to Beate, Miriam and Onur for the happy vibes and random talks whenever I drop by their office.

I am also grateful to the AWI (EcoChem & Polmar) for granting me a 3-month funding (Corona-related contract extension) when my KAAD scholarship ended. I thank the graduate school Polmar for their support and for giving me the opportunity to participate in various courses and trainings. Many thanks as well to the STIBET-DAAD for the 3-month thesis writing grant awarded to me. I also wish to acknowledge the funding that I received from the University of Bremen Central Research Development Fund (01 Impulse Grant) which enabled me to join the 5-week Arctic Marine Molecular Ecology Course at the University Centre in Svalbard (UNIS).

To Joyce, Daphnie, Rhods, Erwin, Gay, Ate Caryl, Ate Dette, Bingles, Martina of KHG-Bremen as well as my KAAD friends, thank you very much for the encouragement and moral support. Thanks for the fun times together. I extend also my gratitude to Tita Rose for her kindness and generosity, and to Stephan and Lena for the friendship.

Most especially, I am grateful to my parents and siblings for always being there to support me in all my endeavors. I know your prayers have guided and protected me throughout these years. I am blessed to have you – you all are my strength, motivation and inspiration. And to my husband, Arjay, thank you very much for your constant love, understanding and support. I appreciate your hard work and everything that you do. I am very grateful that you are by my side while finishing this PhD journey. I share this achievement with you… <3

Universität Bremen

Universität Bremen | Fachbereich 02 | Postfach 33 04 40, 28334 Bremen

Universität Bremen
Fachbereich 2
Prüfungsamt Chemie
z. Hd. Frau Frauke Ernst
Leobener Straße

28359 Bremen
Deutschland

Prüfungsamt
Chemie

Frauke Ernst
Geschäftsstelle
Fachbereich 02
Leobener Str. / NW2
D-28359 Bremen

Verwaltungspavillon 06
Tel. 0421 218-62802
Fax 0421 218-9862802
frauke.ernst@uni-bremen.de
www.fb2.uni-bremen.de

Versicherung an Eides Statt

Name, Vorname	Camoying, Marianne
Matrikel-Nr.	3162805
Straße	
Ort, PLZ	

Ich, Marianne Camoying (Vorname, Name)

versichere an Eides Statt durch meine Unterschrift, dass ich die vorstehende Arbeit selbständig und ohne fremde Hilfe angefertigt und alle Stellen, die ich wörtlich dem Sinne nach aus Veröffentlichungen entnommen habe, als solche kenntlich gemacht habe, mich auch keiner anderen als der angegebenen Literatur oder sonstiger Hilfsmittel bedient habe.
Ich versichere an Eides Statt, dass ich die vorgenannten Angaben nach bestem Wissen und Gewissen gemacht habe und dass die Angaben der Wahrheit entsprechen und ich nichts verschwiegen habe.
Die Strafbarkeit einer falschen eidesstattlichen Versicherung ist mir bekannt, namentlich die Strafandrohung gemäß § 156 StGB bis zu drei Jahren Freiheitsstrafe oder Geldstrafe bei vorsätzlicher Begehung der Tat bzw. gemäß § 161 Abs. 1 StGB bis zu einem Jahr Freiheitsstrafe oder Geldstrafe bei fahrlässiger Begehung.

Ort, Datum / Unterschrift

CONTRIBUTION

Declaration on the contribution of the candidate to a multi-author article/manuscript.
Contribution of the candidate in % of the total workload (up to 100% for each of the following categories).

Chapter 2, Publication 1
Experimental concept and design: ca. 70%
Experimental work and/or acquisition of (experimental) data: ca. 90%
Data analysis and interpretation: ca. 80%
Preparation of Figures and Tables: ca. 100%
Drafting of the manuscript: ca. 80%

Chapter 3, Publication 2
Experimental concept and design: ca. 80%
Experimental work and/or acquisition of (experimental) data: ca. 90%
Data analysis and interpretation: ca. 80%
Preparation of Figures and Tables: ca. 100%
Drafting of the manuscript: ca. 80%

Chapter 4, Publication 3
Experimental concept and design: ca. 10%
Experimental work and/or acquisition of (experimental) data: ca. 20%
Data analysis and interpretation: ca. 85%
Preparation of Figures and Tables: ca. 100%
Drafting of the manuscript: ca. 90%

_____ _____

Ort, Datum Unterschrift